PEOPLE'S DEMOCRATIC REPUBLIC OF ALGERIA
MINISTER OF HIGHER EDUCATION AND SCIENTIFIC RESEARCH
UNIVERSITY YAHIA FARES DE MEDEA



FACULTE DE TECHNOLOGIE

DOCTORAL THESIS

*To obtain the degree of **DOCTOR***

In: Electrical Engineering
Specialty: Electrical Engineering and Electrical Control
Presented by

MOHAMMED ABDULELAH HUSSIEN SAEED ALBASHERI

Thesis title

Study and analysis for the design of Smart Grids

Defended on: 19/02/2025

In front of the jury composed of:

MOUALDIA Abdelhafidh	Professor	Univ. of Médéa	President
BOUCHHIDA Ouahid	Professor	Univ. of Médéa	Supervisor
SOUFI Youcef	Professor	Univ. of Tébessa	Co-Supervisor
KABECHE Nadhir	Professor	Univ. of Médéa	Examiner 1
BOUDANA Djamel	Professor	ENP - Algiers	Examiner 2
BOUKADOUM Aziz	Professor	Univ. of Tébessa	Examiner 3
CHERIFI Abderrazak	Professor	Univ. of Paris Saclay Versailles	Invited

Academic year : **2024/2025**

REPUBLIQUE ALGERIENNE DEMOCRATIQUE ET POPULAIRE
MINISTERE DE L'ENSEIGNEMENT SUPERIEUR ET DE LA RECHERCHE SCIENTIFIQUE
UNIVERSITE YAHIA FARES DE MEDEA



FACULTE DE TECHNOLOGIE

THESE DE DOCTORAT

*Présentée en vue de l'obtention du grade de **DOCTEUR***

Filière : électrotechnique
Spécialité : Électrotechnique et commande électrique
Présentée par

MOHAMMED ABDULELAH HUSSIEN SAEED ALBASHERI

Thème

Etude et analyse en vue de la conception des réseaux électriques intelligents "Smart GRID"

Soutenue le: 19/02/2025

Soutenue publiquement devant le jury composé de :

MOUALDIA Abdelhafidh	Professeur	Univ. de Médéa	Président
BOUCHHIDA Ouahid	Professeur	Univ. de Médéa	Directeur de thèse
SOUFI Youcef	Professeur	Univ. de Tébessa	Co-Directeur de thèse
KABECHE Nadhir	Professeur	Univ. of Médéa	Examinateur 1
BOUDANA Djamel	Professeur	ENP - Algiers	Examinateur 2
BOUKADOUM Aziz	Professeur	Univ. de Tébessa	Examinateur 3
CHERIFI Abderrazak	Professeur	Univ. de Paris Saclay Versailles	Invité

Année Universitaire: **2024/2025**

Acknowledgements

"During the preparation of this thesis, I have received substantial support and encouragement".

I would like to thank the members of my dissertation committee—not only for their time and patience but also for their intellectual contributions to my development as a researcher. To Professor ***MOUALDIA ABDELHAFIDH*** *from the University of Médéa, I am grateful for your role as the Chair of my committee. Your inspiring words during our first meeting motivated me greatly, and I have carried that motivation with me throughout my journey. To Professor* ***KABACHE NADIR*** *from the University of Médéa, Professor* ***BOUDANA DJAMEL*** *from École Nationale Polytechnique–EL Harrach, and Professor* ***BOUKADOUM AZIZ*** *from the University of Tebessa, it is a great honor to have you as jury members. Your constructive feedback and encouragement during the examination process have significantly contributed to the final outcome of this thesis.*

Most of all, I would like to thank my supervisor, Professor ***BOUCHHIDA OUAHID*** *from the University of Médéa. Your guidance and expertise have been invaluable. I am indebted to you for enhancing my research strengths and patiently encouraging me to improve in my weaker areas. Your insightful feedback has inspired me to refine my thoughts and elevate my work.*

I want to acknowledge Professor ***SOUFI YOUCEF*** *from the University of Tebessa for sharing your vast experience in the electrical engineering field. Your excellent collaboration and unwavering technical and mental support have been instrumental. You have been more than just a co-advisor; without your help and motivation, I may not have pursued this challenging area of electrical engineering.*

Finally, I would like to express my appreciation to Professor ***CHERIFI ABDELRREZZAK*** *from the Université Paris Saclay-Versailles for agreeing to serve on my committee. Your presence has strengthened my dissertation and added credibility to my work. I earnestly hope to have the opportunity for future collaborations with you.*

I would also like to thank all the members of the Laboratoire de Recherche en Électrotechnique et Automatique ***LREA****. I wish you all continued success.*

Last but not least, I want to thank my parents, my wife, and my entire family. Your unwavering support during my PhD journey has been invaluable. Thank you for encouraging me through the ups and downs of my academic career. It has been a challenging road, but your confidence in me has enabled me to persevere and succeed. Without your support, I would not be here today. Your encouragement has always motivated me to put forth my best effort in accomplishing my work.

Thank you all"

Mohammed Abdulelah Hussein Saeed ALBASHERI

Publication list

- ***M. A. Albasheri**, O. Bouchhida, Y. Soufi, and A. Cherifi, "Enhanced supervisor energy management technique of DC microgrid-based PV/wind/battery/SC," Electrical Engineering, (Springer), 2024.*

- ***M. A. Albasheri**, O. Bouchhida, Y. Soufi, and A. Cherifi, M. A. H. Mujammal, "Supervisory Energy Management Strategy Based-Fuzzy Logic for a DC Microgrid," International Journal of Dynamics and Control, (Springer), 2024.*

- ***M. A. Albasheri**, O. Bouchhida, Y. Soufi, and A. Cherifi, M. A. H. Mujammal, "Energy Management technique of Hybrid Energy Storage System based DC microgrid," Journal of Energy Systemsl, (DergiPark), 2025.*

- ***M. A. Albasheri**, O. Bouchhida, Y. Soufi, and A. Cherifi, "Enhanced energy storage system efficiency for remote area-based DC microgrid," STUDIES IN ENGINEERING AND EXACT SCIENCES, vol. 5, no. 2, pp. e5367–e5367, Jul. 2024.*

- *M. A. H. Mujammal, A. Moualdia, P. Wira, **M. A. Albasheri**, and A. Cherifi, "Novel Direct Power Control Based on Grid Voltage Modulated Strategy Using Artificial Intelligence," Smart Grids and Energy, (Springer), 2024.*

- *M. A. H. Mujammal, A. Moualdia, S. Boulkhrachef, D. Boudana, P. Wira, and **M. A. Albasheri**, "*Advancing Wind *Energy Conversion: Smart Maximum power point based on M5-Pruned Algorithm for Enhanced Wind Energy Production", Production Engineering, (Springer), 2024.*

- *M. A. H. Mujammal, A. Moualdia, G. Lorenzini, S. Boulkhrachef, P. Wira, **M. A. Albasheri** " Three-Phase PWM Rectifier Control: Enhanced Direct Power Control with Neural Networks from Theory to Superior Reality Performance", Journal Européen des Systèmes Automatisés, (IIETA), 2024.*

- M. A. H. Mujammal, A. Moualdia, S. Boulkhrachef, D. Boudana, P. Wira, and **M. A. Albasheri**, "Next-Generation MPPT: neural network-driven optimization for superior solar performance," STUDIES IN ENGINEERING AND EXACT SCIENCES, vol. 5, no. 2, pp. e7338–e7338, Sep. 2024.

Conferences

- ***M. A. Albasheri**, O. Bouchhida, and Y. Soufi, "Control of a Stand-Alone Variable Speed Wind Turbine with a Permanent Magnet Synchronous Generator," in 2021 18th International Multi-Conference on Systems, Signals & Devices (SSD), (2021), Monastir, Tunisia.*

- ***M. A. Albasheri**, O. Bouchhida, and Y. Soufi, "Indirect Field Oriented Control of Three Phase Induction Motor using Fuzzy Logic controller", in 2021 First International Conference on Energy Transition and Security (ICETS), (2021), Adrar, Algeria.*

- ***M. A. Albasheri**, O. Bouchhida, Y. Soufi, A. Moualdia, and M. Mujammal, "Control And Power Management of DC Microgrid Based Wind/Battery/Supercapacitor," in 2022 IEEE 2nd International Maghreb Meeting of the Conference on Sciences and Techniques of Automatic Control and Computer Engineering (MI-STA), (2022), Sabratha, Libya.*

- ***M. A. Albasheri**, O. Bouchhida, Y. Soufi, A. Cherifi, A. Moualdia, and M. Mujammal, "Improve Lifespan of Battery Energy Storage in Remote Area Power System," in 2023 2nd International Conference on Electronics, Energy and Measurement (IC2EM), (2023), Medea, Algeria .*

Publication list

- *M. A. H. Mujammal, A. Moualdia, O. Bouchhida, and **M. A. Albasheri**, "Upgrade Perturbation and Observation of MPPT Strategy via Fuzzy Logic Controller," in 2023 2nd International Conference on Electronics, Energy and Measurement (IC2EM), (2023), Medea, Algeria.*

- ***M. A. Albasheri**, O. Bouchhida, Y. Soufi, and A. Cherifi, "Enhanced Vector Control of Induction Motor by Fuzzy Logic Controller," in 2024 2nd International Conference on Electrical Engineering and Automatic Control (ICEEAC), (2024), Setif, Algeria.*

- ***M. A. Albasheri**, O. Bouchhida, Y. Soufi, and A. Cherifi, "Energy Management of Wind Energy Hybrid Storage for Remote Area Power System," in 2024 12th International Conference on Smart Grid (icSmartGrid), (2024), Setubal, Portugal.*

- ***M. A. Albasheri**, Y. Soufi, O. Bouchhida, and A. Cherifi, "Control and Energy Management Based on Decoupling Frequency of DC Microgrid," in 2024 21st International Multi-Conference on Systems, Signals & Devices (SSD), (2024), Erbil, Iraq*

- *Hasan Mujammal, M.A., Moualdia, A., Wira, P., **M. A. Albasheri**, Cherifi, A. Novel Direct Power Control Based on Grid Voltage Modulated Technique Using Artificial Intelligence. 12. Eur. Conf. Ren. Energy Sys. (2024), Mallorca, Spain.*

- ***M. A. Albasheri**, Ouahid, B, Abderrezzak, C, Youcef, S, Hasan Mujammal, M.A., Abdelhafidh, M. "Energy Management technique of HESS based DC microgrid,". 12. Eur. Conf. Ren. Energy Sys. (2024), Mallorca, Spain*

- *M. A. H. Mujammal, A. Moualdia, S. Boulkhrachef, D. Boudana, P. Wira, and **M. A. Albasheri**, "Implementation of Smart MPPT Strategy based on Fuzzy Logic Controller for Stand-Alone PV System," IRE DAYS'2024 (2024), Algiers, Algeria.*

- ***M. A. Albasheri**, O. Bouchhida, Y. Soufi, and M. Mujammal, "Enhancing Solar System Performance with Fuzzy Logic-Based Maximum Power Point Tracking," International Conference on Renewable Energies and Power Systems 2024, (2024), Naama, Algeria.*

- ***M. A. Albasheri**, Y. Soufi, O. Bouchhida, and A. Cherifi, "Design, assessment and implementation of Fuzzy Logic for DC Voltage in Microgrid," in 22nd International Multi-Conference on Systems, Signals & Devices (SSD), (2025), Monastir, Tunisia*

Abstract:
This thesis investigates the integration of renewable energy sources within microgrid systems, addressing critical challenges in energy management, techno-economic analysis, and real-world implementation. As nations strive for sustainable and resilient energy solutions, microgrids present a transformative opportunity to enhance energy security and reduce carbon footprints. The research develops a comprehensive modeling framework that combines photovoltaic, wind, and energy storage systems, enabling a deeper understanding of their synergies and operational dynamics. Additionally, a detailed techno-economic analysis is conducted to evaluate lifecycle costs and economic viability, informing stakeholders of cost-effective configurations. The study also explores innovative energy management techniques, particularly through fuzzy logic and adaptive strategies, to optimize energy dispatch and ensure system reliability. Furthermore, the research validates the proposed methodologies through simulations and real-world case studies, bridging theoretical knowledge and practical applications. The findings contribute to the broader discourse on sustainable energy systems and provide a roadmap for future research and policy development.

Keywords: *Microgrid; Renewable energy sources (RES); Hybrid energy storage system (HESS); Energy Management Technique (EMT); Fuzzy logic (FL)*

Résumé :
Cette thèse de doctorat étudie l'intégration des sources d'énergie renouvelables dans les systèmes de microréseaux, en abordant les défis critiques en matière de gestion de l'énergie, d'analyse techno-économique et de mise en œuvre dans le monde réel. Alors que les nations s'efforcent de trouver des solutions énergétiques durables et résilientes, les microréseaux offrent une opportunité transformative pour améliorer la sécurité énergétique et réduire les empreintes carbones. La recherche développe un cadre de modélisation complet qui combine des systèmes photovoltaïques, éoliens et de stockage d'énergie, permettant une meilleure compréhension de leurs synergies et dynamiques opérationnelles. De plus, une analyse techno-économique détaillée est réalisée pour évaluer les coûts de cycle de vie et la viabilité économique, informant les parties prenantes des configurations rentables. L'étude explore également des techniques de gestion de l'énergie innovantes, notamment par le biais de la logique floue et de stratégies adaptatives, pour optimiser le dispatch énergétique et garantir la fiabilité du système. En outre, la recherche valide les méthodologies proposées à travers des simulations et des études de cas réelles, reliant ainsi les connaissances théoriques et les applications pratiques. Les résultats contribuent au discours plus large sur les systèmes énergétiques durables et fournissent une feuille de route pour les recherches futures et le développement des politiques.

Mots-clés: *Micro-réseau ; Sources d'énergie renouvelables (SER) ; Système de stockage d'énergie hybride (SSEH) ; Technique de gestion de l'énergie (TGE) ; Logique floue (FL)*

الملخص :

تستكشف هذه الأطروحة دمج مصادر الطاقة المتجددة ضمن نظم الشبكات الصغيرة، مع معالجة التحديات الأساسية في إدارة الطاقة، والتحليل الاقتصادي التقني، والتنفيذ في العالم الحقيقي. بينما تسعى الدول إلى تحقيق حلول طاقة مستدامة ومرنة، تمثل الشبكات الصغيرة فرصة تحويلية لتعزيز أمن الطاقة وتقليل البصمات الكربونية. تطور الدراسة إطارًا شاملًا للنمذجة يجمع بين الأنظمة الضوئية والطاقة الشمسية والرياح وأنظمة تخزين الطاقة، مما يمكن من فهم أعمق لتآزرها وديناميكياتها التشغيلية. بالإضافة إلى ذلك، يتم إجراء تحليل اقتصادي تقني مفصل لتقييم تكاليف دورة الحياة والجدوى الاقتصادية، مما يوفر معلومات للمعنيين حول التكوينات الفعالة من حيث التكلفة. كما تستكشف الدراسة تقنيات إدارة الطاقة المبتكرة، خاصة من خلال المنطق الضبابي والاستراتيجيات التكيفية، لتحسين توزيع الطاقة وضمان موثوقية النظام. علاوة على ذلك، تصادق الدراسة على المنهجيات المقترحة من خلال المحاكاة ودراسات الحالة الواقعية، مما يربط المعرفة النظرية بالتطبيقات العملية. تسهم النتائج في النقاش الأوسع حول أنظمة الطاقة المستدامة وتوفر خارطة طريق للبحث المستقبلي وتطوير السياسات.

الكلمات المفتاحية: *الشبكة الصغيرة؛ مصادر الطاقة المتجددة (RES)؛ نظام تخزين الطاقة الهجين (HESS)؛ تقنية إدارة الطاقة (EMT)؛ المنطق الضبابي (FL)*

Contents

Publication list IV
Abstract: VI
List of figures XI
List of tables XIII
List of Abbreviations XIV
List of Symbols XV
Generale Introduction 1
Chapter I: Overview of microgrid 6
I.1 Introduction 7
I.2 Concept of microgrids 7
I.2.1 Definition of microgrid 7
I.2.2 Microgrid components 8
I.2.3 Advantages of Microgrids 10
I.3 Classification of microgrids 11
I.3.1 Classifying based on control techniques 11
I.3.2 Classification of MG by size 14
I.3.3 Based on the structure 15
I.3.4 Categorizing MGs According to Source 19
I.3.5 Classification based the operation 20
I.3.6 Classification based applications 22
I.4 Challenges and issues of microgrid 24
I.4.1 Technical challenges in MGs 25
I.4.2 Protection 27
I.4.3 Economic challenges 28
I.4.4 Market challenges 28
I.4.5 Regulatory Challenges 29
I.5 Conclusion 29
Chapter II: Renewable energy and storage system 30
II.1 Introduction 31
II.2 An overall global outlook on renewable energy 31
II.3 Modeling of renewable energy source 32
II.3.1 Photovoltaic model 32

List of tables

II.3.2 Wind energy Model 33
II.3.3 Modelling of the DC-DC converter integrated with PV-Wind energy systems 34
II.3.4 MPPT for renewable energy sources 37
II.4 Energy storage system in microgrid 40
II.4.1 Battery 41
II.4.2 Supercapacitor 43
II.4.3 Energy storage system in microgrid 44
II.4.4 Converter Structures for HESS 46
II.5 Simulation results of renewable energy sources with energy storage 52
II.5.1 Wind energy with energy storage 52
II.5.2 Photovoltaic energy with energy storage 55
II.6 Conclusion 58
Chapter III: Techno-Economic analysis and optimization sizing of microgrid 59
III.1 Introduction 60
III.2 HOMER pro 60
III.2.1 Definition of HOMER 60
III.2.2 The functioning mechanism of HOMER 60
III.2.3 Addressing Issues with HOMER 61
III.3 Literature review 62
III.4 Materials and methods 63
III.4.1 Study locations, load profiles and meteorological data 64
III.4.2 System design 65
III.4.3 Model component systems 68
III.5 Economic assessment 70
III.5.1 The net present cost 70
III.5.2 The levelized cost of energy 71
III.5.3 Capacity shortage fraction 71
III.5.4 Salvage cost 71
III.5.5 Excess and unmet electricity fraction 72
III.5.6 Renewable fraction 72
III.5.7 Power balance constraint 73
III.6 Simulation results 74
III.7 Conclusion 86
Chapter IV: Energy management techniques of microgrid 87
IV.1 Introduction 88

List of tables

IV.2 Classification and comparative investigation of EMS 88
IV.3 Energy management-based frequency decoupling 94
IV.3.1 Convectional method 94
IV.3.2 Proposed energy management technique 96
IV.3.3 Analysis and design the voltage and currents controller 99
IV.3.4 Maximum Power Point Tracking (MPPT) 102
IV.3.5 Load Power Tracking (LPT) 103
IV.3.6 Load Power Shedding (LPS) 103
IV.4 Simulation results of different time constant of LPF 103
IV.5 Simulation results of RES and HESS based frequency decoupling 106
IV.5.1 One-day experimental test 107
IV.5.2 HESS SOC UPPER LIMIT SITUATION 108
IV.5.3 HESS SOC lower limit situation 109
IV.6 Energy management control based fuzzy logic 110
IV.6.1 Balanced power 111
IV.6.2 State of charge (SOC) of battery 112
IV.6.3 State of charge (SOC) of SC 112
IV.6.4 Battery signal 112
IV.6.5 SC signal 112
IV.6.6 Control mode 114
IV.6.7 Simulation results fuzzy logic based EMT 114
IV.7 Energy management based fuzzy logic improved 122
IV.7.1 LPT 125
IV.7.2 LPS 126
IV.8 Conclusion 127
Generale conclusion 129
Bibliography 132

List of tables

List of figures

Fig 1 : A schematic summary of the Methodology outlined. 4
Chapter I: Overview of microgrid
Fig I. 1: Structure of microgrid 8
Fig I. 2: Structure of microgrid 11
Fig I. 3: Control techniques of microgrid 12
Fig I. 4: Structure of AC microgrid 15
Fig I. 5: Structure of DC microgrid 17
Fig I. 6: Structure of hybrid microgrid 18
Fig I. 7: Structure of microgrid 22
Fig I. 8: Structure of microgrid 25
Chapter II: Renewable energy and storage system
Fig II. 1: Additions of renewable power capacity categorized by technology and sector 31
Fig II. 2: Electricity production by technology from 2000 to 2028 32
Fig II. 3: The PV electrical circuit 32
Fig II. 4: DC/DC boost converter 35
Fig II. 5: (a) closed switch mode, (b) open switch mode, (c) switch control signal 36
Fig II. 6: block schematic of the MPPT-using PI control 38
Fig II. 7: variation of insolation 38
Fig II. 8: Waveforms of power with P&O and proposed 39
Fig II. 9: The efficiency of P&O and proposed 39
Fig II. 10: Power and energy density of storage devices 40
Fig II. 11: Classification of energy storage system 41
Fig II. 12: Battery model 42
Fig II. 13: Model of SC 43
Fig II. 14: Bidirectional DC–DC converter charging/discharging equivalent circuit 44
Fig II. 15: Steady state HESS charging/discharging waveforms 45
Fig II. 16: Classification configuration of HESS 46
Fig II. 17: Different HESS topologies 48
Fig II. 18: Comparative of indicators for HESS designs 49
Fig II. 19: Compared battery life with and without supercapacitor 51
Fig II. 20: Total cost expended during the system's 20-year life 52
Fig II. 21: (a): wind speed profile, (b): power without SC, (c): power with SC, d): current of ESS, (e): DC-link voltage, (f): current of PMSG, (g) SOC of ESS (h): zoon out of SOC long time, and (i): comparison of DC link voltage 55
Fig II. 22: Power waveforms of battery alone and battery/SC 56
Fig II. 23: Current load in case of battery alone and battery/SC 56
Fig II. 24: Power balance and current of battery and SC in case of battery alone and battery/SC 56
Fig II. 25: SOC and energy storage consumption in case of battery alone and battery/SC 57
Fig II. 26: DC link voltage in case of battery alone and HESS 57
Fig II. 27: DC link voltage by response time and peak of variation load 58
Chapter III: Techno-Economic analysis and optimization sizing of microgrid
Fig III. 1:Structure of function mechanism of Homer 61
Fig III. 2:schematic summary of the technique outlined in the paper 63
Fig III. 3:The location of the region under investigation 64

List of tables

Fig III. 4:the monthly load profile.....65
Fig III. 5:the daily load profile.....65
Fig III. 6:Visual schematic of six designs.....66
Fig III. 7:Average monthly power production.....75
Fig III. 8: The output power spectrogram of the inverter.....76
Fig III. 9:The energy exchange.....77
Fig III. 10:The excess power, unmet demand load, and capacity shortage.....78
Fig III. 11: SOC of battery for 12 days.....79
Fig III. 12:Hourly SOC of battery.....80
Fig III. 13: The comparison results for all designs.....84
Fig III. 14: Cost distribution of the optimal designs.....85
Chapter IV: Energy management techniques of microgrid
Fig IV . 1: Classification of energy management technique.....91
Fig IV. 2: Low pass filter.....96
Fig IV. 3:Traditional energy management strategy.....96
Fig IV . 4:Power waveforms of HESS on transient zone.....98
Fig IV . 5:Operation zone of HESS.....98
Fig IV. 6:Energy management proposed.....99
Fig IV. 7:Block diagram of SC controller.....101
Fig IV. 8:Block diagram of SC controller.....102
Fig IV. 9:Flowchart of energy management proposed.....102
Fig IV. 10:power evaluations: τ =16s: 8s;4s;2s; 1s;0.4s;0.2s, (a;h).....104
Fig IV. 11:analytic currents energy storages with different time constants τ, (a): battery current, (b): SC current.....105
Fig IV. 12:State of charge of energy storage, (a): SOC of SC, (b): SOC of battery.....105
Fig IV. 13:DC link voltage.....106
Fig IV. 14: (A) irradiation and wind speed profile; (B) power evaluations; (C) Dc link voltage; (D) SOCHESS.....107
Fig IV. 15 :(A) irradiation and wind speed profile; (B) power evaluations; (C) Dc link voltage; (D) SOCHESS.....108
Fig IV. 16:(a) irradiation and wind speed profile; (b) power evaluations; (c) Dc link voltage; (d) SOCHESS.....109
Fig IV. 17:Proposed fuzzy logic energy management system.....111
Fig IV. 18: fuzzy inferential rules.....113
Fig IV. 19:Membership functions.....114
Fig IV. 20:Location Medea, Algeria.....115
Fig IV. 21:Weather data on the 4th June 2022 in Medea, Algeria.....116
Fig IV. 22:Power waveforms.....116
Fig IV . 23:State of charge of HESS.....117
Fig IV. 24:DC link Voltage.....117
Fig IV. 25:Voltage of PMSG.....117
Fig IV. 26:Power waveforms.....118
Fig IV. 27:State of charge of HESS.....119
Fig IV. 28:DC link Voltage.....119
Fig IV. 29:Power waveforms.....121
Fig IV. 30:State of charge of HESS.....121
Fig IV. 31:DC link Voltage.....121
Fig IV. 32:Energy management technique.....122

List of tables

Fig IV. 33:A power management based FLC block 123
Fig IV. 34:Inputs and outputs membership function: (a) P_{net} . (b) SOC_{batt}. (c) SOC_{SC}. (d). $Control_{batt}$ (e) $Control_{SC}$. 123
Fig IV. 35:Surface of relationship of inputs and outputs 124
Fig IV. 36: Operation zone of sub-controls 125
Fig IV. 37:(a) power evaluations; (b) SOC_{HESS}; (c) Current load;(d) DC link voltage 126
Fig IV. 38:(a) power evaluations; (b) SOCHESS; (c) Current load;(d) Dc link voltage 127

List of tables

Table I. 1: List of the benefits and drawbacks of the various MG generating options. 9
Table I. 2: Comparison of control technique of MG 14

Table III. 1: the optimally configured system from previous studies 67
Table III. 2: Technical data of the components used in MG 72
Table III. 3: Definitions of variables. 73
Table III. 4:Summary of the designed optimization results. 82

Table IV. 1: classification of energy management technique 92
Table IV. 2: Comparison of consumption of energy storage 106
Table IV. 3: System parameters description. 115
Table IV. 4: Operating modes with HESS almost empty 119
Table IV. 5: Operating modes with HESS almost fully 120

List of Abbreviations

AC	Alternating Current	NPC	Net Present Cost
CESs	Conventional energy sources	O&M	Operation & Maintenance
DC	Direct Current	P	Power (W)
DCMG	Direct current microgrid	P&O	Perturb and Observe
DG	Diesel Generator	PMS	Power Management Strategy
E	Irradiance (w/m²)	PI	Proportional Integral Controller
ESS	Energy storage system	PI	Proportional Integration
FCL	Fuzzy logic control	PV	Photovoltaic
FC	Fuel Cell	PWM	Pulse Width Modulation
FIS	Fuzzy Inference System	RF	Renewable Energy Fraction
HESS	Hybrid energy storage system	RES	Renewable Energy Sources
HOMER	Hybrid Optimization of Multiple Energy Resources	RES	Renewable Energy Sources
HRES	Hybrid Renewable Energy Source	SC	Supercapacitor
LCC	Life Cycle Cost	SOC	State of Charge
LCOE	Levelized Cost of Energy	SW	Converter Switch
LPS	Load Power Shedding	TSR	Tip-speed Ratio
LPF	Low-pass Filter	T	Temperature (°C)
MG	Microgrid	WT	Wind Turbine
MPPT	Maximum Power Point Tracking		

List of Symbols

I_{pv}	Photovoltaic current	I_{DC}	Load current (A)
L_{PV}, L_W	Converter inductance of the PV and wind (H)	L_b	DC-DC converter inductance of the battery (H)
V_{pv}	Photovoltaic voltage	R_L	Resistance of the load (Ω)
p	Air density	$V_{SC}Rated$	Rated voltage of the SC
V_w	Wind speed (w/m)	E_{SC}	SC energy storage capacity
λ	Tip speed ratio	$K_{P_{SC}}, K_{I_{SC}}$	Proportional and integral gains of the SC PI controller
Q	The battery capacity (Ah),	K_{P_B}, K_{I_B}	Proportional and integral gains of the battery PI controller
v_B	Battery voltage	$K_{P_{DC}}, K_{I_{DC}}$	Proportional and integral gains of the DC link PI controller
v_{SC}	SC voltage	I_{ds}, I_{qs}	Direct and quadratic stator currents(A)
L_{SC}, L_B	DC-DC converter inductance of the SC and battery (H)	V_{ds}, V_{qs}	Direct and quadratic stator voltages (V)
N_S, N_P	The cells in series, and parallel	V_{DC}	DC link voltage
SOC_{SC}	State of charge of SC (%)	η_{DG}	The electrical efficiency of the DG system
SOC_b	State of charge of battery (%)	T_{project}	The project lifespan in years
SOC_{Max}	State of charge maximum (%)	E_{load}	The total electrical load served
SOC_{Min}	State of charge minimum (%)	CRF	The capital recovery factor
SOC_{HESS}	State of charge of HESS (%)	E_{gen}	The total electrical generated
B	Exponential zone time constant inverse (Ah^{-1})	E_{excess}	The excess electricity
I_w	Wind current (A)	E_{Unmet}	The unmet load
C_{DC}	DC bus capacitor (F)		

General Introduction

Background and Context

Microgrids represent a transformative approach in the field of energy systems, particularly as nations strive to reduce carbon footprints and enhance energy security. With the increasing demand for sustainable and resilient energy solutions, the integration of distributed energy resources (DERs) has gained prominence. Microgrids can operate independently or in conjunction with the main grid, offering a flexible and efficient means to manage energy production and consumption at a local level. They facilitate the integration of renewable energy sources, such as solar and wind, while also providing opportunities for energy storage, demand response, and innovative energy management strategies.

The significance of this research lies in its potential to address several critical challenges within the microgrid domain. The exploration of microgrid concepts, renewable energy integration, techno-economic analysis, and energy management techniques is essential for realizing the full potential of microgrids. Technological innovation is a key focus, as investigating advanced modeling techniques for renewable energy sources and energy storage systems contributes to the development of more efficient and reliable microgrid configurations. Additionally, the techno-economic analysis emphasizes the importance of optimizing system design and operational strategies to ensure that microgrids are not only technically feasible but also economically sustainable.

In an era of increasing climate uncertainties and energy supply disruptions, the ability to manage energy resources effectively through innovative management techniques is paramount. This research aims to provide insights into energy management strategies that enhance reliability and performance. Furthermore, the findings can inform policymakers and stakeholders in the energy sector about the benefits and challenges associated with microgrid deployment, paving the way for supportive regulations and incentives. By addressing these areas, this dissertation seeks to contribute to the broader discourse on sustainable energy systems, providing a roadmap for future research and practical applications in microgrid technology.

Research Problem Statement

Integration of Renewable Energy Sources: While significant advancements have been made in the deployment of renewable energy technologies, there is still a lack of comprehensive models that accurately simulate the performance of these systems in microgrid configurations. Current literature often focuses on individual technologies (e.g., photovoltaic or wind) without adequately addressing their integration and interaction within a microgrid context. This research seeks to fill this gap by developing a holistic modeling approach that combines photovoltaic, wind, and energy

storage systems, enabling a better understanding of their synergies and operational dynamics [1],[2],[3],[4],[5].

Techno-Economic Analysis: Existing studies frequently overlook the economic implications of microgrid design and operation. Many analyses fail to incorporate a full range of economic factors, including lifecycle costs, maintenance, and the impact of varying energy prices. This research aims to provide a detailed techno-economic analysis using advanced optimization techniques, thereby offering insights into cost-effective microgrid configurations that can inform decision-making for stakeholders [6],[7],[8],[9],[5].

Energy Management Techniques: While there are various energy management systems (EMS) developed for microgrids, there is a notable absence of comparative studies that evaluate their effectiveness across different scenarios and configurations. The need for robust and adaptive energy management strategies is critical, particularly given the variability of renewable energy sources. This research will explore innovative EMS based on fuzzy logic and other adaptive techniques, addressing the gap in understanding how these approaches can optimize energy dispatch and improve reliability under varying operational conditions [10],[11].

Real-World Implementation and Testing: Many theoretical models and strategies lack validation through real-world case studies. This research intends to bridge this gap by not only modeling microgrid systems but also conducting simulations to validate the proposed methodologies. This approach will contribute empirical data to the current body of knowledge, facilitating a better understanding of practical challenges and solutions in microgrid implementation [12].

Knowledge Gaps Addressed

Integration of Renewable Energy Sources: While significant advancements have been made in the deployment of renewable energy technologies, there is still a lack of comprehensive models that accurately simulate the performance of these systems in microgrid configurations. Current literature often focuses on individual technologies (e.g., photovoltaic or wind) without adequately addressing their integration and interaction within a microgrid context. This research seeks to fill this gap by developing a holistic modeling approach that combines photovoltaic, wind, and energy storage systems, enabling a better understanding of their synergies and operational dynamics.

Techno-Economic Analysis: Existing studies frequently overlook the economic implications of microgrid design and operation. Many analyses fail to incorporate a full range of economic factors, including lifecycle costs, maintenance, and the impact of varying energy prices. This research aims to provide a detailed techno-economic analysis using advanced optimization techniques, thereby offering insights into cost-effective microgrid configurations that can inform decision-making for stakeholders.

Energy Management Techniques: While there are various energy management systems (EMS) developed for microgrids, there is a notable absence of comparative studies that evaluate their

effectiveness across different scenarios and configurations. The need for robust and adaptive energy management strategies is critical, particularly given the variability of renewable energy sources. This research will explore innovative EMS based on fuzzy logic and other adaptive techniques, addressing the gap in understanding how these approaches can optimize energy dispatch and improve reliability under varying operational conditions.

The Main Objectives

The primary objective of this thesis is to enhance the understanding and operational efficiency of microgrid systems through the integration of advanced modeling techniques, renewable energy sources, and innovative energy management strategies. To achieve this overarching goal, the research will focus on the following specific objectives:

1. Develop Comprehensive Modeling Frameworks: Create a holistic modeling approach that accurately simulates the performance of integrated renewable energy sources, including photovoltaic and wind systems, along with energy storage solutions. This framework will enable detailed analysis of system interactions and performance under varying conditions.

2. Conduct Techno-Economic Assessments: Perform a thorough techno-economic analysis of microgrid configurations, evaluating the lifecycle costs, operational efficiencies, and economic viability of different designs. This assessment will provide valuable insights into cost-effective solutions for stakeholders.

3. Explore Innovative Energy Management Techniques: Investigate and develop advanced energy management strategies based on fuzzy logic and other adaptive methods. These strategies will aim to optimize the dispatch of renewable energy while ensuring reliability and resilience in microgrid operations.

4. Validate Models through Simulation: Implement simulations to validate the proposed modeling and management strategies. This objective will bridge the gap between theoretical research and practical applications, providing empirical data to support the findings.

Significance and Potential Impact

The significance of this thesis lies in its potential to advance the field of microgrid technology, addressing critical challenges in renewable energy integration and energy management. By developing comprehensive models and innovative solutions, this work aims to contribute to:

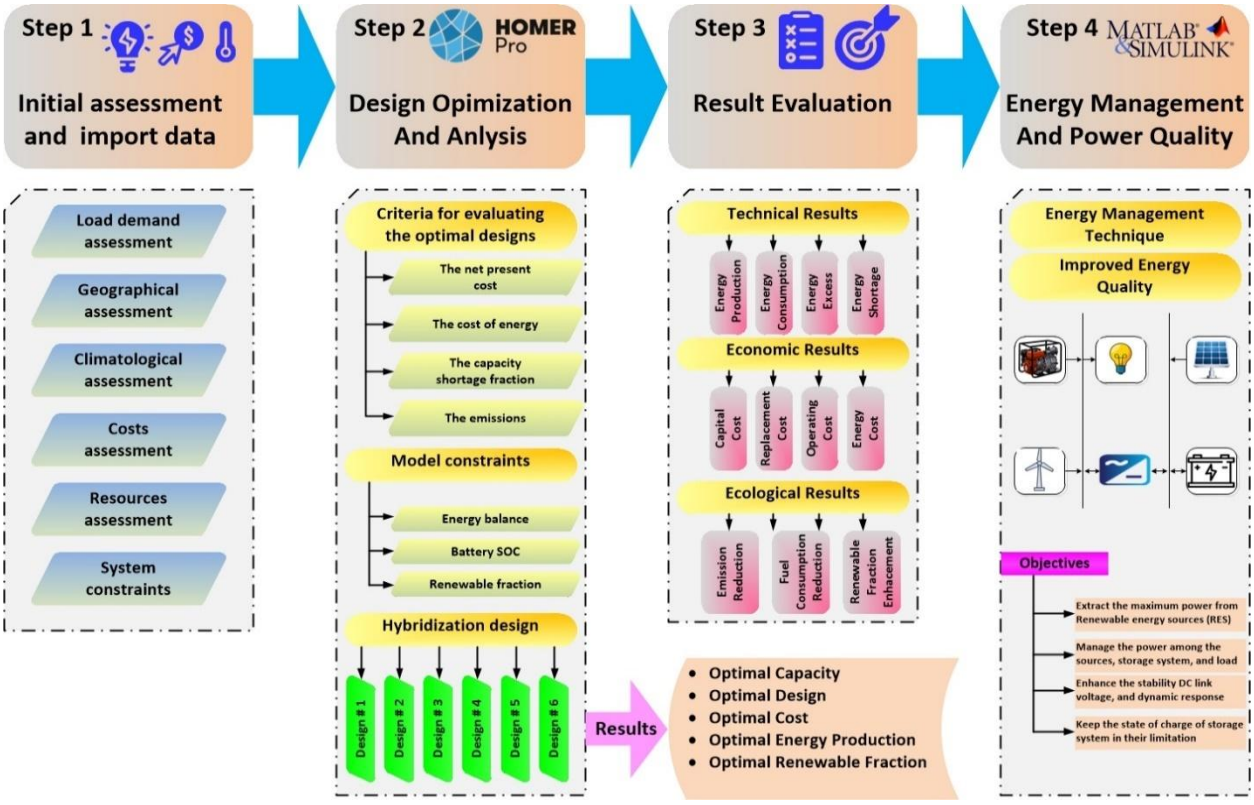
1. Enhanced Energy Resilience: Improved microgrid systems will provide communities with reliable and sustainable energy solutions, particularly in the face of climate change and energy supply disruptions.

2. Economic Benefits: By identifying cost-effective microgrid configurations, this research can help stakeholders optimize their investments and operational strategies, leading to more sustainable energy practices.
3. Policy Guidance: The findings can inform policymakers and industry leaders about the benefits and challenges of microgrid deployment, fostering supportive regulations that encourage the adoption of renewable energy technologies.
4. Academic Contribution: This research will fill critical gaps in the current knowledge base, providing a foundation for future studies in microgrid technology and energy management.

Methodology Overview

This research will employ a multi-faceted methodological approach that integrates both quantitative and qualitative techniques to thoroughly investigate the operational efficiency and economic viability of microgrid systems. The primary research methods include:

1. Modeling and Simulation: A comprehensive modeling framework will be developed using software tools such as HOMER Pro and MATLAB/Simulink. This framework will simulate the performance of integrated renewable energy sources (photovoltaic and wind) and energy storage systems under various scenarios. The models will incorporate real-time data, load profiles, and meteorological conditions to accurately reflect operational dynamics.



2.

Fig 1 : *A schematic summary of the Methodology outlined.*

3. Techno-Economic Analysis: A detailed techno-economic analysis will be conducted to evaluate the lifecycle costs, net present value, and levelized cost of energy for different microgrid configurations. This analysis will utilize financial modeling techniques to assess capital, operational, and maintenance costs, helping to identify the most economically viable solutions.
4. Energy Management Strategy Development: Innovative energy management strategies, including fuzzy logic control and adaptive algorithms, will be developed and tested. These strategies will focus on optimizing energy dispatch, load balancing, and integration of renewable resources while maintaining system reliability.
5. Case Studies and Real-World Validation: The research will include case studies of existing microgrid implementations to validate the proposed models and energy management techniques. Simulation results will be compared with real-world data to assess the accuracy and applicability of the developed methodologies.

Thesis Structure

This thesis is structured into four main chapters, each addressing critical aspects of microgrid technology and the integration of renewable energy. Chapter 1, introduces the concept of microgrids, detailing their components, classifications, and advantages, such as increased resilience and sustainability.

It also examines the challenges involved in implementing microgrid systems. Chapter 2, focuses on integrating renewable energy sources and energy storage within microgrids. It presents modeling techniques for photovoltaic and wind systems, discusses various energy storage technologies, and includes simulation results that demonstrate their performance. Chapter 3, delves into the techno-economic aspects of microgrid design, emphasizing the importance of techno-economic assessments, the application of HOMER software, and evaluating economic metrics like net present cost and levelized cost of energy, leading to significant insights from the analysis. Chapter 4, explores various energy management strategies, including fuzzy logic and adaptive methods, assessing their effectiveness in optimizing energy dispatch and reliability through simulation results. Finally, Conclusion and Future Work summarizes the research findings, discusses their implications for practice and policy, and outlines potential directions for future research. This structure provides a comprehensive examination of microgrid systems and their potential to enhance energy resilience and sustainability.

Chapter I
Overview of microgrid

I.1 Introduction

In recent years, the increasing demand for sustainable energy solutions has prompted significant interest in the concept of microgrids. Microgrids represent a transformative approach to energy generation and distribution, enabling localized control over energy resources while enhancing resilience and reliability. This chapter aims to provide a comprehensive overview of microgrids, beginning with a clear definition of the concept and its fundamental components. Following this, the classification of microgrids based on various criteria, including their operational modes and technological frameworks. Understanding these classifications is essential for identifying the unique challenges and issues that microgrids face, such as integration with existing energy systems, regulatory obstacles, and technological limitations. By exploring these elements, this chapter sets the stage for a deeper examination of microgrid systems and their potential to revolutionise energy management in the context of global sustainability efforts.

I.2 Concept of microgrids

I.2.1 Definition of microgrid

The integration of renewable energy sources (RESs) into conventional electric power systems is leading to a fast transformation. This transformation is characterized by the rising penetration of RESs, which in turn leads to more efficient and environmentally friendly energy production. However, this integration also necessitates the implementation of enhanced control and management functions. Microgrids play a crucial role in the evolution of the distribution level. Since 2004, the concept of MG has been defined as a systematic strategy to harness the potential of distributed generation by considering generation and related loads as a subsystem. Since then, there have been notable advancements and developments[13]. The MG idea was initially developed by the United States' Consortium for Electric Reliability Technology Solutions (CERTS) to efficiently decrease costs and improve power quality worldwide [14]. The U.S. Department of Energy (DOE) Microgrid Exchange Group (MEG) has utilized numerous definitions, including the following [15]. A microgrid is a set of linked loads and distributed energy resources inside defined electrical limits that function as a single controlled unit. The MG is a versatile and controllable system that can operate in either grid-connected or stand-alone modes. It has the ability to decrease the reliance of its users on conventional power generating systems by offering various forms of energy, including electricity and heat, as well as facilitating the trade of auxiliary services[16].

The Consortium for Electric Reliability Technology Solutions (CERTS) and the microgrids programme commenced systematic research and development initiatives throughout the United States and Europe. CERTS, established in 1999 is recognised as the pioneer of the contemporary grid-connected microgrid concept [17]. The CERTS MG was proposed as a potential remedy for the challenges related to the integration of Distributed Energy Resources (DERs) into the electricity system [18],[19]. The primary emphasis was on automated and seamless islands and

grid reconnection, together with passive control techniques [20]. The CERTS MG concept is further evaluated in both experimental test beds and actual microgrid projects [21],[22],[23]. The primary motivation of CERTS was the enhancement of dependability via the integration of renewable sources, rather than the mitigation of emissions of greenhouse gases. The European Union microgrids project investigated analogous technological difficulties, including energy management, secure islanding and reconnection techniques, protective equipment, control methods for both islanded and connected situations, and communication protocols [24]. All the concerns identified in the first studies continue to get significant attention [25].

I.2.2 Microgrid components

Microgrids are intricate systems that consist of a wide variety of linked components. Fig I.1 depicts a schematic representation of a representative microgrid designed for providing electricity to residential areas in remote locations. The home microgrid is linked to a variety of generating and storage components, allowing it to function in a connection mode via the point of common coupling. The microgrid has the capability to engage in energy exchange with the major grid. Comprehending the frequently used power production technologies and their potential uses is essential for assessing a prospective microgrid operation. Table 1 highlights the alternatives for MG generation together with their respective pros and downsides.

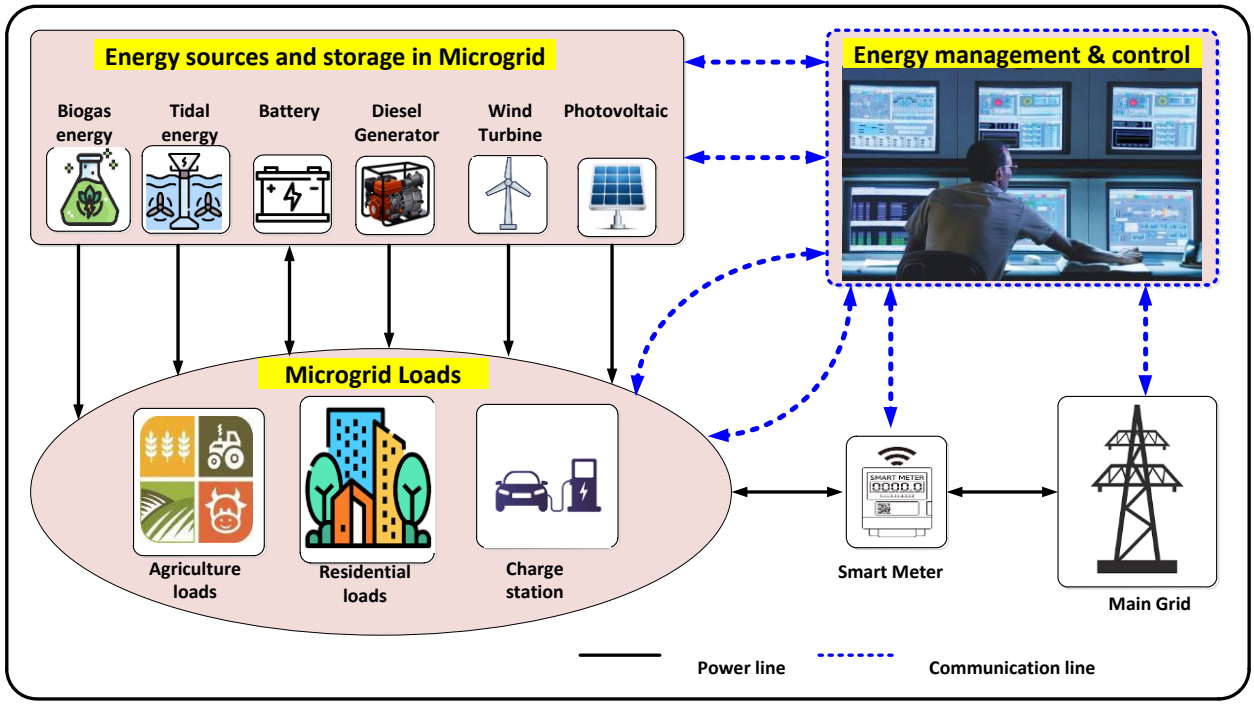


***Fig I. 1**: Structure of microgrid*

- Productions: The MG producing system may include several renewable and non-renewable production sources. A variety of non-renewable generating sources exist, including natural

gas generators, biogas generators, and combined heat and power (CHP) systems. Renewables generation includes sources such as solar, wind, hydro, and biofuels [26],[27].

- The Energy Storage System (ESS): energy storage devices serve several tasks in Microgrids (MGs), including maintaining power quality, peak load reduction, frequency management, stabilising the output of Renewable Energy Sources (RESs), and supplying backup power for the system. ESS is also crucial to the optimisation of MG costs [28].
- Loads: Microgrids (MGs) exhibit two primary categories of loads: (i) essential loads that must be met under all circumstances, and (ii) deferrable loads that may be modified for load balancing within the MG, hence optimising economic power output [23].
- Point of Common Coupling: The Point of Common Coupling (PCC) serves as a vital element, functioning as the physical interface between the microgrid (MG) and the main grid. It functions as the interface for the exchange of electrical energy between the microgrid and the broader power system. The PCC integrates diverse equipment and systems to provide connection, power exchange, control, and safety between the microgrid and the utility grid. This involves elements such as circuit breakers, protection relays, and synchronisation apparatus. The isolated MG lacks PCC [29],[30].

Table I. 1: List of the benefits and drawbacks of the various MG generating options.

Elements	Advantages	Disadvantages
Solar energy [31],[32]	• Reduced maintenance expenses • Varied uses • Mitigates carbon emissions	• Dependence on sun • Initial capital • Expenditure Necessitates • Energy storage systems • Necessitates an inverter
Wind energy [33]	• Location-independent • Minimises carbon impact • Low manufacturing expenses	Dependent on wind velocity Visual and auditory pollution
Battery storage [34],[35]	• Carbon neutrality in savings • Retrofit capability • Rate optimisation and management • Immediate power accessibility	• Spatial limitations • Battery longevity • Restricted energy storage
Diesel generator [36],[37]	• Fast start-up • High load acceptance dispatchability • 20% low-load operating • Fuel storage • Excellent transient response	• High fuel prices • High emissions
Gas generator [38],[39]	• Improved fuel economy • Low pollution • (CHP) solution • Capable of part-load operating at 35%	• Prolonged start-up • Time and restricted transient responsiveness Expensive fuel reserve Recently, gasoline prices have surged considerably
Biogas [40],[41]	• Economical fuel source • Mitigates land and water emissions • Byproduct as fertiliser	• Integration expenses • Fuel treatment and filtration • Necessitates appropriate biomass

Fuel cell [42],[43],[44]	• Minimal Carbon • Remarkably silent • Beneficial for Combined Heat and Power applications.	• Hydrogen extraction incurs high costs • Significant infrastructure investment is necessary for hydrogen

I.2.3 Advantages of Microgrids

- Market stability: Investments in the grid helps mitigate risk. It serves as a safeguard against unpredictable and possibly costly contingency or emergency energy costs. It furthermore provides safeguarding against variable electricity expenses [45].
- Economic advantage: According to regional market regulations and policies, MGs may reduce peak load pricing, participate in demand response (DR) financial markets, and offer frequency management services to the broader grid. They may generate revenue by reducing peak load expenses, participating in demand response markets, and providing frequency control services to the grid [46].
- Uninterrupted supply: Although the electrical infrastructure in several modern nations is generally reliable, any disruption may be expensive and hazardous. Extreme weather, aging, physical assaults, and cyberattacks are increasingly threatening the nation's energy system today [47]. Functioning in island mode may guarantee a continuous electrical supply by detaching from the main grid and using on-site generation [48].
- Renewable integration: Renewable Energy Sources (RESs) play a crucial role in meeting global energy needs. The current global energy crisis has created unprecedented momentum for renewable energy sources. The predicted growth of renewable capacity over the next five years is expected to exceed prior projections. The IEA forecasts that renewable energy will increase by around 2400 GW from 2022 to 2027. This signifies an 85% acceleration relative to the increase seen in the preceding five years. The projected increase is over 30% more than the previous year's prediction, representing the most significant upward adjustment to date. Consequently, MGs are gaining significance for harnessing the advantages of RESs [49].
- Enhanced dependability and resilience: The ability of microgrids to operate in isolation enables them to maintain power delivery to consumers during a power outage. The capability to island is also crucial for isolating errors by segregating distribution feeds [50].
- Enhance power quality: Equipment may need a greater electrical supply than the electric system can provide. Implementing an MG enables enhanced control over its characteristics, which is crucial for sensitive equipment in healthcare, advanced manufacturing, laboratories, and other institutions [51].
- The relationship of microgrids (MGs) to the utility grid: MGs serve as fundamental components of smart grids. In other words, future utility grids may consist of a network of linked microgrids that regulate energy demand and supply at both micro and macro levels.

- Grid support: Microgrids mitigate grid congestion and peak demand. They also provide other grid services, including energy, capacity, and ancillary services [52].

I.3 Classification of microgrids

An extensive literature review was performed to examine the main architectures and designs of existing MGs in order to provide guidance to designers in selecting inherently safe and resilient design solutions. MGs may be classified into many categories based on their uses, their infrastructure, and the specific needs of end-users [10], (as seen in Fig I.2).

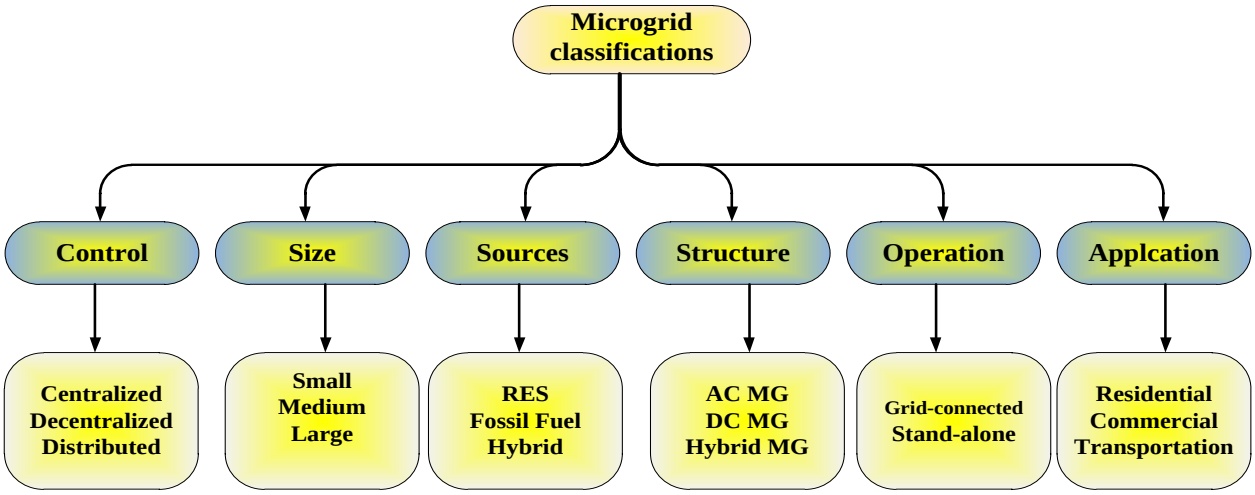


***Fig I. 2**: Structure of microgrid*

I.3.1 Classifying based on control techniques

Control techniques classify MG systems into three main categories as shown in Fig I.3 [53].

I.3.1.1 Centralized Control Methods

To implement centralized control in microgrids (MGs), a central controller (MGCC) system and a digital network of communications connect the controller with energy sources and loads, as illustrated in Fig I.3. The MG central controller (MGCC) collects data from the distributed generation (DG) units and transmits command signals to each unit for centralized control methods. Small-scale Distributed Cooperative Microgrid Generators (DCMGs) may be directly regulated by master-slave control schemes[54],[55]. For larger-scale microgrids, hierarchical control is preferred because to its autonomy and reliability [56],[57]. The local converter control serves as

the fundamental control level inside the hierarchical control structure. Secondary and tertiary

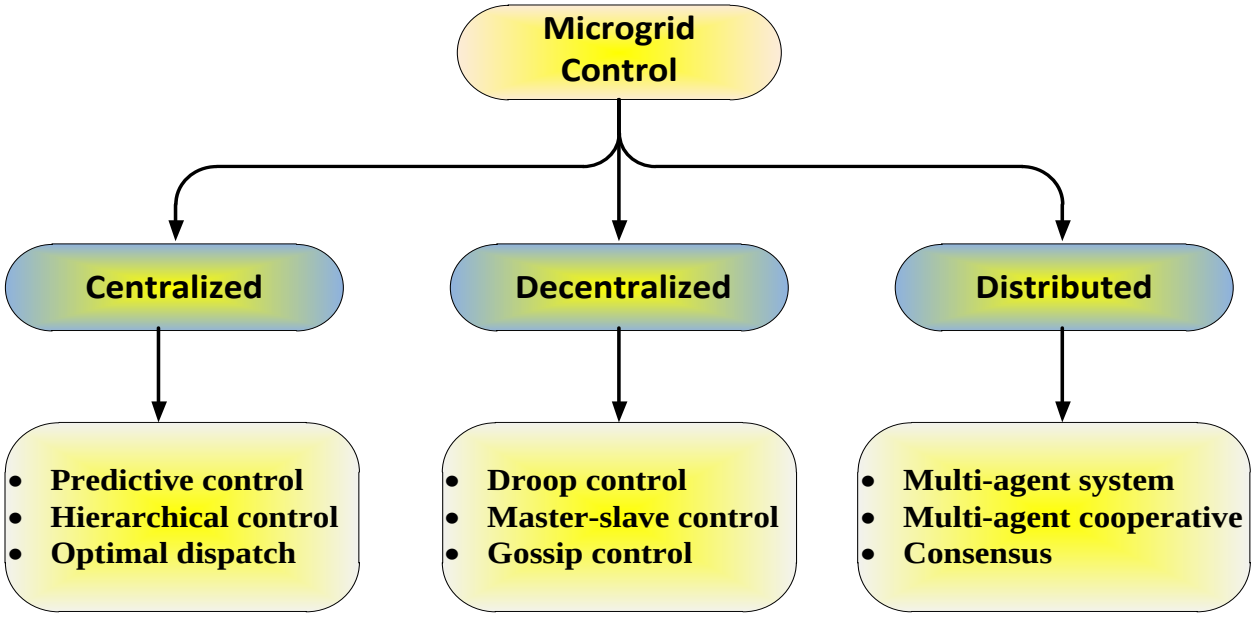


***Fig I. 3**: Control techniques of microgrid*

control levels govern DC voltage, manage power flow, and oversee grid-interactive control goals, including unit commitment and global optimization, which are coordinated functions. The hierarchical control structure has been established as one of the most effective control systems [58]. The structure has elementary, secondary, and tertiary levels [59]. The principal control mechanism is decentralized control, including voltage and current regulation loops, distributed generation maximum power point tracking (MPPT) control, and state of charge estimate for each storage unit. It exhibits a rapid dynamic response to real-time control [60]. Secondary control pertains to voltage regulation and enhancement of load-sharing efficiency. It pertains to regulating the DC bus voltage [61],[62]. The tertiary control level is capable of scheduling responses, forecasting distributed generation output, assessing power quality, and optimizing overall performance. All of these responsibilities are facilitated by the energy management approach executed at the MGCC level [63]. This approach has many drawbacks associated with the decentralized architecture, such as single-point failure, reduced battery longevity, and limited scalability [64].

I.3.1.2 Decentralized Control Methods

Each distributed generation unit autonomously produces its control signal in decentralized control methods. The most prevalent decentralized control systems are droop control, power line signaling (PLS), and distributed DC bus signaling (DBS) [65]. Recently, the decentralized administration of microgrids has concentrated on using blockchain or other distributed ledgers to enable peer-to-peer transactions among prosumers or energy assets[66] . In these methodologies, the blockchain will maintain immutable energy transactions derived from digitally signed energy-

related data collected by intelligent equipment situated at the prosumers' locations. At the microgrid level, a blockchain network is built, whereby the prosumer, as a network participant, sustains the blockchain and gets alerts from peer nodes upon the generation of new energy transactions. Prosumers may engage in energy trading to enhance their profitability or support microgrid goals, including demand-supply equilibrium, minimizing reliance on the main grid, and augmenting local renewable energy use. In these instances, smart contracts execute the control logic. Demand response systems may similarly be executed in microgrids via blockchain overlays. Intelligent contracts will oversee the demand response process for accuracy, adherence, and regulation in accordance with established criteria. These may encode, execute, and enforce arbitrary agreements between entities, whether human or machine, offering a transparent, verifiable, and secure framework for, for example, responding to demand signals and trading energy flexibility. The droop control method is the most used approach. Determining the droop parameters is challenging, since current sharing, precision, and system stability are contingent upon these factors [67]. Furthermore, without adequate communication, complete management is unattainable. These control systems have several advantages, including simplicity and independence from digital communication technology; but, the lack of input from other units automatically limits their efficacy. Moreover, given that the effectiveness and reliability of these methods are always dependent on the interpretation of the voltage on the common DC bus, the accuracy of voltage sensors is essential [68].

I.3.1.3 Distributed Control Methods

Distributed control is a methodology whereby there is no central controller, and local controllers (LCs) only communicate with one another. Distributed control techniques may execute functions similar to centralized systems using digital communication. They gather and evaluate data employing consensus-based methods or direct methods, enhancing reliability by removing any single point of failure [69]. The distributed control method may efficiently manage voltage variations while achieving tertiary objectives such as load sharing or economic dispatch [70]. Distributed control offers a degree of information awareness comparable to that of centralized control. This facilitates the attainment of objectives like output current sharing, autonomous voltage restoration, power distribution, enhancement of global efficiency, and status of charge (SoC) balancing [71]. A key advantage of this technology is that it enables the system to maintain full performance despite the failure of specific communication lines, provided the communication system remains intact. Distributed control is, thus, resistant to solitary sources of failure [72]. Nonetheless, its principal disadvantage is in the complexity of its analytical assessment of performance, especially under nonideal conditions [73]. Furthermore, comprehensive mathematical analysis remains challenging, especially under nonideal circumstances such as communication delays, measurement noise, and insufficient electrical control systems. Consequently, this form is unattainable for large-scale microgrids [74].

Table 2 delineates a comparison of centralized, decentralized, and distributed microgrid control systems.

***Table I. 2**: Comparison of control technique of MG*

Metric	Centralized	Decentralized	Distributed
Quantity of users	Single	Multiple	Multiple
Optimization	✓✓✓	✓	✓✓
Flexibility	✓	✓✓✓	✓
Communication	✓✓✓	✓	✓✓✓
Cost	✓✓✓	✓	✓✓
System failure	✓✓	×	××
Data acquisition	From all components	Local data	Local and neighboring data

I.3.2 Classification of MG by size

Microgrids may be classified into three categories based on their size: small, medium, and large-scale microgrids [75].

I.3.2.1 Small Scale Microgrid

Small-scale microgrids produce low-capacity power from renewable energy sources. Nevertheless, some MGs may use diesel engine sets as a source of electricity in conjunction with or in lieu of renewable energy sources (RESs). A small-scale microgrid may have a generating capacity of up to 10 MW [76]. Small-scale microgrids may provide electricity to residential structures, small regional power systems, islands, and isolated places [77].

I.3.2.2 Medium-Scale Microgrid

Medium-scale microgrids provide power of moderate capacity from renewable energy sources, oil, or coal. The generating capacity for a medium-scale microgrid may exceed 10 MW and approach 100 MW. This sort of MG has the ability of servicing industrial zone applications [78].

I.3.2.3 Larg Microgrid

Large-scale microgrids produce high-capacity power using oil or coal. The generating capacity of a large-scale microgrid may exceed 100 MW. This sort of MG has the capability of supplying industrial zone site applications [79].

I.3.3 Based on the structure

The microgrid is categorized based on its power type as an AC MG, a DC MG, and a hybrid MG [80].

I.3.3.1 AC Microgrid

In AC microgrids, the primary components that need synchronization are active power, reactive power, unbalanced components, and harmonics. In DC microgrids, the primary element requiring regulation is DC electricity. Consequently, the control mechanism of a DC microgrid is less complex than that of an AC microgrid [81]. The architecture of the AC microgrid is shown in Fig I.4. Prior to the connections, DC-AC inverters are used to convert the direct current (DC) electricity supplied by photovoltaic (PV) systems into alternating current (AC). Rectifiers convert AC power into DC electricity to provide DC loads. AC load gets straight supply from the AC bus without any transformation. The converters provide the connectivity between the wind power generating system and the AC bus for the management of active and reactive power. Interconnection with the main grid is simplified since it requires simply phase alignment between the main grid and the AC microgrid [82].

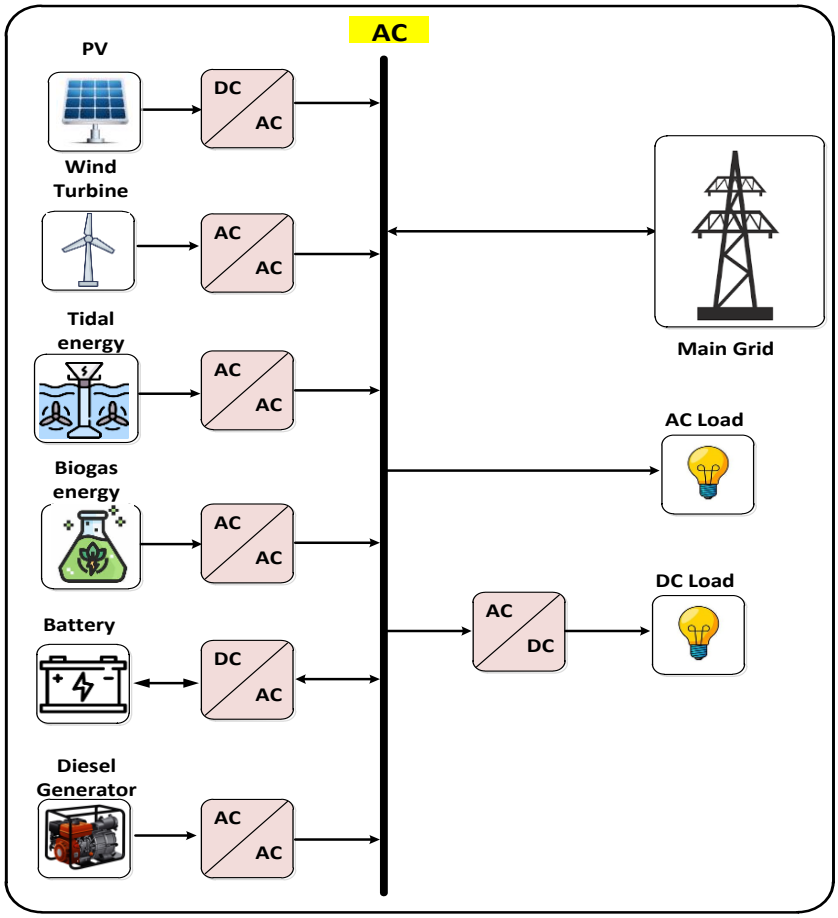


***Fig I. 4**: Structure of AC microgrid*

I.3.3.1.1 Advantages of AC Microgrid

1. The notable benefit of an AC microgrid is the use of a highly efficient transformer. The transformer enables the voltage of AC microgrids to be increased or decreased for distribution purposes and for local loads next to the microgrid, respectively.
2. Due to frequent zero voltage crossings, protection solutions for AC circuits are beneficial since circuit breakers interrupt fault current arcs at these zero crossings.
3. Independent regulation of reactive power enables the attainment of steady voltage.
4. In grid-tied mode, the AC microgrid will disconnect itself upon the occurrence of any fault situation. AC loads get direct power from the AC microgrid and are unaffected by interruptions occurring in the main grid [83].

I.3.3.1.2 Disadvantages of AC Microgrid

1. AC electricity must be converted for use with DC loads, including battery charging, PCs, and DC fluorescent lighting. Consequently, efficiency diminishes as a result of these transformations.
2. The use of power electronic converters generates harmonics in the primary grid.
3. The interconnection of DC renewable sources is complex, since the DC output from these sources must be transformed to AC via inverters [84].

I.3.3.2 DC Microgrid

The DC link may be directly connected to various DC loads without any conversion, hence reducing the cost of power electronics converters and enhancing efficiency [85].

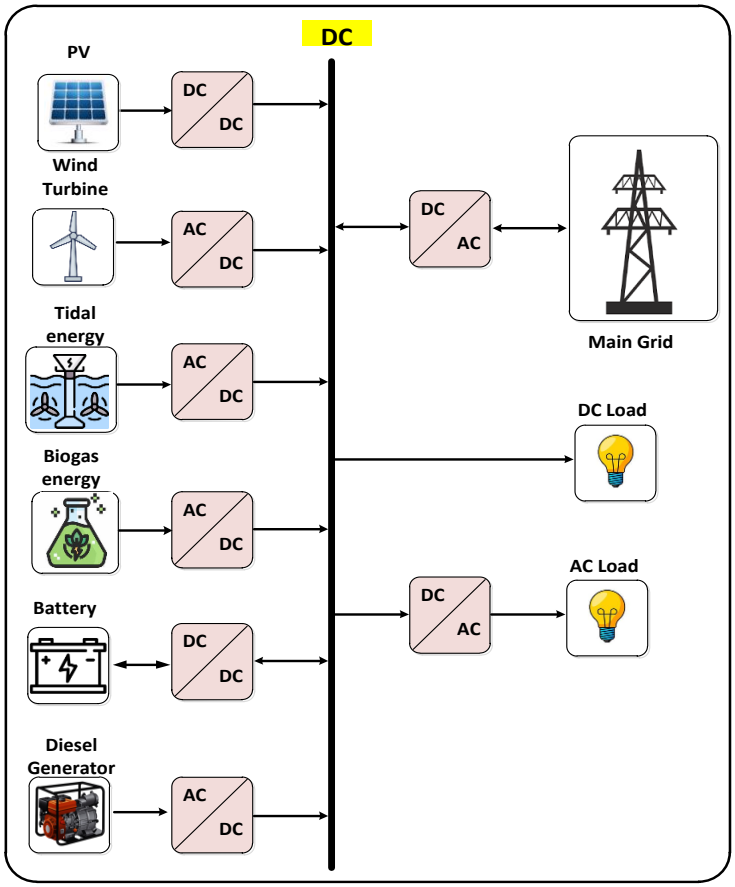


***Fig I. 5**: Structure of DC microgrid*

The advancement of DC RES is propelling study in the domain of DC microgrids. The architecture of the DC microgrid is illustrated in Fig I.5.

I.3.3.2.1 Advantages of DC Microgrid

1. A battery storage system may be immediately integrated to provide backup power. The backup storage system will provide electricity during high demand periods or in the lack of any distributed engine.
2. Direct connecting minimizes power conversions and enhances system efficiency.
3. Facilitated connectivity of renewable energy sources [86].
4. Battery storage in a DC microgrid will consistently provide electricity to the load throughout any disruptions in the AC main grid.
5. The power converter loss and operational costs of the DC system may be reduced, since just a basic inverter unit linked to the AC main grid is necessary.

I.3.3.2.2 Disadvantages of DC Microgrid

1. In the existing power system configuration, the majority of load units need AC electricity.

2. Voltage transition in a DC system is less organized than in an AC system.
3. To convert AC power to DC power, a rectifier is necessary for the integration of AC generators[87].

I.3.3.3 Hybrid Microgrid

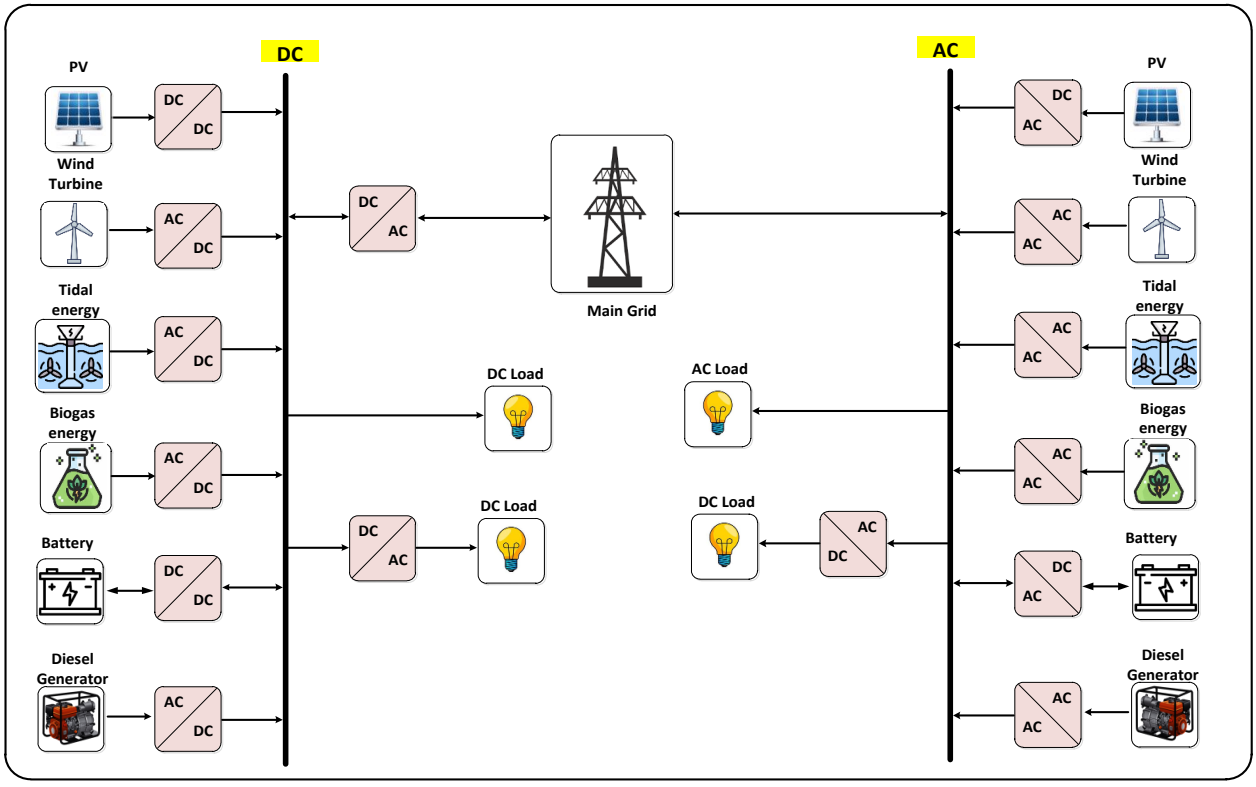


***Fig I. 6**: Structure of hybrid microgrid*

The distinct structures of the two DC and AC microgrids are integrated to create a hybrid microgrid. Consequently, a hybrid AC-DC microgrid encompasses the advantages of both DC and AC microgrids [88].

A genuine hybrid AC-DC microgrid design is shown in Fig I.6. The bidirectional AC-DC converter is used to interconnect AC and DC microgrids. DC-DC boost converters are used to link DC power generators, such as fuel cells (FC) and solar panels, to a DC microgrid [34,35]. DC-DC buck converters facilitate the connection of DC loads, such fluorescent lights and electric cars, to a DC microgrid. Bidirectional DC-DC converter is used to link energy storage systems to DC microgrids [89]. Alternating current (AC) loads, such as AC motors, are directly linked to the AC microgrid. Power will migrate from the DC microgrid to the AC microgrid during the AC microgrid's overloaded situation [90]. Throughout this procedure, the primary converter will operate as an inverter. Under the overloaded state of a DC microgrid, power will transfer from the AC microgrid to the DC microgrid, with the interlinking converter operating as a rectifier [91],[92].

The primary aim of a bidirectional AC/DC converters are to regulate the power transfer seamlessly between a DC microgrid and an AC microgrid, while maintaining the stability of the DC bus voltage in the DC microgrid and the AC bus voltage and frequency in the AC microgrid [40–42].

I.3.3.3.1 Advantages of Hybrid Microgrid

1. A hybrid AC-DC microgrid reduces the number of conversions in a standalone DC or AC microgrid, providing stable, uninterrupted, and high-quality electricity to various loads. It also mitigates conversion losses that arise after successive conversions [93].
2. Hybrid architecture may cut equipment costs, remove various transformation components, and limit frequency conversion devices, therefore decreasing losses and enhancing the reliability and efficiency of the complete system. It not only prevents blackouts but also supports local demand [94].
3. The hybrid AC-DC microgrid has two distinct grids linked to various loads and generating units, each exhibiting fundamentally different characteristics and capable of independent management [88].
4. Power electronic equipment (e.g., inverters, bidirectional converters, and boost converters) are used to link several components, resulting in a substantial introduction of harmonics of different orders into the grid. Diverse filtering methods may be used to eradicate these harmonics in both grids.
5. An extra inverter or rectifier is unnecessary. It reduces the total expenditure.
6. The hybrid AC-DC microgrid offers auxiliary services, including an uninterruptible power supply and improved power quality.
7. The majority of generator units used in the hybrid AC-DC microgrid are environmentally benign. It also contributes to mitigating the greenhouse impact [47,48].

I.3.3.3.2 Disadvantages of hybrid microgrid

1. The distinct characteristics of AC and DC microgrids complicate the system and have resulted in many significant operational challenges owing to their interplay.
2. The primary concern is the reduction of power loss, achievable by minimizing power transfer between the AC and DC micro-grids during the power conversion process.
3. The integration of dispersed generation within two subgrids with unique features is challenging [95].

I.3.4 Categorizing MGs According to Source

I.3.4.1 Renewable Microgrid

A microgrid powered by distributed renewable resources is referred to as a renewable microgrid. Renewable microgrids typically consist of renewable energy sources and batteries.

They provide power to consumers while implementing lower carbon solutions globally. Nonetheless, the unpredictable and sporadic production of renewable energy sources complicates the efficient functioning of microgrids. Additionally, addressing the time-varying demand becomes a critical difficulty for an isolated microgrid. Energy Storage Systems (ESS) are among the most attractive technologies for optimizing the use of renewable energy and are widely used for balancing demand and supply in microgrids. The primary problem is to synchronize storage systems, dispersed renewable energy sources, and fluctuating power demand. Consequently, an Energy Management System (EMS) is essential for renewable Microgrids (MGs) [96],[97].

I.3.4.2 Fossil Fuel Microgrid

MGs driven by fossil fuel (natural gas/diesel) generators, capable of supplying electricity to distant regions. They can operate in both isolated and grid-connected settings. For several years, energy sources such as steam and gas turbines, together with diesel generators, have been the conventional means of producing localized power in a microgrid. These, however, have a detrimental impact on both the environment and the economy [88]. The fossil fuels necessary to operate these MGs are costly to acquire and transport, and transportation itself incurs a carbon footprint. Numerous towns using diesel generators encounter this issue consistently. Manufacturers are investigating cleaner alternatives due to these effects [98].

I.3.4.3 Hybrid Microgrid

A hybrid MG system integrates renewable energy sources (RESs), fossil fuel generators (diesel/gas), and/or batteries to function in both isolated and grid-connected configurations. Hybrid microgrids using renewable energy sources are supplanting entirely diesel or natural gas microgrids as a more favored alternative. Hybrid vehicles significantly reduce fuel use while also being more cost-effective, dependable, and ecologically sustainable throughout their lifespan. Nevertheless, hybrid systems need fuel-powered generators, resulting in unavoidable noise and emissions [99],[14].

I.3.5 Classification based the operation

The execution of decentralized energy systems is contingent upon the degree of decentralization. In rural decentralization, the system is governed by local involvement, and energy is provided to satisfy local demands. In some instances, surplus electricity may be sent to the grid. Conversely, industry-level decentralization may occur, when the electricity produced as a by-product of industrial processes (such as bagasse co-generation) primarily serves internal requirements, with any excess being sent to the grid. The degree of decentralization influences whether the system functions in grid-connected (GC) [100],[101] or stand Alone (SA) mode [102],[103].

I.3.5.1 Grid-connected Systems

Two categories of grid-connected systems may be identified. In the first kind, the primary objective of the GC system is to meet local power demands, with any excess generation being sent to the grid, while electricity is sourced from the grid during shortages. The alternative is utility scale, where decentralized stations are administered by utilities similarly to major electric power plants. All output from the GC systems is sent into the central power grid, disregarding local requirements. The significant characteristics of GC systems are as following [104].

- A grid-linked energy system is an autonomous decentralized power system linked to an electrical transmission and distribution network, known as the electricity grid. They are optimal for sites near the grid [105].
- The operating capacity is dictated by the source of supply. The system operates just when energy sources are accessible.
- Due to the supply-driven functioning, the system may need to disregard local demand during periods of supply source unavailability [106].
- The system may either satisfy local demand with any excess sent to the grid, or it may only exist to supply the grid.
- The connection to the grid facilitates the establishment of relatively large-scale systems, therefore allowing them to function at elevated plant load factors, enhancing the economic feasibility of the operation.
- In a grid-linked power system, the grid functions as a battery with infinite storage capacity. It addresses seasonal load fluctuations. The total effectiveness of a grid-connected system surpasses that of a stand-alone system due to the virtually unlimited storage capacity, allowing generated electricity to be stored without the necessity of discarding any excess production.
- Systems using renewable sources such as biomass, wind, and solar photovoltaic will see significant demand on these resources, since they typically function at large scales and need more biomass for operation [107].

I.3.5.2 Stand-alone systems

Stand-alone systems generate electricity autonomously from the utility grid; hence, they are referred to as stand-alone. These are more appropriate for the most isolated areas where the grid cannot reach and no other energy sources exist. Stand-alone systems constitute the predominant kind of solar installations in remote areas globally, since they often represent the most economical option for applications far from the utility grid. Examples include lighthouses and other distant installations, supplemental power units for emergency services or military purposes, and industrial plants using sensitive electronics. The SA systems have inherent drawbacks such as a poor capacity factor, high battery prices, and limited power storage capacity,

necessitating the disposal of surplus energy produced. The salient characteristics of SA systems are enumerated as follows [108].

- In SA energy networks, the operating capacity aligns with the demand.
- The requirements of the local area take precedence.
- These systems are optimal for distant areas where operation at low plant load factors is necessary.
- Operation is mostly seasonal, since conventional stand-alone systems often rely on renewable energy sources such as solar photovoltaic, which are not consistently accessible year-round.
- This does not impose strain on biomass and other renewable energy sources, since it needs less resources for small-scale applications.
- These systems are not linked to the utility grid, necessitating batteries for the storage of energy generated during off-peak demand hours, which incurs additional battery and storage expenditures; alternatively, the surplus power produced must be discarded.

I.3.6 Classification based applications

Microgrids provide electricity in a reliable, resilient, and ecologically sustainable way, making them applicable across many sectors. Fig I.7, illustrates the most important applications of the microgrid. The following are many critical applications of microgrids:

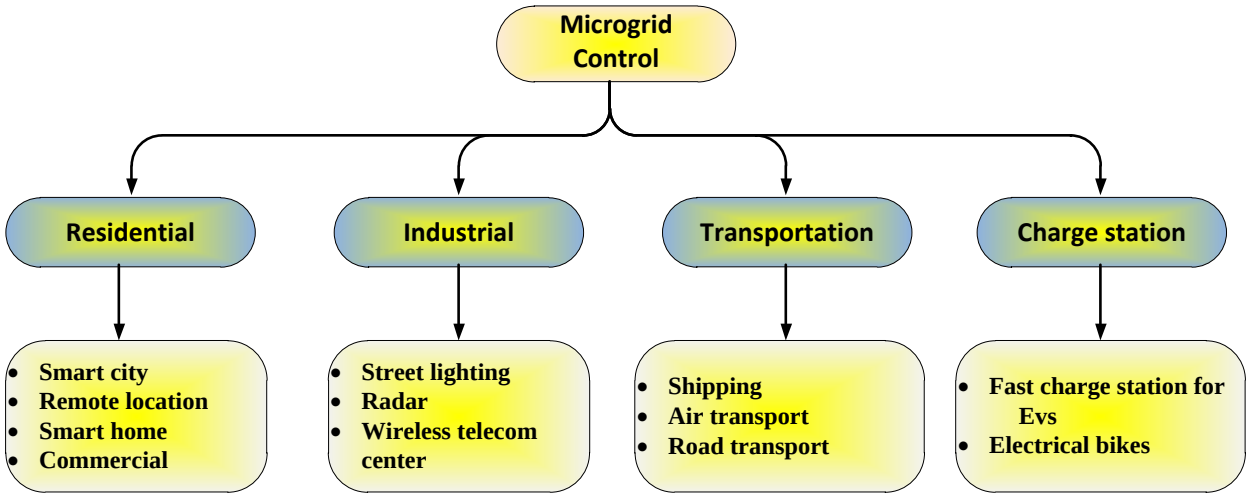


***Fig I. 7**: Structure of microgrid*

I.3.6.1 Smart Cities and Urban Applications

Microgrids facilitate the evolution of urban infrastructures into smart cities by integrating advanced technologies such as the Internet of Things (IoT), energy management systems, and demand response mechanisms [109]. Intelligent energy systems and dependable electrical networks characterize smart cities. They support the integration of renewable energy sources, recharge electric cars, enhance energy efficiency, promote demand-side management, and provide

novel energy-related value-added services [110]. In the power paradigm, these technical attributes and information and communication networks are essential [111].

I.3.6.2 Isolated and remote applications

A community or utility microgrid often resembles an island microgrid [112]. The primary difference is that, in most instances, there will be no connection to the electrical grid. In some instances, a cable connection to the mainland power grid may be feasible if the distance between the island and the mainland permits [113]. Conversely, the efficiency of the decision-making process may be expedited based on the island's existing power supply infrastructure. For physically distant or remote towns and underdeveloped nations, "off-grid" microgrids prioritise dispersed and varied energy sources. Numerous distant microgrids are being established to ultimately integrate into a bigger grid system as countries in the developing world enhance their electrical infrastructure. Other distant microgrids are designed to be autonomous in order to maintain energy security [114].

I.3.6.3 Smart home applications

microgrids may enhance energy independence and resilience via the installation of advanced energy management systems, photovoltaic panels, and battery storage solutions. Furthermore, the growing prevalence of DC residential loads, such laptops and LEDs, is enhancing the reliability of DCMGs for residential applications [115]. The 380-400 V DC bus voltage is predominantly used in this application due to its alignment with the Emerge Alliance building requirements [116].

I.3.6.4 Commercial applications

Commercial buildings have seen a substantial rise in energy consumption attributable to their features, such as elevated consumption ratios and considerable size [117]. Microgrids has the capacity to reduce energy expenses and mitigate the risks associated with power interruptions. The buildings may significantly contribute if managed in a coordinated way as flexible assets connected with the microgrids. Research initiatives are required to facilitate the digital transformation of buildings by developing technology enablers and interoperability frameworks that permit their coordinated functioning. According to, a 380 V DC bus voltage is a suitable selection for these structures [118]. Zero-net energy (ZNE) buildings are more appealing and using microgrid technology as a power system. The use of photovoltaic systems and batteries on roofs is a promising approach for the implementation of Distributed Clean Microgrids (DCMGs) in these structures. Furthermore, structures yearly dissipate 13% of energy as a result of AC/DC conversion [119],[120]. These losses may be mitigated with the use of DCMGs. Its compatibility with residential and commercial structures makes it an exceptional alternative for power distribution in

metropolitan areas. This enables city residents to engage in the energy market by trading electricity between themselves. This may provide economic and technological advantages.

I.3.6.5 Industrial applications

Electric motor drives use over 40% of the supplied power [42]. Connecting the used converters to a DC bus facilitates the usage of regenerative (braking) power [43]. The standard DC bus architecture may serve as a cost-effective and energy-efficient solution for most industrial applications. Consequently, using DCMGs for this application is a dependable choice. The direct current (DC) characteristic facilitates superior plug-and-play capabilities, allowing the future installation or disconnection of distributed generators (DGs) or loads without disrupting the operation of the microgrid (MG) [121].

I.3.6.6 Transportation applications

The majority of contemporary propulsion systems rely on AC-supplying mechanisms. Nonetheless, the developing propulsion technology may position DC-supplying systems as superior alternatives [44]. Consequently, DCMGs are proposed as ideal options for forthcoming transportation systems, including electric ships, more electric airplanes (MEA) [122], advanced electric cars (EVs) [123], ships [124], and hybrid electric automobiles [125]. MGs-based hybrid power systems (HPSs) are emerging as a key option for various applications. The majority of electric vehicles use batteries with other storage devices, such as supercapacitors. Moreover, hybrid electric car fuel cells are rapidly used due to their benefits, such as elevated power density and alternative storage methods.

I.3.6.7 Fast chargers station for electric automobiles

Plug-in electric vehicles (PEVs) are increasingly recognized in the realm of energy decarbonization [126]. However, they need specialized charging stations because to the elevated consumption rate. Conversely, a microgrid, functioning as an autonomous power system, promotes self-consumption, hence reducing strain on the main grid [127]. Furthermore, owing to their compliance with the direct current characteristics of charging power, DC microgrids are regarded as the superior choice for charging station infrastructures in comparison to their alternating current counterparts. Furthermore, it is compatible with photovoltaic generators often used in urban environments [126].

I.4 Challenges and issues of microgrid

Notwithstanding the prospective advantages, MG growth encounters some hurdles and constraints, as elucidated. The primary problems of MGs may be categorized into four areas [128],[129], as seen in Fig I.8.

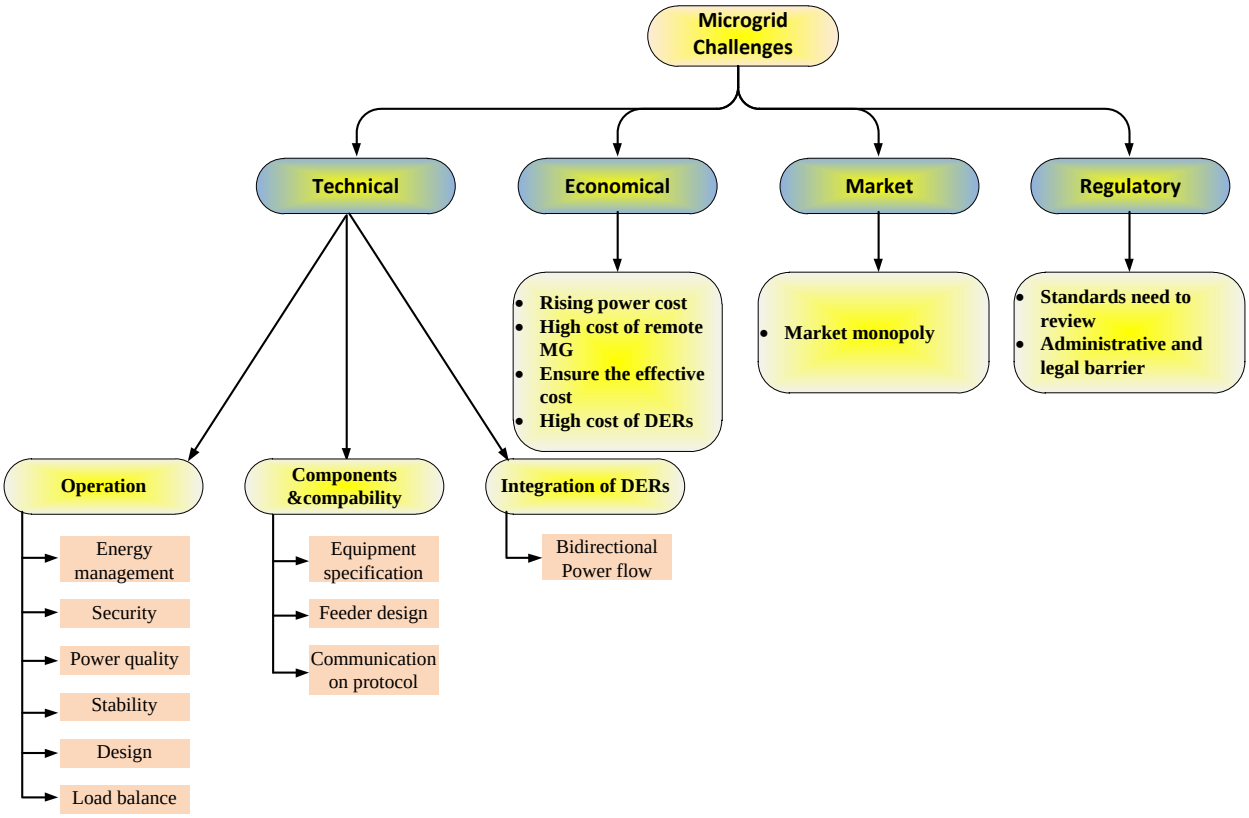


***Fig I. 8**: Structure of microgrid*

I.4.1 Technical challenges in MGs

I.4.1.1 Operations and Management

The following are the main managerial and operational challenges encountered by an MG:

- Issues during start-up: Challenges during the initiation of island mode: The system's frequency and voltage may be influenced by the significant current influx during the first phases of island mode activation. This may result in the generators tripping and shutting down during the starting phase. To resolve this, an examination of energy generating techniques in island mode is necessary, along with the creation of tailored controls appropriate for microgrid operations.
- Energy management: Generally, energy control encompasses several fine-tuning factors. Subsequently, the parameters must be simulated to identify the optimal solutions. Determining an optimal value in MGs is a complex endeavour due to the diverse ambiguity and vague examples, alongside the clearly defined precise occurrence [130],[131].
- Suitable design: Microgrids, especially those based on renewable energy, need distinct design, modelling, and planning criteria compared to traditional fuel-based systems, with which the majority are already familiar [132],[133]. A significant issue that diminishes the

lifespan of MGs is suboptimal design [134]. The design of renewable microgrids requires a comprehensive knowledge of the available energy resources and user needs [135]. It is crucial to evaluate how fluctuations in energy resource availability and demand might impact the dependability and availability of energy supply. Consequently, effective MG design continues to be a difficulty.

- Identifying the modes of operation of the microgrid: Each integrated power source and load scenario inside the microgrid must be delineated for circumstances such as temporary switching or emergency load shedding. The functioning of an MG, including diverse loads and generators with distinct operating characteristics, renders this phase crucial and demanding [136].
- System security: Contingency planning and emergency measures, including demand-side management, load shifting, islanding, or unit shutdown, are essential for maintaining system security. In contingency circumstances, production must be planned economically to align with system loads and load-end voltage/frequency. System security in a microgrid must be maintained via emergency procedures and contingency planning, including load shedding, distributed resource management, islanding, and unit shutdown.
- Ensuring power quality: The active and reactive power balance of the microgrid must be maintained in the near term.
- Supervisory Control and Data Acquisition: The Control Centers (CCs) and Management Centers (MCs) of the Microgrid (MG) shall integrate SCADA-based metering, control, and protection functionalities. Provisions must be included for system diagnostics using state estimation functions.
- Control system analysis: Optimal performance of an MG requires effective design and functional evaluation. The operational mode and configurations of the microgrid are critical in the design of the microgrid control system. To effectively manage the operational situation, the control system must include every viable control approach [137].
- Load flow analysis: Load flow must be examined under all microgrid operating conditions and configurations to ascertain current flow and voltage levels. The task involves cataloguing relevant loads and assessing their crucial thresholds. Furthermore, specifying the timings of varied profiles of load may increase the complexity [138],[139].
- Balancing power production and consumption: This is a common challenge faced by microgrids. It is essential to maintain a constant equilibrium between demand and generation of electricity.
- Instability in the isolated system may arise from abrupt or substantial changes in loads. System stability analysis: Given the importance of microgrid stability, it is essential to predict, observe, and assess the transient events resulting from both typical and atypical disturbances. MGs consist of many sources of energy and components. Maintaining system stability while using inertia-based generators, static converter-based photovoltaic systems, wind energy, and energy storage devices is problematic. Additionally, there are other types

of converters, including those using electrical power sources and virtual synchronous generators. Manufacturers and designers must do a thorough analysis and establish a strong correlation of equipment to ensure system stability [140],[141].

I.4.1.2 Component and compatibility

- Equipment specs: the details and single-line diagrams of the system are the key aspects to examine.
  During the formulation of power system analyses. Consequently, the principles for elucidating and exhibiting the MG's operational characteristics are crucial [142],[143].
- Designing feeder for MG: Feeders are currently constructed according to reliable sources of power production and distribution, in accordance with the current power system. Nonetheless, a hurdle arises when the need for feeders in microgrids goes unmet [142],[144].
- Telecommunications infrastructure and communication protocols: Effective energy management, protection, and control need networks of communications and communication protocols [145].

I.4.1.3 Integration of Distributed Energy Resources

When a microgrid (MG) is linked to the grid, transmission of electricity between the main grid and the MG occurs in both directions. Concerns with voltage escalation emerge due to the integration of several dispersed generators into the grid, representing a significant technical barrier. Due to the intermittent nature of solar PV, it often induces transient voltage fluctuations, which interfere with the functioning of power control and protection systems, thereby reducing the lifespan of the equipment. [146].

Bidirectional power flows: The integration of distributed generation (DG) units at low voltage levels inside the network might result in reverse power flows, which complicate protection coordination, create unfavourable power flow patterns, affect fault current distribution, and hinder voltage regulation.

I.4.2 Protection

The following are the principal protection concerns that an MG may encounter:

- Assessment of short-circuit current: Short-circuit current (SCC) thresholds are often determined by the maximum and lowest values resulting from power system breakdowns. The challenge arises from the significant variability in SCC between operational configurations due to differing energy sources and load [147],[27].
- Earthing: Neutral earthing is a critical and complex matter in MGs concerning the protection strategy. The MG transitions between power sources, utilises many energy sources (including turbines and converters), and connects with the main grid. The

installation of earthing is mostly regulated by local grid standards; nevertheless, the installation and maintenance of neutral earthing may provide specific challenges [148].

- The evaluation of protection and coordination: Given the evident fluctuations and poor SCC, research on protection is necessary. The MG configuration must include efficient protective equipment and personnel safety, together with coordinated and sequenced functioning of protective devices. In MGs, the conventional protective strategy may prove challenging or ineffective, requiring creativity and compromise [149].

I.4.3 Economic challenges

MG investments continue to be significant. Certain components, such as fuel cell energy storage systems, smart grid infrastructure, and grid management applications remain financially unviable without financial support. Guaranteeing economic functionality: Generation scheduling, economic load delivery, and successful power flow operations must be used to attain cost-effective operations. The economic functioning of the MG must be facilitated by economic load delivery, generator planning, and efficient power flow operations [150].

- Rising energy production costs: The development of a hybrid system will result in an overall increase in complexity, which may raise the cost of generating power.
- Reimbursement of fixed costs: Infrastructure costs are included into utility rates. Individual consumers will acquire less energy from the utility if incentivised to produce their own power. Some will also produce surplus power for sale to utility companies. Customers using net metering will maintain their connection to the grid and may profit from this infrastructure without incurring its fixed costs. Consequently, users that do not implement net metering will incur the repercussions of infrastructure costs. Utilities are apprehensive that an increasing number of customers choosing net metering may hinder their capacity to finance the substantial infrastructure enhancements required for a contemporary, sustainable grid [46].
- Supplementary expenses for the isolated MG: The installation of the MG in rural areas complicates maintenance and escalates transportation costs.
- Elevated expenses of DERs: Microgrids have a considerable drawback regarding installation expenditures. This may be alleviated by obtaining a government subsidy to encourage investment. To fulfil environmental and carbon capture objectives, this should be implemented at least temporarily. A worldwide objective has been established to enhance renewable energy production and reduce carbon emissions by 50% by the year 2050.

I.4.4 Market challenges

Market monopoly: If microgrids are allowed to autonomously deliver electricity to priority loads during main grid interruptions, the critical issue is who would determine the price for energy supply during the outage. Due to the disconnection of the main grid and the resultant loss of regulatory oversight in the electrical market, microgrids may use their monopolistic position to

sell energy at exorbitant costs. Consequently, to facilitate the sustainable development of MGs, appropriate market infrastructure must be designed and executed [151].

I.4.5 Regulatory Challenges

Standards need evaluation: MG is an emerging industry. Standards and standards for the integration of micro sources and their involvement in both conventional and deregulated power markets, together with safety and protection recommendations, should be established. Standards like as G59/1 and IEEE 1547 should be evaluated and revised to effectively integrate MGs with active distribution networks. Additionally, an examination of IEEE 2030.7-2017 – IEEE Standard for the Specification of Microgrid Controllers is required. Administrative and legal impediment: In several nations, there is an absence of standardized law or regulation governing the functioning of microgrids. Certain governments are advocating for the development of green power microgrids, while standardized laws have not yet been developed for future execution [152].

I.5 Conclusion

This chapter has outlined the essential concepts and classifications of microgrids, emphasizing their role in modern energy systems. We have identified the various types of microgrids and discussed the challenges that accompany their implementation and operation. As the energy landscape continues to evolve, addressing these challenges is crucial for harnessing the full potential of microgrids. The insights gained from this chapter provide a foundation for further exploration of innovative solutions and strategies that can enhance the effectiveness and resilience of microgrids. Future research will be vital in overcoming the identified issues, thereby facilitating the broader adoption of microgrids in pursuit of sustainable energy goals.

Chapter II
Renewable energy and storage system

II.1 Introduction

As the global energy landscape undergoes a significant transformation, renewable energy has emerged as a pivotal player in addressing the challenges posed by climate change and energy security. In 2023, projections indicate a remarkable increase in renewable power capacity, driven by robust policy support across more than 130 countries. This chapter provides a comprehensive overview of the current state and projected growth of renewable energy, highlighting the unprecedented advancements in solar photovoltaic (PV) and wind energy sectors, particularly in China. Furthermore, the chapter delves into the modeling of renewable energy sources, including detailed analyses of photovoltaic systems, wind energy models, and integrated systems utilizing hybrid energy storage solutions (HESS). By examining various converter structures and their operational impacts within microgrid systems, this chapter underscores the importance of technological innovation in optimizing energy efficiency and reliability. Through simulation results, we will evaluate the performance of renewable energy systems, providing insights into operational costs and system efficacy under varying conditions.

II.2 An overall global outlook on renewable energy

In 2023, renewable power capacity additions are predicted at 507 GW, about 50% more than in 2022, driven by ongoing policy support in over 130 countries, resulting in a notable shift in the worldwide development trajectory. The global acceleration in 2023 was primarily fueled by the year-on-year growth in the People's Republic of China's flourishing solar PV industry (+116%) and wind energy sector (+66%). Renewable energy capacity expansions are projected to rise over the next five years, with photovoltaic and wind energy comprising a historic 96% of the total, due to their lower generating costs compared to both fossil and non-fossil alternatives in the majority of nations, and ongoing supportive policies.

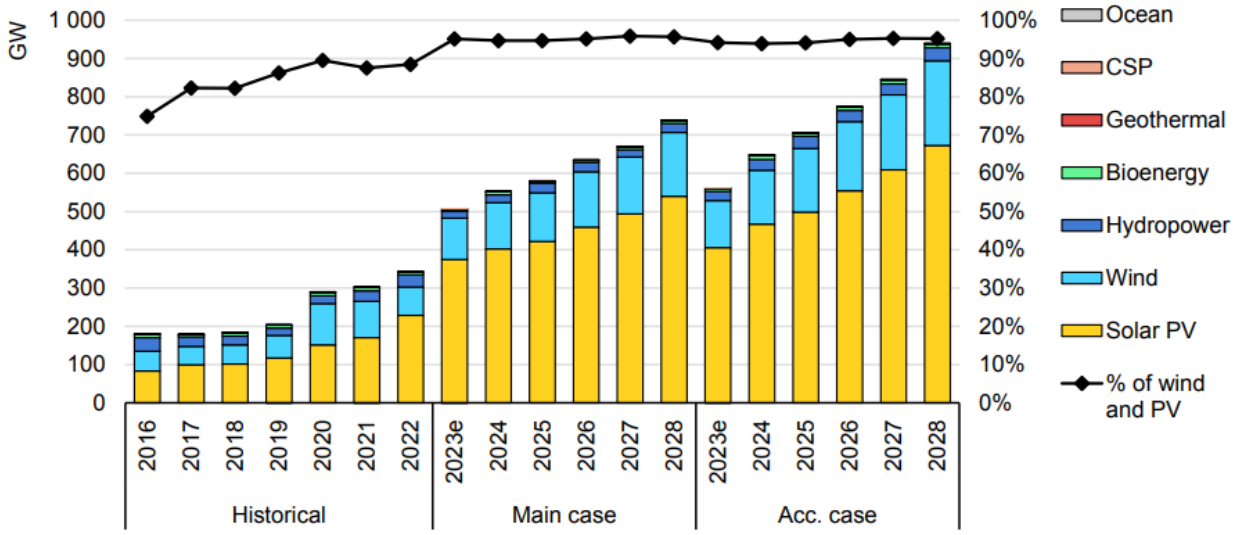


***Fig II. 1**: Additions of renewable power capacity categorized by technology and sector*

By 2028, the potential for renewable power production is anticipated to reach around 14,400 TWh, reflecting an increase of over 70% from 2022. In the next five years, many renewable energy milestones may be attained [153]:

1. In 2024, variable renewable energy output exceeds hydropower.
2. In 2025, renewable energy will exceed coal-fired power output.
3. In 2025, wind energy will exceed nuclear power production.
4. In 2026, solar photovoltaic energy will exceed nuclear power production.
5. In 2028, solar photovoltaic energy output exceeds that of wind energy.

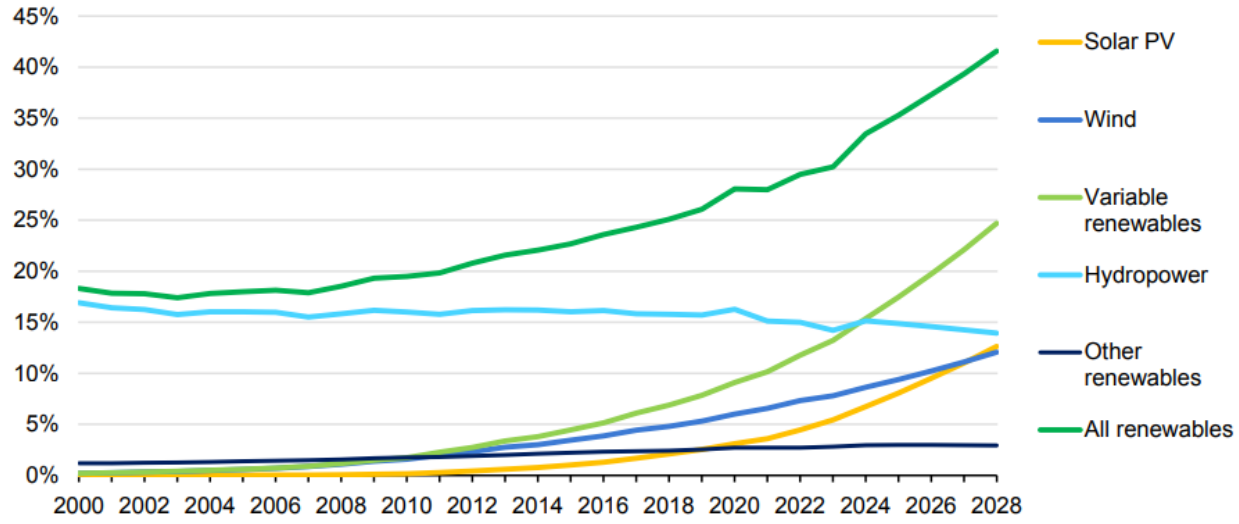


***Fig II. 2**: Electricity production by technology from 2000 to 2028*

II.3 Modeling of renewable energy source

II.3.1 Photovoltaic model

The electrical structure of the selected photovoltaic model is illustrated in Fig II.3. It consists of a single diode and a photocurrent. The leakage currents are represented by a shunt resistor Rp. An internal resistance denoted by a series resistor Rs that signifies the current flow. The photovoltaic current I_{pv} is defined by [154], [155];

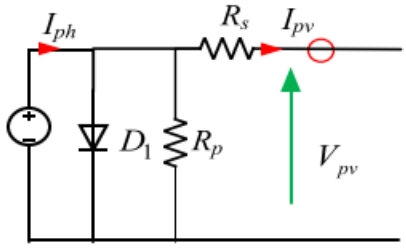


***Fig II. 3**: The PV electrical circuit*

$$I_{pv} = I_{ph} - I_s \left[exp\left(\frac{q\left(V_{pv} + R_s \cdot I_{pv}\right)}{AN_s K T_j} \right) - 1 \right] - \frac{V_{pv} + R_s \cdot I_{pv}}{R_{sh}} \quad \text{II.1}$$

The saturation current Is I_s expressed by the following the following formula:

$$I_s = I_{s,0} \left(\frac{T_n}{T} \right)^3 \left[exp\ \frac{qE_g}{AK} \left(\frac{1}{T_n} - \frac{1}{T} \right) \right] \quad \text{II.2}$$

Where $I_{s,0}$ represents the short-circuit current estimated at 25 °C and 1 kW/m². The photocurrent I_{ph} is defined as;

$$I_{ph} = (I_{ph,n} + K_I \Delta T) \frac{G}{G_n} \quad \text{II.3}$$

where $\Delta T = T - T_n$.

II.3.2 Wind energy Model

The wind turbine rotor transforms the kinetic energy of the wind into mechanical rotational energy, the mechanical power produced by a wind turbine may be described using the following equation.

$$P_{WT} = \rho A C_p(\lambda, \beta) V_w^3 \quad \text{II.4}$$

The variables in the equation are defined as follows: ρ represents the air density, A represents the area swept by the rotor blades, andC_p is the power coefficient of the wind turbine. β represents the blade pitch angle, V_w represents the wind speed, and λ represents the tip speed ratio. The tip speed ratio is defined as:

$$\lambda = \frac{R * \omega_m}{V_W} \quad \text{II.5}$$

ω_m represents the angular speed of the turbine rotor, R is the radius of the turbine blade. The equation governing the mechanical motion of a wind turbine system is as follows:

$$T_t + T_e = J \frac{\omega_m}{\mathrm{d}t} + B_{f^*} \omega_m \quad \text{II.6}$$

The total mechanical torque of the wind turbine T_t, the electromagnetic torque of the generator T_e, the total inertia of the system J, and the coefficient of viscous friction B_f.The velocity of the wind is transformed into useful electricity energy. It is constituted of a boost converter, a rectifier, a direct-drive permanent magnet synchronous generator (PMSG), a variable speed wind turbine, and no gearbox used[156].

The PMSG was modeled in the synchronous rotating d-q reference space, with the d-axis perpendicular to the magnet flux vector. When viewed from this perspective, the PMSG's model expressions may be formulated as follows[157]:[158]

$$V_{ds} = R_s \cdot I_{ds} + \frac{\psi_{ds}}{dt} - w_e * \Psi_{qs} \quad \text{II.7}$$

$$V_{qs} = R_s \cdot I_{qs} + \frac{d\psi_{qs}}{dt} + w_e * \Psi_{ds} \quad \text{II.8}$$

The components of the stator flow vector may be written in this reference frame as follows [159]:

$$\psi_{ds} = L_d * I_{ds} + \psi_{PM} \quad \text{II.9}$$

$$\psi_{qs} = L_q * I_{qs} \quad \text{II.10}$$

The expression for the electromagnetic torque of PMSG may be stated as follows:

$$T_e = p\frac{3}{2}(I_{ds} * \psi_{ds} - I_{ds} * \psi_{qs}) \quad \text{II.11}$$

Where the: V_{ds}, V_{qs} - d-q are stator voltage vector elements; Ids, Iqs are stator current vector elements of d-q; and Stator resistance R_s; d-q components of the stator flux vector (ds, qs). Inductances of stator direct and quadrature axes (L_d, L_q); A permanent magnet (PM) produces a magnetic field known as a field pm. The number of pole pairs in the PMSG is denoted by p.

II.3.3 Modelling of the DC-DC converter integrated with PV-Wind energy systems

A boost converter is utilised with PV-Wind for DC-DC conversion as shown in Fig II.4. The current of PV or wind and voltage PV or wind are regarded as state variables for the converter, while D represents the duty cycle that governs the converter's operation. The maximum power

point tracking (MPPT) or Load power tracking (LPT) control algorithm

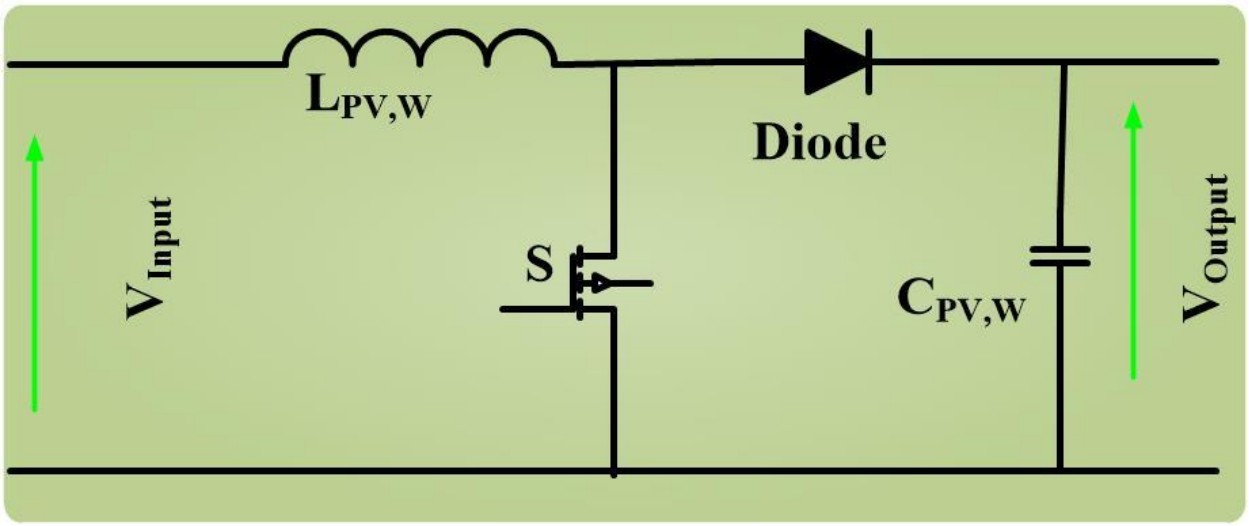


***Fig II. 4**: DC/DC boost converter*

determines the value of D, which ranges from 0 to 1. For the purpose of simplifying the converter's modelling, it is presumed to be lossless. The control signal for the switch $T_{pv,W}$ is depicted in Fig II.5 (c) as a rectangular signal with frequency f, where the duration is modulated by the duty cycle D. The duty cycle is defined as the ratio of the conduction duration of the switch $T_{pv,W}$, to the switching period T_D, expressed by the following equation.

$$D_{pv,W} = \frac{T_{ON}}{T_{OFF}} \quad \text{II.12}$$

$$T_D = T_{ON} + T_{OFF} \quad \text{II.13}$$

T_{OFF} denotes the switch's blocking duration ($T_{OFF} = (1 - D_{pv,W})\, T_D$), whereas T_{ON} signifies the switch's conduction time ($T_{ON} = D_{pv,W} T_D$). Two operational phases, namely the active and freewheel phases, may be identified based on the status of the two switches $T_{pv,W}$and $D_{pv,W}$, as seen in Fig II.5 (a).

- Active phase

Upon closure of the switch at t = 0, for a length of $T_{pv,W}$and $D_{pv,W}$, the diode experiences reverse bias. The same circuit is seen in Fig II.5 (b). The voltage across the inductance is represented by the following formula:

$$v_{L_{pv,W}} = V_{pv,W} = L_{pv,W} \frac{di_{pv,W}}{dt} \quad \text{II.14}$$

The equation that describes the progression of current via the inductor is derived by resolving the differential Equation. It may be articulated as follows:

$$i_{L_{pv,W}} = \frac{V_{pv,W}}{L_{pv,W}} t + I_{L_{pv,W}Min} \quad \text{II.15}$$

- Freewheeling phase

When the switch is open at time ($t = D_{pv,W}T_D$)., for a length of ($1 - D_{pv,W}$) T_D), the inductive current cannot change instantly. The voltage across the inductor is articulated as follows:

$$v_{L_{pv,W}} = V_{pv,W} - V_{Output} = L_{pv,W} \frac{di_{pv,W}}{dt} \quad \text{II.16}$$

$$v_{L_{pv,W}} = V_{pv,W} - V_{Output} = L_{pv,W} \frac{di_{pv,W}}{dt} \quad \text{(II.16)}$$

The development of the current via the inductance is derived by solving differential Equation (4). It may be articulated as follows:

$$i_{L_{pv,W}} = \frac{V_{pv,W} - V_{Output}}{L_{pv,W}} (t - D_{pv,W} T_D) + I_{L_{pv,W}Max} \quad \text{II.17}$$

The temporal average of Equations (6) and (8) yields an average model of this converter. It is articulated as follows:

$$L_{pv} \frac{di_{pv}}{dt} = V_{pv} - (1 - D_{pv}) V_{dc} \quad \text{II.18}$$

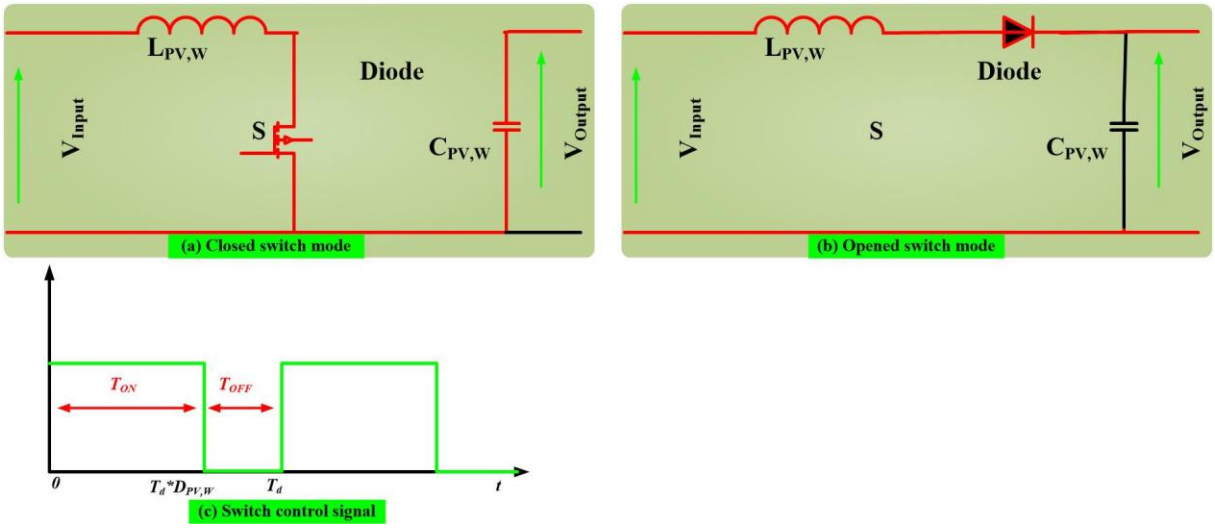


***Fig II. 5**: (a) closed switch mode, (b) open switch mode, (c) switch control signal*

II.3.4 MPPT for renewable energy sources

MPPT techniques has used to extract the maximum energy from RES.MPPT is used in most situations and depends on the state of charge of the HESS and the power difference between the generated power and the demanded power. A block schematic of a PI control system used to execute MPPT of PV, and wind system with a boost converter is illustrated in Fig II.6. The outer loop reference voltage $V_{input}{}^{*}$ may be generated using any voltage-based MPPT technique. The MPPT algorithm requires measurements of the PV/Wind system's current I_{input} and voltage V_{input} (e.g., P&O). The adjustable voltage loop regulates the boost converter's input capacitor voltage, namely the PV/Wind systems output voltage. As a result, the MPPT algorithm provides the reference for this loop [160].

A linear proportional integral (PI) regulator with the output current via the input capacitor I_C is used to regulate the voltage error. While the DC–DC converter doesn't really regulate the capacitor current directly, a feedforward adjustment may be incorporated to calculate the DC–DC converter current reference; in the situation of the boost converter, this is the inductor current I_L .an MPPT block calculates the optimal voltage for maximum power, while Proportional-Integral (PI) controllers adjust the system to minimize voltage and current errors. The compensation stage refines current values, and the Pulse Width Modulated (PWM) signal adjusts the switch duty cycle to maintain optimal power flow, ensuring efficient and stable operation [161], as LPT, which is activated when the energy storage devices reach full capacity and the electricity generated from renewable energy sources exceeds the power demand. The LPT controls the voltage of the DC link by compared the DC voltage measured V_{DC} and voltage reference V_{DC_ref}. Moreover, effectively control the power generated by the Permanent Magnet Synchronous Generator (PMSG) and Photovoltaic (PV) systems to meet the required load demand [162],[160]. To validate the MPP tracking for the PV simulation system, it compares the suggested MPPT technique with the P&O MPPT method under various ambient circumstances. This comparison demonstrates the effectiveness and accuracy of the suggested MPPT method in tracking the maximum power output across multiple scenarios.

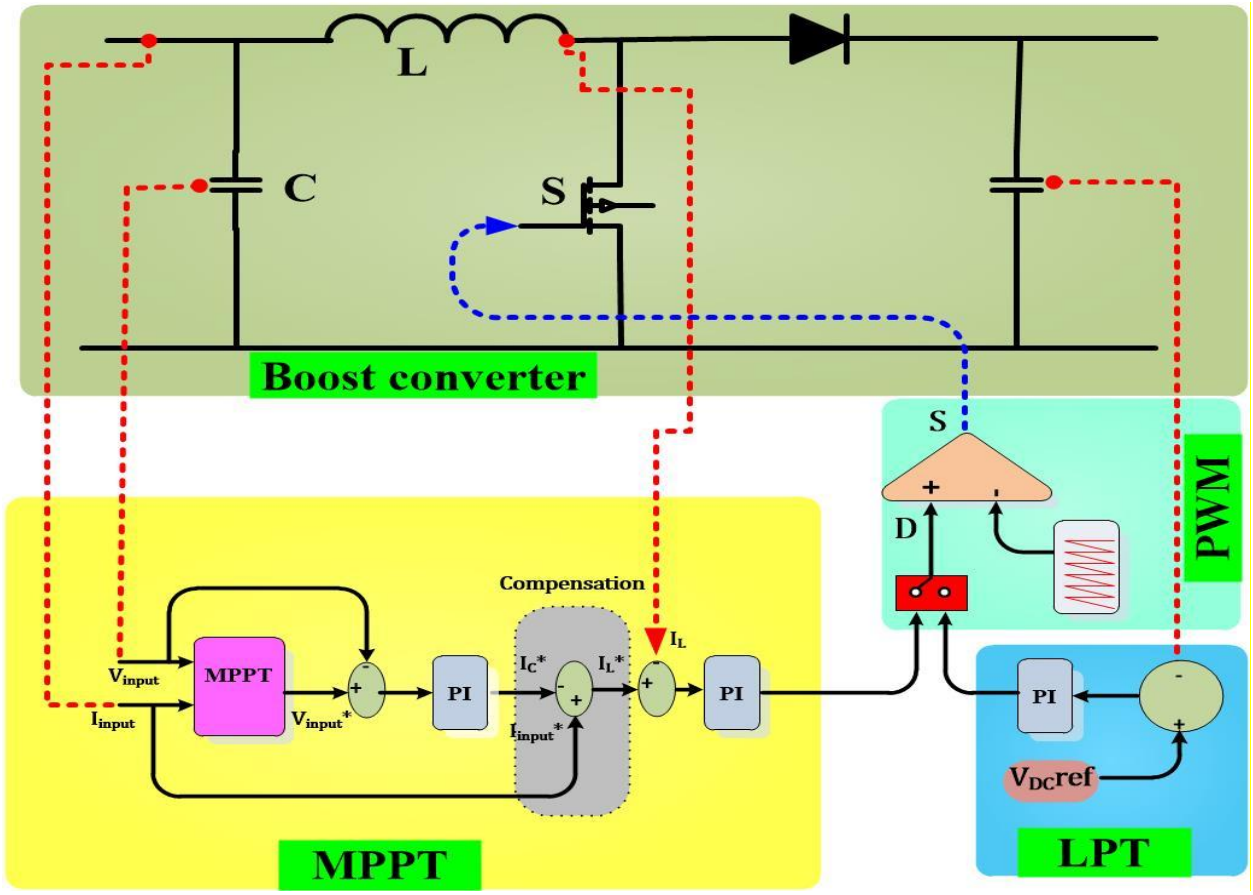


***Fig II. 6**: block schematic of the MPPT-using PI control*

The simulation is carried out using MATLAB/Simulink. The solar radiation undergoes a quick shift in the form of a unit step while maintaining a constant temperature of 25°C, as seen in Fig II.7. The sun radiation begins at an intensity of 500 w/m^2 and persists until 0.3 seconds, after which it increases to 600 w/m^2 At 0.6 seconds, the solar radiation experiences a significant fall to 400 w/m^2. By 0.9 seconds, it then increases to reach 600 w/m^2 at 1.2 seconds. Subsequently, it continues to grow at a rate of 100 w/m^2 every 0.3 seconds.

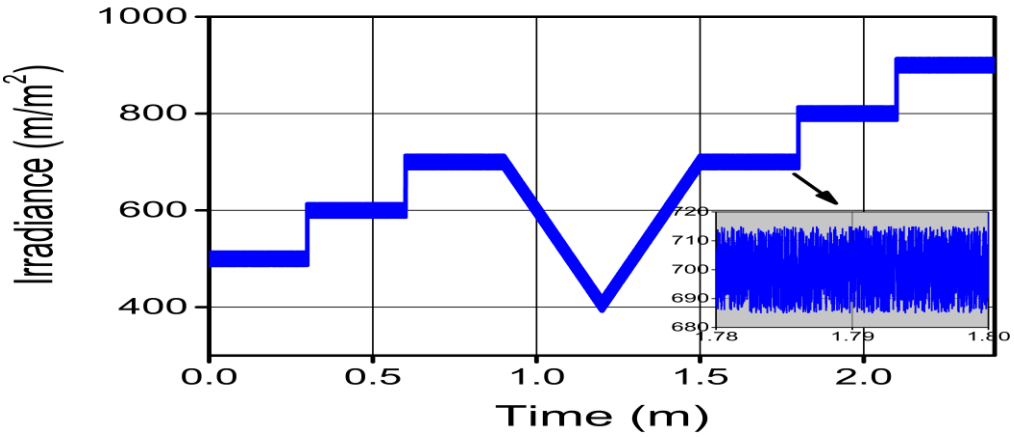


***Fig II. 7**: variation of insolation*

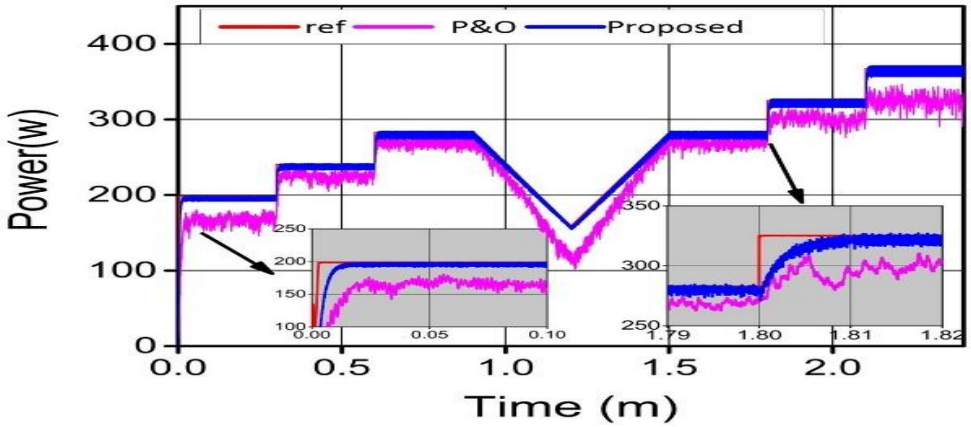


***Fig II. 8**: Waveforms of power with P&O and proposed*

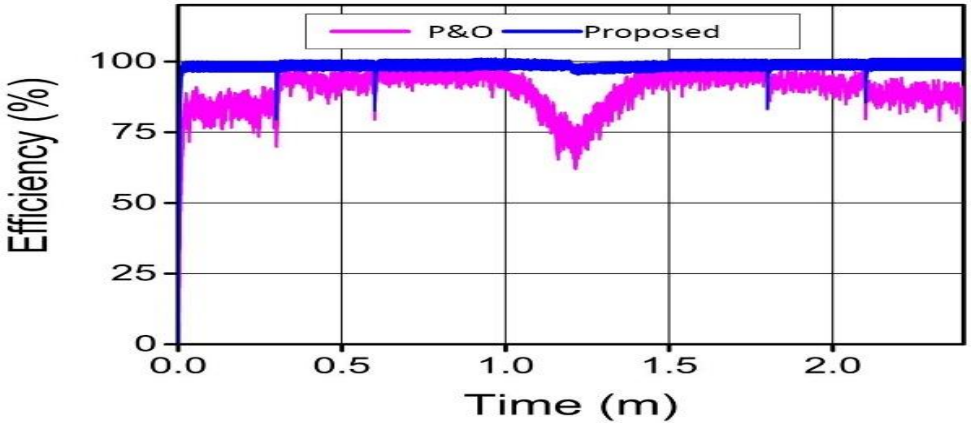


***Fig II. 9**: The efficiency of P&O and proposed*

In Fig II.8, visually illustrate the contrast between P&O and proposed MPPT algorithm. The relevant qualitative comparison is shown. Based on the observed data, the following conclusions may be drawn:

- The P&O MPPT method exhibits more oscillation at the maximum power point (MPP), resulting in larger power loss compared to the proposed MPPT method.
- The period for settling of the FLC MPPT system is shorter compared to the P&O MPPT system. The proposed MPPT system offers improved power stability.
- The proposed MPPT reduces overshoot, resulting in minimal oscillations at the output.
- The use of fuzzy logic based MPPT increases the level of complexity of the system.

The proposed MPPT technology effectively achieved maximum power tracking. The tracking efficiency achieved with the proposed MPPT approach is 98.77%. The greatest power measured and the corresponding photovoltaic (PV) system. When comparing the tracking achieved using FLC with that gained using the P&O MPPT approach, it was found that the P&O method successfully tracked the maximum power. However, the oscillation around the maximum power

was greater compared to the FLC method. However, the tracking efficiency achieved with the P&O MPPT technique is 92%, which is lower than that achieved with the proposed MPPT method.

II.4 Energy storage system in microgrid

Power and energy density are two characteristics of energy storage systems (ESS), exemplified by batteries that possess low power and high energy density; yet, issues arise in power management due to their slow dynamic response. Conversely, SCs and FES are capable of satisfying substantial power requirements. No modern energy storage system technology can concurrently meet the energy and power density requirements as seen in the Ragone plot in Fig II.10. The classification of ESS is shown in Fig II.11. Given this restriction, it is imperative to include different energy storage systems, referred to as a hybrid energy storage system (HESS). As a result, the advantages of each ESS are consolidated inside the integrated system to fulfill specific needs, withstand adverse circumstances, reduce system size and cost, and enhance system performance and efficiency. HESS further mitigates dynamic stress in storage components, enhancing their lifespan and optimizing functionality [163],[95]. HESS is a synthesis of HPS and HES. HPS rapidly adjusts and may provide brief bursts of power injection or absorption.

It effectively diminishes high-frequency oscillations. The elevated expense of HPS, however, restricts its widespread use. HES has substantial ESS potential and aids in mitigating low-frequency fluctuations, albeit its economical nature. HPS mostly comprises SC, FES, and SMES, while HES predominantly consists of PHES, CAES, FC, and vanadium redox batteries [164], [165].

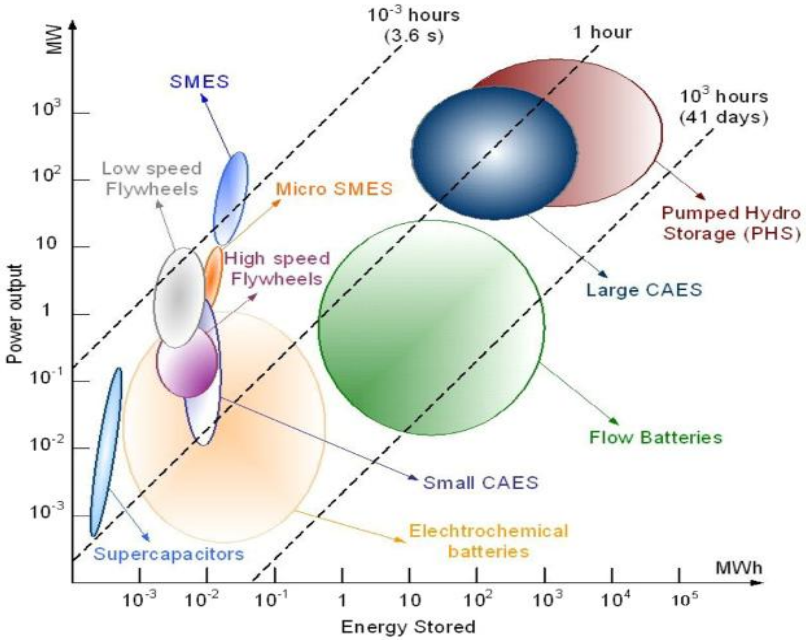


***Fig II. 10**: Power and energy density of storage devices*

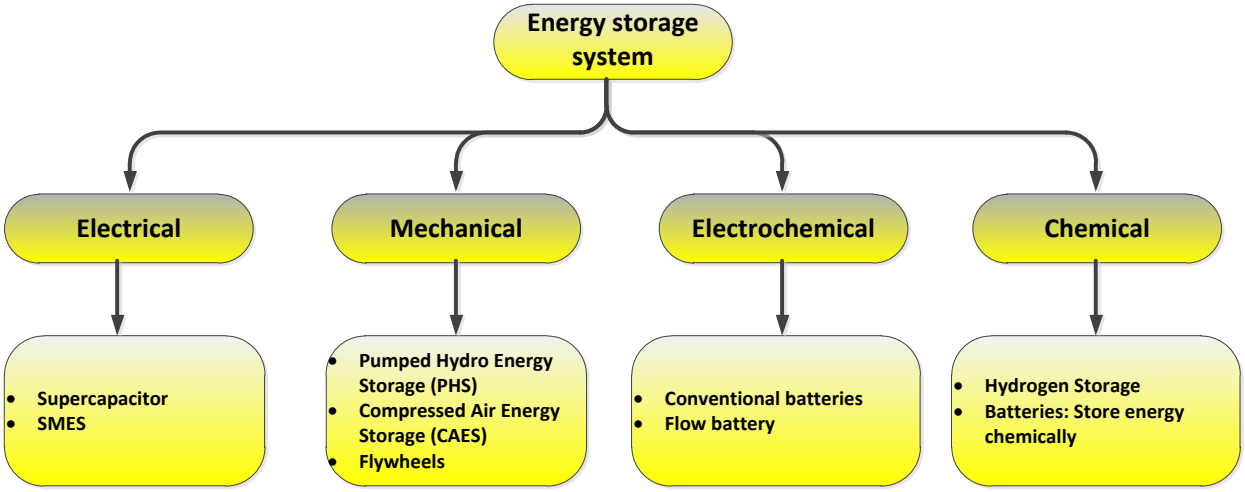


***Fig II. 11**: Classification of energy storage system*

II.4.1 Battery

The battery has significant promise as a technology for regenerative energy storage in hybrid systems due to its low self-discharge rate, rapid dynamic response, and high energy density. An analogous circuit for the battery is employed to examine its behavior, as seen in Fig II.12. The nonlinear voltage is modified according to the charging method to maintain the battery's capacity within an acceptable performance range. In discharge mode, the voltage is calculated as follows [166]:

$$V_{b,dis} = f_1(I_b t, I_b^*, I_b) \quad \text{II.19}$$

$$V_{b,dis} = V_o - K\frac{Q}{Q - \int_0^t I_b dt} I_b^* - K\frac{Q}{Q - \int_0^t I_b dt} \cdot \int_0^t I_b dt + A_b exp\left(-B \cdot \int_0^t I_b dt\right) \quad \text{II.20}$$

where, $V_{b,dis}$- non-linear voltage during discharging mode, V_o - constant voltage. I_b^* - dynamics of low-frequency currents. I_b - battery output current. A_b - exponential voltage; K - polarization constant (V·A·h^{-1}), B - Exponential Capability Ah^{-1}, Q - battery capacity.

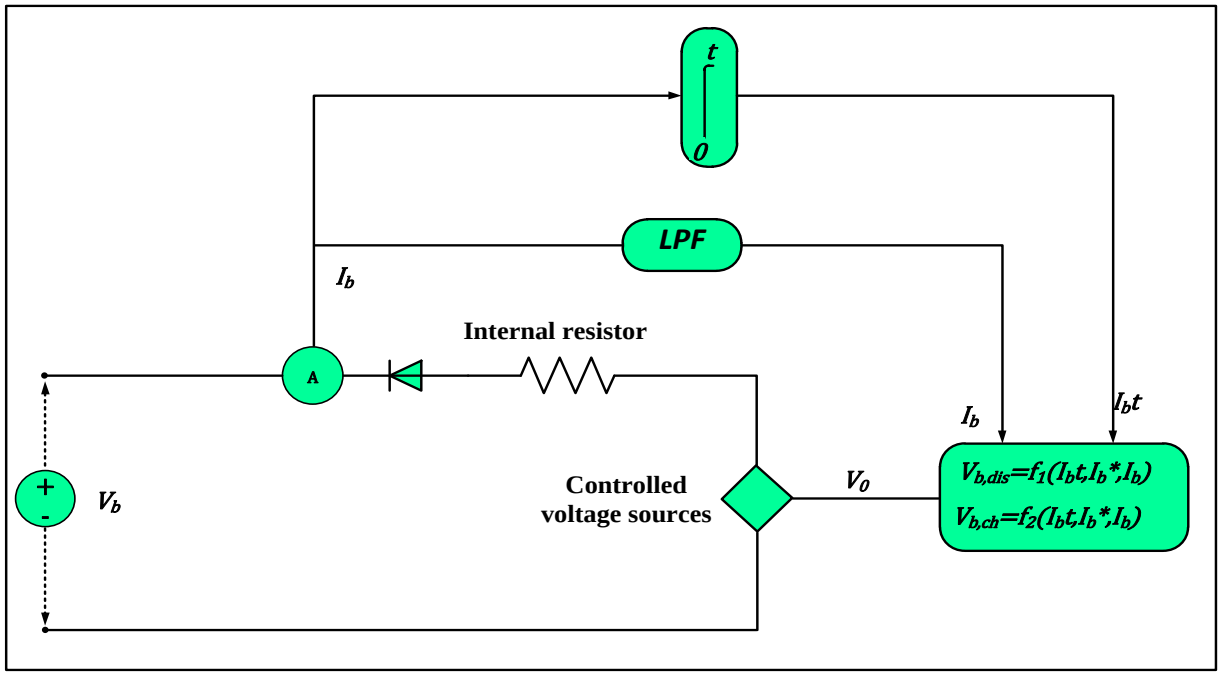


***Fig II. 12**: Battery model*

The polarization resistance $K\frac{Q}{Q-\int_0^t I_b dt}\cdot\int_0^t I_b dt$ is calibrated for the charge mode to demonstrate performance during the last phase of the charging process due to the battery's rapidly escalating voltage. Consequently, the voltage is established by [31].

$$V_{b,ch} = f_2(I_b t, I_b^*, I_b) \quad \text{II.21}$$

$$V_{b,ch} = V_o - K\frac{Q}{Q-\int_0^t I_b dt}I_b^* - K\frac{Q}{Q-\int_0^t I_b dt}\cdot\int_0^t I_b dt + A_b exp\left(-B\cdot\int_0^t I_b dt\right) \quad \text{II.22}$$

where, $V_{b,ch}$ denotes the nonlinear voltage during the charging phase. The output voltage of the battery model is articulated as follows [32]:

$$V_b = V_o + R_b I_b - \frac{KQ_b}{Q_b + \int I_b dt} + A_b exp\left(B_b \int I_b dt\right) \quad \text{II.23}$$

The battery's state of charge (SOC) may be determined by using the maximum capacity and the variation of current charge.

$$SOC = 100\left(1 + \frac{\int I_{bat} dt}{C_{bat}}\right) \quad \text{II.24}$$

Where B_b stands for the battery's internal resistance, V_0 for its open circuit voltage, I_b for its charging current, K for its polarization voltage, C_b for its capacity, A_b for its exponential voltage, and B_b for its exponential capacity.

It is important to keep in mind that the energy restrictions of the battery should be seen as the state-of-charge limits as well as the charging and discharging speeds [36].

$$SOC_{MIN} \leq SOC_t\ (t) \leq SOC_{MAX} \qquad \text{II.25}$$

II.4.2 Supercapacitor

The supercapacitor functions as a high-power density electrical component with a rapid dynamic response. To compensate for the maximum power demand due to abrupt load fluctuations, the hybrid system may either discharge more power or save additional regenerative energy. This work uses the Stern model to develop a supply chain model [168]. Fig II.11, illustrates the corresponding circuit of the SC model.
The output voltage of supercapacitors may be expressed as, [169].

$$V_{SC} = \frac{N_S Q_T}{N_P C_{cell}} - R_{SC} I_{SC} \qquad \text{II.26}$$

Where Q_T is the total electric charge (in coulombs), N_S are the cells in series, N_P are the cells in parallel, R_{SC} is the internal resistance, and I_{SC} is the SC's current. The SC voltage V_{SC} and the SC capacitance Q_{SC} are the two factors that determine the SC energy E_{SC}[37]:

$$E_{SC} = \frac{Q_{SC} * V_{SC}^2}{2} \qquad \text{II.27}$$

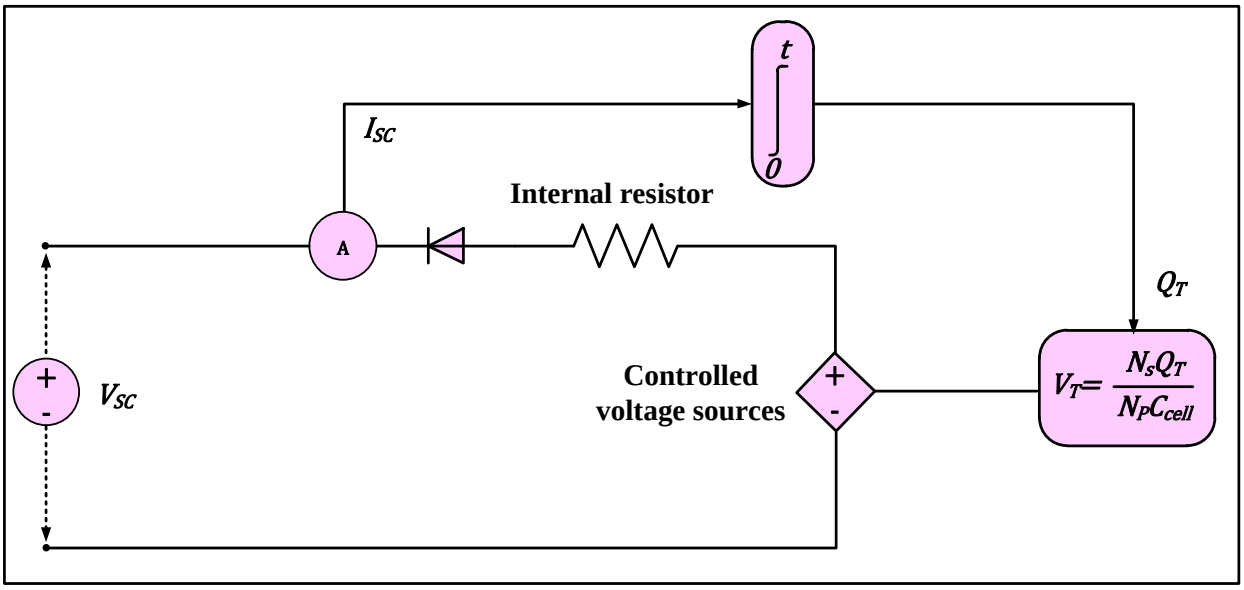


***Fig II. 13**: Model of SC*

$$V_{SC} = \frac{N_S Q_T}{N_P C_{cell}} - R_{SC} I_{SC} \qquad \text{II.28}$$

As a result, if the voltage of the capacitor changes, there will be a corresponding shift in the amount of energy that has been stored, and the SOC_{SC} may be calculated as follows:

$$SOC_{SC} = \left(SOC_{SC}(t_0) - \frac{\int I_{SC} dt}{Q_{SC}} \right) * 100\% \qquad \text{II.29}$$

II.4.3 Energy storage system in microgrid

The operation of the microgrid with a Hybrid Energy Storage System (HESS) is delineated, and the bidirectional DC-DC converter is used to control the HESS. Fig II.14, illustrates that the system comprises four switching devices configured in a bidirectional DC-DC converter arrangement. The converter design specifies a battery voltage less than the DC utility grid voltage but more than the SC voltage. The battery legs are thus associated with higher-frequency inductance L_b . The following sections examine several sorts of operations.

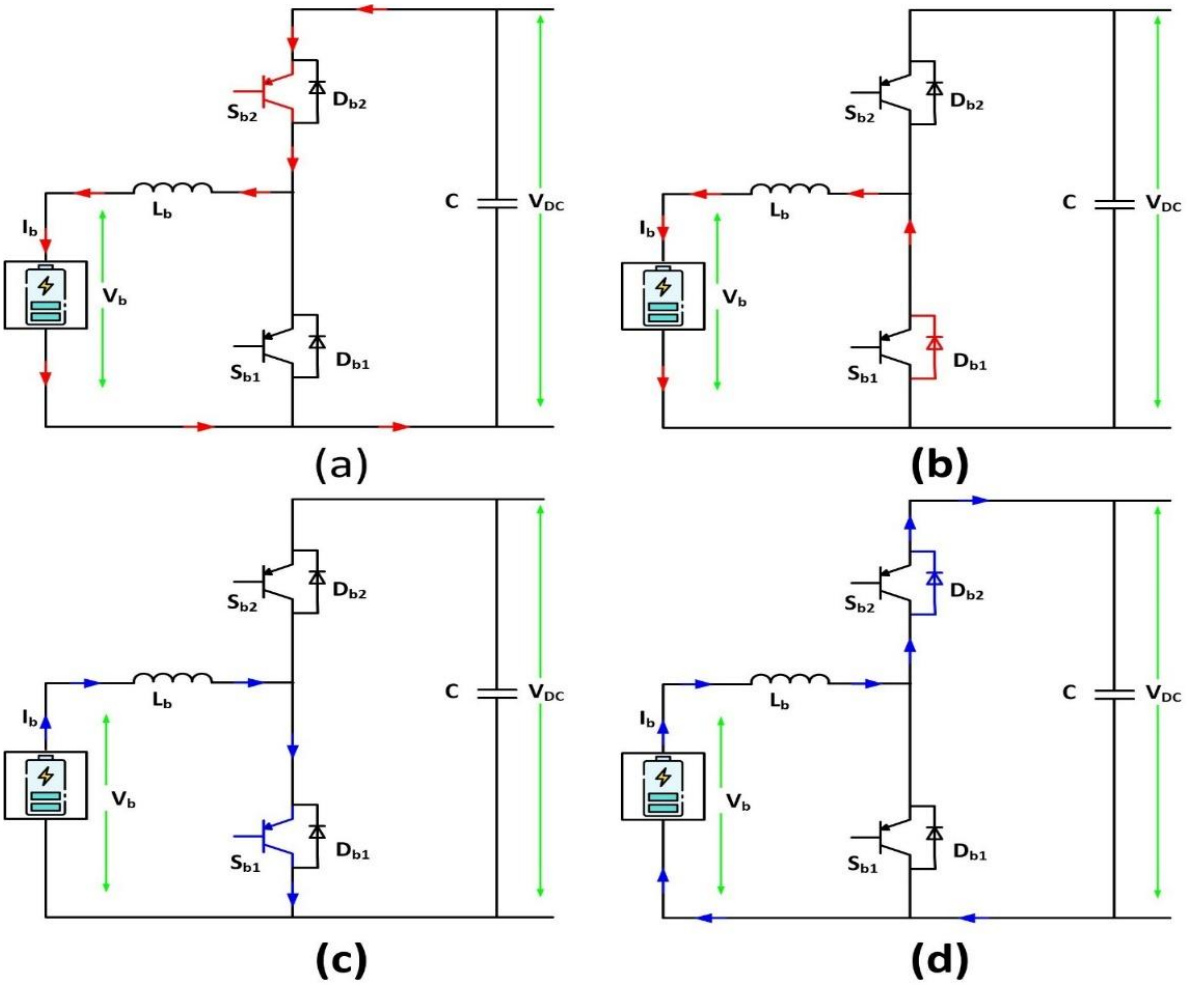


***Fig II. 14**: Bidirectional DC–DC converter charging/discharging equivalent circuit*

- HESS charging mode.

When power generation surpasses the required load or when the demand diminishes, excess power in the DC microgrid results in an increase in the DC grid voltage level. The additional power will be used to charge the HESS, therefore stabilizing the DC microgrid. Consequently, power from the DC grid is sent to the HESS in this condition. As seen in Fig II.14, the actions of the DC-DC converter in this condition may be divided into two distinct time intervals. Switch S_{b1} is activated with a duty cycle during the time interval T1, charging the inductances L_b and Lsc with its respective source V_b. As seen in Fig II.15, the current increases according to the profiles of $(V_{DC} - V_b / L_b$. Subsequent to this period (during T2), two switch devices are deactivated, allowing I_b to traverse D_{b1}.

$$V_b = d_b * V_{DC} \qquad \text{II.30}$$

where d_b is the duty cycles. Energy is conveyed from the DC grid to the HESS. The DC grid network has more potential than the HESS. The bidirectional converter is then used in buck mode to replenish a hybrid energy storage system (HESS).

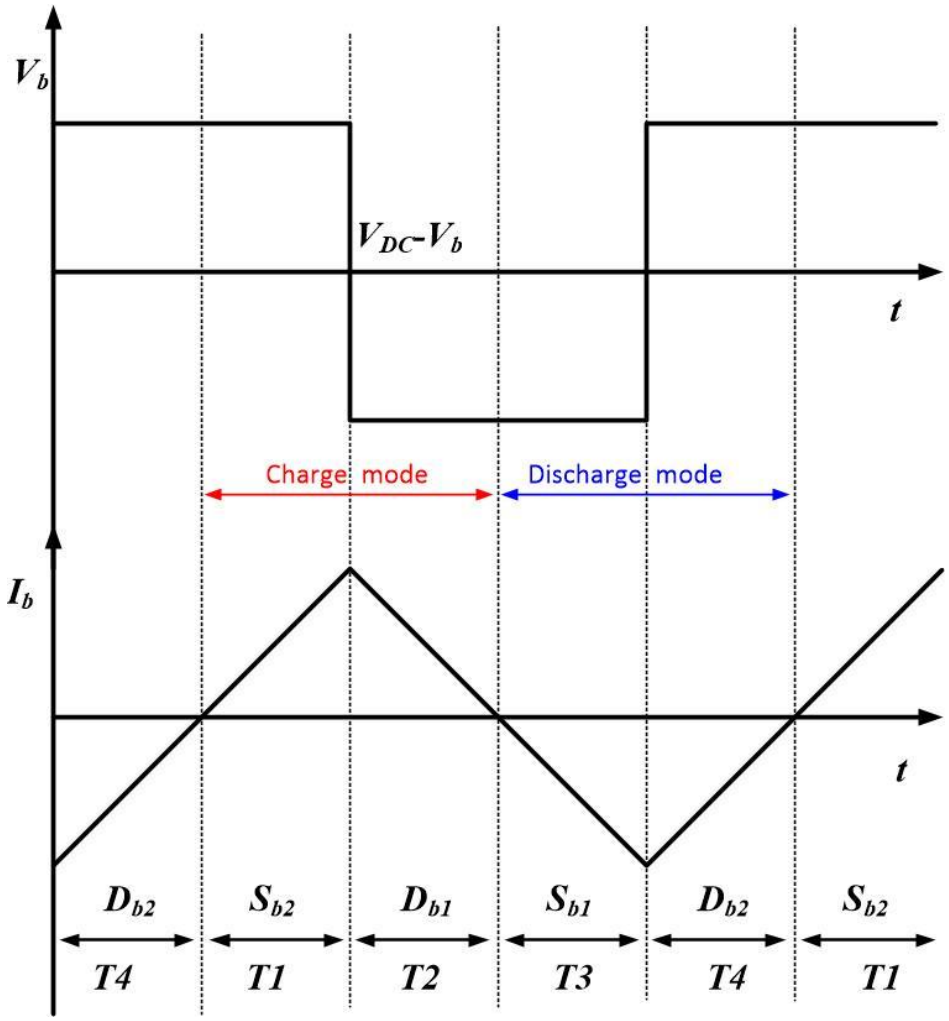


***Fig II. 15**: Steady state HESS charging/discharging waveforms*

- HESS discharging mode.

The voltage in a DC microgrid diminishes as power generation decreases or when demand surpasses producing capacity. HESS must provide power throughout this timeframe. In this condition, power is conveyed from the HESS to the DC grid via the proper management of S_{b1}. As seen in Fig II.14, when switch S_{b1} is actuated during each time interval T3, the inductors L_b mostly collect energy in a reverse manner, and the reverse current flow $I_b$increases at a rate of V_b/L_b. The power transmits via HESS to the DC grid in the ways shown in Fig II.15, after its timespan T3 (during timespan T4) when the cumulative voltages of the battery and inductance exceed the DC grid voltage.

$$V_{DC} = \frac{V_b}{1 - d_b} \qquad \text{II.31}$$

The switches S_{b1} and S_{b2} function complementarily. Only one gate circuit is required for each switching leg.

II.4.4 Converter Structures for HESS

HESS is interconnected with MG, using various converter topologies that significantly influence system performance, operation, and cost implications. Different converter topologies used to integrate HPS and HES for HESS combination are primarily classified into three categories: passive, semi-active, and completely active, as seen in Fig II.16. The primary distinctions among these topologies lie in the quantity and positioning of DC-DC converters that enable bidirectional power transfer between HESS components. The majority of researches used the buck-boost converter as a DC-DC converter and utilized a state-space model for the modeling of DC-DC converters [171],[172].

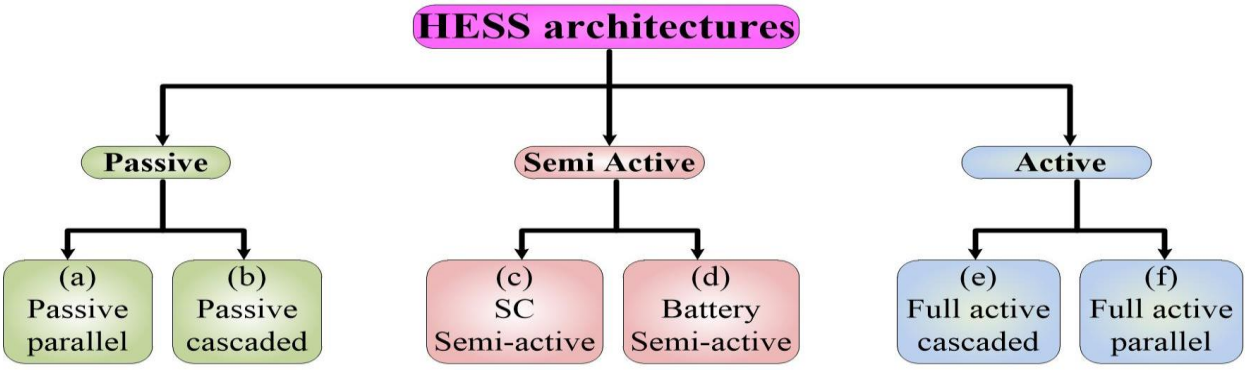


***Fig II. 16**: Classification configuration of HESS*

II.4.4.1 Passive HESS:

The passive topology refers to a simple arrangement in which the terminals of battery and SC are directly connected to the DC bus in series or parallel, as shown in Fig II.17,(a,b), [173]. The electrical properties and time constant of the HESS component play a crucial role in

determining power-sharing in the microgrid (MG). The significant differences in terminal voltages between battery and SC prevent the full use of SC expertise, leading to decreased flexibility and poor volumetric performance. The Passive-HESS architecture is vulnerable to cascading failures caused by direct bus connections during changes in circumstances. The passive architecture is similar to parallel functional synchronous generators, with load distribution determined by the impedance ratio. The output properties of the battery and its internal resistance, which are influenced by factors like as temperature and instantaneous state of charge (SOC), determine the outcome in this case[174]. The combination of a battery and a supercapacitor (SC) requires the SC voltage to be greater than both the DC bus voltage and the battery voltage. The SC cannot fully use its absolute limit, which ultimately reduces its effectiveness [175]. This is the original design of HESS topology and is seldom used in real-world applications.

II.4.4.2 Semi-active HESS:

There are two kinds of semi-active designs, which include connecting a DC-DC converter with one of the HESS sources, as shown in Fig II.17 (c,d). Semi-active topology provides little control flexibility.

- **Battery semi-active**

In a battery/SC, the battery current is able to reject transients when the power converter is connected to the battery. However, the necessity to regulate the load voltage restricts the range of operating voltages for the supercapacitor. The SC's direct connection results in voltage fluctuations on the DC bus. In order to maintain a stable DC bus voltage, it is necessary to use a high-capacity SC, which results in an increased cost [176].

- **SC semi-active**

In a battery/SC, the SC may operate across a wide range of voltages when it is coupled to a power converter. However, it is important to note that load transients can still impact the current of the battery [177]. The DC bus voltage will remain constant as a result of the direct connection of the battery. However, the chosen converter must be able to endure significant variations in voltage and sudden changes in current, which leads to an increase in cost. Semi-active topology provides a limited degree of control flexibility. This architecture is only used in situations when there is little need for control and a substantial cost limitation.

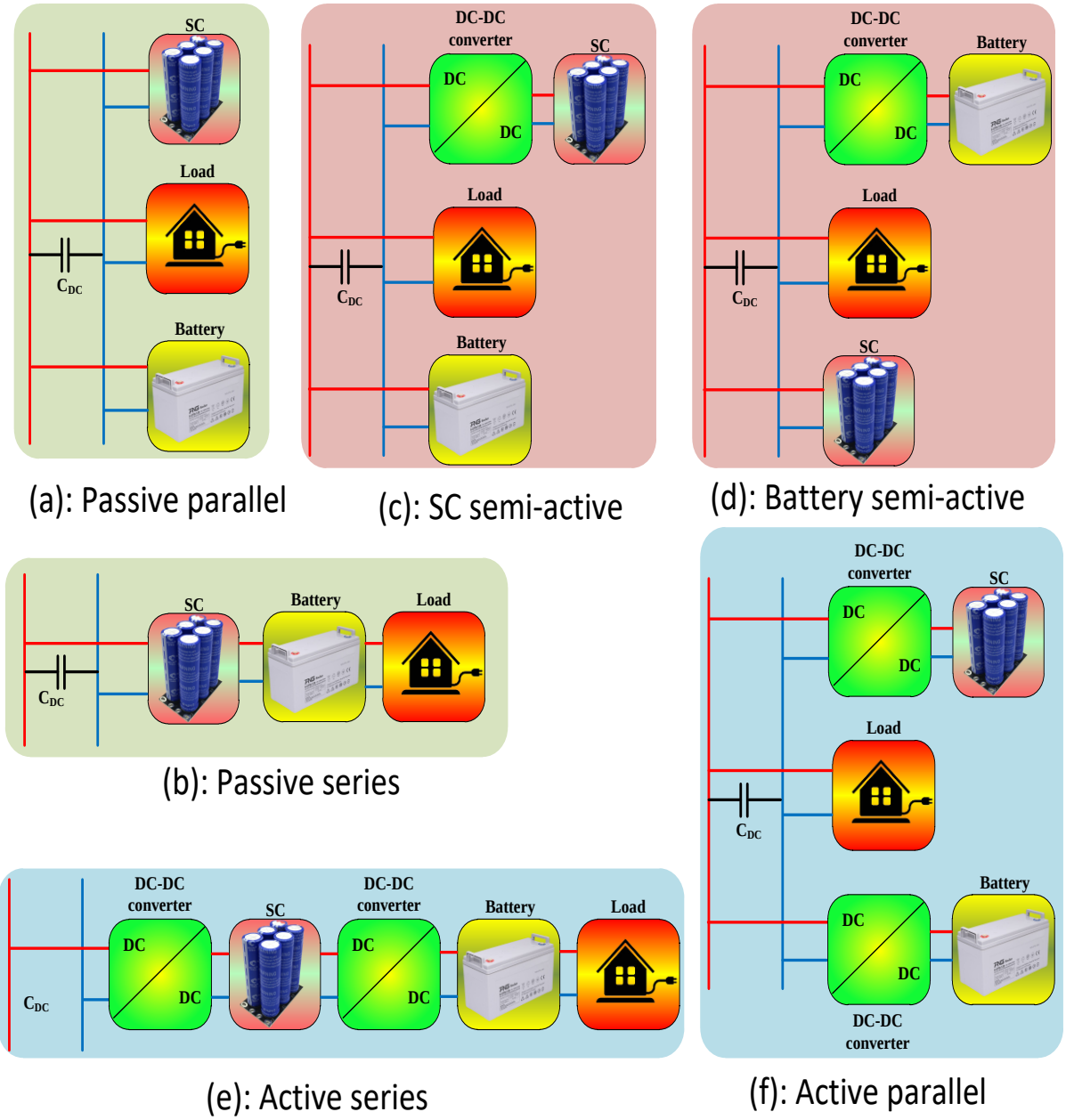


***Fig II. 17**: Different HESS topologies*

II.4.4.3 Full active HESS

An active design includes of private bi-directional DC/DC converters for every single (ESS) device, as shown in Fig II.17 (e,f). The primary advantage of an active topology is that it actively regulates the power of each ESS. However, it also adds complexity, causes losses, and increases costs. Active topologies can be categorized into cascaded and parallel configurations. In reference [178], a parallel active topology was proposed for a battery and supercapacitor (SC) ESS, which were connected to the AC bus independently by individual DC/AC converters and then fed energy to the grid. This topology enhances conversion efficiency and reduces power handling

phases. The parallel active topology is broadly employed in MG. The active topology has several advantages [179]:

1. Separated control of HESS units offers extra flexibility.
2. Various control strategies can be employed.
3. The system voltage is independent of the voltage levels of ESS units.
4. It enhances the intrinsic fault tolerance capacity.

Various indicators of HESS topologies are shown in Fig II.18. The active design offers superior flexibility, controllability, and voltage stability; however, it is accompanied by higher costs compared to alternative topologies. Additionally, it has more space limits.

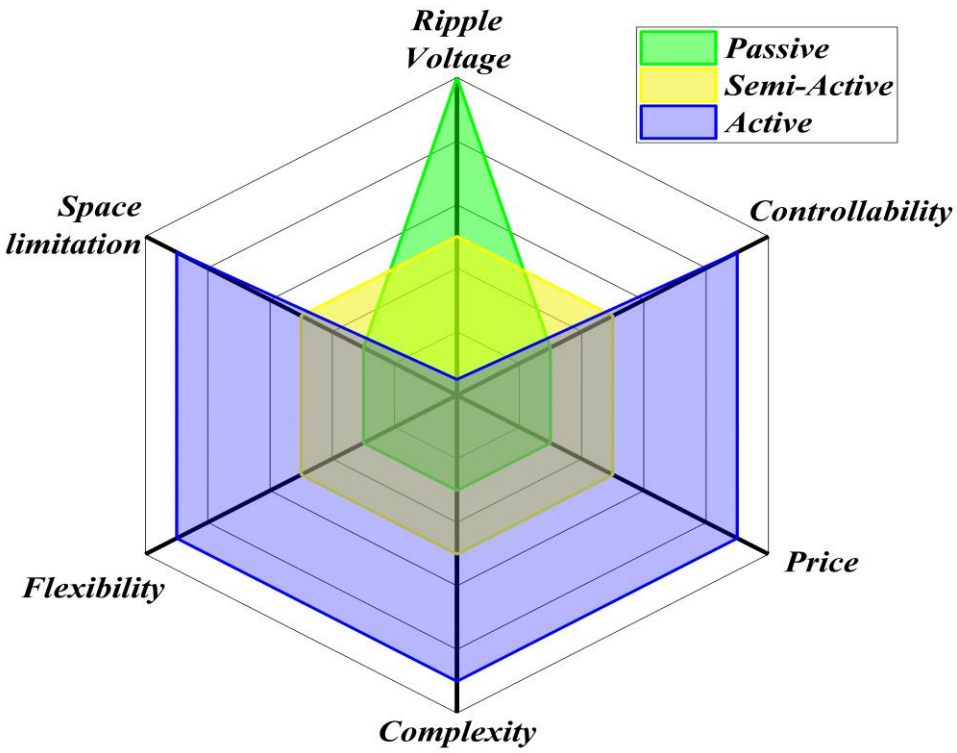


***Fig II. 18**: Comparative of indicators for HESS designs*

II.4.4.4 Cost assessment of HESS

The daily residential average load in the simulation test system is around 240 W, with the peak load reaching $P_{\text{Load_max}}$ = 610 W. The daily energy load requirement is E_{Load}= 210W * 24h = 5.04kWh.

To satisfy this load requirement, the installed capacity of photovoltaic (PV) systems and batteries is determined, resulting in P_{PV} = 205W and E_b = 7200VAh, as shown in [180]. Furthermore, if a supercapacitor is used in conjunction with a photovoltaic and battery system, the net needed installed capacities for each component are P_{PV}= 205W, E_b = 5760VAh, and C_{SC} = 99F (at V_{SC} = 24V). For a comprehensive economic analysis, three cost components are evaluated: the

original cost, the current value of repairs, and the expenses associated with usage and maintenance [181].

II.4.4.5 Initial cost

The initial expenditure associated with acquiring components of the system for the first time is referred to as the "startup cost." The launch pricing of this product is stated as

$$C_{\text{init}} = C_{pv(\text{init})} + C_{\text{batt}(\text{init})} + C_{sc(\text{init})} \quad \text{II.32}$$

where $C_{pv(\text{init})}$ represents the initial cost of the photovoltaic modules, $C_{\text{batt}(\text{init})}$ denotes the initial investment in the battery energy storage systems, and $C_{sc(\text{init})}$indicates the first expenditure for the supercapacitors [182],[183].

II.4.4.6 Present value replacement cost

The expense of fixing system components nearing the end of their service life is included into the current purchase price of these components. This cost also accounts for inflation and interest rates, which may impact the system's present worth. The equation for determining the cost of repairs $C_{rep}$is [184];

$$C_{rep} = C_{\text{unit}}\, C_{\text{nom}} \sum_{i=1}^{N_{rep}} \left[\frac{1+f_0}{1+K_d}\right]^{\frac{N_i}{N_{rp+1}}} \quad \text{II.33}$$

where f_0 represents the inflation rate of the replacement unit, kd denotes the interest rate of the replaced element, N_{i} indicates the number of years, and C_{nom} signifies the value of a system component. Utilizing the Schiffer balanced Ah capacity model, the impact on BESS lifespan via the use of supercapacitors is examined. This technique calculates the lifetime of the BESS by accounting for the corrosive loss $C_c$and degradation C_{dcg} of its materials. A Battery Energy Storage System (BESS) is considered to have reached the end of its useful life when its capacity C_0 falls below 80% of its rated capacity C_0.
The residual capacity of the BESS may be computed as

$$C_r = C_0 - C_c - C_{dcg} \quad \text{II.34}$$

Fig II.19, illustrates the residual battery capacity both with and without the supercapacitor. The battery replacement occurs after 3.5 years when just the battery is used in the system; however, the incorporation of a supercapacitor extends the battery's lifespan by almost an additional 2 years. Consequently, lowering the replacement cost C_{rep}.

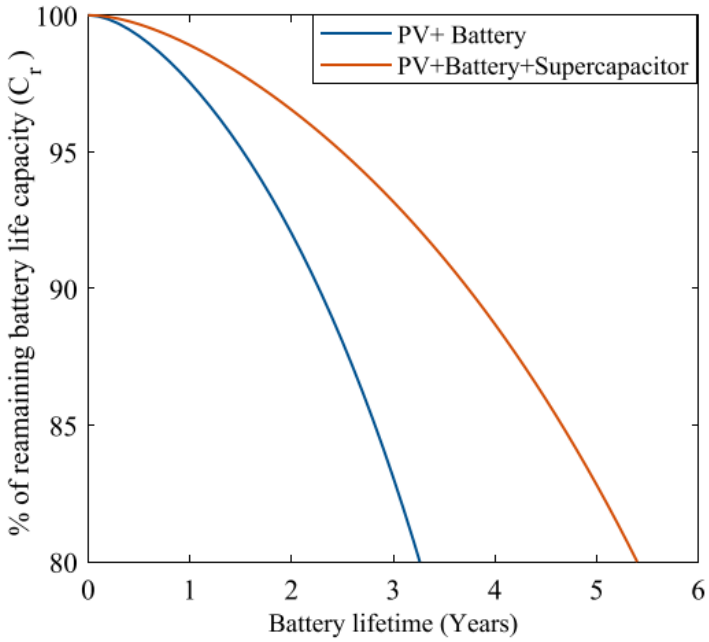


***Fig II. 19**: Compared battery life with and without supercapacitor*

II.4.4.7 Value of operation and maintenance cost:

This cost includes the expenses associated with operating and maintaining each component of the gadget during its lifespan. It is given as

$$C_{0\&m} = \begin{cases} C_{(0\&m)o}\left[\frac{1+f_o}{1+K_d}\right]\left[1-\left(\frac{1+f_o}{1+K_d}\right)^n\right], k_d \neq f_1 \\ C_{(0\&m)o} x n \; k_d \neq f_1 \end{cases} \quad \text{II.35}$$

$C_{0\&m}$denotes the initial operation and maintenance costs, f_1 signifies the inflation rate for these expenses, and n indicates the lifetime in years. The functioning of a supercapacitor necessitates little cost due to the absence of dynamic or moving components.

II.4.4.8 Life cycle cost

The life cycle cost LCC encompasses the initial capital expenditure of the system, the present value of replacement costs for system components across its lifespan, and the present value of operational and maintenance expenses over the system's duration. Therefore, the life cycle cost is defined as [185], [186];

$$LCC = C_{\text{init}} + C_{crep} + C_{o\&m} \quad \text{II.36}$$

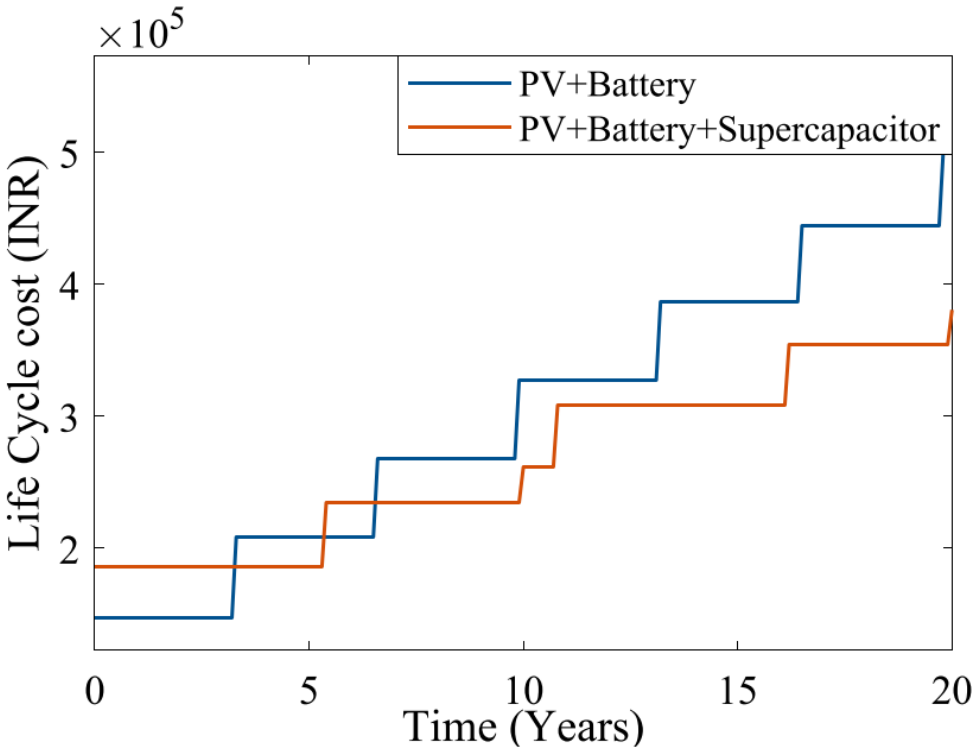


***Fig II. 20**: Total cost expended during the system's 20-year life*

II.5 Simulation results of renewable energy sources with energy storage

II.5.1 Wind energy with energy storage

The RAPS energy-based wind energy employing HESS, battery, and SCs was simulated under varying circumstances in MATLAB/Simulink to evaluate its efficacy [187]. The simulations assume that the battery and SCs are charged and discharged to various degrees. A comparison of the two different simulation designs is provided below. The first test of the exam involves simulating the RAPS without the SCs, and the second test involves simulating the RAPS with the SCs. These experiments were conducted with identical wind velocity and load variation patterns. It cannot utilize an actual RAPS cycle for the test, but in this simulation test, it provided most scenarios: the load was varied.

The findings of the simulation tests are shown in Fig II.21. (a), illustrates the wind speed proposed [12.8,14.7,12.8,10.5,9,7] m/s. Wind power varies in reaction to variations in wind speed, as seen in Fig II.21. (b), and Fig II.21. (c) [600,700,600,500,400,300] watt.

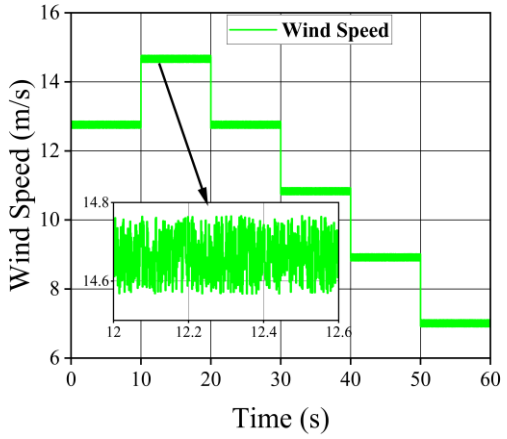
In Fig II.21. (b), the power waveforms of RAPS battery without SC, during the period 0 to 10s and 25s to 60s the power load needs are more than the power generated by wind turbine the battery compensates this deficit of power. And second case is the period from 15s to 20s the power production from wind are more than power needs, the battery absorbed the excess power. In interval from 10s to 15s the power generated is satisfied the power needs. As shown in Fig II.21.

(c), the power waveforms of RAPS battery with SC, the SC provides the rapid fluctuations in wind power and load, that reduce the stress on battery.

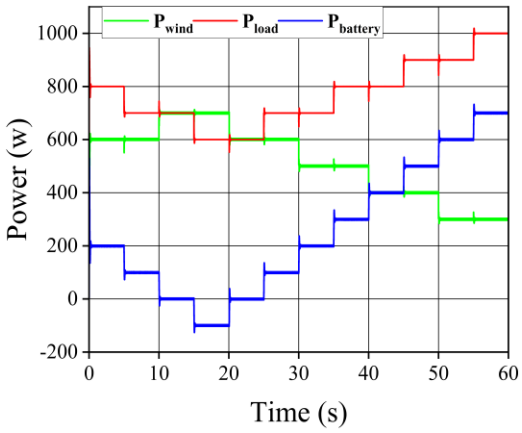
Fig II.21. (d), depicts the batteries and SC currents, with SCs satisfying transient currents and reducing the impacts of peak currents on the batteries in case of hybridization. however, the battery alone provides the transient term and long term together that is impacted in lifespan and effectiveness of battery.

Fig II.21. (e), displays the DC bus voltage, the DC bus voltage reaches the reference at 100v in less than 0.1 seconds for the HESS. Conversely, the battery alone takes 0.55 seconds. The HESS provides faster reaction speed and 5 times less tracking time compared to other criteria like response or tracking time. During steady state, the Hybrid Energy Storage System (HESS) provides a more reliable reaction with little or insignificant deviations around the reference when compared to using just the battery. Unlike the HESS, it is noticeable that the variation of the DC bus voltage is more pronounced when using just the battery. The variance in the battery alone reaches 4V, corresponding to a relative deviation of 4%. On the other hand, the variation is less than 0.5V for HESS, representing a relative deviation of 0.5% of the DC bus voltage, making it eight times smaller. The findings indicate that the HESS effectively regulates the DC bus voltage with little departure from its reference value, outperforming the battery system alone.

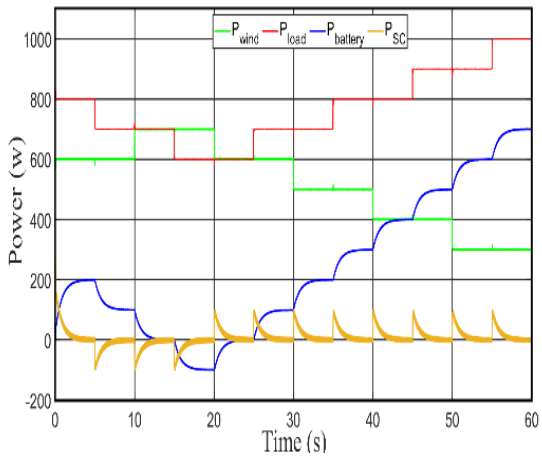
In Fig II.21. (f), the stator current of the PMSG is shown and the stator current's zoom. Fig II.21. (g) shown the state of charge of battery in two cases with SC and without SC. And the state of charge zoom out of long period is displayed in Fig II.21. (h), and comparison of the dynamic behaviors of the DC link voltage illustrated in Fig II.21.(i)



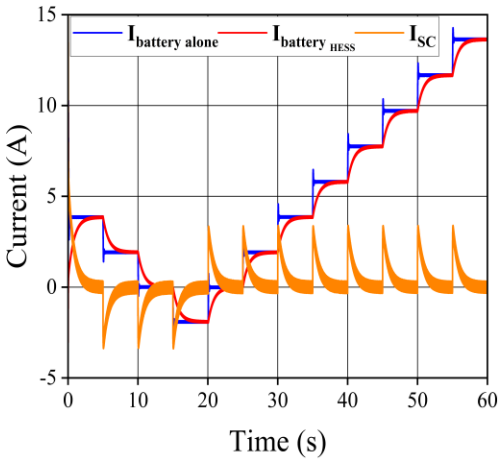
(a)



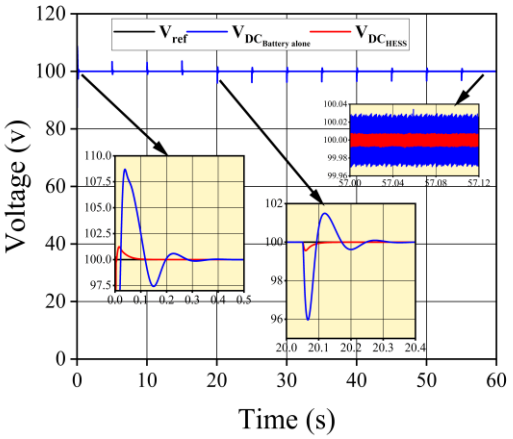
(b)


P wind
P load
P battery
P SC
Power (w)
Time (s)

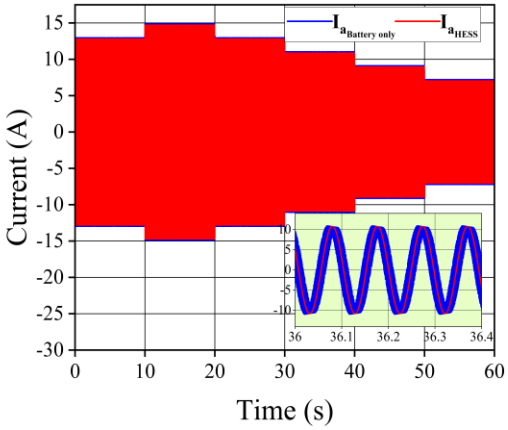
(c)


I battery alone
I battery HESS
I SC
Current (A)
Time (s)

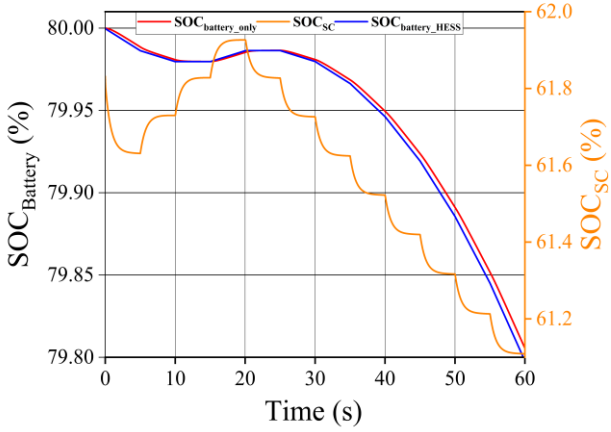
(d)


V ref
V DC Battery alone
V DC HESS
Voltage (v)
Time (s)

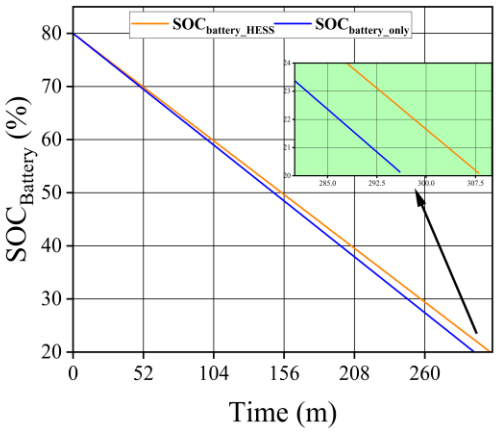
(e)


I a Battery only
I a HESS
Current (A)
Time (s)

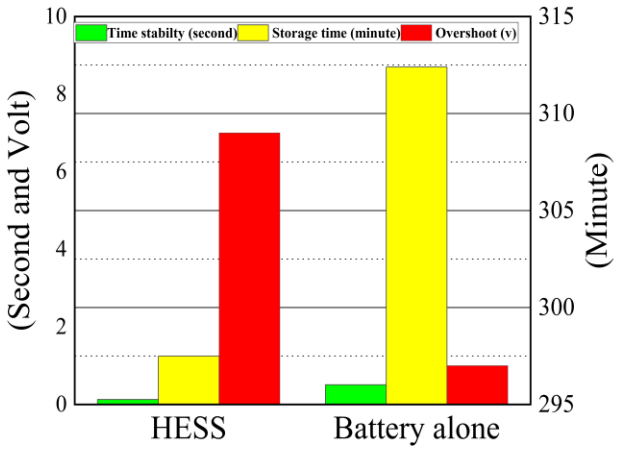
(f)


SOC battery_only
SOC SC
SOC battery_HESS
SOC Battery (%)
SOC SC (%)
Time (s)

(g)


SOC battery_HESS
SOC battery_only
SOC Battery (%)
Time (m)

(h)



(i)

Fig II. 21*: (a): wind speed profile, (b): power without SC, (c): power with SC, d): current of ESS, (e): DC-link voltage, (f): current of PMSG, (g) SOC of ESS (h): zoon out of SOC long time, and (i): comparison of DC link voltage*

II.5.2 Photovoltaic energy with energy storage

In this test a comparatives simulation between battery alone and battery with SC were obtained. Figs II.22 – II.27, provide comprehensive details on the power waveform and current load for both cases: the battery operating independently and the battery combined with SC, respectively. Whereas, the battery/SC more stability and the fast response dynamic to the variations of PV production and load demand. Furthermore, Fig II.22, demonstrates the power stability and efficiency of the battery alone and the current battery/SC. The states of charge of HESS present in fig II.25. The integration of SC decreases the discharge of battery by 2.25 % for each charge/discharge cycle. likewise, Fig II.26, demonstrates the ability of the battery alone and the battery/SC combination to accurately monitor the DC bus voltage.

The obtained findings demonstrate that the battery/SC successfully reduces the impact of load and PV disturbance, ensuring that the DC bus voltage remains at its desired value of 100 V. Additionally, it efficiently distributes the power flow between the battery and the supercapacitor. Furthermore, the findings indicate that, during transient periods, the battery/supercapacitor combination has less significant variations in magnitude compared to the battery alone. In order to showcase the effectiveness of the battery/supercapacitor (SC), we recognize the voltage overshoot/undershoot and settling time required to restore the direct current (dc) bus voltage in the aforementioned scenarios. The spider graph visually depicts the comparison between a battery only and a battery combined with a supercapacitor.

The settling time for the battery/SC system is 0.16 seconds, whereas the settling time for the battery alone is 0.41 seconds. The deviation in load fluctuation of ± 0.5kW results in an overshoot of

15.86% and an undershoot of -21.29% when using just the battery. When using both the battery and the SC, the overshoot is reduced to 1.58% and the undershoot is -1.63%, as shown in fig II.27.

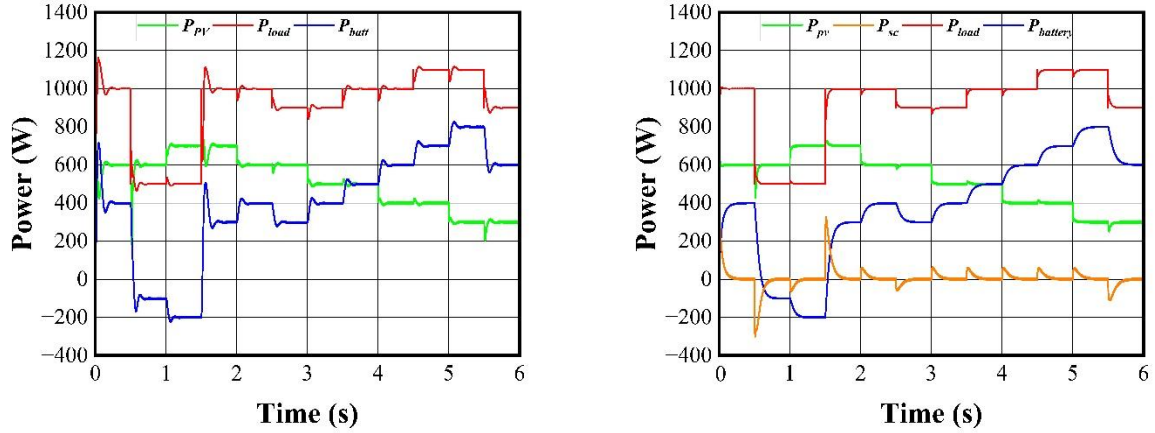


***Fig II. 22**: Power waveforms of battery alone and battery/SC*

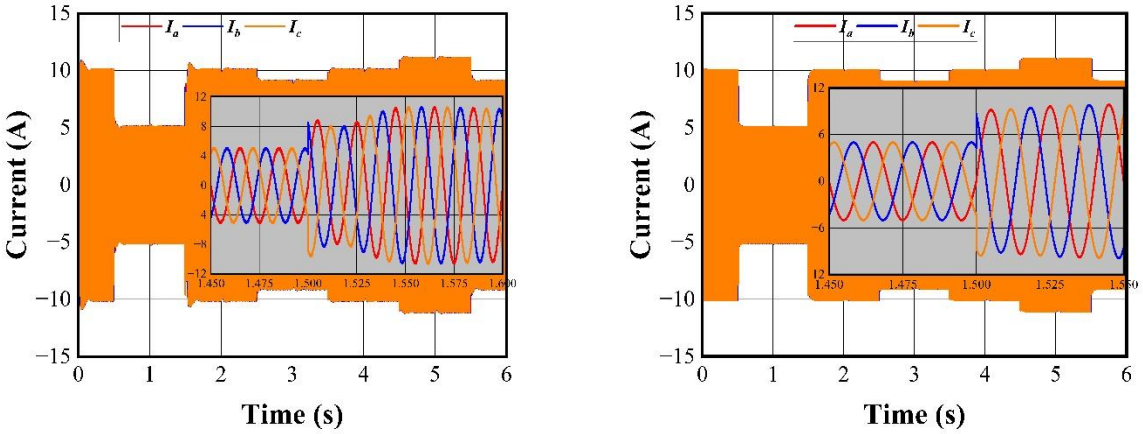


***Fig II. 23**: Current load in case of battery alone and battery/SC*

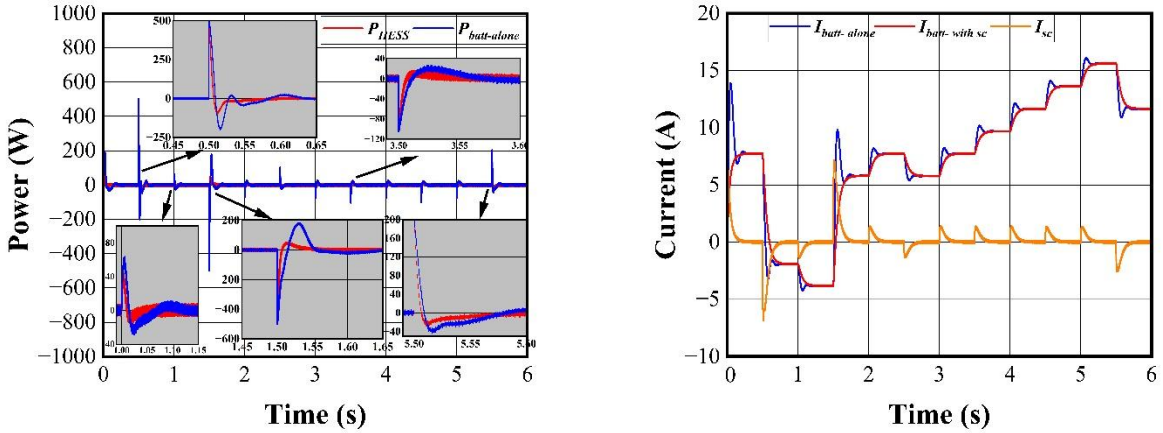


***Fig II. 24**: Power balance and current of battery and SC in case of battery alone and battery/SC*

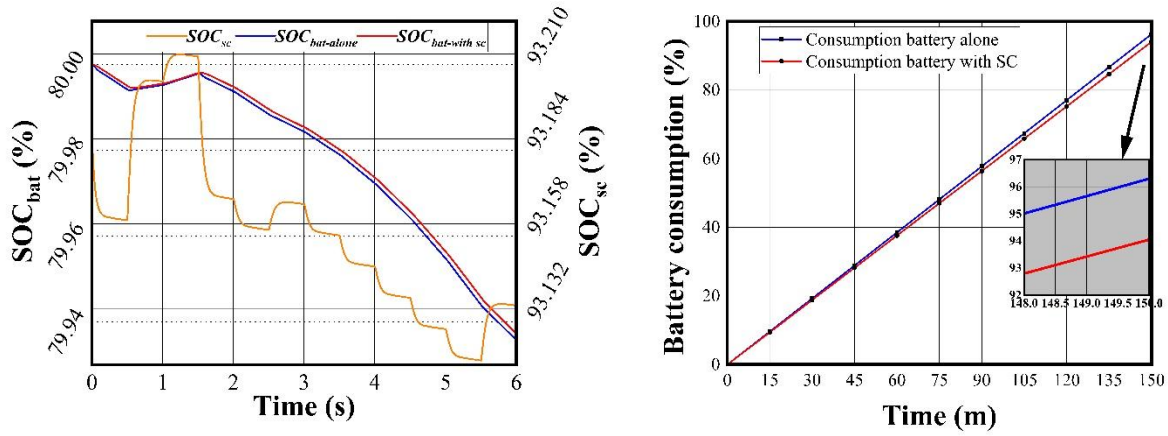


***Fig II. 25**: SOC and energy storage consumption in case of battery alone and battery/SC*

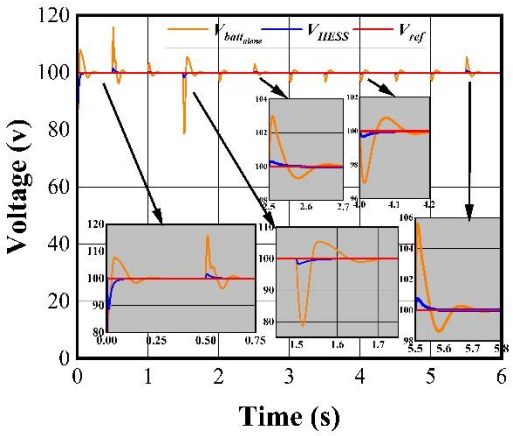


***Fig II. 26**: DC link voltage in case of battery alone and HESS*

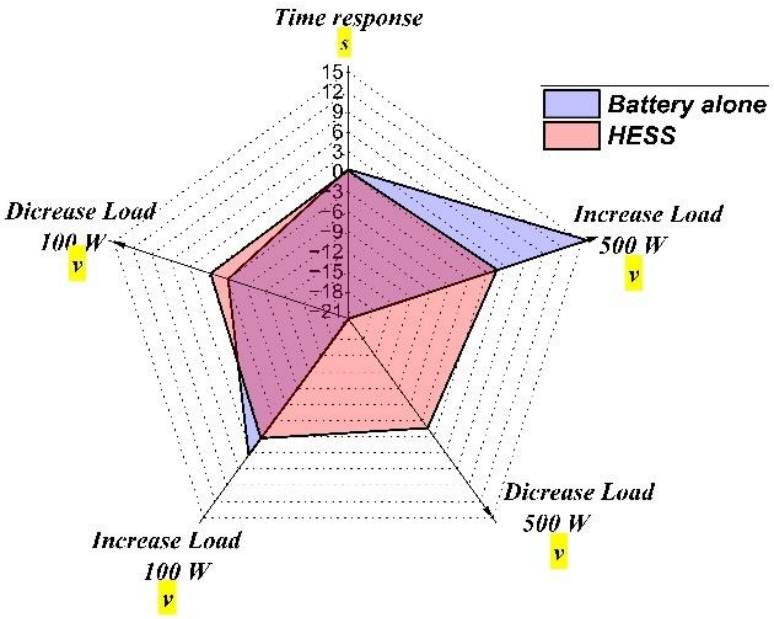


***Fig II. 27**: DC link voltage by response time and peak of variation load*

II.6 Conclusion

In conclusion, this chapter has presented a global overview of renewable energy developments, emphasizing the significant capacity additions and technological advancements witnessed in 2023. The remarkable growth of solar and wind energy highlights the potential for renewable sources to reshape the energy landscape. Additionally, the exploration of modeling techniques for PV and wind energy systems, alongside the integration of hybrid energy storage systems, reveals critical insights into system performance and operational efficiency. The simulation results demonstrate the comparative advantages of utilizing supercapacitors alongside batteries, illustrating the dynamic interplay between different energy storage solutions. As we move forward, addressing the operational and maintenance costs will be essential for maximizing the benefits of renewable energy systems. This chapter lays the groundwork for further exploration of innovative strategies and technologies that can enhance the integration of renewable energy within microgrids, ultimately contributing to a sustainable energy future.

Chapter III

Techno-Economic analysis and optimization sizing of microgrid

III.1 Introduction

This chapter delves into the utilization of HOMER (Hybrid Optimization of Multiple Electric Renewables) as a micropower optimization model for designing both off-grid and grid-connected power systems. HOMER aids in the systematic evaluation of various system configurations by analyzing numerous technological options, fluctuating costs, and energy supply availability. The key functionalities of HOMER—simulation, optimization, and sensitivity analysis—enable comprehensive assessment of potential system designs. By simulating energy balances, optimizing cost-effective configurations, and analyzing sensitivity to variables, HOMER provides a robust framework for optimizing hybrid renewable energy systems (HRES). This chapter outlines the methodology and effectiveness of HOMER in facilitating sustainable energy solutions across diverse applications.

III.2 HOMER pro

III.2.1 Definition of HOMER

HOMER (Hybrid Optimization of Multiple Electric Renewables), the micropower optimization model, streamlines the assessment of designs for both off-grid and grid-connected power systems across diverse applications. When designing a power system, several choices on the system's layout must be made, particularly concerning the components to be included into the design. What is the quantity and size of each component that should be utilized [188]. The multitude of technological possibilities, along with the variability in technology prices and the availability of energy supplies, complicates these considerations. The optimization and sensitivity analysis methods of HOMER provide the evaluation of several potential system configurations.

III.2.2 The functioning mechanism of HOMER

III.2.2.1 Simulation

HOMER replicates system operations by performing energy balance calculations at each time step throughout the year. At each time interval, HOMER evaluates the electric and thermal demand against the energy that the system can provide, subsequently calculating the energy flows to and from each system component. For systems including batteries or fuel-powered generators, HOMER determines the operational status of the generators and the charging or discharging of the batteries at each time step. HOMER does energy balance calculations for each system configuration under consideration. It then assesses the feasibility of a design, specifically its capacity to provide the specified electric demand, and evaluates the costs associated with the installation and operation of the system over the project's lifespan. The system cost estimates include expenses including capital, replacement, operation and maintenance, fuel, and interest.

III.2.2.2 Optimization

HOMER Pro has two optimization techniques. The original grid search technique evaluates all viable system configurations specified by the Search Space. The new HOMER Optimizer employs a patented derivative-free method to identify the most cost-effective system. HOMER thereafter presents a compilation of configurations, arranged by net present cost (sometimes referred to as lifespan cost), enabling the comparison of system design alternatives.

III.2.2.3 Sensitivity Analysis

When sensitivity variables are designated as inputs, HOMER iteratively conducts the optimization procedure for each specified sensitivity variable. For instance, if you choose wind speed as a sensitivity variable, HOMER will simulate system configurations within the specified range of wind speeds.

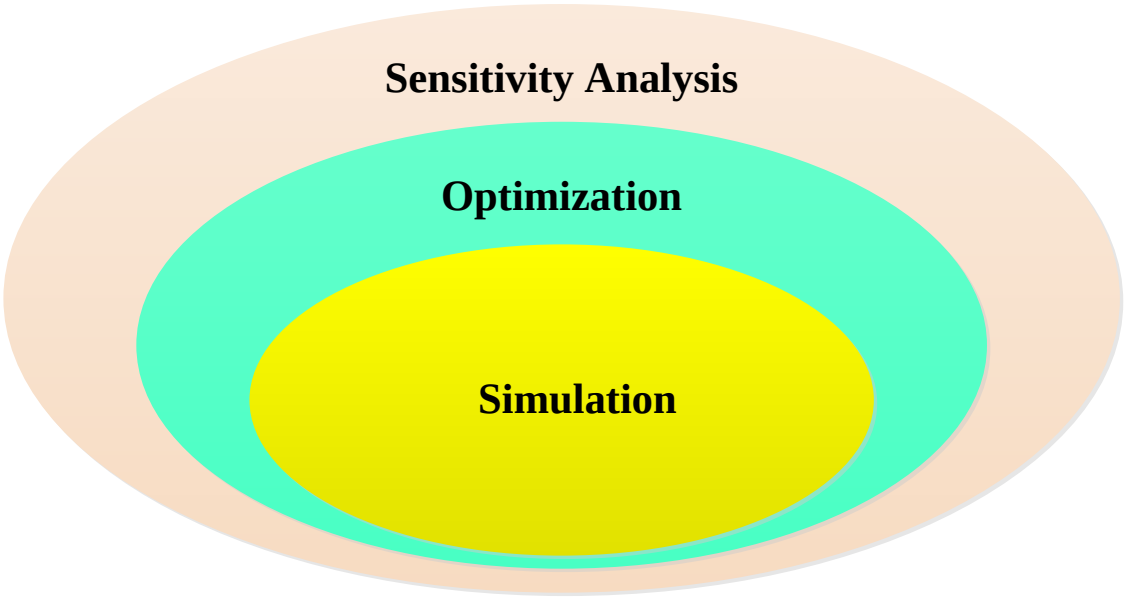


***Fig III. 1**:Structure of function mechanism of Homer*

III.2.3 Addressing Issues with HOMER

HOMER streamlines the design process for distributed generation (DG) systems, applicable to both grid-connected and off-grid scenarios. The optimization and sensitivity analysis algorithms of HOMER enable the assessment of the economic and technical viability of several technology alternatives while accommodating fluctuations in technology expenses and energy resource accessibility. Effective use of HOMER necessitates comprehension of its three fundamental capabilities: simulation, optimization, and sensitivity analysis, as well as their interrelations.
Simulation, Optimization, Sensitivity Analysis

III.2.3.1 Simulation

HOMER fundamentally functions as a simulation model. It will endeavor to replicate a functional system for all conceivable configurations of the equipment you desire to evaluate. Depending on the issue configuration, HOMER may mimic hundreds or even thousands of systems.

III.2.3.2 Optimization

The optimization phase occurs subsequent to all simulations. The simulated systems are organized and refined based on your specified criteria, allowing you to identify the optimal matches. While HOMER is primarily an economic optimization model, it also allows for the minimization of fuel use.

III.2.3.3 Sensitivity analysis

This optional stage enables you to simulate the influence of uncontrollable factors, such as wind speed and fuel prices, and see how the best system adapts to these fluctuations.

III.3 Literature review

The HOMER Pro platform has been used for the optimum capacity sizing of the developed solar, wind, and battery hybrid renewable energy systems (HRES). This program is classified as one of the most comprehensive and potent optimization tools for assisting in the conceptualization of HRES, among 51 optimization tools assessed in [150] and current sizing methodologies examined in [189]. In accordance with this criterion, HOMER Pro was used to devise and model the design optimization of the produced HRES, taking into account actual renewable resources and load profile data. This program has been efficiently used to reduce modeling risk by evaluating all choices and hybridization situations. Examples of most recent studies based on HOMER include but are not limited to the following: electrification of rural villages, such as small Peruvian communities [190], or the over 100 households in a village in [191] , remote islands of which typical examples are represented by a remote community settlement in the North-West of Western Australia comprising 100 dwellings and several small commercial buildings and factories [31] and the Pratas island in Taiwan considering a load demand for electricity mainly owing to the air-conditioning system [192], industrial and commercial buildings, such as the Ethiopian industrial park [33], university buildings in the United Arab Emirates [36], and academic research building in India [35,36], urban cities characterised by hot [193], and cold [32], climatic conditions; reverse osmosis desalination plant [39], water irrigation system considering contemporaneously energy and economic aspects [40] or COE and environmental impacts [180],[126], coastal community [128].

III.4 Materials and methods

Fig III.2, illustrates the flowchart of the implemented techno-economic design methodology. A pre-HOMER evaluation was conducted, using the site resource and load demand data. Furthermore, financial parameters of the project and comprehensive specifications of several energy technologies were gathered. Subsequently, in the investigation of all viable energy system

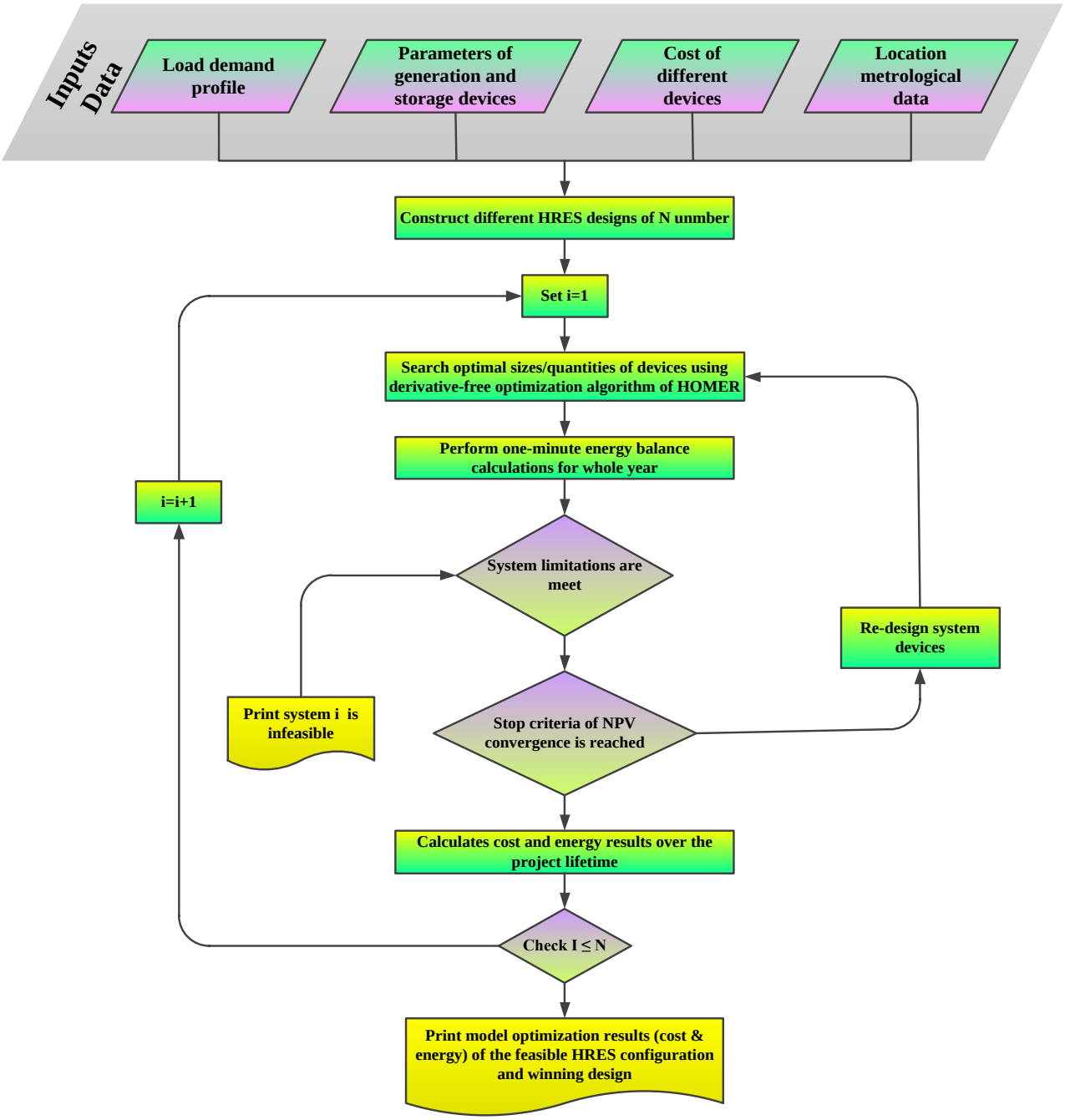


Fig III. 2*:schematic summary of the technique outlined in the paper*

configurations, HOMER developed many hybridization scenarios using the available technological alternatives to meet the load demand and adhere to any additional limits put on

the model. Subsequently, load balancing calculations for each minute throughout the year were performed to assess the viability of each HRES scenario. Utilizing 1-minute power balancing in the design process, rather than the 1-hour resolution often reported in the literature, yielded a more favorable perspective on the total expenses of the HRES, facilitating precise decision-making towards the ideal solution. Techno-economic simulations and optimization assessments were performed for each viable system to ascertain the appropriate dimensions of various components, aiming to minimize the overall net current cost and cost of energy (COE) [194]. Upon achieving the precise convergence value and verifying all viable systems, the optimization concluded, resulting in the selection of a list of possible optimized designs. The HRES configuration that yielded the most favorable outcomes for the research goals was designated as the optimal option for sustainable electrification of the specified location. According to the research literature reported and summarized in Table 1, nearly all of the case studies examined just two features (the technical and economic elements) while designing and optimizing operations. Furthermore, it suffered from a deficiency in implementation control and energy management approaches, resulting in reduced reliability and effectiveness.

III.4.1 Study locations, load profiles and meteorological data

An analysis is conducted to determine the feasibility and suitable size of the microgrid in distinct location in south of Yemen, as seen in Fig III.3. The coordinate for Lahj is 13º03'32.1N, 45º02'22.6E. the electricity consumption patterns of homes are used that fall under the category of small consumers, the peak power requirements are 4.28 kW, and the average is 22.83 kWh/day. The monthly and daily load consumption are illustrated in fig III.4 and III.5.



***Fig III. 3**:The location of the region under investigation*

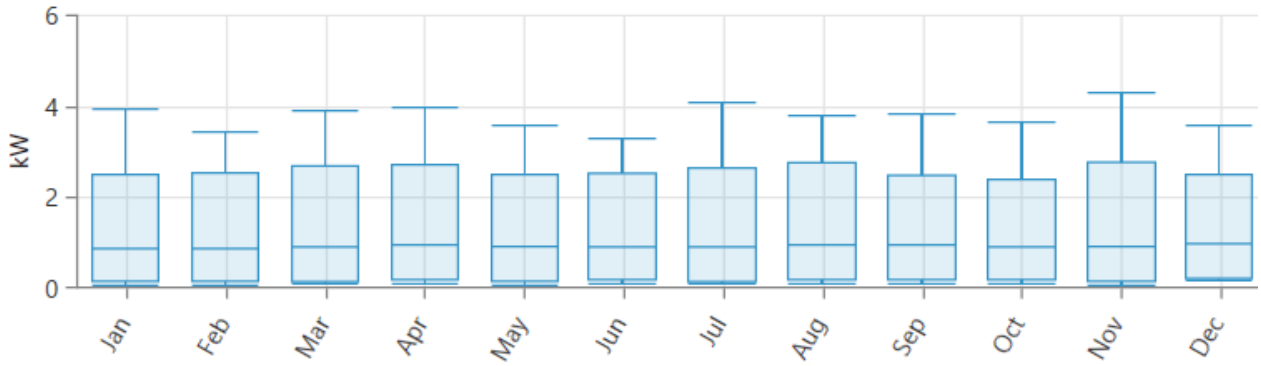


***Fig III. 4**:the monthly load profile*

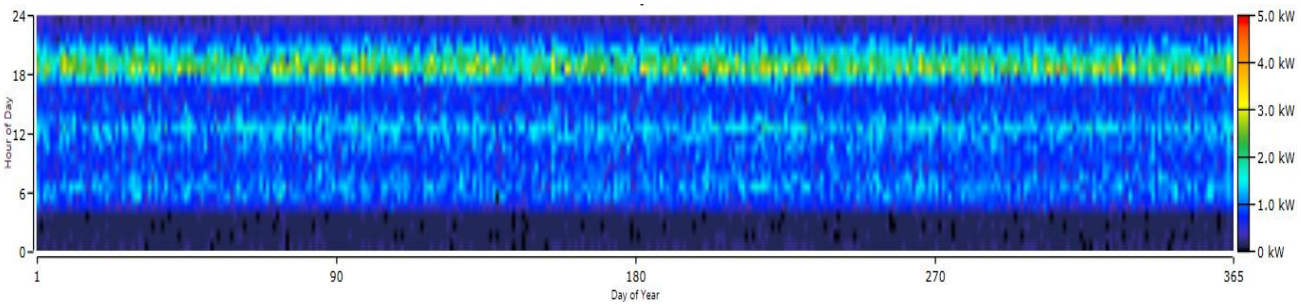


***Fig III. 5**:the daily load profile*

III.4.2 System design

The design was produced using HOMER software, taking into account local circumstances, cost factors, energy resources, and other key simulation parameters. The HOMER optimisation was run for one year in hourly stages to satisfy electrical requirement with the lowest NPC. Several combinations for the distant location were considered, including PV, WT, DG, and battery. As a result, six combinations known as designs #1 to #6 were simulated, as shown in fig 3.6.

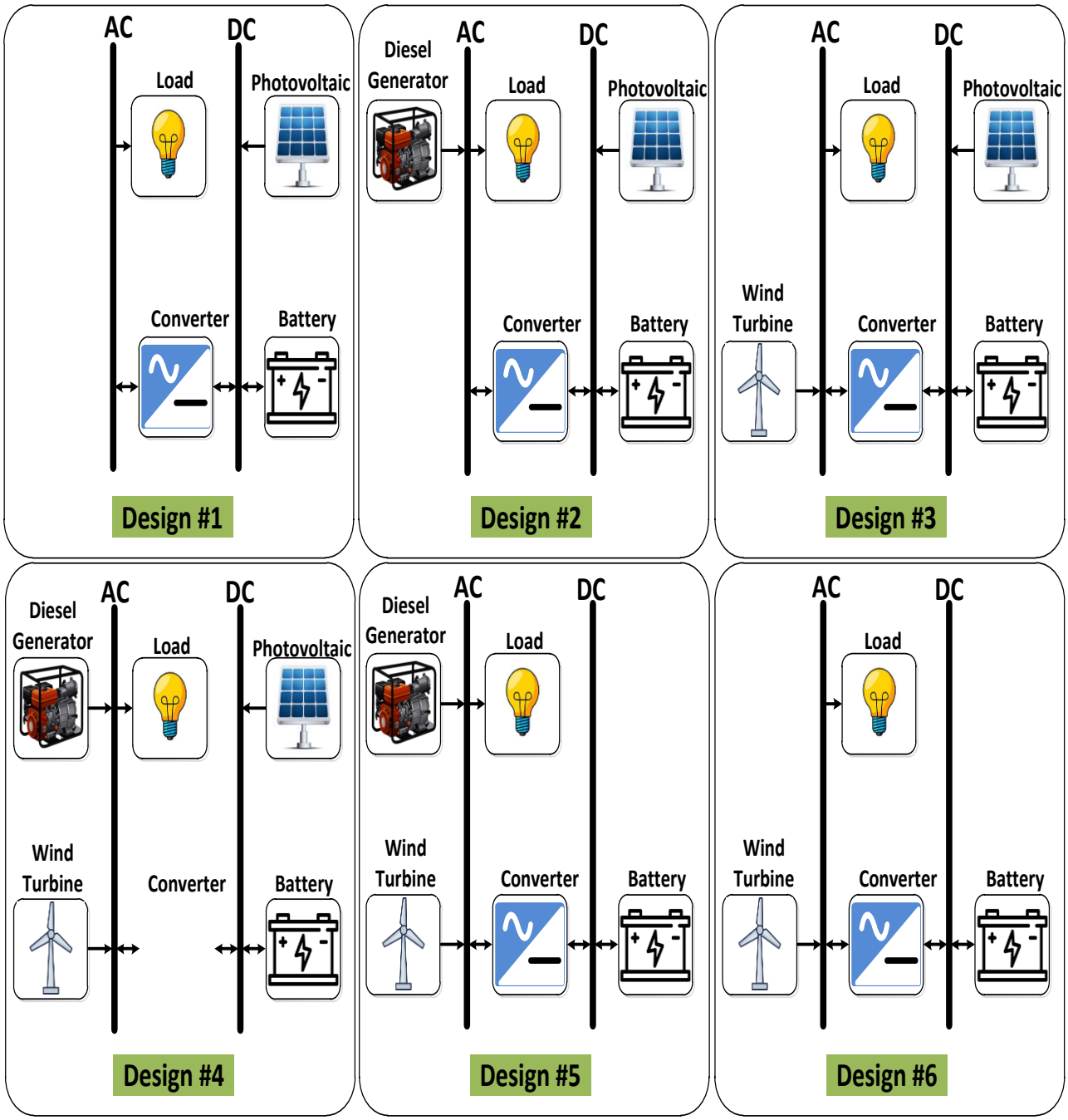


***Fig III. 6**:Visual schematic of six designs*

***Table III. 1**: the optimally configured system from previous studies*

Ref	year	location	MG configuration	mode	EMS applying	Techno-economic	Objectives
[194]	2020	Egypt	PV/WT/DG/ battery	Off-grid	Yes	Yes	design optimization analysis capacity of RES Ensured the stability of the system despite different weather conditions and changes in load. Maintained plenty stored energy at all times
[195]	2023	Malawi	PV/WT/biogas/ battery	On-grid	No	Yes	Performing a techno-economic analysis Reduced grid demand
[193]	2018	Iran	PV/WT/battery	Off-grid	No	Yes	optimal sizing of an off-grid house
[196]	2024	Morocco	PV/biogas/battery	Off-grid	No	Yes	optimal capacity of RES, and achieving the most effective COE reducing greenhouse gas emissions,
[197]	2022	Egypt	PV/WT/battery	remote areas	No	Yes	Investigating the technological and economic feasibility
[198]	2023	Sudan	PV/DG/battery	isolated areas	No	Yes	the optimal sizing of HPS analyzing technical, economic, and environmental aspects.
[199]	2022	Cameroon	PV/FC/Electrolyzer /Biogas/battery/H_2	isolated area	No	Yes	investigated the techno-economic feasibility
[199]	2016	Spain	PV/FC/Electrolyzer /WT/battery/H_2	Off-grid	Yes	Yes	Optimize the cost of energy Increase lifespans of energy system
[200]	2023	Australia	PV/WT/FC/DG	remote island	No	Yes	Techno-economic analysis and optimal sizing of microgrid components.
[38]	2018	KSA	PV/WT/DG/ Battery	Off-grid	No	Yes	analyze the Loss of Power Supply Probability (LPSP), the Cost of Electricity (COE), and the Renewable Factor (RF)

III.4.3 Model component systems

III.4.3.1 Photovoltaic

The electrical power produced from solar PV panels depends on the solar irradiance calculated by HOMER. The power generated from solar PV $P_{S,pv}$is computed as [189]-[201] :

$$P_{S,pv}(t) = P_{Rt,pv} \times d_{loss,pv} \times (I_h(t)/I_{STC}) \times \left[1 + \alpha_{T,p}(T_c - T_{STC})\right] \quad \text{III.1}$$

The variables in the equation are defined as follows: $d_{loss,pv}$ represents the derating factor for PV panels, I_h represents the solar irradiation on an hourly average, I_{STC} indicates the solar irradiation at STC, $\alpha_{T,p}$ represents the temperature co-efficient, T_c refers to the temperature of the PV cell, T_{STC} represents the temperature of the PV cell at STC, and$P_{Rt,pv}$ represents the rated power of a solar PV panel. The technological and economic characteristics of PV model utilised in the research are provided in Table 3.2 and 3.3.

III.4.3.2 Wind Turbine

The WT generator set has a power rating $P_{Rt,WT}$ at the wind speed v_{Rt} that is considered the standard. The electrical output power from the wind turbine generator set, denoted as $P_{WT,G}$ may be calculated using equation [202]-[159].

$$P_{WT,G}(t) = \begin{cases} 00 \le v(t) \le v_{\text{Cuin}}\, v(t) \ge v_{\text{Coff}} \\ v^3(t)\left(\frac{P_{Rt,WT}}{v_{Rt}^3 - v_{Cuin}^3}\right) - v_{C\text{ in}}^3\left(\frac{P_{Rt,WT}}{v_{Rt}^3 - v_{Cuin}^3}\right) v_{\text{Cuin}} < v(t) < v_{Rt} \\ P_{Rt,WT} v_{Rt} \le v(t) < v_{\text{Coff}} \end{cases} \quad \text{III.2}$$

where the cut-in, cut-off, and rated wind speeds are denoted by v_{Cuin} , v_{Coff} , and v_{Rt}, respectively. In Tables 3.2 and 3.3, the techno-economic parameters of the WT model were studied.

III.4.3.3 Deisel Generator

Diesel generators (DG) work as a supplementary power source by supplying backup power and assisting renewable energy sources during times of low electricity output. To ensure a constant flow of electricity and to adapt its output power production to meet unexpected spikes in demand, DG turns on during quiet days or nights when wind and solar power are not sufficient [203].

$$F_C = f_{g,r} \times P_r + f_{go} \times P_r(t) \quad \text{III.3}$$

F_C and P_r indicate the fuel price and output power production from the DG. The variables $f_{g,r}$and f_{go} reflect the intercept coefficient (L/h/kW-rated power) and slope (L/h/kW-output power) of the DG fuel curve. Furthermore, the fuel cost in DG may be expressed as.

$$C_f(t) = P_f \times f_c(t) \quad \text{III.4}$$

The electrical efficiency of the DG may be calculated using the equation.

$$\eta_{DG} = \frac{3.6 \times P_g}{\rho_f \cdot F_c \cdot H_{llf}} \quad \text{III.5}$$

ρ_f, H_{llf}, and η_{DG} represent the fuel density of diesel (kg/m3), the lower heating value of diesel fuel (MJ/kg), and the electrical efficiency of the DG system, respectively. The electrical efficiency of the DG mostly depends on the lower heat value. The particular information on the DG specification and the price used in this research can be found in Tables 3.2 and 3.3.

III.4.3.4 Battery

Batteries are used in hybrid renewable energy systems to store surplus energy and release it when there is an inadequate or nonexistent supply of electricity from renewable sources. Accurate determination of the state of charge (SOC) is essential for measuring energy. The state of charge (SOC) of the battery is determined by the passage of time and may be mathematically computed [191].

$$\frac{\text{SOC}\ (t)}{\text{SOC}\ (t-1)} = \int_{T-1}^{T} \frac{P_b(t)\eta_{\text{batt}}}{V_{\text{batt}}}\, dt \quad \text{III.6}$$

The voltage of the battery is denoted as V_{batt} , the battery's input/output power is represented by P_b, and η_{batt} t refers to the round-trip efficiency of the battery. If the value of $P_b(t)$ is positive, it indicates that the battery is currently being charged. Conversely, if the value is negative, it indicates that the battery is being discharged. Additionally, the round-trip efficiency of a battery may be defined as follows:

$$\eta_{\text{batt}} = \sqrt{\eta^c_{\text{batt}}\, \eta^d_{\text{batt}}} \quad \text{III.7}$$

where η^c_{batt} represents the charging efficiency of the battery and η^d_{batt} represents the discharging efficiency of the battery. The capacity of the battery bank $C_n(Ah)$ is defined as follows:

$$C_n(Ah) = \frac{N_{\text{batt}}}{N_{\text{batt}}^{s}} C_b(Ah) \quad \text{III.8}$$

The variable $C_b(Ah)$ represents the capacity of a single battery, N_{batt} represents the total number of batteries, and N_{batt}^{s} represents the number of batteries linked in series.

III.4.3.5 Converter

The capacity of the converter should be configured to meet the maximum load demand $P_{\text{Load}}^{\text{Max}}$, even in the absence of power delivery on the AC bus. The capacity of the converter is calculated as follows [204]:

$$P_{\text{con}}(t) = P_{\text{Load}}^{\text{Max}}(t)/\eta_{\text{con}} \quad \text{III.9}$$

η_{con} denotes converter efficiency.

III.5 Economic assessment

III.5.1 The net present cost

It is possible to calculate the (NPC) by adding up all of its lifetime expenses and subtracting all of its lifetime revenues. All of the system's expenses, such as the costs of initial, replacement, operation, maintenance, and salvage, considering rate of inflation and interest [190].

$$\text{NPC} = \text{TIC} + \text{TOC} + \text{TRC} + \text{TSC} \quad \text{III.10}$$

$$\text{TIC} = \sum_{\text{k=1}}^{\text{Ncomp}} \text{N}_\text{k} \cdot \text{IC}_\text{k} \quad \text{III.11}$$

$$\text{TOC} = \sum_{k\in \text{ counp}} \sum_{y=1}^{T_{\text{med}}} \frac{1}{\left[1+\left(\frac{d_n-f_r}{1+f_r}\right)\right]^{y}} N_k \cdot \text{ OM}_{\,k} \quad \text{III.12}$$

$$TRC = \sum \frac{1}{\left[1+\left(\frac{d_n-f_f}{1+f_f}\right)\right]^{T_k}} \cdot N_k \cdot RC_k \quad \text{III.13}$$

$$\text{TSC} = \sum_{\text{k}\in \text{ conmp}} \frac{1}{\left[1+\left(\frac{\text{d}_1-f_\text{k}}{1+f_\text{z}}\right)\right]^{T_\text{k}}} \cdot \left(\frac{\text{T}_{\text{k,rem}}}{\text{T}_\text{k}}\right) \cdot \text{N}_\text{k} \cdot \text{RC}_\text{k} \quad \text{III.14}$$

Where (TIC) is the total initial cost, total operating cost (TOC), total replacement cost (TRC), and total salvage cost (TSC) are the corresponding totals for the components. On the other hand, the total capital, operational, replacement, and salvage expenses of unit k are represented by $\text{IC}_{\,k}$,

OMC $_k$, $\mathrm{RC_k}$, and $\mathrm{RSC_k}$, respectively. In addition, T_{project} stands for the project lifespan in years, T_{k} for the overall lifetime of the k component, and $\mathrm{T_{k,rem}}$ for the remaining life of the component at the conclusion of the project in years. $\mathrm{N_k}$ is the quantity of k-type units, d_{r} is the percentage of real savings, $\mathrm{d_n}$ is the percentage of nominal savings, and f_{r} is the percentage of inflation.

III.5.2 The levelized cost of energy

The levelized cost of energy (COE) is the average cost per kWh of useable electrical energy generated by the system. To determine the COE, divide the entire annualised cost by the total electric load provided, using the following the following formula [190], [205]:

$$COE = \frac{\mathrm{NPV} \cdot \mathrm{CRF}\left(\mathrm{d_r}, T_{\mathrm{project}}\right)}{\mathrm{E_{load}}} \quad \text{III.15}$$

$$\mathrm{CRF}\left(\mathrm{d_r}, \mathrm{p}\right) = \frac{\left(\frac{\mathrm{d_a} - \mathrm{f_r}}{1 + \mathrm{f_t}}\right) \cdot \left[1 + \left(\frac{\mathrm{d_n} - \mathrm{f_r}}{1 + \mathrm{t_t}}\right)\right]^{T_{\mathrm{project}}}}{\left[1 + \left(\frac{\mathrm{d_a} - \mathrm{f_t}}{1 + \mathrm{f_t}}\right)\right]^{T_{\mathrm{project}}} - 1} \quad \text{III.16}$$

Where, $\mathrm{E_{load}}$ is total electrical load served, CRF is capital recovery factor

III.5.3 Capacity shortage fraction

(CSF) is also referred to as the loss of power supply probability and is often used as an energy concept to quantify the possibility of an insufficient energy supply to an energy demand [206]. This study defines CSF as the dependability measure, and it is possible to calculate the ratio of energy deficit to load demand over a certain time frame [207]. A number of one indicates that the load is never served, while a value of zero indicates that the load demand is continuously met.

$$CSF = \frac{\sum_{t=1}^{8760} \mathrm{E_{load}}\,(t) - E_{gen}(t)}{\sum_{t=1}^{8760} \mathrm{E_{load}}\,(t)} \quad \text{III.17}$$

III.5.4 Salvage cost

The salvage cost refers to the expected value of a system component after the end of its useful life, assuming linear deterioration. The salvage value of a component grows linearly with its remaining lifespan. Furthermore, the salvage value is determined based on the expense of replacing the item, rather than its initial purchase cost. The mathematical equation for this connection, as used in the following manner, is represented as [208],[209]:

$$C_{\mathrm{sal}} = C_{\mathrm{repl}} \frac{R_{\mathrm{rem}}}{R_{\mathrm{comp}}} \quad \text{III.18}$$

The variables R_{rem} and C_{repl} reflect the cost of replacing the component and the lifespan of the component, respectively. R_{rem}, which is equal to T_{project}, represents the lifespan of the project, which is 25 years.

III.5.5 Excess and unmet electricity fraction

The excess electricity fraction is defined as the ratio of the total amount of excess electricity divided by the total amount of electrical production. it computes using the following equation [188]:

$$f_{\text{excess}} = \frac{E_{\text{excess}}}{E_{\text{prod}}} \quad \text{III.19}$$

The unmet load fraction refers to the percentage of the overall yearly electrical load that was not fulfilled due to inadequate generating capacity. The equation representing the unfulfilled load percent is shown below [188]:

$$f_{\text{unmet}} = \frac{E_{\text{Unmet}}}{E_{\text{load}}} \quad \text{III.20}$$

III.5.6 Renewable fraction

The renewable factor (RF) refers to the amount of electricity generated by renewable energy sources (RES) to fulfil the HMG system's basic load requirement. Radio frequency (RF) explains the limitation on the quantity of power generated by renewable energy sources (RES) as opposed to conventional energy sources (CES). If RF is 100%, it indicates that the load is getting all of its power only from RES. The computation of the RF for the proposed system may be written as:

$$Rf\% = \left(1 - \frac{\sum P_{DG}}{\sum P_{PV} + P_{WT}}\right) \quad \text{III.21}$$

***Table III. 2**: Technical data of the components used in MG*

Elements	Capital	O&M	Replacement	Fuel
Photovoltaic (PV)	1200 $/kW	4 $/kW/year	900 $/kW	-
Wind turbine	2300 $/kW	10 $/kW/year	1650 $/kW	-
Battery	250 $/unit	5 $/unit/year	250 $/unit	-
Diesel Generator	1000 $/kW	0.05 $/op.hour/year	900 $/kW	-
Converter	300 $/kW	-	300 $/kW	0.3 $/L

***Table III. 3**: Definitions of variables.*

Elements	Specification	Value/Unit
Photovoltaic (PV)	Rating of PV panel	1 kW
	Derating factor	85 %
	Temperature coefficient	−0.4 %/°C
	Temperature at standard test conditions (T_{STC})	25 °C
	Lifetime	25 years
Wind turbine (WT)	Rated power	1 kW
	Cut in speed (V_{cin})	2.8 m/s
	Cut out speed (V_{co})	20 m/s
	Rated wind speed (V_{rat})	13 m/s
	Hub height	18 m
	Lifetime	20 years
Diesel Generator (DG)	Rated capacity	1.2 kW
	Fuel curve slope	0.234 L/h/kW
	Fuel curve intercept	24.7 L/h
	Carbon monoxide 1	0.64 g/L of fuel
	Lower heating value	43.2 MJ/kg
	Fuel density	820 kg/m^3
	Carbon content	88 %
	Lifetime	15,000 h
Battery	Nominal capacity (C_b)	2.3 kWh
	Nominal voltage (V_{batt})	12 V
	Max charging current (Imax)	192 A
	Minimum state of charge	30 %
	Maximum state of charge SOC_{Max}	100%
	Round trip efficiency	97 %
	Lifetime	10 years
Converter	Converter's efficiency	95 %
	Relative capacity	100 %
	Lifetime	15 years

III.5.7 Power balance constraint

Based on the power balance equation, there should be a balance between power production and consumption at any given interval. Equation 23 represents the off-grid HMG load demand, which may be met by using power generation from renewable energy sources (RES) and diesel generation (DG). In addition, any excess electricity produced by (RES) and (DG) is used to charge the batteries, and the deficit of electricity to meet the load needs may compensate by the battery [210].

$$P_{PV} + P_{WT} + P_{DG} \pm P_{\text{batt}} = P_{\text{load}} \qquad \text{III.21}$$

III.6 Simulation results

This section provides the specific results collected from the case study. The findings are organized into two primary sections: the outcomes of the design optimization and the results of energy management technique.

Fig III.7, illustrates the monthly average power generation for suitable hybrid designs derived from photovoltaic, wind, and diesel generators for electricity demand community. The photovoltaic array module accounted for 100% of the yearly power generation for design #1 and #2. Subsequently, it was succeeded by the PV (71.7%) and (72.9%). Wind energy production was 28.3% for design #3 and 27.1% for design #4, respectively. The power generated in design #5 was mostly from wind generators (90.5%) and supplemented by diesel generators (9.5%), with diesel use occurring only in May, June, and September. In design #6, all electrical energy was generated by wind turbines. The peak power generation occurred during the period of November to March (dry season). It is prudent to note that the smallest value was observed during the June to September period (rainy season). This finding may be elucidated by the presence of cloud cover throughout the rainy season.

Fig III.8, demonstrates the output power spectrogram of the inverter. It indicates a rise in power between 18:00 and 20:00, which corresponds to the peak electricity demand time displayed. The energy exchange on random days in January was investigated to confirm the 12-day power balancing efficiency throughout all designs in Fig III.9. subsequent to the excess power, unmet demand load, and capacity shortage during the same time illustrated in Fig III.10.
The fig III.11 illustrate the state of charge (SOC) of batteries over 12 days for six designs. Design #1 shows significant fluctuations, with SOC varying between 20% and 100%, and an overall declining trend. Design #2 exhibits moderate fluctuations, maintaining SOC between 30% and 80%. Designs #3 and #4 both start with low SOC, then rise to stabilize between 60% and 100%, with less variability. In contrast, designs #5 and #6 rapidly achieve near-full charge and maintain SOC around 90% to 100%, with minimal fluctuations, indicating superior charge retention. Overall, designs #5 and #6 perform best in sustaining high SOC levels consistently, while Design #1 displays the most variability.

The fig III.12 illustrate the state of charge (SOC) for six battery designs over a year, highlighting daily and hourly variations. Designs #1 to #4 exhibit relatively stable SOC levels, predominantly maintaining high charge states with occasional reductions, as indicated by consistent yellow regions. In contrast, designs #5 and #6 display significant fluctuations, with frequent and pronounced decreases in SOC, evident from the darker bands. This pattern suggests that the first four designs demonstrate superior charge retention and stability, while the latter two exhibit potential inefficiencies and greater variability in performance. Overall, designs #1 to #4 are more effective in sustaining higher SOC levels over the observed period.

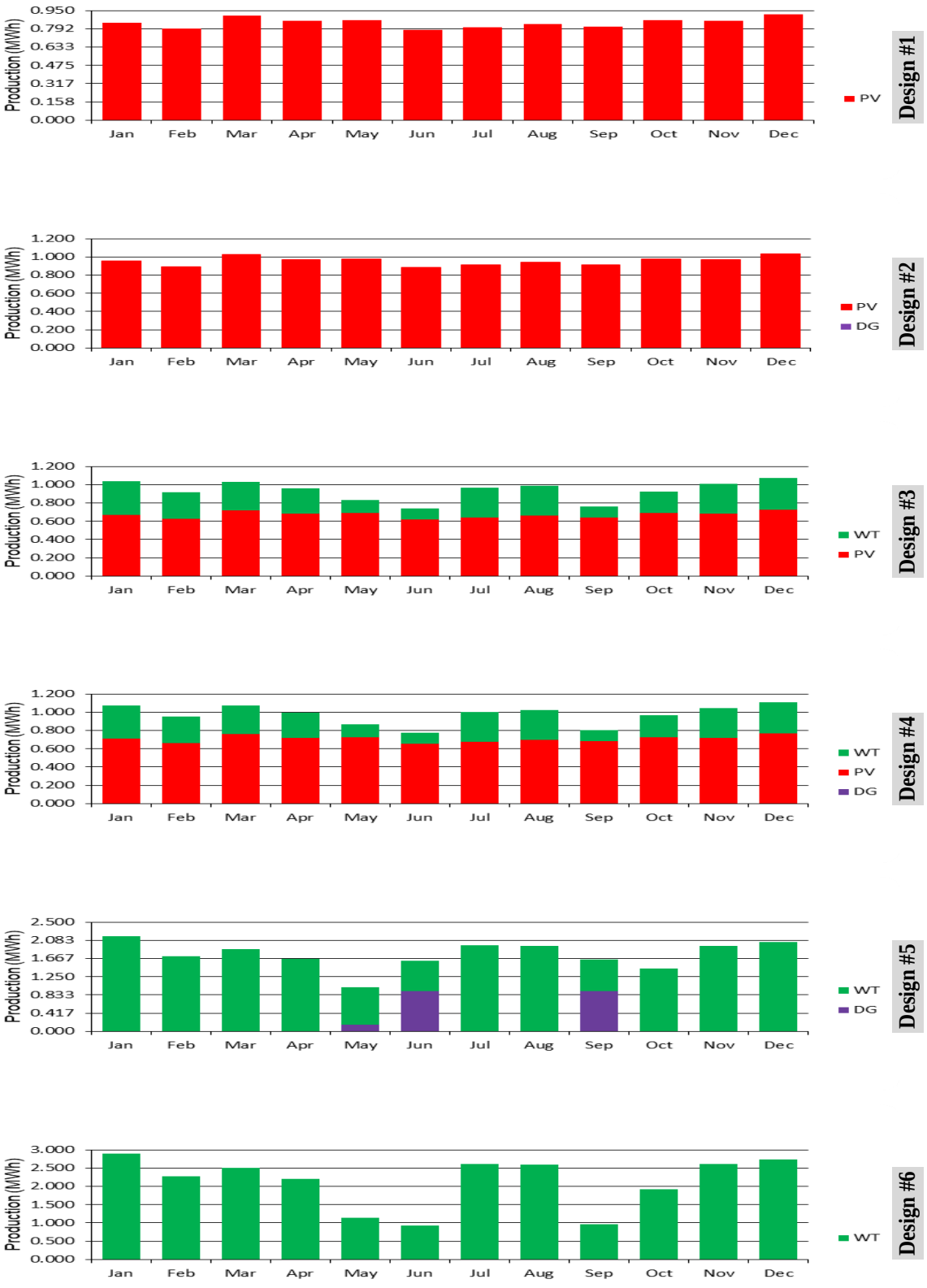


***Fig III. 7**:Average monthly power production*

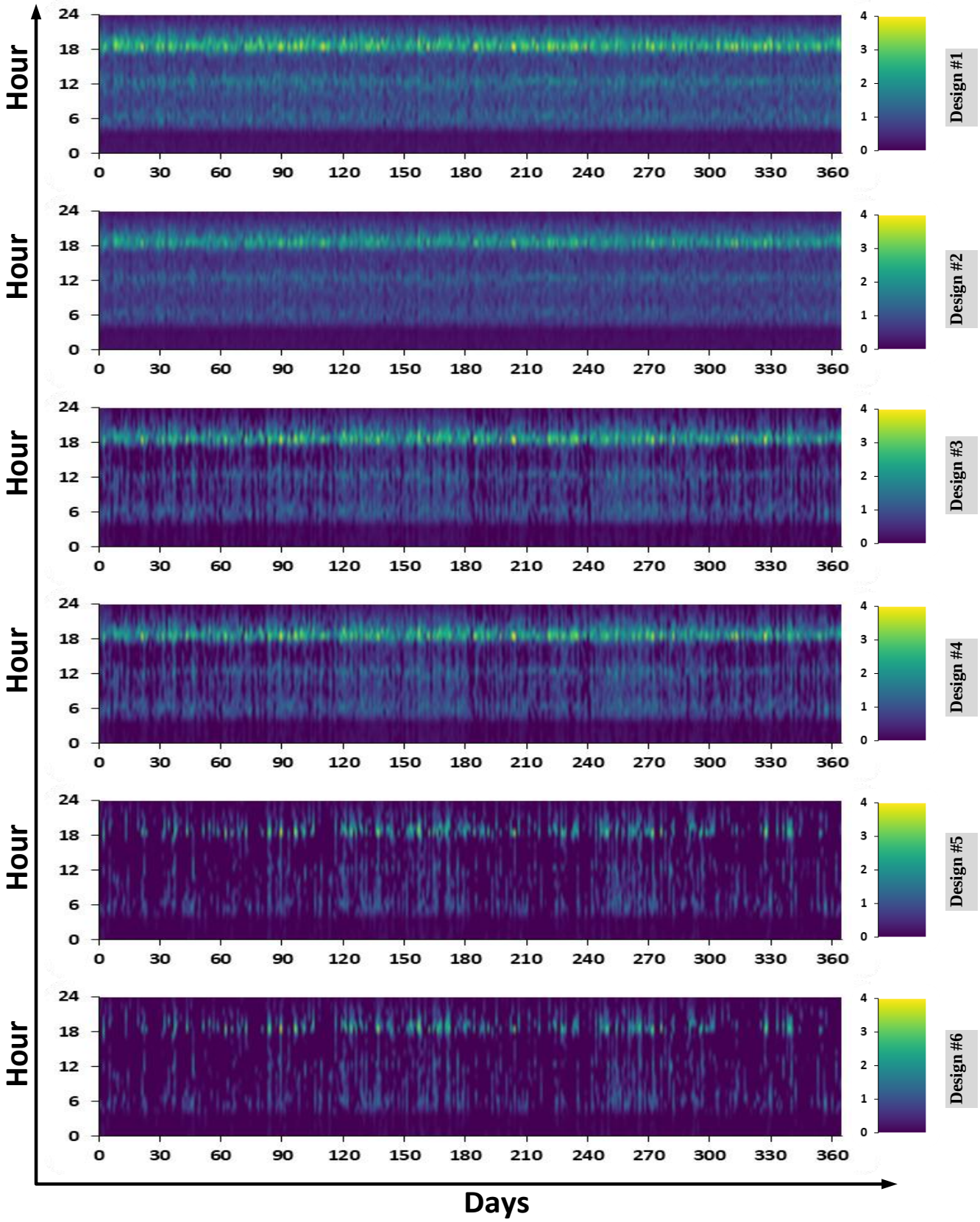


***Fig III. 8**: The output power spectrogram of the inverter*

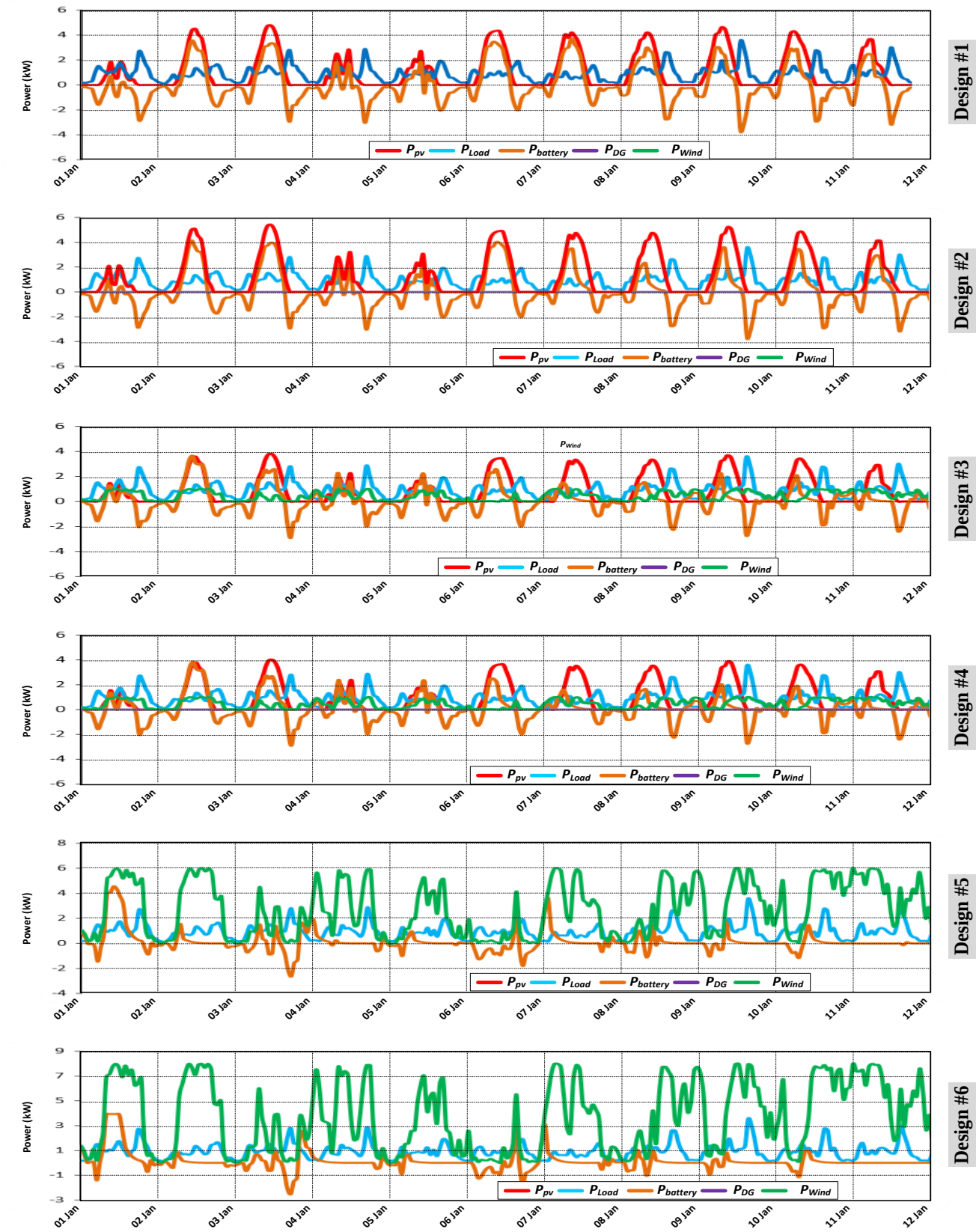


***Fig III. 9**:The energy exchange*

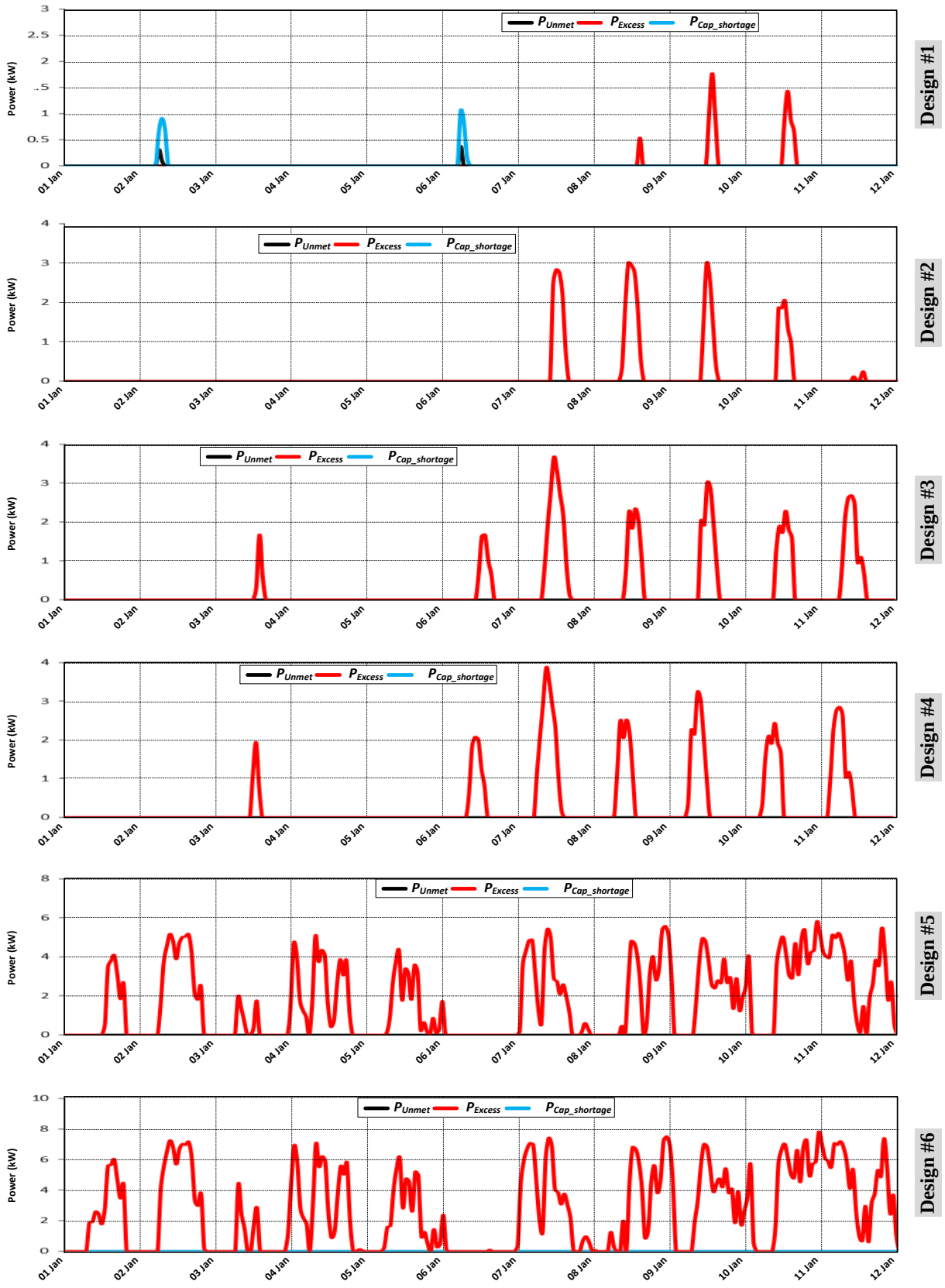


***Fig III. 10**:The excess power, unmet demand load, and capacity shortage*

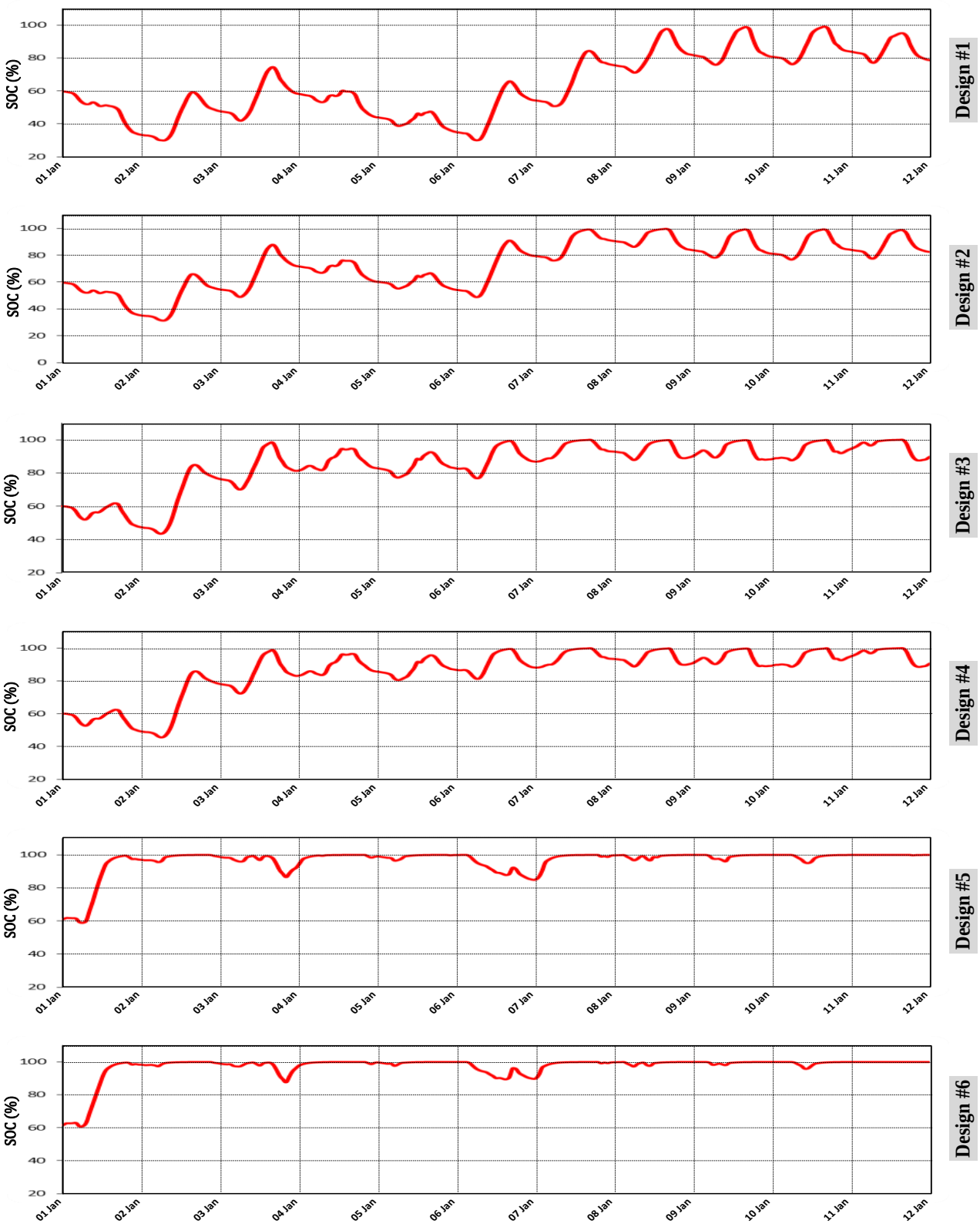


Fig III. 11: SOC of battery for 12 days

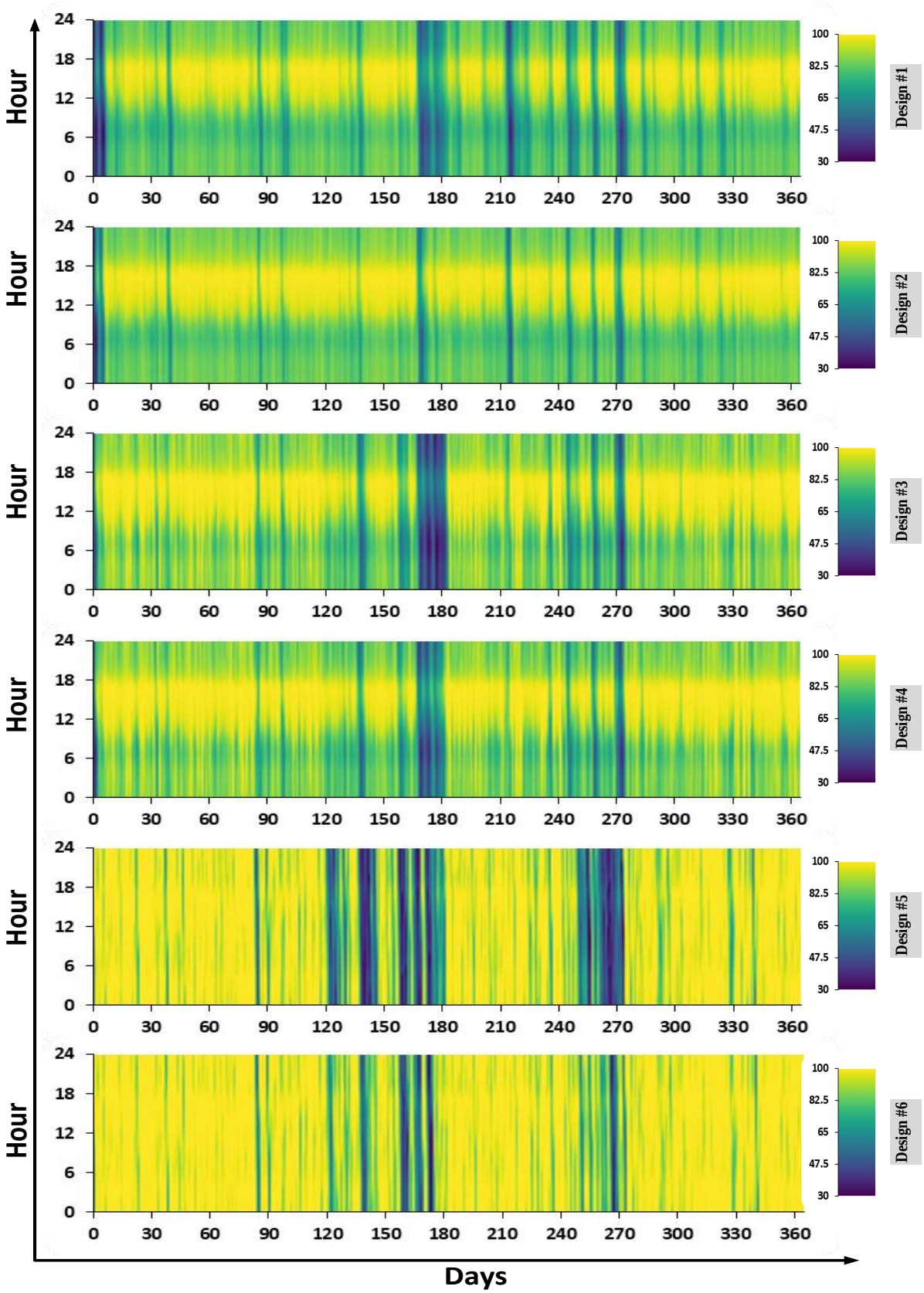


***Fig III. 12**:Hourly SOC of battery*

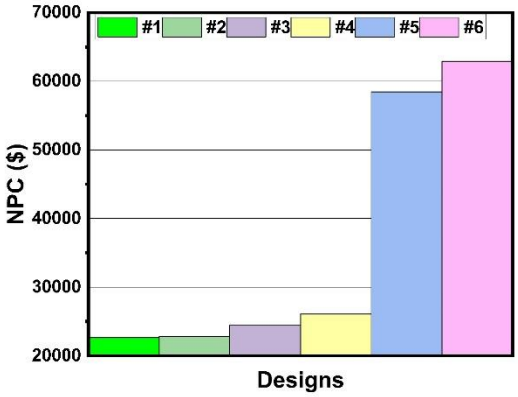
The following findings of the design optimization, with a specific emphasis on the economic, energy, and environmental performance of the ideal system. The HOMER optimizer evaluated six viable energy options that combined photovoltaic (PV), wind turbines (WT), diesel generator (DG) and battery. The comprehensive design optimization findings are summarized in Table 3.4, shows the optimum capacity of each component in various energy options, as well as the economic, energy, and reliability performance of each viable design. The energy choices have been evaluated in a higher order based on their economic performance. The primary susceptible outcomes may be summarised as follows:

- The most efficient energy option that met the electricity demand of the studied area was the PV/battery design, which has a net present value (NPV) of $22647.71and a cost of energy (COE) of $0.0849 per kilowatt-hour (kWh). In opposition, the WT/ battery has the lowest cost-effectiveness, with a NPV of $62888.8and a COE of $0.235886/kWh. The most efficient energy design consisted of 4.819746-kW photovoltaic panels, 29 units batteries, and a 3.975545-kW inverter.
- A suitable system's higher economic performance is determined by the largest number of PV ratings. Therefore, the original capital cost was at its lowest, amounting to $113262.41. On the other hand, the remaining designs incurred the greatest initial capital cost since they used wind turbines (WT) and diesel generators (DG) in the system.
- The majority of viable options are environment-friendly and beneficial due to the absence of fuel-based energy generation sources in the systems designed. Thus, the most of designs achieved a renewable percentage (R_f) of 100%, except for designs #2 and #5, which achieved 98.77% and 84.07% respectively. This indicates that the suggested energy system is very desired, particularly in light of the growing need to protect the environment.
- The designs #5 and #6 generated the most energy among all possible designs, with an annual output of 20383.18 kWh and 25409.58 kWh, respectively. The optimal design #1 generated a total of 10141.14 kWh/year, whereas the average load usage amounted to 8332 kWh/year. In the same proportion, design #5 and #6 have the most excess of energy with 11724.25 kWh (57.52 %), and 16803.12 kWh (66.13 %), respectively. And the excess energy of the optimal design #1 is 1208.187 kWh (11.91 %).

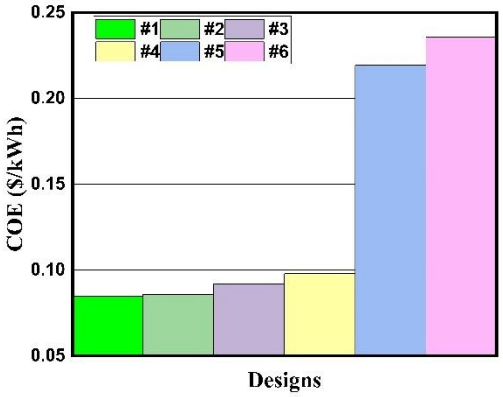
***Table III. 4**:Summary of the designed optimization results.*

	DESIGN	DESIGN #1	DESIGN #2	DESIGN #3	DESIGN #4	DESIGN #5	DESIGN #6
Optimal Capacity	Architecture/PV (kW)	4.819746	4.791667	3.833333	4.428211		
	Architecture/Wind			1	1	6	8
	Architecture/DG (kW)		1020		1020	1020	
	Architecture/Battery	29	29	24	26	30	30
	Architecture/Conv (kW)	3.975545	4.739583	4.083333	5.126642	5.982447	3.939736
Economic Results	Cost/NPC ($)	22647.71	22854.24	24468.88	26100.56	58467.46	62888.8
	Cost/COE ($)	0.084912	0.085672	0.091738	0.097841	0.219172	0.235886
	Operating cost ($/yr)	293.1681	230.8629	340.8123	285.3296	1004.978	1068.519
	Initial capital ($)	13262.41	15463.54	13558.33	16966.2	26294.73	28681.92
	Fuel cost ($/yr)	0	15.62473	0	0	203.1215	0
	Cost/O&M ($/yr)	77.27898	77.19666	78.33334	84.71284	150.39	180
Technical and Environmental Results	Ren Frac (%)	100	98.77594	100	100	84.08727	100
	Total Fuel (L/yr)	0	43.40202	0	0	564.2263	0
	Cap Short (%)	0.109363	0	0.069816	0	0	0.109911
	Elec Prod (kWh/yr)	10141.14	10184.06	11241.84	12493.51	20383.18	25409.58
	Elec Cons (kWh/yr)	8331.495	8332.95	8331.722	8332.95	8332.95	8327.999
	Excess Elec (%)	11.91372	12.26719	22.13756	29.92756	57.51921	66.12906
	Excess Elec (kWh/yr)	1208.187	1249.297	2488.67	3739.003	11724.25	16803.12
	Unmet load (%)	0.017463	5.67E-15	0.014746	4.00E-15	2.42E-15	0.059409
	Unmet load (kWh/yr)	1.455198	4.73E-13	1.228795	3.33E-13	2.02E-13	4.950544

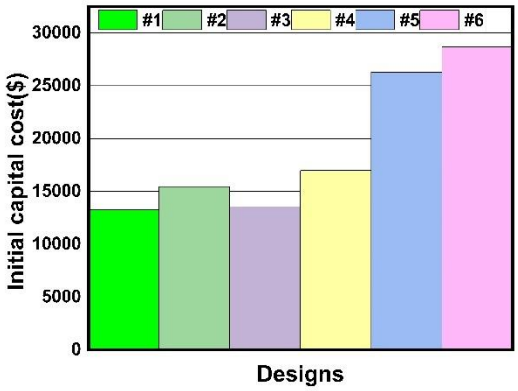
The unmet load ratio of the optimal design #1 is 0.017 %, and the design #6 has the maximum of unmet load with 4.95 kWh/yr (0.059 %). In contrast, the unmet load of designs #2, #4, and #5 are almost non-existent.



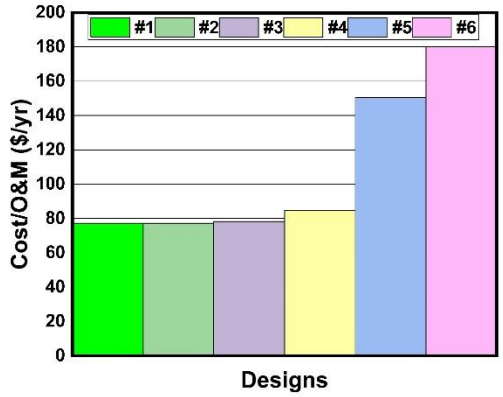
(a): Net present cost



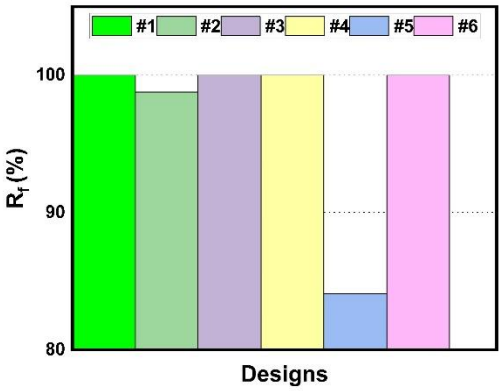
(b): The cost of energy



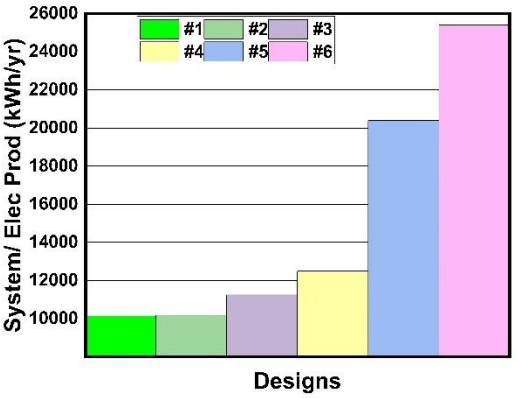
(c):Intial capital cost



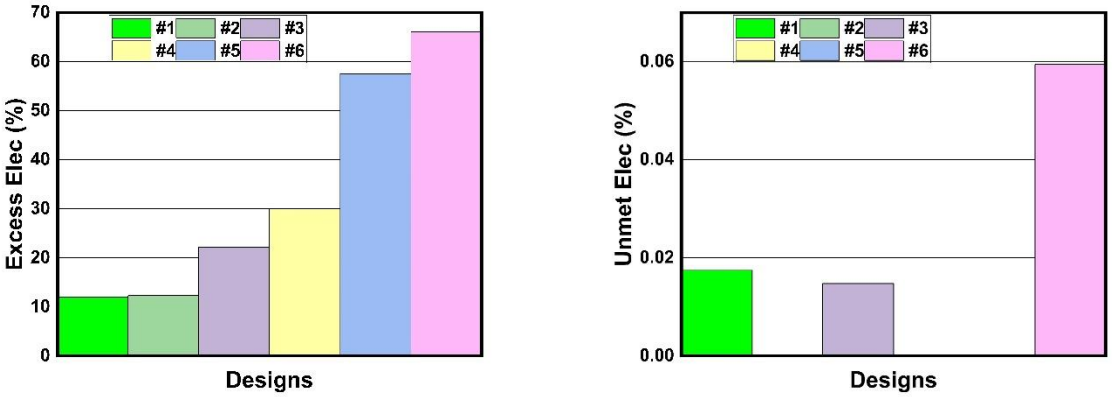
(d): the cost of Operting and maintenance



(e):Renewable fraction



(f): Electricity production



(g):Excess electricity (f) Unmet electricity

***Fig III. 13**: The comparison results for all designs*

The pie charts illustrate the cost distribution for six designs, covering capital, replacement, operation and maintenance (O&M), fuel, and salvage costs. Design #1 allocates 42.8% to capital costs and 35.8% to replacement, with notable salvage costs at 13.5%. Design #2 is similar, with 43.3% capital and 30.7% replacement, and higher salvage at 19.2%. Design #3 has 35.8% capital and 39.9% replacement, with minimal O&M at 6.6%. Design #4 shows 36.7% capital and 35.8% replacement, with O&M at 5.9%. Design #5 uniquely includes 4.4% fuel costs, with 23.8% capital and 41.6% replacement, alongside higher O&M at 7.6%. Design #6 emphasizes replacement costs at 47.5%, with the lowest capital at 24.2% and minimal O&M at 4.9%. Overall, designs #1 and #2 focus on capital and salvage, Design #6 on replacement, and Design #5 on a more varied cost structure including fuel.

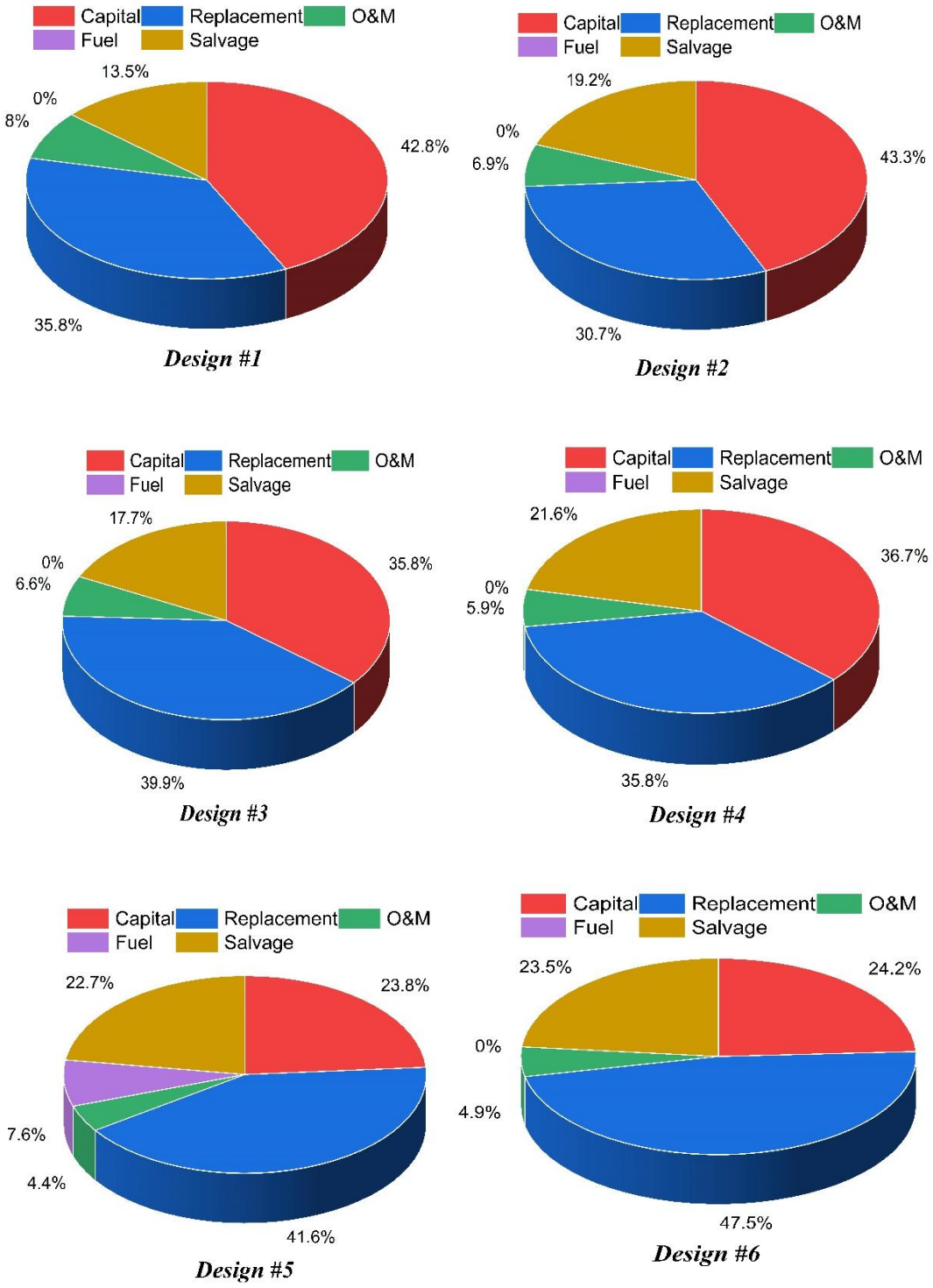


***Fig III. 14**: Cost distribution of the optimal designs*

III.7 Conclusion

HOMER proves to be an indispensable tool in the design and optimization of hybrid renewable energy systems. Through its simulation, optimization, and sensitivity analysis capabilities, HOMER allows for an in-depth evaluation of technical and economic viability of multiple configurations. The application of HOMER in case studies, ranging from rural electrification to urban energy solutions, demonstrates its versatility and effectiveness in minimizing costs and maximizing renewable energy utilization. The results highlight HOMER's ability to adapt to various environmental conditions and energy demands, ultimately leading to sustainable and cost-efficient energy solutions

Chapter IV
Energy management techniques of microgrid

IV.1 Introduction

As the integration of renewable energy sources (RES) into microgrid systems becomes increasingly prevalent, the need for effective energy management systems (EMS) has never been more critical. This chapter focuses on the classification and comparative investigation of various EMS strategies, with a particular emphasis on filter-based control techniques. We will explore conventional filter-based methods and introduce a proposed energy management technique tailored for DC microgrids. The analysis will encompass the design and analysis of voltage and current controllers, crucial for maintaining system stability and efficiency. Through a series of simulations conducted in the MATLAB-Simulink environment, we will evaluate the proposed EMS under different operational scenarios, examining factors such as state of charge (SOC) limits for hybrid energy storage systems (HESS). By analyzing the performance of the fuzzy logic energy management system (FL-EMS) within the context of fluctuating renewable energy production, this chapter aims to provide valuable insights into optimizing microgrid operations and enhancing energy reliability.

IV.2 Classification and comparative investigation of EMS

To fully capitalize on the benefits of the hybrid power generating system and hybrid energy storage, the authoritative ordinance power must be effectively allocated among the various power sources using an energy management strategy (EMS) [211]. The appropriate EMS has additional obstacles, including the reduction of fuel consumption, operational costs, and strain on energy sources, while still achieving maximum efficiency [212],[213].

Ultimately, sustaining the bus voltage at a certain level. In the recent past, several researchers have used various forms of EMS for FC hybrid power systems to attain the aforementioned objectives. Moreover, several research have been conducted to categorize these EMSs [214],[215]. One of the standard categories categorizes EMS into two primary groups. Fig VI.1: Offline and Online Emergency Management Systems. Offline Energy Management Systems (EMSs) are categorized depending on the comprehensiveness of the load profile information and operational circumstances, including rule-based EMSs and optimization-based EMSs. Online EMSs are categorized into three subtypes: immediate optimization-based EMSs, predictive EMSs, and learning-based EMSs.

Reference [216], introduced an Energy Management System (EMS) utilizing a Smart Management System (SMS) with droop control for a hybrid power model of tramways incorporating Proton Exchange Membrane Fuel Cells (PEMFC), batteries, and supercapacitors. The SMS facilitates the distribution of load power among the available power sources, while droop control ensures the stability of the DC bus voltage by restricting circulating currents. In [217] presented an Energy Management System (EMS) that integrates a combination of State Machine Strategy (SMS) and Equivalent Consumption Minimization Strategy (ECMS) for a hybrid tramcar system utilizing a fuel cell and supercapacitor. The proposed EMS effectively coordinates multiple

power sources, ensuring operation within their optimal efficacy range, and has achieved a reduction in hydrogen consumption of 4.18% and 0.56% compared to the state machine strategy and equivalent consumption minimization strategy, respectively.In [218], a novel Energy Management System (EMS) utilizing a Frequency Decoupling Strategy (FDS) through fuzzy control for hybrid electric vehicles (HEVs) powered by fuel cells, batteries, and supercapacitors is proposed. The controller partitions the power demand into three frequency levels employing Haar wavelet, and a genetic algorithm is utilized to optimize the membership functions of the proposed controller.
In [219], the authors implemented Fuzzy Logic Control and a Rule-Based Algorithm on a hybrid power system comprising Fuel Cells, Batteries, and Supercapacitors. They employed a backtracking search algorithm in conjunction with sequential dynamic programming to optimize the parameters of the fuzzy logic, resulting in a 10.92% enhancement in fuel economy through the proposed Energy Management System (EMS).

In [220], an Energy Management System (EMS) utilizing Dynamic Programming (DP) and State Machine Systems (SMS) for a hybrid Fuel Cell/Supercapacitor (FC/SC) power system has been introduced. DP is employed to determine the optimal distribution among the power sources, while SMS utilizes the outcomes of DP to adjust the threshold values of its states. The proposed EMS has been validated using the RT-LAB real-time simulator, demonstrating an 18.82% reduction in hydrogen consumption over 800 seconds compared to conventional SMS.

In [221], an EMS using a Mixed-Integer Linear Programming method was developed, proposing a multi-objective design and operation (D&O) optimization strategy aimed at minimizing costs and fuel cell deterioration. A comparison between multi-objective D&O optimization and single-objective optimization (focused only on cost minimization) shown a 65% reduction in FC deterioration with multi-objective D&O. In [222], a hybrid genetic method for HEV was presented, using the quadratic programming approach. The suggested approach demonstrates superior convergence speed and flexibility relative to the conventional GA technique. In [223], energy sources were minimized using a novel optimization technique called the Quantum Butterfly Optimization Algorithm (QBOA) for hybrid fuel cell electric vehicles. The proposed Energy Management System (EMS) was compared with the Adaptive Energy Management Strategy (AEMS), a conventional discrete wavelet transform power-splitting technique, and additional comparisons among QBOA, Butterfly Optimization Algorithm (BOA), and Particle Swarm Optimization (PSO). The findings indicated a reduction of 10% in weight and 16% in cost of the hybrid system. In [224], an Energy Management System (EMS) using Equivalent Consumption Minimization Strategy (ECMS) was introduced, delivering optimum performance for hybrid fuel cell/battery power systems via an adaption approach of the equivalent factor informed by State of Charge (SoC) feedback signals.

A novel Energy Management System (EMS) incorporating Cost Optimization for Finite Horizon Strategy (CO-FHS) and Adaptive Equivalent Consumption Minimization (A-ECMS) has been presented in [225]. This EMS integrates a battery State of Charge (SoC) penalty term within

A-ECMS to ensure the efficient operation of charge and discharge cycles. CO-FHS optimizes fuel consumption based on Vehicle-to-Vehicle (V2V) technology. The findings indicate that A-ECMS outperforms on highways, whereas CO-FHS is superior for urban driving, achieving an average fuel efficiency improvement of 5% compared to the Finite State Machine Strategy (FSM).In [226], an Energy Management System (EMS) using the Degradation-Conscious Equivalent Consumption Minimization Strategy (D-ECMS) for the fuel cell hybrid system was presented. A comparison of the Rule-Based (RP) control approach, the original EMCS, and D-ECMS has been presented. The findings indicated an enhancement in battery and fuel cell degradation of the suggested energy management system relative to other methods, but with increased hydrogen usage.

In terms of battery State of Charge (SoC) maintenance, ECMS and D-ECMS outperform RP; moreover, D-EMCS achieved savings of 1.01% and 34.43% in worldwide costs compared to ECMS and PR, respectively. In [227], a novel Energy Management System (EMS) was introduced, integrating Artificial Neural Network (ANN) and Passivity Based Control (PBC) for hybrid fuel cell/battery/supercapacitor electric vehicles. The ANN is employed to ascertain the controller's references, specifically the battery current reference and the remaining hydrogen quantity, prior to distributing the load demand among the power sources. Owing to its simplicity, ease of installation, cheap cost, and potential for enhancement via the adjustment of its controller gain levels. Furthermore, PI is regarded as one of the most prevalent and practical control strategies.

In [228], a PI controller was used for the operation of a phosphoric acid fuel cell (PAFC), and the findings demonstrated the efficacy of their technology even under varying dynamic situations. In [229], an enhanced PI controller was created that accounts for the efficiency of fuel cells in hybrid fuel cell/battery passenger boats; the suggested energy management system demonstrated reduced hydrogen consumption and less stress on the fuel cell relative to other methods. In [230], an Energy Management System (EMS) using a Proportional-Integral (PI) controller for a hybrid power system fueled by Fuel Cells (FC) and Supercapacitors (SCs) was proposed. This method regulates the DC bus voltage in accordance with the load's requirements by allocating power among the sources. In [231], a multi-scheme strategy was introduced that selects its Energy Management System (EMS) based on system inputs.

The proposed EMS schemes include: SMS, ECMS, Charge Depleting Charge Sustaining (CDCS) strategy, and the classical PI controller. This multi-scheme strategy resulted in a 16.7% reduction in hydrogen consumption and an 8% increase in maximum energy during 8 hours of daily operation for the passenger vessel. A novel adaption mechanism for the comparable factor used by EMCS has been developed. The novel technology used a fuzzy PI controller, and the suggested strategy was implemented in a hybrid electric car with both an internal combustion engine and an electric motor. Table 1 delineated the benefits and drawbacks of the primary EMSs.

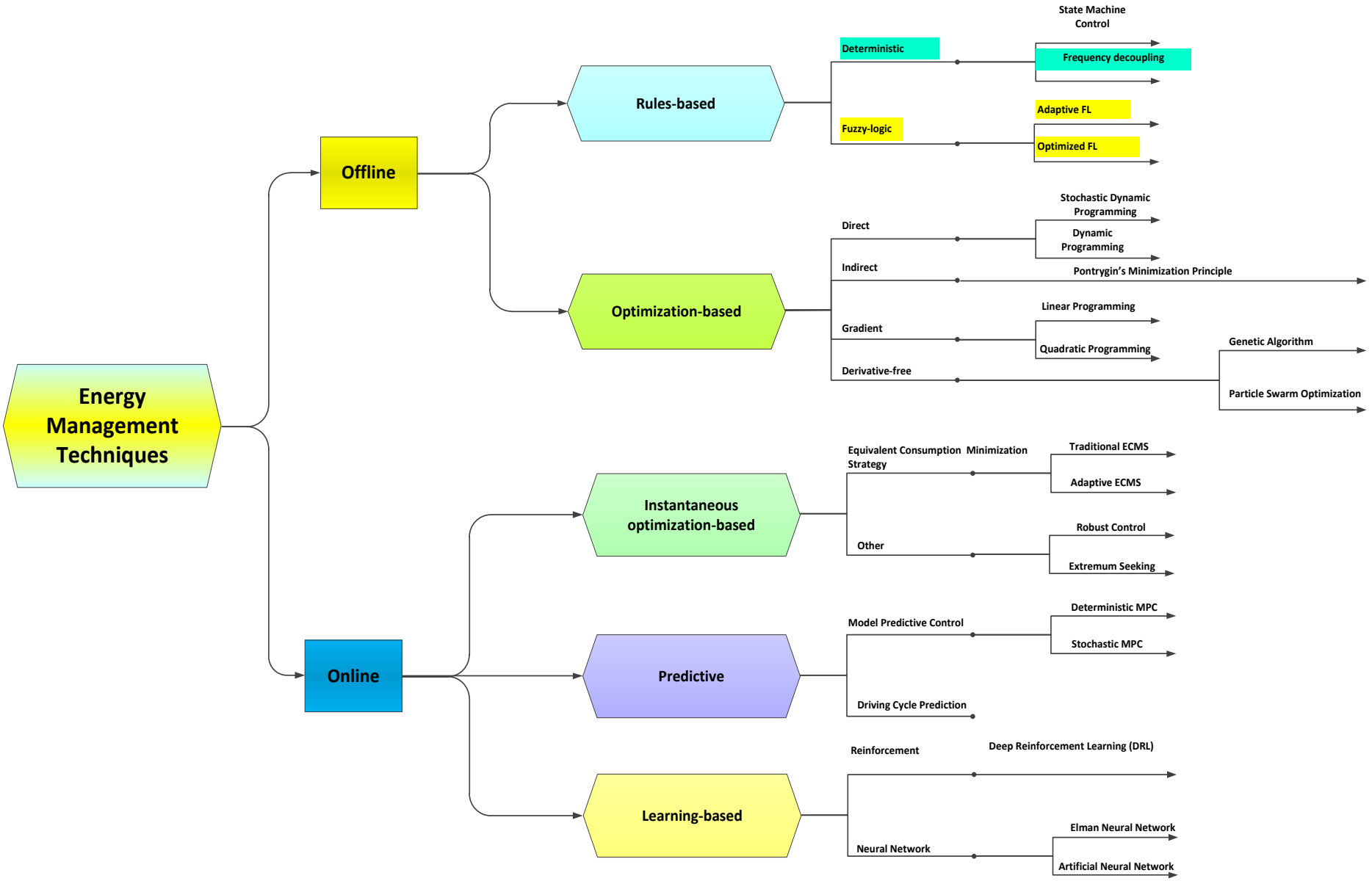


***Fig IV . 1**: Classification of energy management technique*

***Table IV. 1**: classification of energy management technique*

	Type	Technique	Advantages	Disadvantages	Ref
Offline	Ruled-based	Deterministic	• Simple to implement using a look-up table. • Basic Architecture.	The final operational points may not be ideal owing to the failure to account for future load situations.	[216],[217] ,[218],[232] ,[233],[234] ,[235],[236]
		Fuzzy-logic	• Implementation is straightforward, contingent upon the degree of similarity across data sets.	• Limited flexibility resulting from the difficulty in finding an appropriate membership function based on diverse inputs.	[219],[237] ,[238]
	Optimization-based	Direct	• Serve as a standard for other EMSs. • Attains almost ideal fuel efficiency.	• Reduced adaptability. • Increased computational complexity. • Necessitates a load profile database.	[239],[238] ,[240],[241]
		Indirect	• The optimal control for global trajectory.	• Advanced mathematics. • Model approximation is necessary to minimize computational cost.	[242]
		Gradient	• Rapid calculation.	• Strong model simplification • Requirement for derivative information pertaining to the goal function • Intricate mathematics	[243],[244]
		Derivative-free	• Global optimality. • Excellent global search efficacy.	• Optimal solution not achieved within a restricted number of repetitions. • Reduced flexibility.	[245],[246]

Online	Instantaneous optimization-based	ECMS	• Online execution. • Increased adaptability.	• Potential for attaining local optimum solutions. • Sensitivity of the driving cycle about the comparable factor.	[247]
		Robust Control	• Resilience in the presence of unclear parameters. • Increased versatility.	• Computational difficulty arising from the nonlinear time-variant model. • Increased model complexity.	[248]
		Extremum Seeking	The system model is unnecessary, allowing for the optimization of performance in systems where the process model is imprecisely understood.	• Complexity pertains to its execution. • Potential for local optima. • Gradual convergence.	[249]
	Predictive	Model Predictive Control	• Address limitations directly. • Improve the transient performance of the hybrid system. • Increased versatility with less computational demands.	• Intricate methodology. • Requirement for a joint chance restriction.	[250]
		Driving cycle Prediction Reinforcement	• It forecasts the load profile for the EMS, hence optimizing fuel efficiency. • Model-free control	• Diminished fuel efficiency in the presence of several unpredictable variables. • Labor-intensive in terms of database preparation.	[225]
		Neural Network	• More versatile due to their capacity to operate with partial information. • Capacity for parallel processing.	• Require an extended duration. • Necessitate more data for training capacity.	[232]

IV.3 Energy management-based frequency decoupling

Energy management-based frequency decoupling is a method that employs a filter to refine the input signal prior to its application to the plant. The filter may eliminate noise, disruptions, or other undesired elements from the input signal. This may enhance the control system's performance by increasing its robustness to disturbances and minimizing chattering in the output signal. Filtered-based control is relevant to several applications, including hybrid energy storage systems (HESS) that integrate multiple energy storage types such as batteries and supercapacitors. These systems accumulate renewable energy from sources like as solar and wind power and provide electricity to the grid during peak demand or when renewable sources are inaccessible. Diverse filter types may be used for filter-based control in HESS, with the choice contingent upon particular criteria such as frequency response, system stability, and cost factors. The Filtered-Based Method (FBM) is a control approach used in Hybrid Energy Storage Systems (HESS) that utilizes a filter to improve system performance. FBM enhances the HESS output, enabling superior energy management in systems that include batteries and supercapacitors. A primary benefit of FBM is its ability to mitigate the peak demand of the HESS. The filter mitigates the output fluctuations of the HESS, hence reducing the likelihood of the HESS needing to provide substantial power in a short period.

This may alleviate stress on the HESS components and prolong their lifetime. Another benefit of FBM is its potential to enhance the efficiency of the HESS. The filter reduces the noise and disruptions present in the output of the HESS. The noise and disturbances may diminish the operational efficiency of the HESS. By mitigating these factors, FBM can enhance the efficiency of the HESS. FBM may enhance the longevity of HESS components by alleviating the stress imposed on them. The filter mitigates the output fluctuations of the HESS, hence reducing the likelihood of the HESS needing to provide a substantial quantity of power in a short timeframe. FBM may mitigate the expenses associated with HESS by minimizing energy wastage. The filter reduces the noise and disruptions present in the output of the HESS. Ultimately, FBM may enhance the dependability of the HESS. The filter makes the HESS less vulnerable to disruptions.

Disruptions may lead to inconsistent operation or complete failure of the HESS. By minimizing disturbances, FBM may enhance the dependability of the HESS. FBM is an effective control approach that enhances the performance of HESS in several aspects. FBM may enhance HESS as a more dependable and economical energy storage system by diminishing peak power consumption, augmenting efficiency, bolstering reliability, extending lifetime, and lowering costs [201],[251].

IV.3.1 Convectional method

The architecture of a filtered-based control (FBC) system comprises a DC bus voltage loop designed to sustain a stable DC voltage and alleviate disturbances arising from fluctuations in source and load conditions [157].

$$C_{DC}\frac{d_{C_{DC}}}{dt} = I_{\text{HESS}} + I_{RES} - I_{\text{Load}} \quad \text{IV.1}$$

C represent the equivalent capacitance, IHESS denote the total HESS current for voltage control, I_{RES} signify the RES current, and I_{Load} indicate the load current.
The imbalanced current power $I_{\text{HESS}} = I_{RES} - I_{\text{Load}}$ is seen as a disturbance mitigated by the HESS. Furthermore, for a hybrid energy storage system (HESS) consisting of a supercapacitor (SC) and a battery energy storage system (BESS), equation IV.2, indicates that the total HESS current is the aggregate of the SC and BESS currents. This equation facilitates the computation of individual component currents for HESS control, guaranteeing efficient and safe operation[252].

$$I_{HESS} = I_{\text{bat}} + I_{SC} \quad \text{IV.2}$$

When the generated power aligns with the load demand, the HESS stays dormant. In the event of an imbalance when demand surpasses the RES power, the HESS provides electricity to the load. If the produced power above the load requirement, the HESS accumulates energy. Nevertheless, prudence is necessary. It is advisable to circumvent situations in which the hybrid energy storage system (HESS) either delivers current when its energy storage level is critically low or consumes current when fully charged, as this may lead to inadequate current supply, damage to the HESS, inability to store additional energy, or potential harm from forced energy storage. Effective management of the HESS is essential for safe and efficient functioning. Fig VI.3 illustrates a simplified schematic of voltage regulation inside the filtered-based control (FBM) system. The system utilizes a proportional-integral (PI) controller inside the bus voltage loop to provide the reference current I_{HESS} for the purpose of maintaining a constant bus voltage. The disturbance current (iun) is mitigated by the PI controller, which assesses the actual and intended bus voltages to provide an error signal. The controller output modifies the reference current, therefore regulating the HESS to either provide or absorb current for the stabilization of bus voltage. The PI controller facilitates efficient disturbance compensation by dynamically adjusting the reference current I_{HESS} as required. Fig VI.3 illustrates that the hybrid energy storage system (HESS) distributes its total current between the battery energy storage system (BESS) and the supercapacitor (SC) using a low-pass filter in the standard filtered-based method (FBM) energy management system (EMS). The low-pass filter divides the reference current into low-frequency ${I_{batt}}^*$ and high-frequency ${I_{SC}}^*$ components, which regulate the Battery Energy Storage System (BESS) and Supercapacitor (SC), respectively, while preserving the overall Hybrid Energy Storage System (HESS) current.

$$\begin{cases} FT_{LPF}(s) = \dfrac{1}{1+sT_f} \\ {I_{batt}}^*(s) = {I_{HESS}}^*(s) * FT_{LPF}(s) \\ {I_{HF}}^*(s) = {I_{HESS}}^*(s) - {I_{batt}}^*(s) \end{cases} \quad \text{IV.3}$$

F(s) represents a low-pass filter. The existing loops, often executed using proportional-integral (PI) controllers, govern the currents of the BESS and SC, aligning them with their respective references. Under steady-state circumstances, the total HESS current I_{HESS}^{*} is equivalent to the sum of the BESS and SC currents $I_{batt}^{*} + I_{SC}^{*}$. During transient situations, the current loops may have a slower response compared to the voltage loop, hence impacting bus voltage regulation.

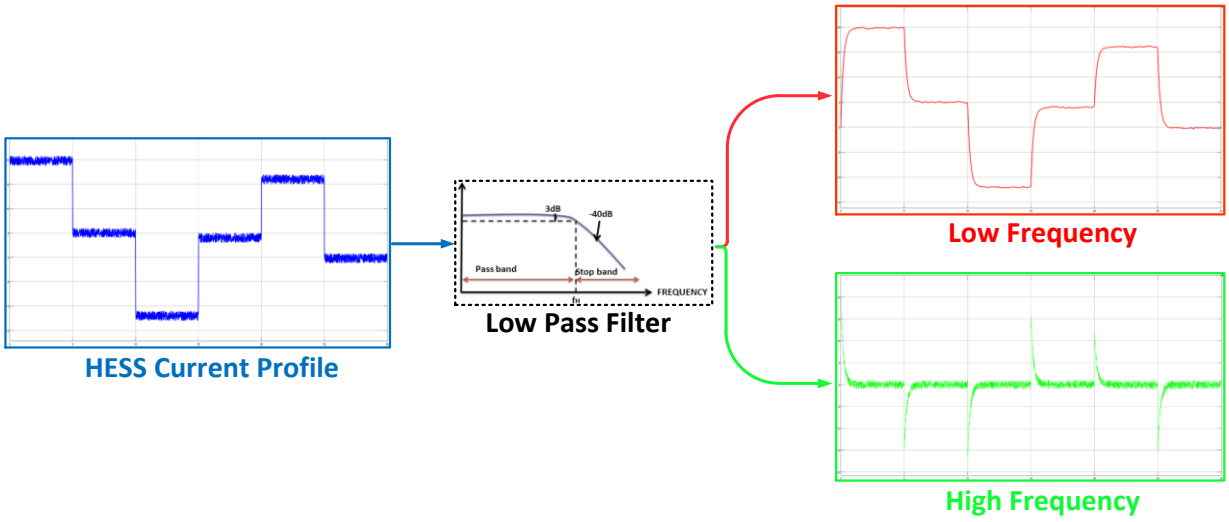


Fig IV. 2: Low pass filter

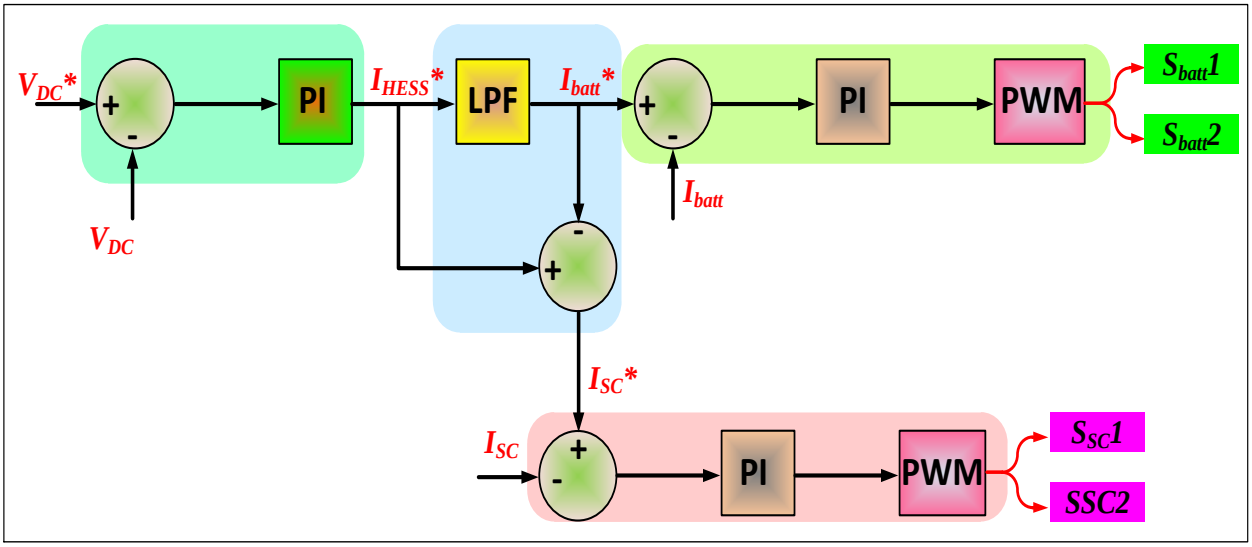


***Fig IV. 3**:Traditional energy management strategy*

IV.3.2 Proposed energy management technique

The conventional method is failed to eliminate the disparity caused by errors in comparing V_{DC} and V_{DC}^{*}. Also, the slow reaction of the battery caused it, where the battery current I_{bat} was not following the reference current I_{bat}^{*} instantly. Hence, the unremunerated battery power is expressed as [253];

$$P_{uncomp}(s) = [\ {I_{HF}}^{*}(s) - [\ {I_{batt}}^{*}(s) - I_{batt}(s)]] * V_{batt}(s) \quad \text{IV.4}$$

The power uncompensated P_{uncomp} could be compensated by Supercapacitor, Hence the current reference of SC is described as follows;

$${I_{SC}}^{*} = [\ {I_{HF}}^{*}(s) - [\ {I_{bat}}^{*}(s) - I_{bat}(s)] * \frac{V_{Batt}(s)}{V_{SC}(s)} \quad \text{IV.5}$$

The energy state of HESS can be obtained by calculating the integral of the power, and the initial energy state E_{initial} .

$$E(t) = E_{\text{initial}} + \int P_{HESS}(t)dt \quad \text{IV.6}$$

The difference in energy ΔE is the quantitative measure of the difference between the highest and lowest points. The following equation describes the difference energy magnitude of HESS;

$$\Delta E = E_{max} - E_{min} \quad \text{IV.7}$$

Fig IV.5 illustrates the combined power requirements of the HESS, the battery, and the supercapacitor (SC) power while the HESS is using the low-pass filter (LPF). The overall power required for the HESS corresponds to the necessary power flow of the DC link, indicating the power flow of the HESS when a single ESS is used. The integral of power in relation to time represents the amount of work required, which corresponds to the region enclosed by the power curve and the x-axis. The total work done for the DC bus is equal to the sum of the areas between the total power demand curve and the x-axis, which includes both the orange and the yellow areas. The phase delay of the low-pass filter in the HESS results in a delay among the total power request and the battery power. This delay, denoted as $\boldsymbol{\Delta t}$, is seen as a time difference between the crossing of zero points of the total power

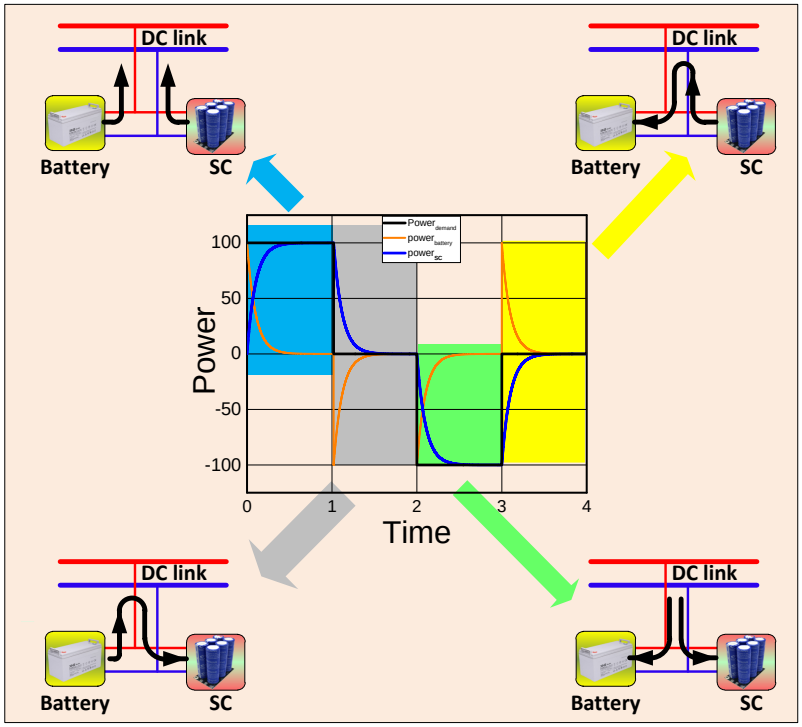


***Fig IV . 4**:Power waveforms of HESS on transient zone*

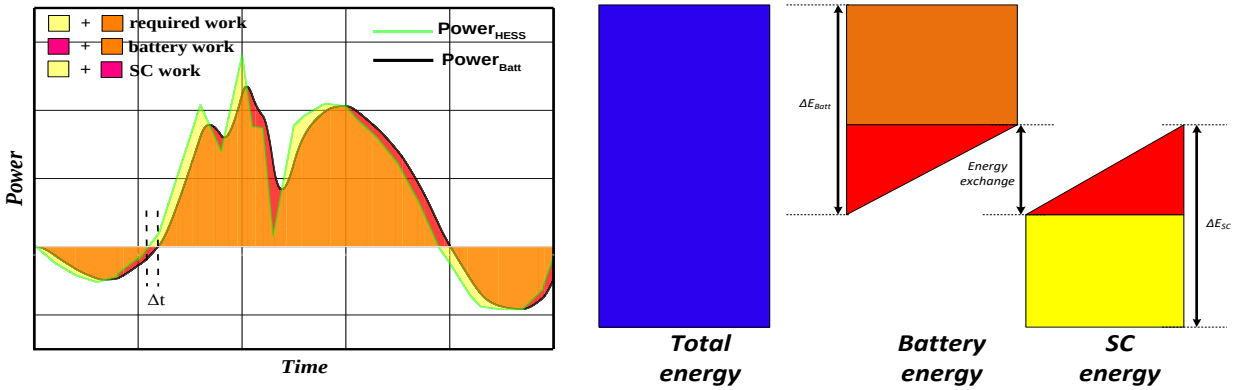


***Fig IV . 5**:Operation zone of HESS*

demand and the battery power. Hence, the total work performed by the battery is equal to the combined areas of the orange and red regions. Furthermore, power need and the battery signify the work performed by the SC in the HESS. This includes the combined areas of both the yellow and red areas. As demonstrated in Fig IV.5 graphical representation of the required capabilities might be clarified. The blue area represents whole energy, the orange areas correspond to battery energy, and the yellow areas correspond to SC energy. Therefore, the red areas represent the exchange of energy throughout the HESS.

IV.3.3 Analysis and design the voltage and currents controller

To control the energy flows among the various elements, the DC link is regulated by a PI controller. The bi-directional converter linked to the SCs is accountable for determining the parameters of this regulator in this scenario. A resistance R_L is present in this model, linked in parallel with the load. The mathematical equations for the suggested converter are described as follows [254]:

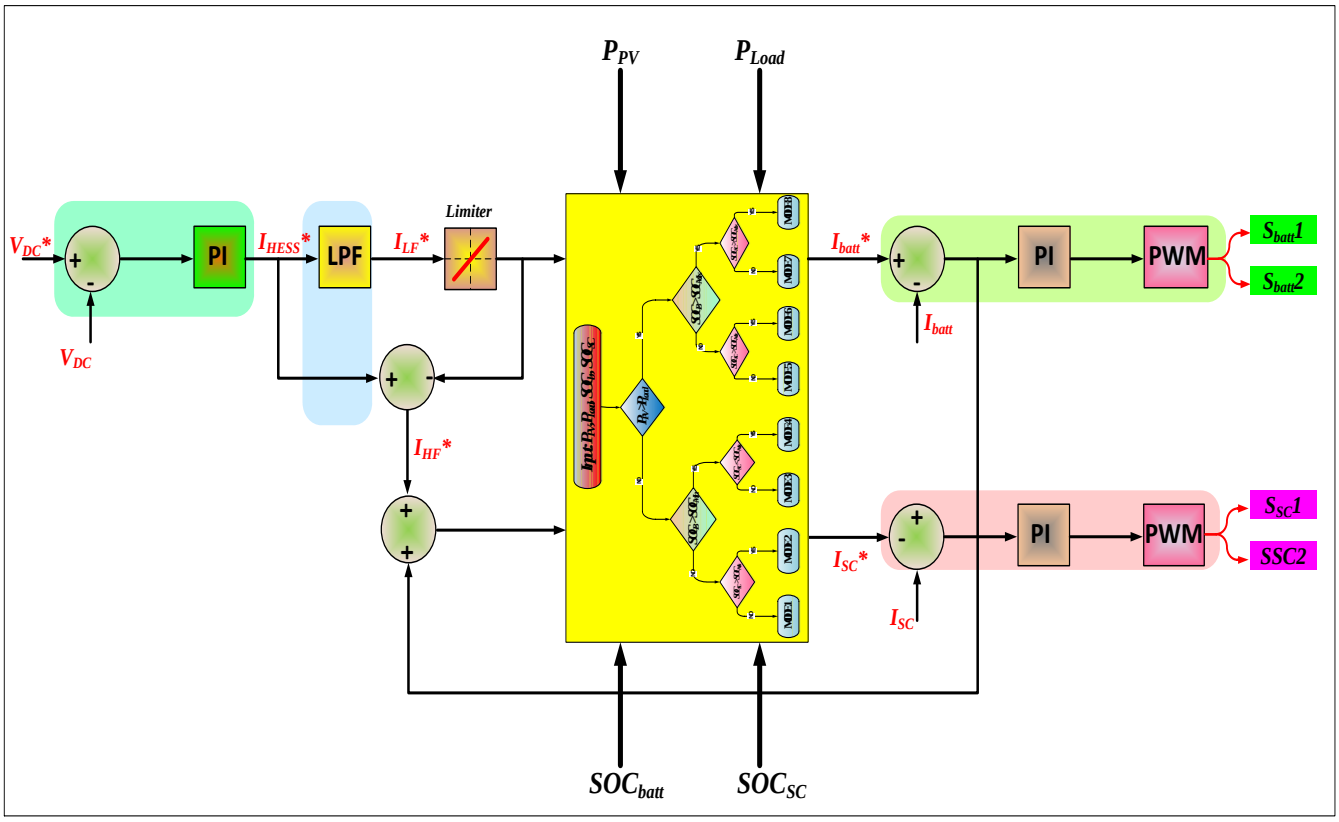


***Fig IV. 6**:Energy management proposed*

$$C_{DC}\frac{dV_{DC}}{dt} = i_{L_{SC}}(1 - d_{SC}) - \frac{V_{DC}}{R_L} - I_{DC} \quad \text{IV.8}$$

$$L_{SC}\frac{dI_{L_{SC}}}{dt} = V_{SC} - (1 - d_{SC})V_{DC} \quad \text{IV.9}$$

By using the formulas provided above, one can derive the following formula:

$$C_{DC}\frac{dV_{DC}}{dt} = i_{L_{SC}}\frac{V_{SC}}{V_{DC}} - \frac{V_{DC}}{R_L} - I_{DC} \quad \text{IV.10}$$

The representation of the transfer function of DC link voltage is developed as follows;

$$FTx(s) = \frac{V_{DC(s)}}{I_{DC}(s)} = \frac{V_{SC}R_L}{\frac{R_L C_{SC}}{2}s + 1} \quad \text{IV.11}$$

The equation presented the transfer function of the PI controller.

$$C_{dc}(s) = K_{p_{DC}} + \frac{K_{i_{DC}}}{s} \quad \text{IV.12}$$

resulting in:

$$FTBF\ (s) = \frac{K_{P_{DC}}R_L V_{SC}\left(s+\frac{K_{i_{DC}}}{K_{P_{DC}}}\right)}{K_{p_{DC}}R_L V_{SC}\left(s+\frac{K_{i_{DC}}}{K_{p_{DC}}}\right)+s\left(\frac{R_L C_{SC}}{2}s+1\right)} \quad \text{IV.13}$$

resulting in:

$$FTBF(s) = \frac{K_{p_{DC}}R_L V_{SC}\left(s+\frac{K_{i_{DC}}}{K_{p_{DC}}}\right)}{\frac{R_L C_{SC}}{2}s^2+\left(K_{p_{DC}}R_L V_{SC}+1\right)s+K_{p_{DC}}R_L V_{SC}\frac{K_{i_{DC}}}{K_{p_{DC}}}} \quad \text{IV.14}$$

By comparing the denominator with the equivalent of the canonical form, we obtain

$$\begin{cases} K_{i_{DC}} = \frac{\omega_n^2 C_{SC}}{2V_{SC}}, & \omega_n^2 = \frac{2}{C_{SC}}V_{SC}K_{i_{DC}} \\ K_{p_{DC}} = \frac{\xi\omega_n R_L C_{SC}-1}{R_L V_{SC}}, & 2\xi\omega_n = \frac{2}{R_L C_{SC}}\left(K_{p_{DC}}R_L V_{SC}+1\right) \end{cases} \quad \text{IV.15}$$

The equation used for controlling the bi-directional converter is as follows:

$$V_{SC} = L_{SC}i_{L_{SC}}(s)s + R_{\text{Load}}\, i_{L_{SC}}(s) + (1 - D_{SC}(s))V_{DC} \quad \text{IV.16}$$

As a result, the following equation is established to connect the duty cycle DSC with the present I_{SC}:

$$\frac{I_{SC}(s)}{D_{SC}(s)} = \frac{\frac{V_{DC}}{R_{Load}}}{1+\frac{L_{SC}}{R_{Load}}s} \quad \text{IV.17}$$

The corrector's transfer function is as described below:

$$G_{SC}(s) = \frac{K_{i_{SC}}\left(1 + \frac{K_{P_{SC}}}{K_{i_{SC}}}s\right)}{s} \quad \text{IV.18}$$

The system's transfer function is made simpler by assuming a pole/zero and applying compensation: $\frac{K_{p_{SC}}}{K_{i_{SC}}} = \frac{L_{SC}}{R_{\text{Load}}}$. The newly developed closed-loop transfer function has become;

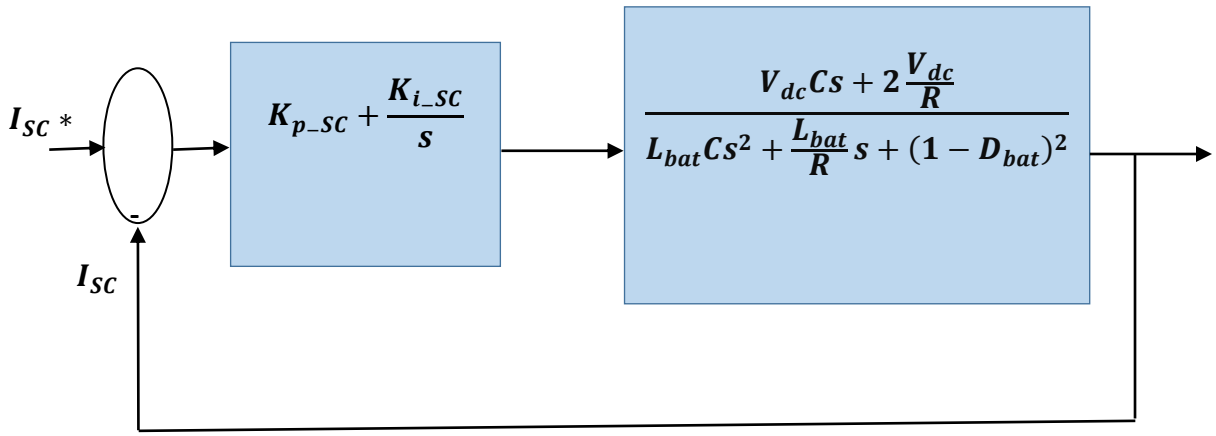


***Fig IV. 7**:Block diagram of SC controller*

$$CLTF_{SC}(s) = \frac{1}{1+\frac{R_{Load}}{V_{dc}K_{i_{SC}}}s} \text{ where, } \tau_{SC} = \frac{R_{Load}}{V_{DC}K_{i_{SC}}} \quad \text{IV.19}$$

Then,

$$K_{p_{SC}} = \frac{L_{SC}}{\tau_{SC}V_{DC}} \text{ and, } K_{i_{SC}} = \frac{R_{Load}}{\tau_{SC}V_{DC}} \quad \text{IV.20}$$

In the same method for battery, we obtain;

$$\text{CLTF}_{batt}(s) = \frac{1}{1+\frac{R_{Load}}{V_{DC}K_{i_{batt}}}s} \text{ where, } \tau_{batt} = \frac{R_{Load}}{V_{DC}K_{batt}} \quad \text{IV.21}$$

Then,

$$K_{p_{batt}} = \frac{L_{batt}}{\tau_{batt}V_{DC}} \text{ and, } K_{i_{batt}} = \frac{R_{Load}}{\tau_{DC}V_{DC}} \quad \text{IV.22}$$

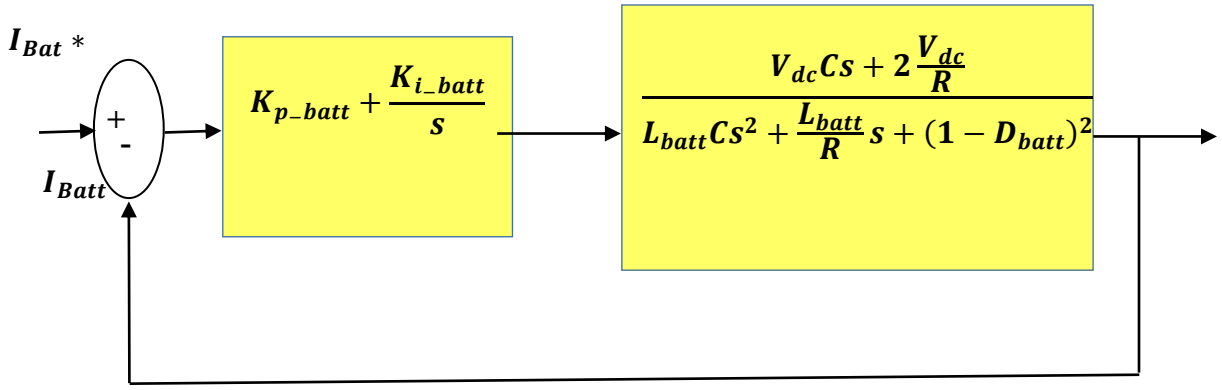


***Fig IV. 8**:Block diagram of SC controller*

The flowchart of energy management control strategy is illustrated in Fig IV.9. This diagram illustrates the functioning modes of the energy management technique (EMT) by providing charge/discharge to the battery and the Super Capacitor (SC) for various State of Charge (SOC) situations. The maximum state of charge $SOC_{\max}$ is 80%, whereas the minimum state of charge $SOC_{\min}$ is 20%.

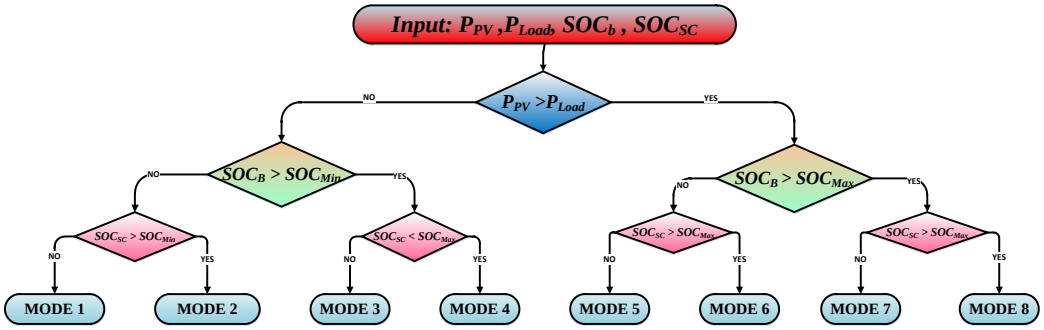


***Fig IV. 9**:Flowchart of energy management proposed*

As illustrated in Fig IV.9, there are height different modes to consider. Control techniques for controlling DC bus voltage throughout all operating states using storage devices and PV solar are described below.

IV.3.4 Maximum Power Point Tracking (MPPT)

Using MPPT control when the Photovoltaic/wind power may be lower or greater than the load power demand. While still maintaining limitations on the battery state of charge. As a result, the storage devices operating in charged/discharged scenarios. Fig 2.6, depicts a schematic diagram of a typical controller design employed to accomplish the MPPT of a PV and wind energy integrated with a boost converter. Any voltage-based MPPT method may create the control loop reference voltage. The PV or wind energy readings are necessary for the MPPT algorithm (e.g., P&O) to work correctly.

IV.3.5 Load Power Tracking (LPT)

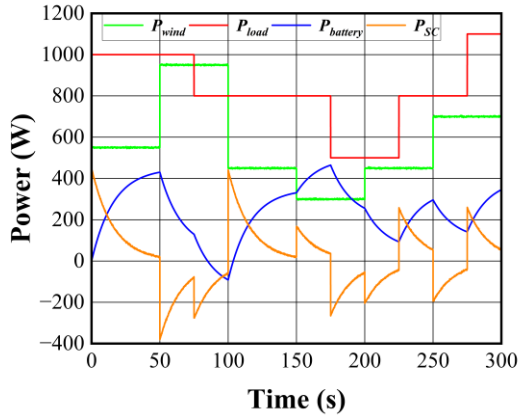
Iin this state, the wind and solar power are either greater than the load power, and the level of charge of the storage devices are full charged, in this control mode the power produce by RESs follow the power load as reference power.

IV.3.6 Load Power Shedding (LPS)

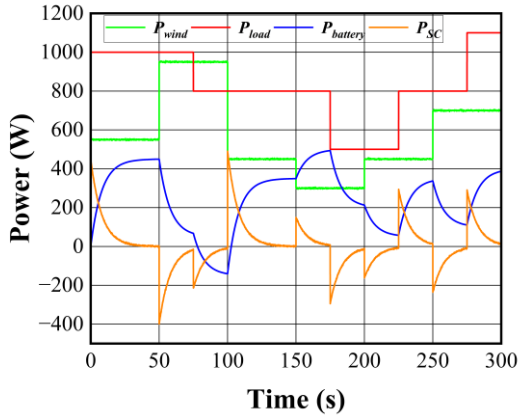
In this case, the photovoltaic and wind power are much less than the load power, and the storage devices are entirely emptied. As a result, the loads are limited to the essentials, and the storage devices regulate the DC link voltage. In this case the load decrease to the essential load.

IV.4 Simulation results of different time constant of LPF

To confirm the efficacy of the EMS suggested and system control, simulated results were executed using MATLAB-Simulink environmental. seven simulation scenarios are evaluated with various filter constants τ [0.2, 0.4, 1, 2, 4, 8, and 16]. [980, 460, 290, 460, 720w] represents the variance in wind power produced. The intended load power ranges from 500w to 1100w. This variable was selected to be less and greater than wind energy production.
The simulation findings of the evaluation with a similar changes in wind power and load consumption for varying time constants are illustrated in Fig IV.10 (a-h).



(a)



(b)

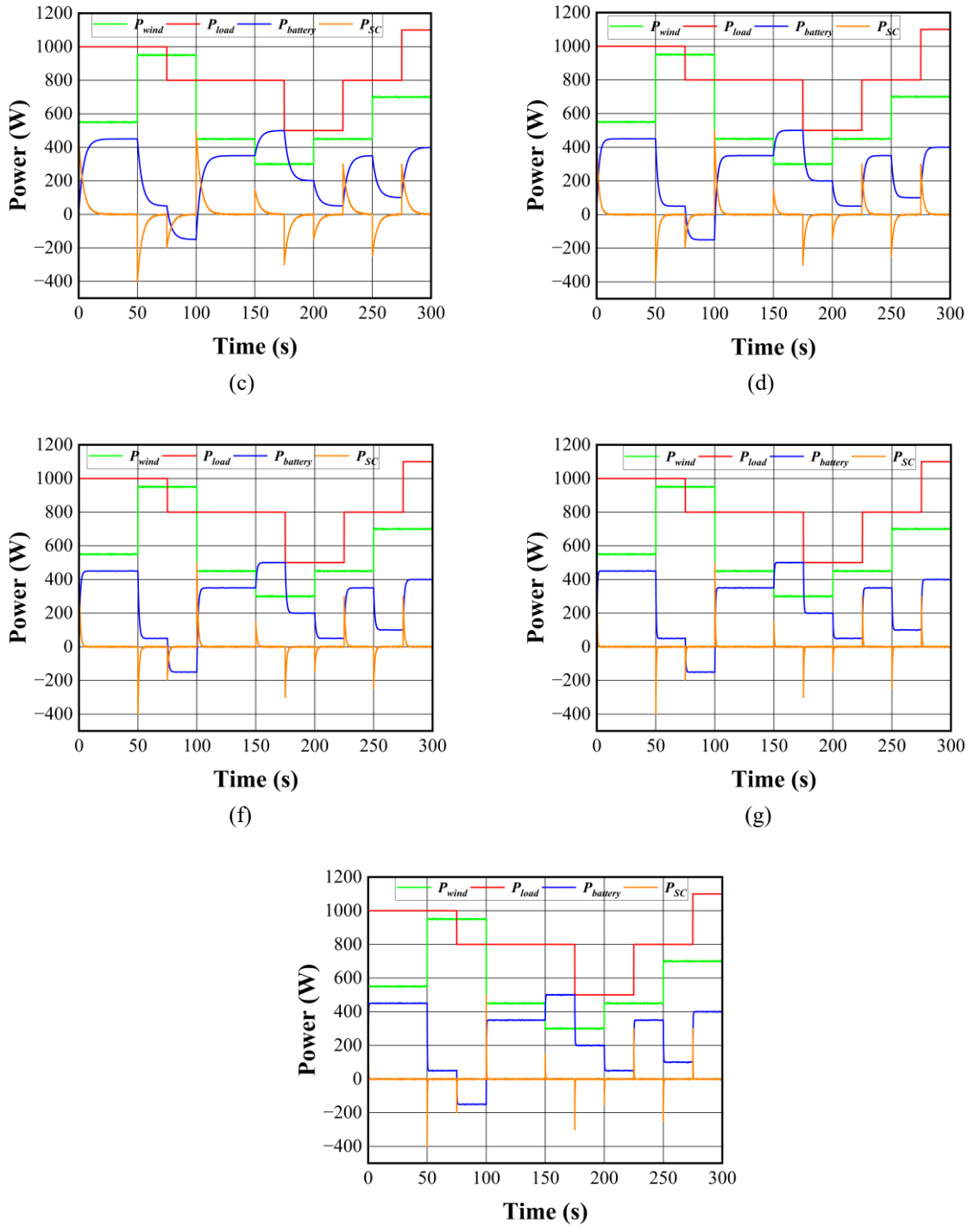
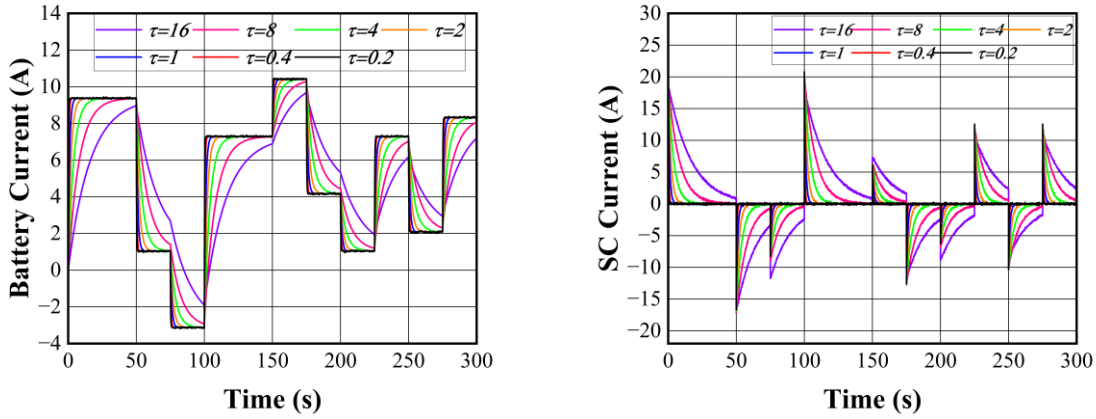


***Fig IV. 10**:power evaluations: τ =16s: 8s;4s;2s; 1s;0.4s;0.2s, (a;h)*

Fig IV.11 (a,b), is shown the battery current and the current of SCs, respectively. A longer time constant may assist in reducing the stress on the battery produced by abrupt variations in the load current. As a consequence, reaction times to rapid changes in load are also slower. In contrast, small Tc, fast response by the battery resulting increase battery stress and minimize the lifespan of battery.

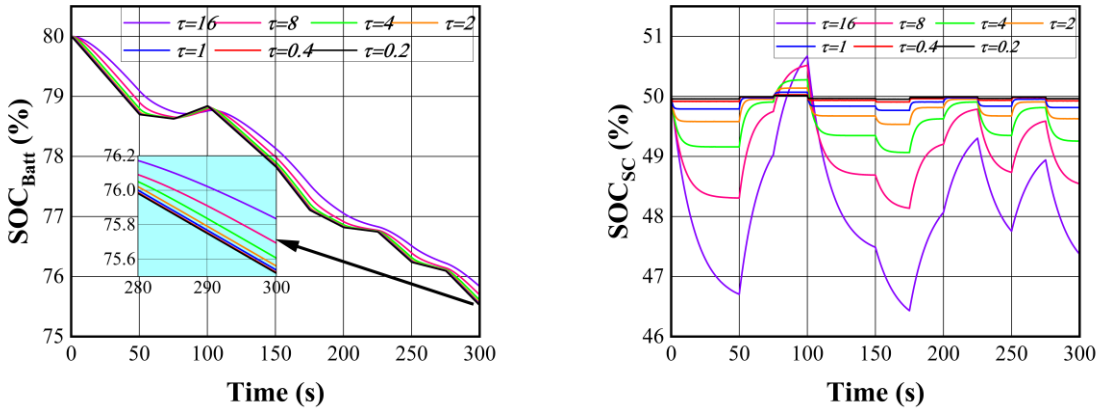
Just the peak current is eliminated by the SCs. Nevertheless, when the τ increases, the SCs are able to get rid of the peak current and guarantee an extended charging and discharging current.



(a) (b)

***Fig IV. 11**:analytic currents energy storages with different time constants τ, (a): battery current, (b): SC current*

Fig IV.12, (a) shows a comparison of the SOC of SCs for various values of τ. By an increase in the filter constant τ, the SOC_{SC} reduces charge and discharge rates. Fig IV.12, (b) shows a comparison of the SOC_{batt} for various values of. As the filter constant rises, it affects the SoC of batteries. decreased charge/discharge rate as a consequence



(a) (b)

***Fig IV. 12**:State of charge of energy storage, (a): SOC of SC, (b): SOC of battery*

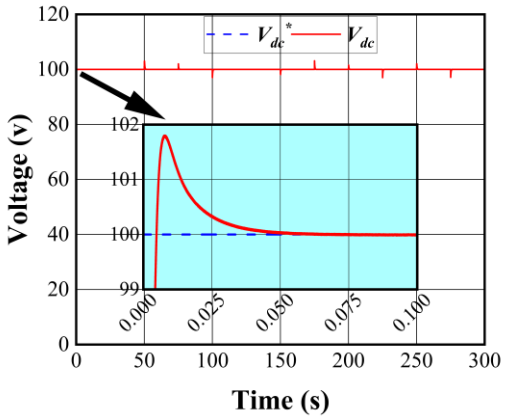


***Fig IV. 13**:DC link voltage*

Fig IV.13, depicts a curve of the DC link voltage, which remains constant at 100 V over the full serving range, with slight variations due to changes in wind production and load requirements. Table 1 shows the estimated SOC_{batt} and SOC_{SC} for one hour and the energy consumption by battery and SC for 300s. An increase in the filter constant lowers the SOC battery usage. For τ = 0.2 s, the consumption of the SOC_{batt} is 53.772 %, while for τ = 16 s, the consumption is 49.98 %.

***Table IV. 2**: Comparison of consumption of energy storage*

Time constant (s)	SOC_{batt} at 300s (%)	Consumption of SOC_{batt} for 300s (%)	Consumption of SOC_{batt} for 1 hour (%)	SOC_{SC} at 300s (%)	Consumption of SOC_{SC} for 300s (%)	Consumption of SOC_{SC} for 1 hour (%)
16	75.835	4.165	49.98	47.370	2.63	31.56
8	75.694	4.306	51.672	48.545	1.455	17.46
4	75.607	4.393	52.716	49.255	0.7451	8.9412
2	75.560	4.44	53.28	49.628	0.372	4.464
1	75.537	4.463	53.556	49.814	0.186	2.232
0.4	75.524	4.477	53.724	49.925754	0.07424	0.891
0.2	75.519	4.481	53.772	49.9628	0.0372	0.4464

IV.5 Simulation results of RES and HESS based frequency decoupling

A simulation environment is used to test the viability of the suggested energy management plan. The purpose is to evaluate all feasible scenarios as well as do a one-day continuous test for the planned DC microgrid.

IV.5.1 One-day experimental test

Unlike the next two experiments, which try to illustrate all different possibilities, the goal of the one-day experiment is to illustrate and verify the efficacy and implementation of the full system strategy in a real-life situation. As a result, no human intervention is required during the test. It is to validate that the hybrid battery/SC power system can perform well with the actual power (PV/Wind) and load profile under the direction of the suggested strategy. The data of irradiation and wind speed throughout the one-day test 0 to 24 obtained from a real location for a one-day dynamic tests, which was executed in October 2023 at Medea, Algeria. One second in the simulation study presented one hour in a real scenario. Fig IV.14 (A), depicts the actual sun light and air velocity on this day. Fig IV.14 (B), depicts the planned DC microgrid's power evolution over the course of one day. The load is provided by the battery and Wind power during the period (0 to 5) and (20 to 24). SCs respond immediately and quickly to the deficiency or surplus in situations of fluctuation in power generation or power load. The extra power generated by (PV/wind) is utilized to charge the batteries during the period (5 to 20). The waveform of the DC bus voltage is shown in Fig IV.14 (C), which is maintained constant at 100v, there are slight fluctuations (fewer than 2% of the rated DC link voltage). throughout the working range. The evolutions of SOC_{HESS} in Fig IV.14 (D), indicate that storage capacities are respected. Both supplying and absorbing energy, the battery and SC are effective.

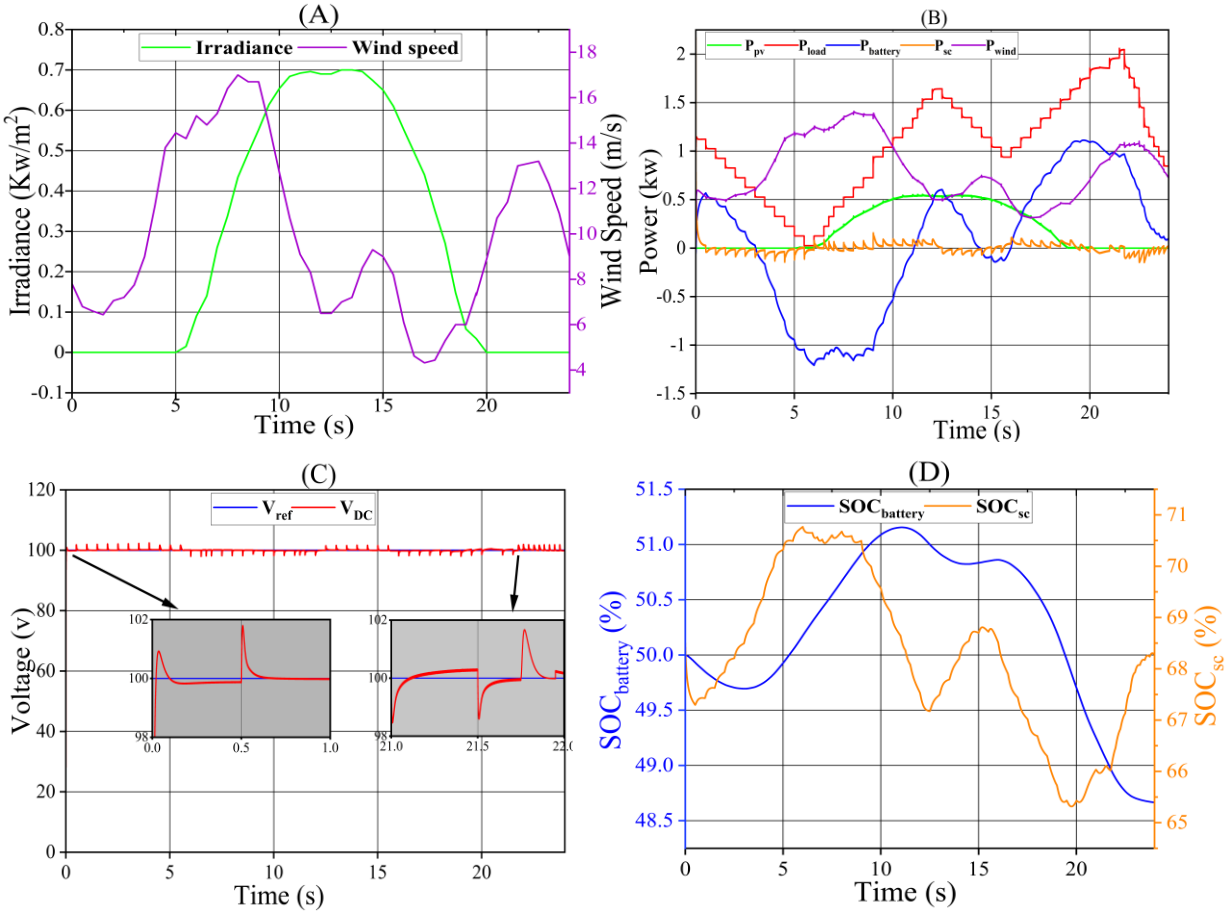


***Fig IV. 14**: (A) irradiation and wind speed profile; (B) power evaluations; (C) Dc link voltage; (D) SOCHESS*

IV.5.2 HESS SOC UPPER LIMIT SITUATION

Fig 4.15 (A), demonstrates the variations in sunlight irradiation and wind velocity. Fig 4.15. (B and D), depict the operating results when the battery and SC are fully charged. In the first interval (mode 4), the power production is less than the power load, and SOC_B and SOC_{SC} are upper than SOC_{Max} ,the SC is discharged to compensate for the shortfall. Then, (mode 3), SC discharge to reach lower than SOC_{Max} .similar in in (mode 1), battery discharge to cover the deficit, SOC_B is lower than SOC_{Max} .In (mode 9), the power generation increased to be more than power load in this case the battery and SC absorbed the surplus power to reach at SOC_{Max} .Where the SC is fully charged and SOC_{SC} equally SOC_{Max} in (mode 10). After fully charge of SC the surplus power absorbed by the battery. As appear that the surplus or deficit power is absorbed and supplied by the battey and SC. Where (PV/wind) are operated in MPPT control to extract the maximum power. At the end in (mode 11) the HESS are fully charge. As a consequence, PV is converted from MPPT to LPT mode in order to share the load demand. In Fig 4.15 (C). DC link voltage kept constant in followed the reference value 100v through all the modes.

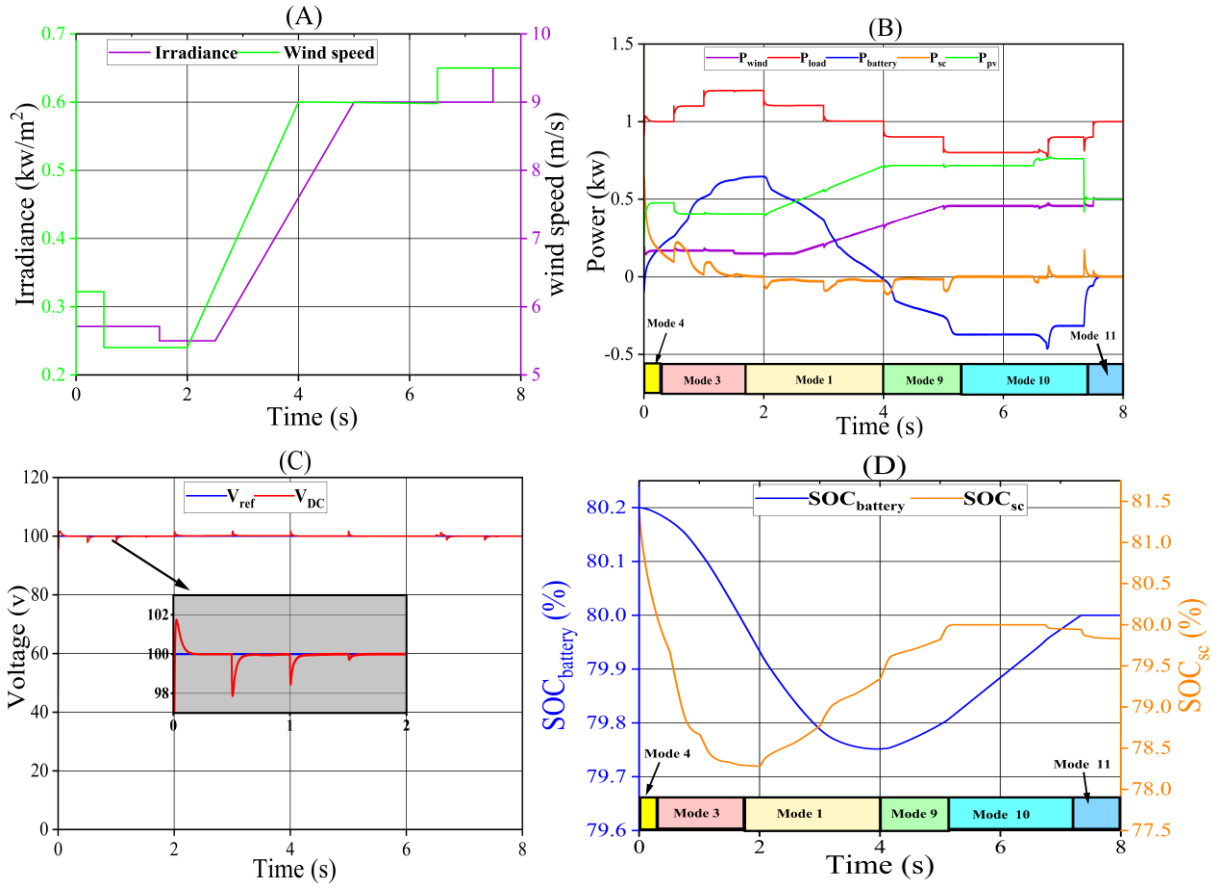


Fig IV. 15 *:(A) irradiation and wind speed profile; (B) power evaluations; (C) Dc link voltage; (D) SOCHESS*

IV.5.3 HESS SOC lower limit situation

Fig IV.16 (A), demonstrates the variations in sunlight irradiation and wind velocity. In Fig IV.16 (B), PV, wind, load, battery and SC power variations are shows, where the SOC_B and SOC_{SC} are illustrated in Fig IV.16 (D).

the operation scenario is as follows: In (mode 5) the power produced from PV and wind are more than load required, the excess power is absorbed by battery and SC that their SOC are lower than SOC_{Min}. SOC_{SC} is rapidly charged to reach its SOC upper than SOC_{Min} in (mode 6). In (mode 7) battery is continuously charge to reach more then SOC_{Min}.

In the end of (mode 7), the power generation is decreased to be lower than the demand load in (mode 8), where the SC is supplied power deficit. In (mode 1), the power deficit is increased, this power is compensated by the battery. However, SOC_B is discharged to reach the SOC_{Min}, in (mode 9), where control mode switched from MPPT to LPS to reduce the load to the essential load at 0.5 kw. Fig IV.16 (B) demonstrates that the utilization of HESS in the system simulation effectively mitigates the adverse impact of peak currents on the batteries, and appears exponentially. SC additionally decrease the variation of the DC bus voltage when there are sudden changes in the load and variations in photovoltaic (PV) or wind power, as seen in Fig IV.16 (C).

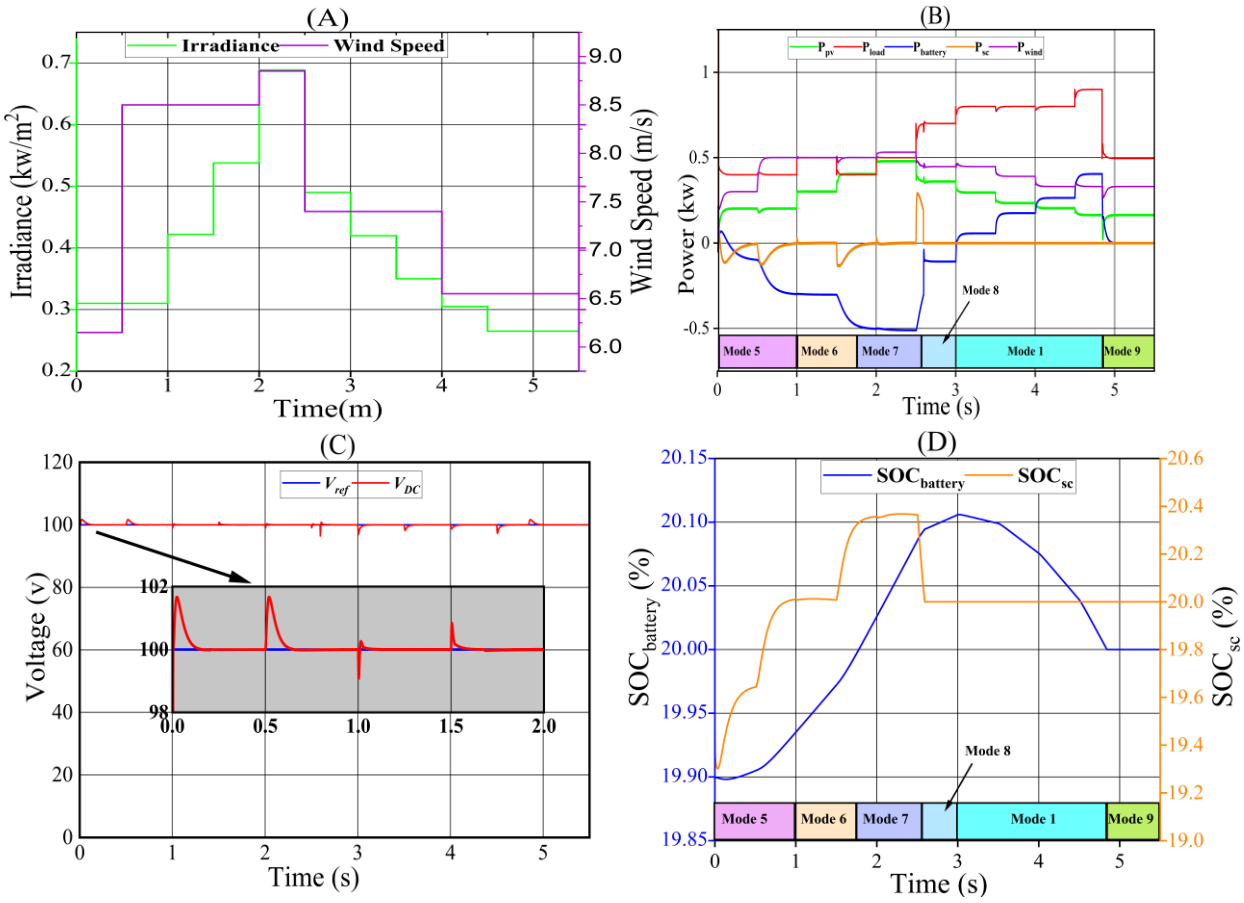


***Fig IV. 16**:(a) irradiation and wind speed profile; (b) power evaluations; (c) Dc link voltage; (d) SOCHESS*

IV.6 Energy management control based fuzzy logic

The electricity produced by RESs fluctuates during the day because of changes in irradiance, temperature, and wind speed. To satisfy the requirement for load, it is crucial to have an energy management system (EMS), Fig IV.17, depicts the Fuzzy logic energy management system (FL-EMS) for DCMG with HESS. Despite both load and power source fluctuations. The DC link voltage is controlled using PI control. The control method for this voltage regulation is shown in Fig IV.17. To regulate the voltage, the PI controller calculates the desired current for the DC bus, represented as (I_{DC_ref}), and sets the desired voltage for the DC bus as V_{DC_ref}= 48 V. The converter is given with current references ($I_{\text{b_ref}}$) and (I_{SC_ref}) via the usage of FL-EMT. The present references will ensure that the DC bus voltage remains constant irrespective of the supplied load. The total value of the references being used must always meet the requirements stated in the following Equations provide a precise explanation of the voltage in the DC connection.

$$I_{DC_ref} = I_{\text{b_ref}} + I_{SC_ref} \quad \text{IV.23}$$

$$C_{DC}\frac{d_{C_{DC}}}{dt} = I_{\text{b}} + I_{SC} - I_{\text{Load}} \quad \text{IV.24}$$

I_{b} , I_{SC}, and I_{Load} indicate the currents being pulled from the batteries, the short circuit (SC), and the load, respectively. The word "C_{DC}" stands for the capacity of the DC bus, which defines the ability of the DC bus voltage to be distributed to all sources and loads. The system is provided with two reference currents: one for the batteries, written as (K_{Battery}), and one for the supercapacitor, denoted as (K_{SC}). These reference currents are used for the management of HESS, (RES) and the load is controlled by the third output of FL (Control mode), as shown in Fig IV.17. In order to regulate the instantaneous voltage fluctuations that occur in the SCs, a low-pass filter is added to the DC bus current, which is known as additionality. To ascertain the values of I_{SC_ref} and $I_{\text{b_ref}}$. When determining the reference values of currents, it is important to consider both the state of charge of the battery (SOC_b) and the state of charge of the supercapacitor (SOC_{SC}). To achieve this goal, a switch is used to choose the appropriate reference current. The current is then regulated by a FL, as seen in Fig IV.17, (b).

Fuzzy logic-based EMS has been developed for this reason, since it more effectively handles uncertainty using linguistic variables and inference rules. As shown in Fig IV.18, and IV.19. the suggested EMS has been built using Mamdani Fuzzy Inference System (FIS) and Fuzzy Logic Designer.

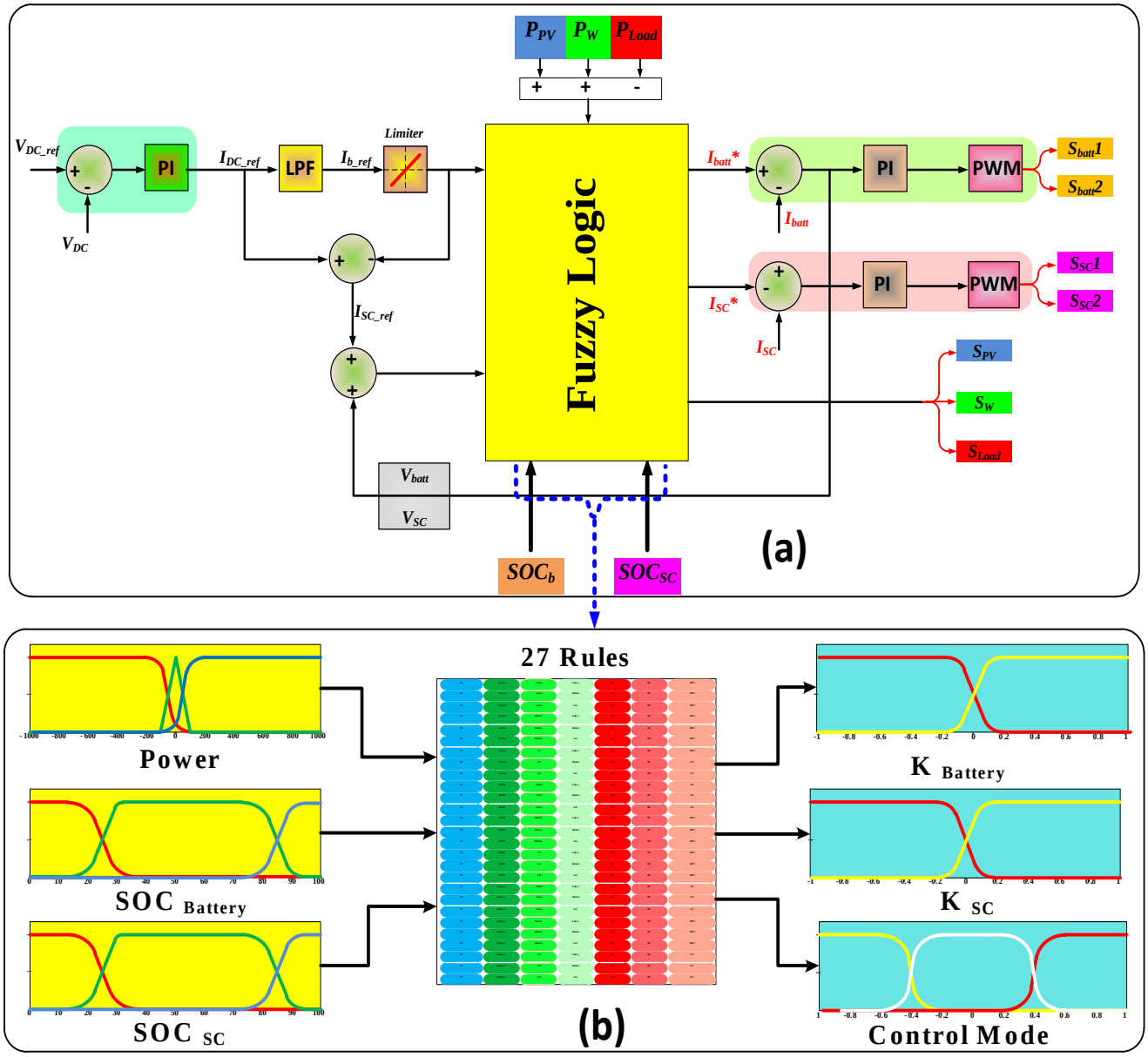


***Fig IV. 17**:Proposed fuzzy logic energy management system*

It is composed of three inputs, three outputs, and 27 rules that have been developed specifically for energy management. Fig 4.18, displays a set of rules for FLEMS that are based on intuition and has been simulation. The following is how the input and output parameters have been constructed with regard to their corresponding membership functions:

IV.6.1 Balanced power

The power in DC MG that must be balanced under fluctuating power production from RESs and electricity load variables is called to as power balance, and it was computed in the following way [255]:

$$P_{balance} = P_w + P_{PV} - P_{\text{load}} \qquad \text{IV.25}$$

Power input has three membership functions Excess(E), Deficit(D) and Balance (B). This parameter's range represents the power between 1 KW to -1 KW, as seen in Fig 4.19 (a)

IV.6.2 State of charge (SOC) of battery

The membership functions of the Battery SoC and SC are Empty(E), Medium(M), and Full(F). As shown in Fig. 4.19 (b), the range of this parameter represents the battery and SC SoC%, which may vary from 0 to 100%.

IV.6.3 State of charge (SOC) of SC

There are three levels of membership function inside the SoC of SC: low, medium, and high. The values that fall inside this parameter's range represent the SC SoC%, and they may be anywhere from 0% to 100%, as shown in Fig 4.19 (c)

Output of Fuzzy logic

IV.6.4 Battery signal

Where: $\mathbf{K_{battery}}$: The control signal of the battery converter's switch, $K_{battery}$ input has two membership functions (on and off), where ON signifies that the battery may charge or discharge and OFF indicates that the battery has been turned off. The $K_{battery}$ is represented by the values that lie within the range of this parameter, which may vary from -1 to 1, as illustrated in Fig 4.19 (d).

IV.6.5 SC signal

Where: $\mathbf{K_{sc}}$: The control signal of the battery converter's switch, Ksc input has two membership functions (on and off), where ON signifies that the SC may charge or discharge and OFF indicates that the SC has been turned off. The Ksc is represented by the values that lie within the range of this parameter, which may vary from -1 to 1, as illustrated in Fig 4.19 (e).

Rule number	Inputs Variables			Outputs Variables		
	Power	$SOC_{Battery}$	SOC_{SC}	$K_{Battery}$	K_{SC}	Control mode
01	Excess	Empty	Empty	ON	ON	MPPT
02	Excess	Empty	Medium	ON	ON	MPPT
03	Excess	Empty	Full	ON	OFF	MPPT
04	Excess	Medium	Empty	ON	ON	MPPT
05	Excess	Medium	Medium	ON	ON	MPPT
06	Excess	Medium	Full	ON	OFF	MPPT
07	Excess	Full	Empty	OFF	ON	MPPT
08	Excess	Full	Medium	OFF	ON	LPT
09	Excess	Full	Full	OFF	OFF	LPT
10	Deficit	Empty	Empty	OFF	ON	LPS
11	Deficit	Empty	Medium	OFF	ON	LPS
12	Deficit	Empty	Full	OFF	ON	LPS
13	Deficit	Medium	Empty	ON	ON	MPPT
14	Deficit	Medium	Medium	ON	ON	MPPT
15	Deficit	Medium	Full	ON	OFF	MPPT
16	Deficit	Full	Empty	ON	OFF	MPPT
17	Deficit	Full	Medium	ON	ON	MPPT
18	Deficit	Full	Full	ON	ON	MPPT
19	Balance	Empty	Empty	ON	ON	LPS
20	Balance	Empty	Medium	ON	ON	LPS
21	Balance	Empty	Full	ON	ON	LPS
22	Balance	Medium	Empty	ON	ON	MPPT
23	Balance	Medium	Medium	ON	ON	MPPT
24	Balance	Medium	Full	ON	ON	MPPT
25	Balance	Full	Empty	ON	ON	LPT
26	Balance	Full	Medium	ON	ON	LPT
27	Balance	Full	Full	OFF	ON	LPT

***Fig IV. 18**: fuzzy inferential rules*

IV.6.6 Control mode

Control mode outputs have three membership functions: Maximum Power Point Tracking (MPPT), Load Power Tracking (LPT), and Load Power Shedding (LSC)

IV.6.6.1 MPPT control

Using MPPT control when, the Photovoltaic / wind power may be lower or greater than the load power demand. While still maintaining limitations on the battery state of charge. As a result, the DC link voltage has been controlled by the storage devices operating in charged/discharged scenarios.

IV.6.6.2 LPT control

In this state, the wind and solar power are either greater than the load power, and the level of charge of the storage devices are full charged

IV.6.6.3 LSC

In this case, the photovoltaic and wind power are much less than the load power, and the storage devices are entirely emptied. As a result, the loads are limited to the essentials, and the storage devices regulate the DC link voltage.

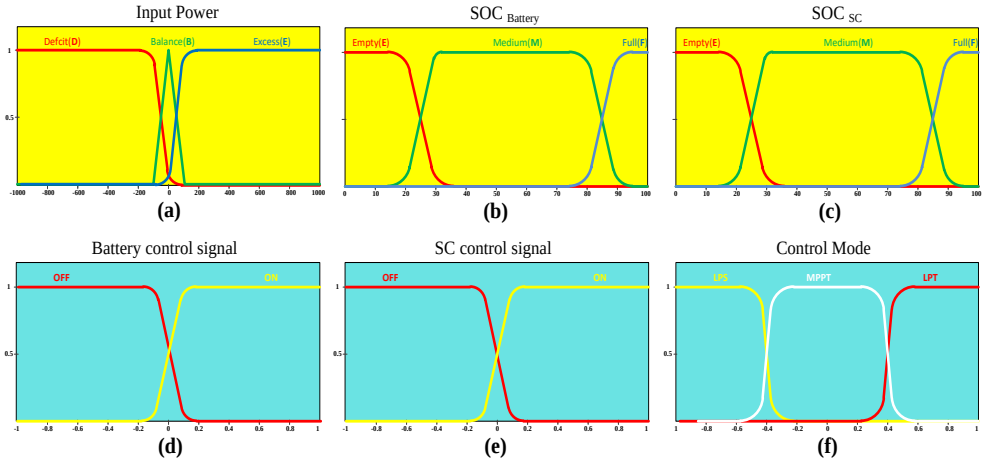


***Fig IV. 19**:Membership functions*

IV.6.7 Simulation results fuzzy logic based EMT

MATLAB/Simulink was used to build a rule-based FL for in-depth investigation and technical performance evaluation of the proposed EMT by three tests. First, a one-day test was conducted with real data. 2) Conduct the test with the HESS almost empty. 3 Run the test using HESS at around full charge. Table 4.3 shows all components of the system with their parameters used in the simulation

***Table IV. 3**: System parameters description.*

Parameters	Specifications
PV solar	P=200 W, V_{MP}=47.06V, I_{MP}=4.26A, N_S=1, N_P=2
Wind turbine	P=1 kW, Diameter=2.8 m, Working wind speed (3~25) m/s
PMSG	P=1 kW, V=220 V, I=12 A, Rated Rotate Speed= 180 rpm
Battery	Capacity=20 Ah, Rated voltage=24V
SC	Capacitance= 41.666 F, Rated voltage= 32.4V
Converters	L_{pv}=0.0016 mH, L_W=0.0026 mH, L_{SC}=0.00103 mH, L_{Bat}=0.0055 mH, C_{DC}=1200 µF

IV.6.7.1 One day test

The test was carried out for a small house, which is in the city of Medea-Algeria, at a latitude of 36◦27212′ S and a longitude of 2◦78565′ E. for one day in June 2024 as shown in Fig 4.20. The Medea region has a hot summer (June to September) and good solar potential. With an average annual wind speed of around 8.675 m/s, Fig 4.21, which shows daily averages of global irradiance on a horizontal plane collected on June 4, 2022. The purpose of the one-day experiment is to show and demonstrate the usefulness of the entire system approach in an actual-life scenario. Therefore, there is no human involvement at any point in this test.



***Fig IV. 20**:Location Medea, Algeria.*

It is to confirm that the hybrid PV/Wind/battery/SC power system can function effectively with the actual PV and Wind power and load profile while under the direction of the suggested approach.Fig 4.22. depicts the suggested DC microgrid's performance over the course of one day in terms of power evolution. When (0 to 3.4) and (11.6 to16.5) occurs, PV and wind power are utilized to provide the load, with any excess power going towards charging the battery, the PV and wind are unable to satisfy the power demand load during the intervals (3.4 to 11.6) and (16.5 to the end) and the battery covers the deficit. Where, SC reacts quickly and handles transient values as well as sudden changes in load or power product.

Totally observance of the state of charge of SOC_b and SOC_{SC} evolution is shown in Fig 4.23. as can be seen in Fig 4.24, the DC line voltage development hardly changes over time. The waveform of the PMSG voltage during the change in wind speed is shown in Fig 4.25.

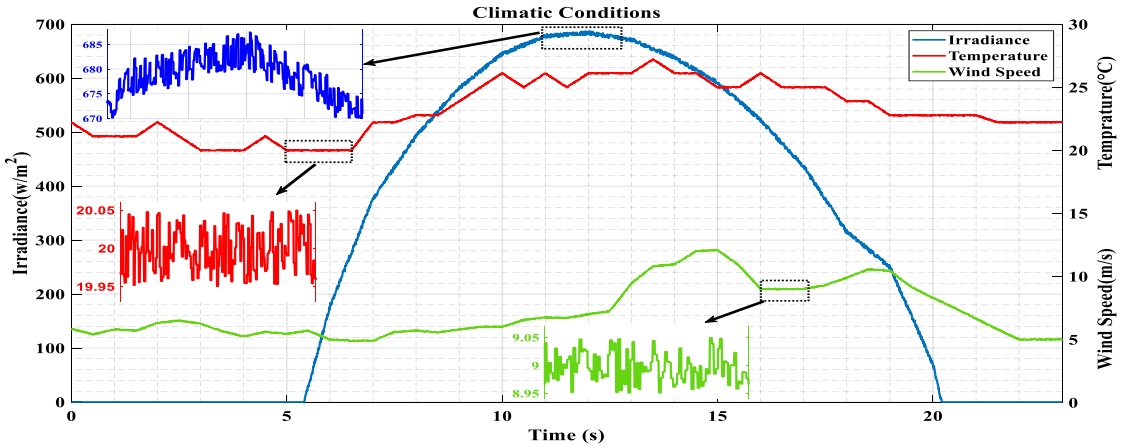


***Fig IV. 21**:Weather data on the 4th June 2022 in Medea, Algeria.*

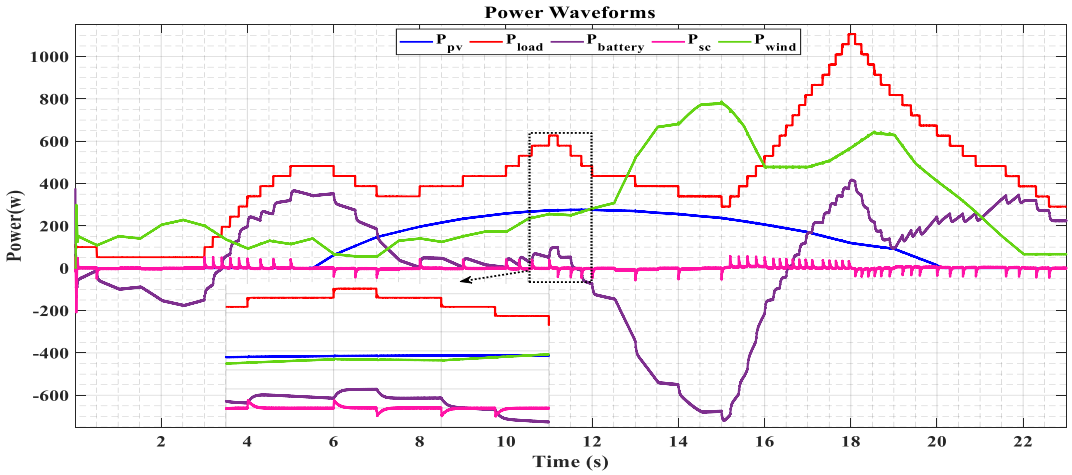


***Fig IV. 22**:Power waveforms*

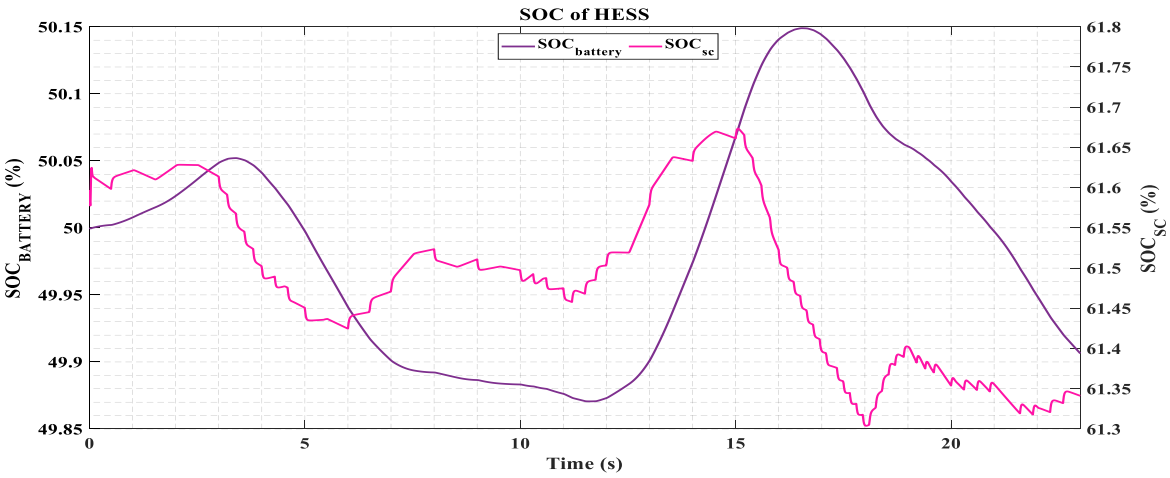


***Fig IV . 23**:State of charge of HESS*

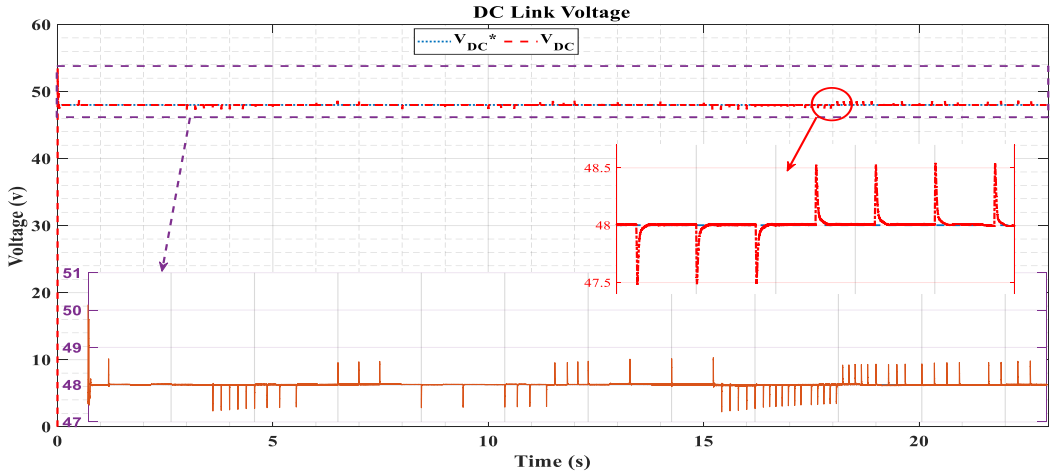


***Fig IV. 24**:DC link Voltage*

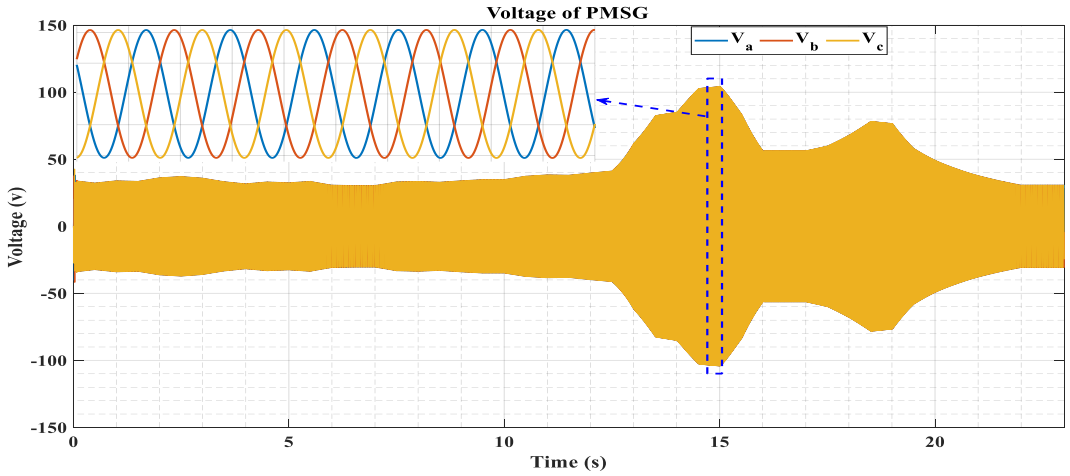


***Fig IV. 25**:Voltage of PMSG*

IV.6.7.2 HESS almost empty.

As illustrated in Fig 4.26 amd 4.28, the effectiveness of the proposed FL-EMT is validated across all modes of operation by varying power generation, load demand, HESS SoCs, and control modes.To ensure that we cover all of the bases described in Table 4, we run the simulation for a total of 2.7 s.

The system is initiated at t = 0 s when the power production is balanced with the required load, RES are operating in MPPT mode, and $SOC_b$and SOC_{SC} are fewer than SOC_{Min}. At t = 0 s, the supercapacitor absorbs excess power until the battery reaches a stable state and the DC link voltage stabilizes at the rated value. In case 19 and 01, corresponding to 0-0.275 s, HESS are furnished and absorbed the average deficit and excess power. It is can notice from 0.275s to 1.2s, the battery keep on charge/discharge to compensate excess/deficit power .Where, SOC_b is more then lower limits, until SOC_b reach on lower limits at t=1.2s , where, the battery is stopped and power defict is compensated by SC only. the control mode is switched from MPPT to LPS and the load is decreased to essential load 120W, at t=1.51s.

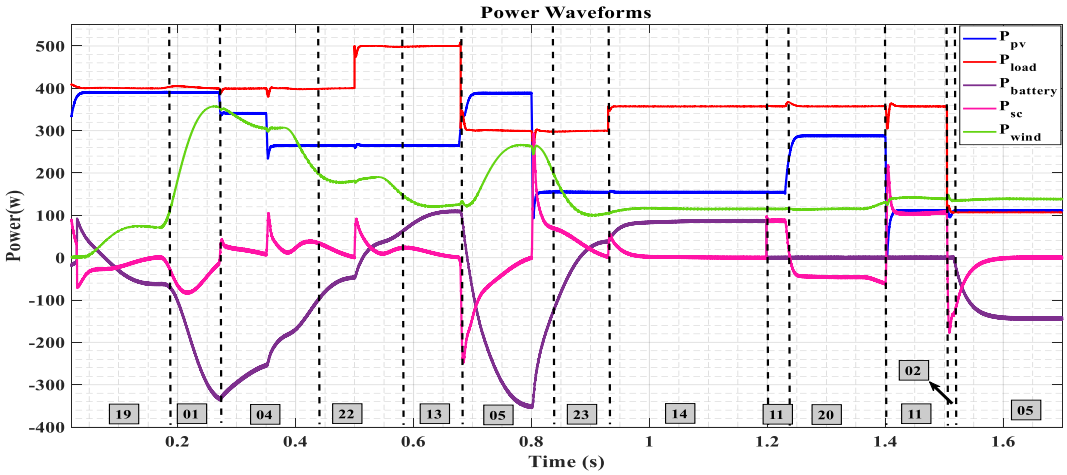


***Fig IV. 26**:Power waveforms*

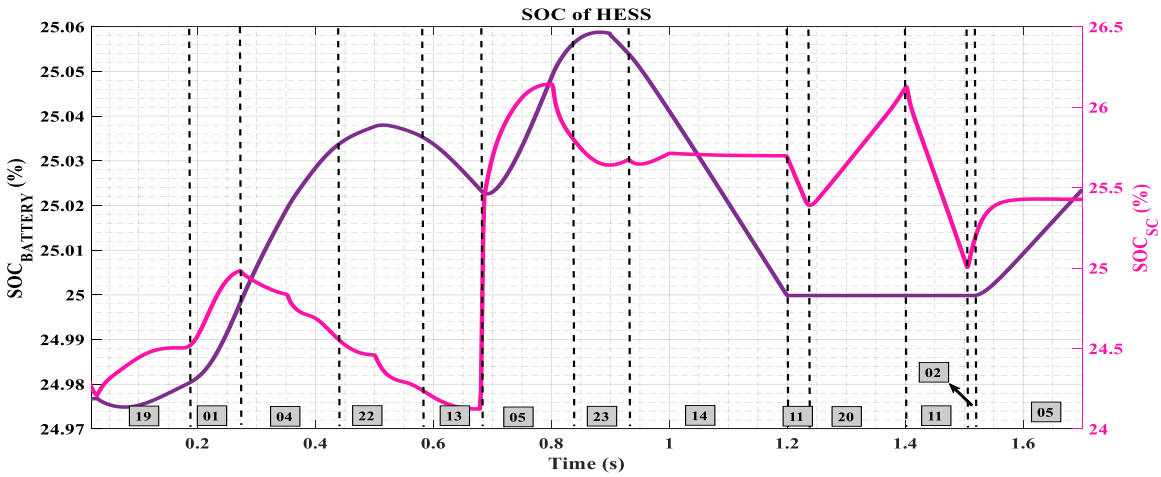


***Fig IV. 27**:State of charge of HESS*

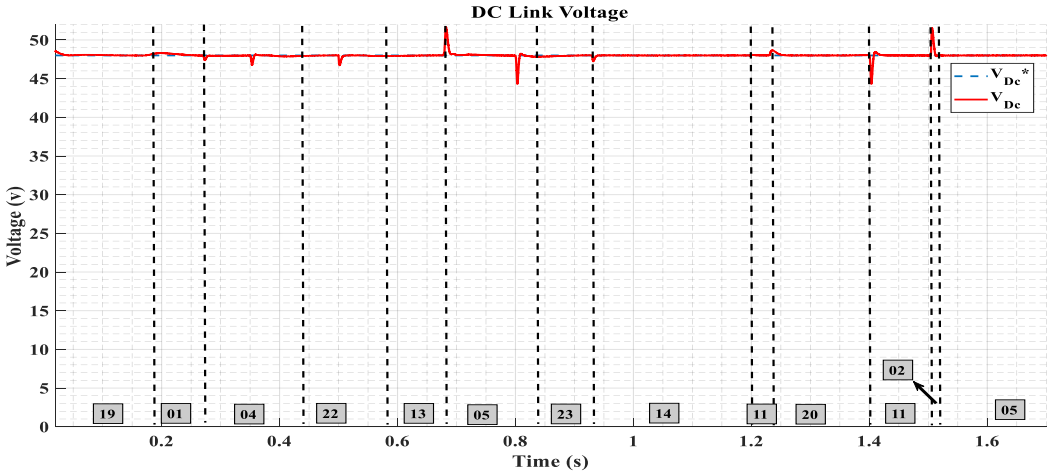


***Fig IV. 28**:DC link Voltage*

***Table IV. 4**: Operating modes with HESS almost empty*

Cases	Sim-Time	SOC_b	SOC_{SC}	K_B	K_{SC}	Control mode
Case 19	00 : 0.185	SOC_b<25	SOC_{SC}<25	ON	ON	MPPT
Case 01	0.185 0.275	SOC_b<25	SOC_{SC}<25	ON	ON	MPPT
Case 04	0.275 : 0.44	SOC_b >25	SOC_{SC}<25	ON	ON	MPPT
Case 22	0.44 : 0.58	SOC_b >25	SOC_{SC}<25	ON	ON	MPPT
Case 13	0.58 : 0.68	SOC_b >25	SOC_{SC}<25	ON	ON	MPPT
Case 05	0.68 : 0.84	SOC_b >25	SOC_{SC} >25	ON	ON	MPPT
Case 23	0.84 : 0.94	SOC_b >25	SOC_{SC} >25	ON	ON	MPPT
Case 14	0.94 : 1.20	SOC_b >25	SOC_{SC} >25	ON	ON	MPPT

Case 11	1.20 : 1.35	SOC_b =25	SOC_{SC} >25	OFF	ON	MPPT
Case 20	1.35 : 1.40	SOC_b =25	SOC_{SC} >25	OFF	ON	MPPT
Case 11	1.40 : 1.505	SOC_b =25	SOC_{SC} >25	OFF	ON	MPPT
Case 02	1.505: 1.52	SOC_b =25	SOC_{SC} >25	OFF	ON	LPS
Case 05	1.52: End	SOC_b >25	SOC_{SC} >25	ON	ON	LPS

IV.6.7.3 HESS almost Full.

As illustrated in Fig 4.29 and 4.31, the simulation is initiated with SOC of battery and SC are more than their SOC_{Max}. And P_{Load} is greater then the power that produce by RES. The battery and SC are discharged to supply the gaping power (cases 18, and 27). It can be observed during the period (0.42 to 1.88s), SOC_b on limitaton and appear that HESS are charged where the excess power available and discharge to supply the load on deficit case. At t=1.88s batty his fully chaged and the excess power is absorbed by SC. The control mode is switched from MPPT to LPT at t=2.42s where HESS are completely charged and the power produce from RESs follow load domend.

***Table IV. 5**: Operating modes with HESS almost fully*

Cases	Sim-Time	SOC_b	SOC_{SC}	K_{Ba}	K_{SC}	Control mode
Case 18	00 : 0.19	$SOC_b > 85$	$SOC_{SC} > 85$	ON	ON	MPPT
Case 27	0.19 : 0.325	$SOC_b > 85$	$SOC_{SC} > 85$	ON	ON	MPPT
Case 24	0.325 : 0.425	$SOC_b < 85$	$SOC_{SC} > 85$	ON	ON	MPPT
Case 15	0.425 : 0.61	$SOC_b < 85$	$SOC_{SC} > 85$	ON	ON	MPPT
Case 24	0.61 : 0.85	$SOC_b < 85$	$SOC_{SC} > 85$	ON	ON	MPPT
Case 06	0.85 : 0.99	$SOC_b < 85$	$SOC_{SC} > 85$	ON	ON	MPPT
Case 14	0.99 : 1.26	$SOC_b < 85$	$SOC_{SC} < 85$	ON	ON	MPPT
Case 23	1.26 : 1.41	$SOC_b < 85$	$SOC_{SC} < 85$	ON	ON	MPPT
Case 05	1.41 : 1.79	$SOC_b < 85$	$SOC_{SC} < 85$	ON	ON	MPPT
Case 08	1.79 : 1.9	$SOC_b = 85$	$SOC_{SC} < 85$	OFF	ON	MPPT
Case 26	1.9 : 2.02	$SOC_b = 85$	$SOC_{SC} < 85$	OFF	ON	MPPT
Case 17	2.02 : 2.11	$SOC_b = 85$	$SOC_{SC} < 85$	OFF	ON	LPT
Case 27	2.42 : 2.43	$SOC_b = 85$	$SOC_{SC} = 85$	OFF	ON	LPT

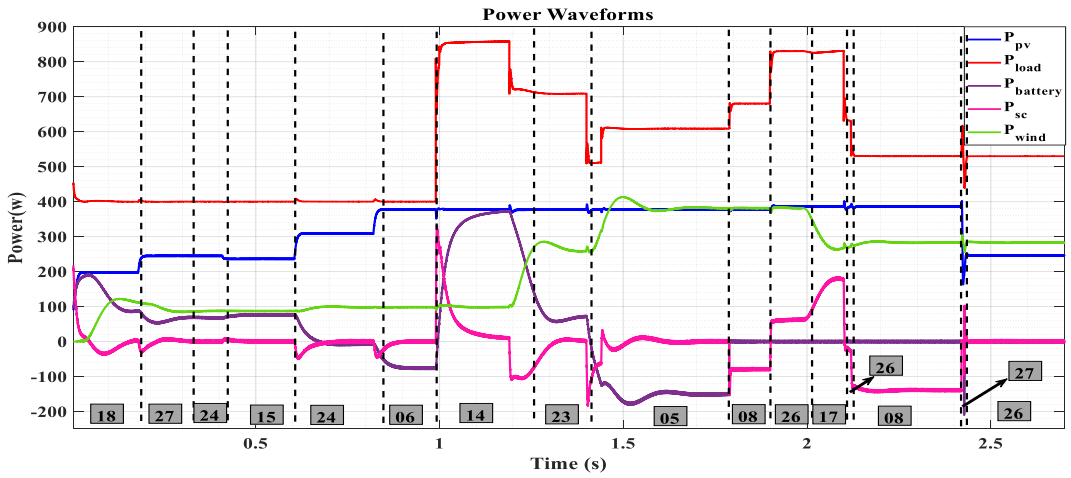


***Fig IV. 29**:Power waveforms*

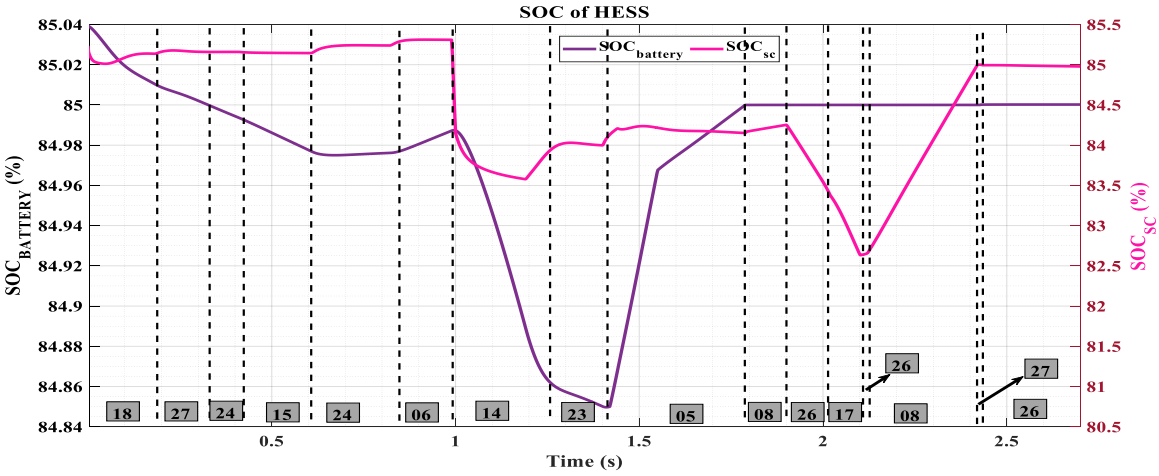


***Fig IV. 30**:State of charge of HESS*

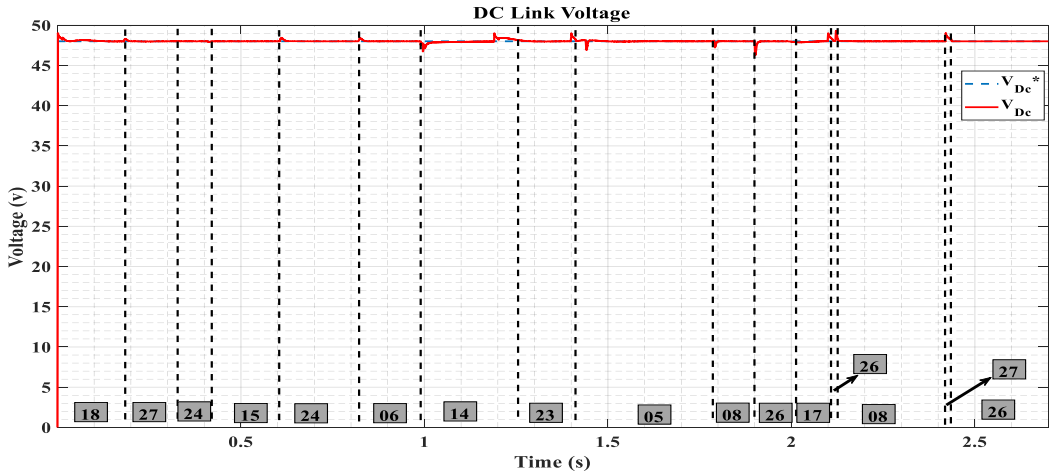


***Fig IV. 31**:DC link Voltage*

IV.7 Energy management based fuzzy logic improved

Fuzzy logic control-based power management is designed with three inputs variables and two outputs variables. The membership functions (MFs) of the power net P_{gap} are categorized into five levels (High Positive, Positive, Balance, Negative, High Negative) to meet the criteria of the suggested FL-PMT. These levels indicate the power values, which are selected from a range of -2000 to 2000. the 2nd and 3rd inputs are SOC_{batt}, SOC_{SC} respectively. The membership functions (MFs) of SOC_{batt}, SOC_{SC} are categorized into three levels (Empty, Moyen, Full) the range of SOC is selected between [0 : 100], the minimum of the state of charge SOC_{Min} is 20%, and the maximum of the state of charge SOC_{Max} is 80%. The membership function results that have been optimised are shown in Fig 4.34.

The optimisation results for the fuzzy logic-based energy management system (EMT) are shown in Fig4.34 (a). In the figure, (a) corresponds to the membership function for the input power demand, (b) represents the input state of charge (SOC) of the battery, (c) represents the input SOC of the supercapacitor (SC), and (d,e) represent the control outputs for the battery and SC, respectively. Fig 4.35, illustrates the fuzzy output surfaces for all possible combinations.

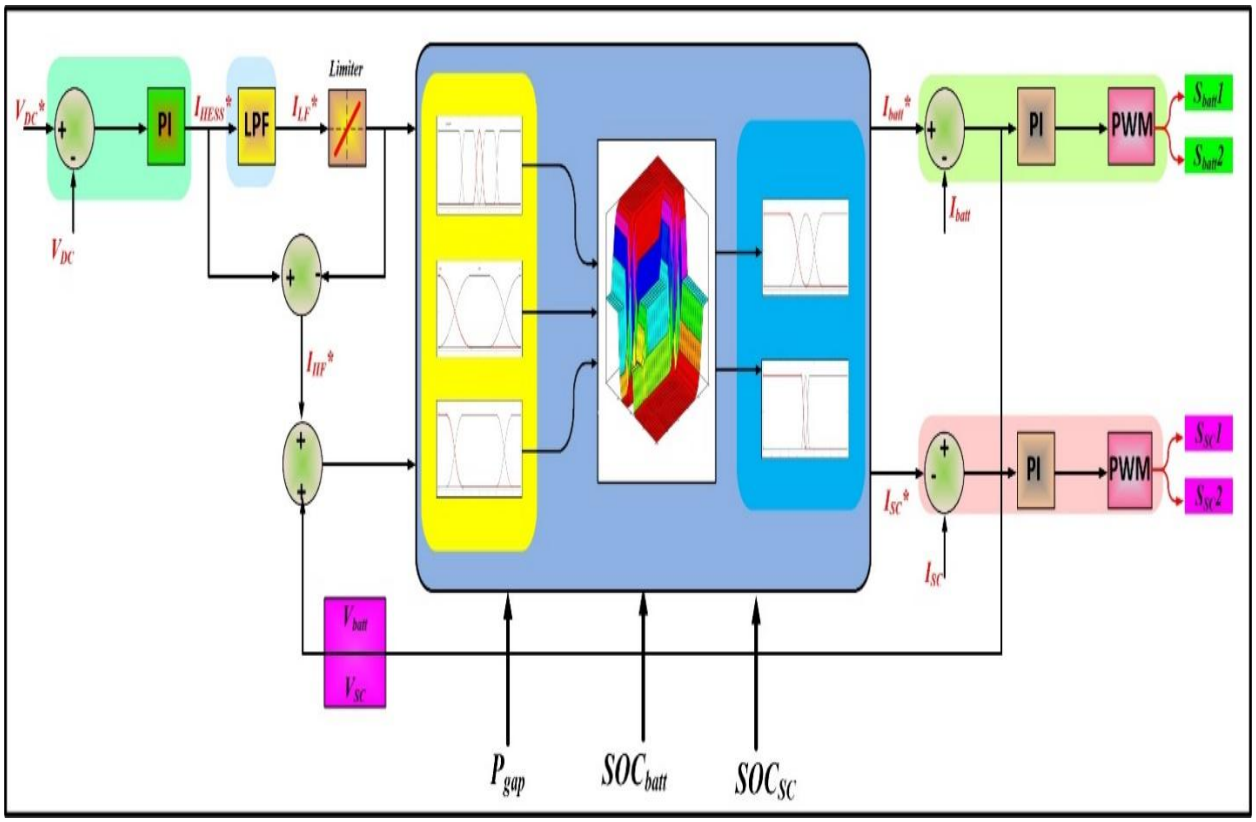


***Fig IV. 32**:Energy management technique*

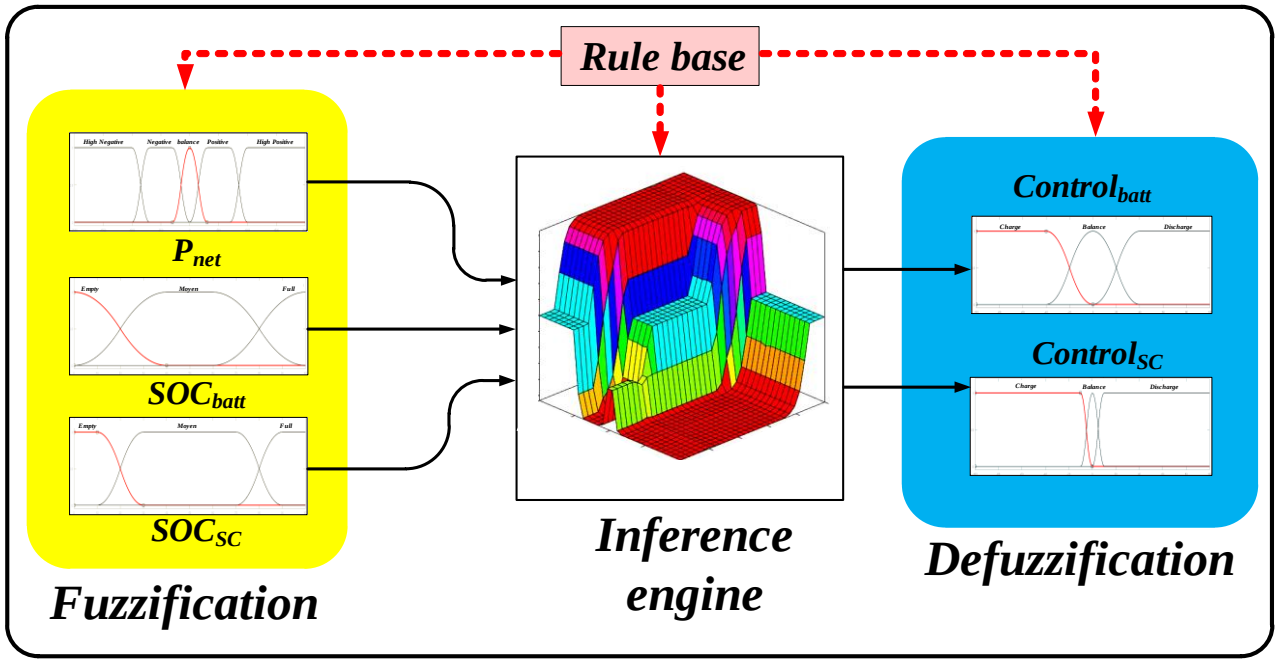
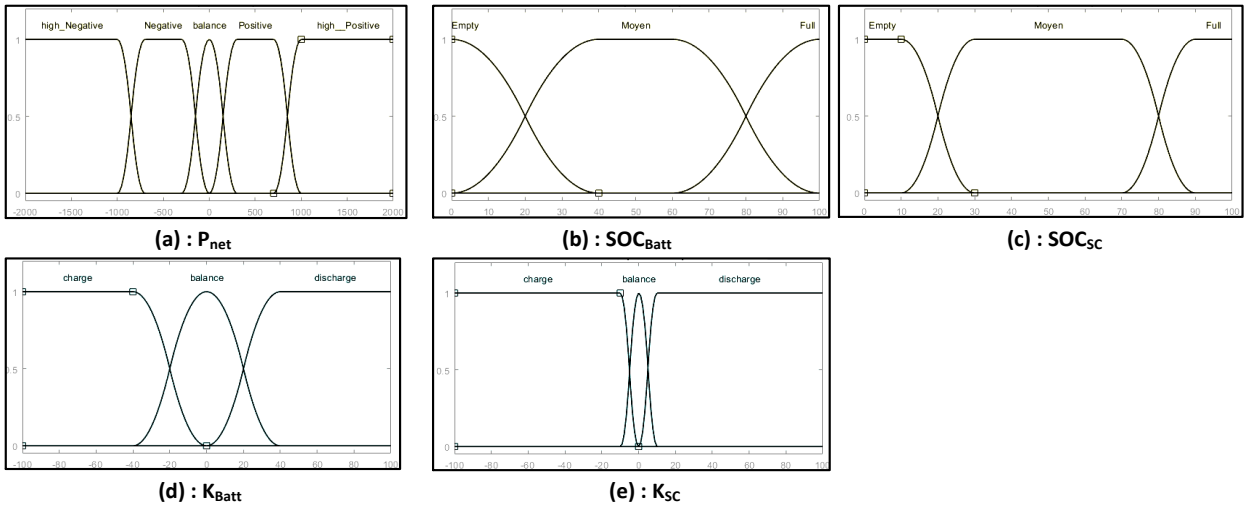


Fig IV. 33:A power management based FLC block



(a) : P_{net} (b) : SOC_{Batt} (c) : SOC_{SC}

(d) : K_{Batt} (e) : K_{SC}

Fig IV. 34:Inputs and outputs membership function: (a) P_{net} . (b) SOC_{batt}. (c) SOC_{SC}. (d). $Control_{batt}$ (e) $Control_{SC}$.

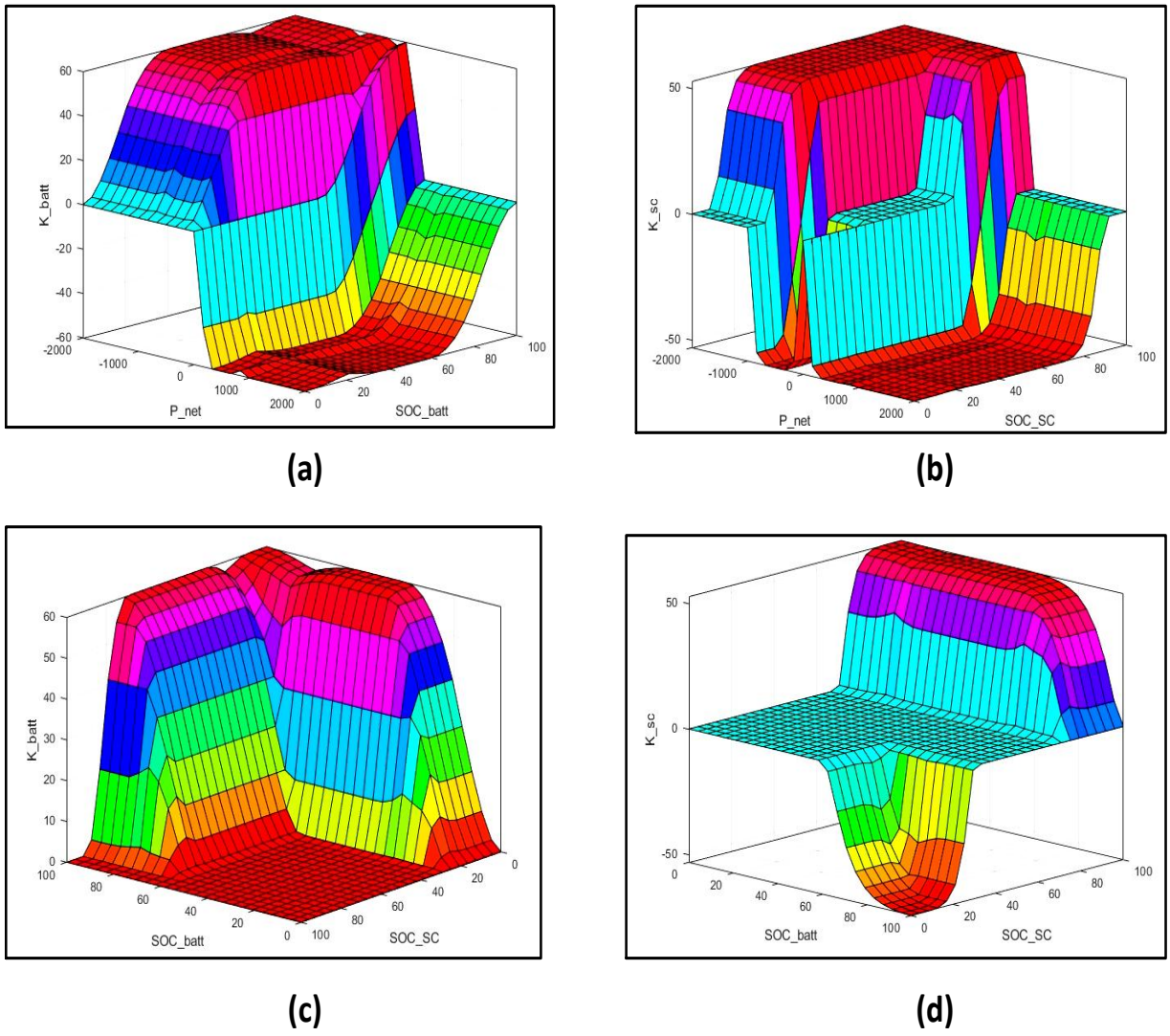


***Fig IV. 35**:Surface of relationship of inputs and outputs*

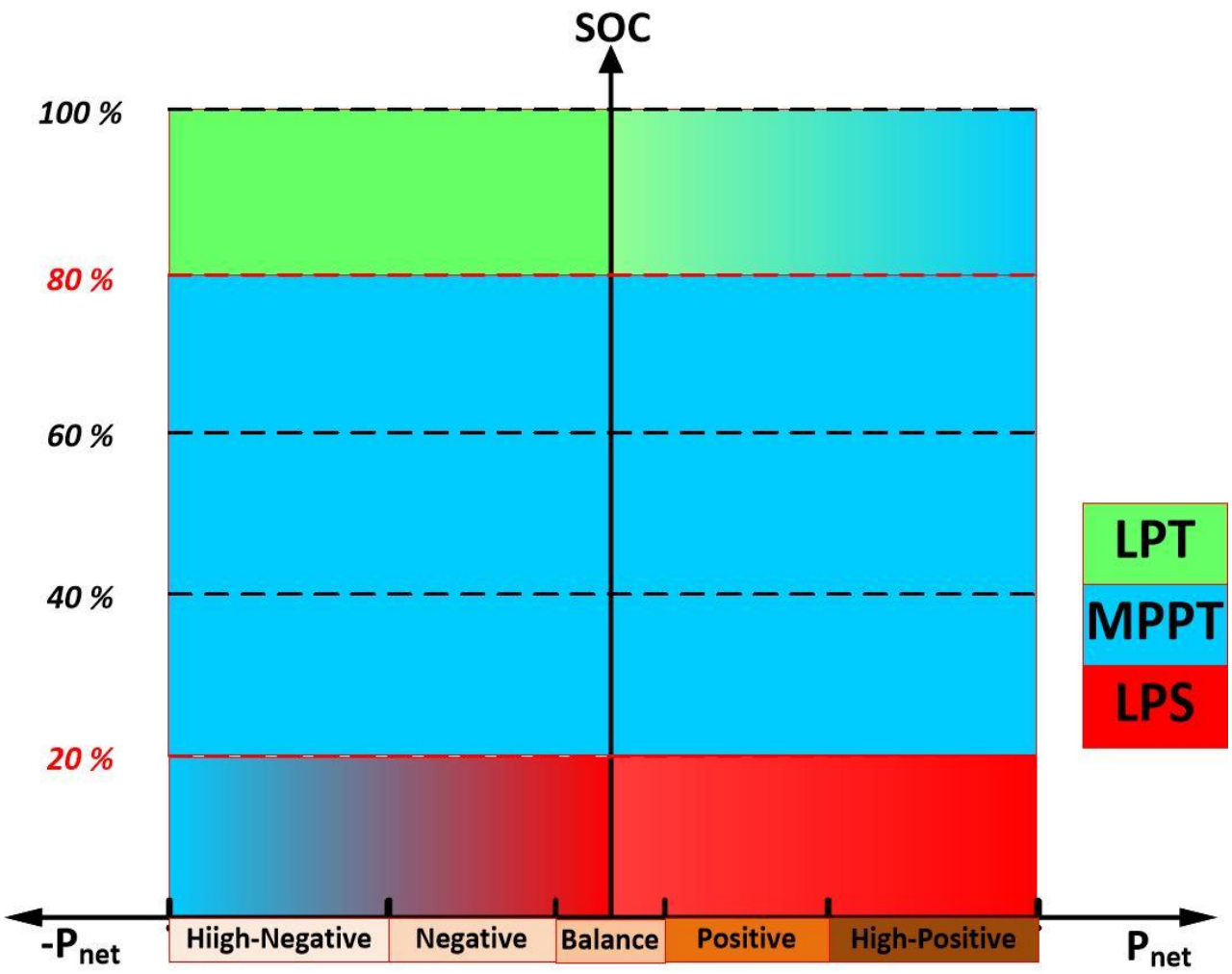


***Fig IV. 36**: Operation zone of sub-controls*

As illustrated in Fig 4.36. there is t different control modes. Control techniques for controlling RES, HESS and power load.

IV.7.1 LPT

In this scenario, the state of charge (SoC) of the battery is close to its maximum limit, SOC_{Max}, as seen in Fig 4.37(b). The performance of the suggested (EMS) is assessed under changing Pload (load power) and Ppv (photovoltaic power) situations. The DC microgrid has an initial load of 750W, and the state of charge (SoC) of the battery is slightly below 80%, as seen in Fig 4.37 (a) and (b). To prevent overcharging the batteries while the battery state of charge (SoC) is at its maximum, the suggested (EMS) activates the photovoltaic (PV) local control, which enables the PV system to function in load power tracking (LPT) mode and prevents further charging of the battery. Throughout this cycle, the DC-link voltage is consistently maintained at a level of 100V as shown in fig 4.34 (d). At time t = 0.5s, 1.5s, and 3.5s, the total load Pload in the DC microgrid is reduced by 200W at each instance. Conversely, the Ppv experienced a rise, reaching a value over 800W at

t=1s, and thereafter decreased to around 450W by t=2.75s Fig 4.37(a). Since the power generated by the power source (Ppv) exceeds the power used by the load (Pload), the battery undergoes charging and reaches its full capacity at t=4.43s. When the load demand increases, the battery begins to discharge, causing the state of charge (SoC) to drop below its upper limit. According to the data, the suggested EMS allows the photovoltaic system to run in maximum power point tracking (MPPT) mode at a time of 5.5 seconds. Fig 4.37 (d) displays the graphical representation of the current flowing through the load.

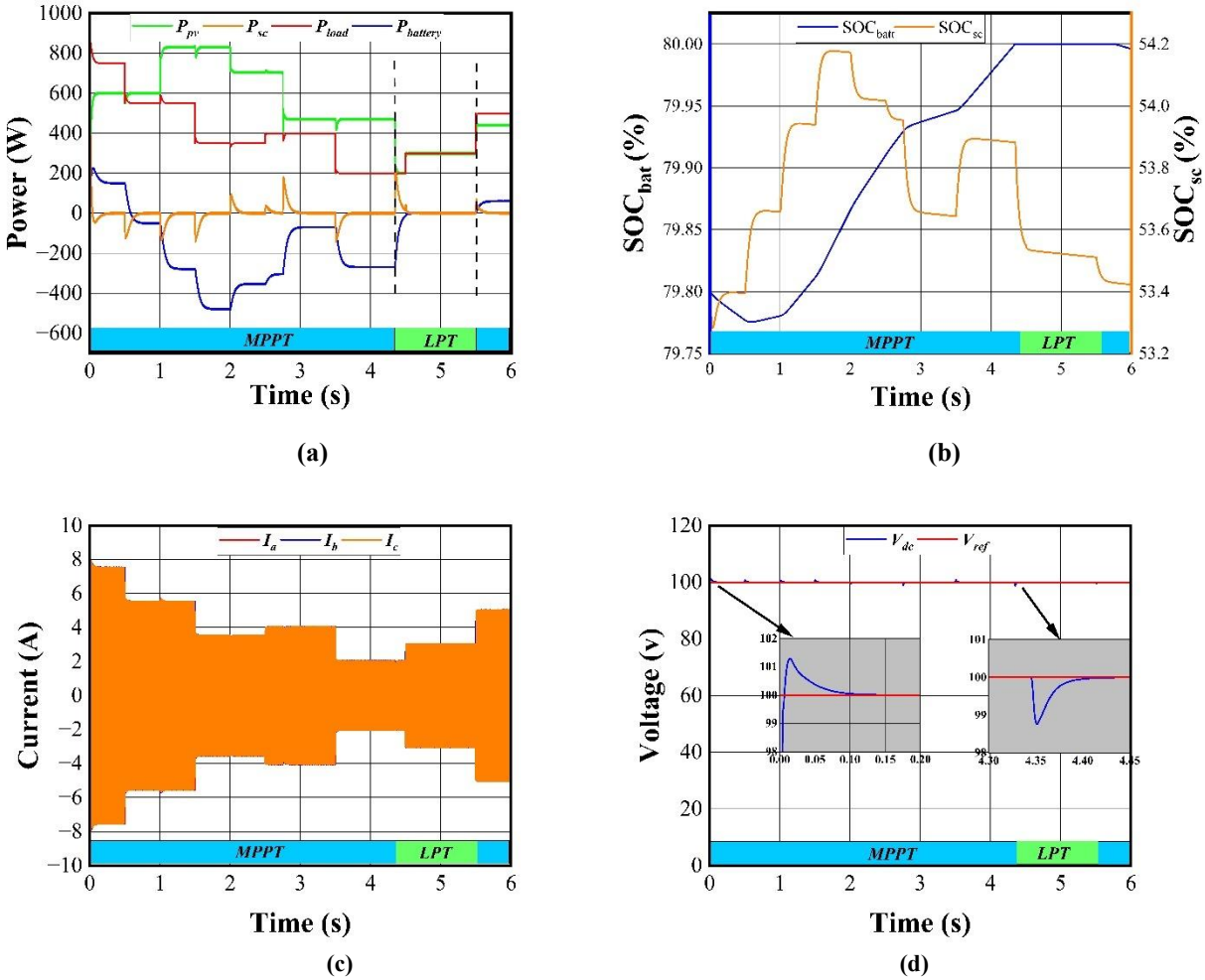


***Fig IV. 37**:(a) power evaluations; (b) SOC_{HESS}; (c) Current load;(d) DC link voltage*

IV.7.2 LPS

In this scenario, the state of charge (SOC) of the battery is close to its minimum limit (SoC_{min}) as seen in Fig 4.38(b). The performance of the suggested (EMS) is assessed under varying of load and Ppv . In Fig. 4.38 (a) and (b), the DC microgrid had an initial demand greater than the power generated by the photovoltaic (PV) system, and the state of charge (SOC) of the battery was slightly over 20%. The demonstrated EMS-operated PV system in MPPT mode, as illustrated in Fig 4.38 (c), (d), ensures that the battery is depleted to meet the load requirement while preventing excessive

discharge. The load demand was redirected to the important load at t = 1.17s, with the load being Pload = 200W.The battery provides for the lack of power demand in LPS mode. When the power consumption of Pbatt is below 20W, it leads to a reduced discharge rate of battery. At a time of 2 seconds, the peak power voltage (Ppv) surpassed the power load (Pload) and then returned to its typical demand.

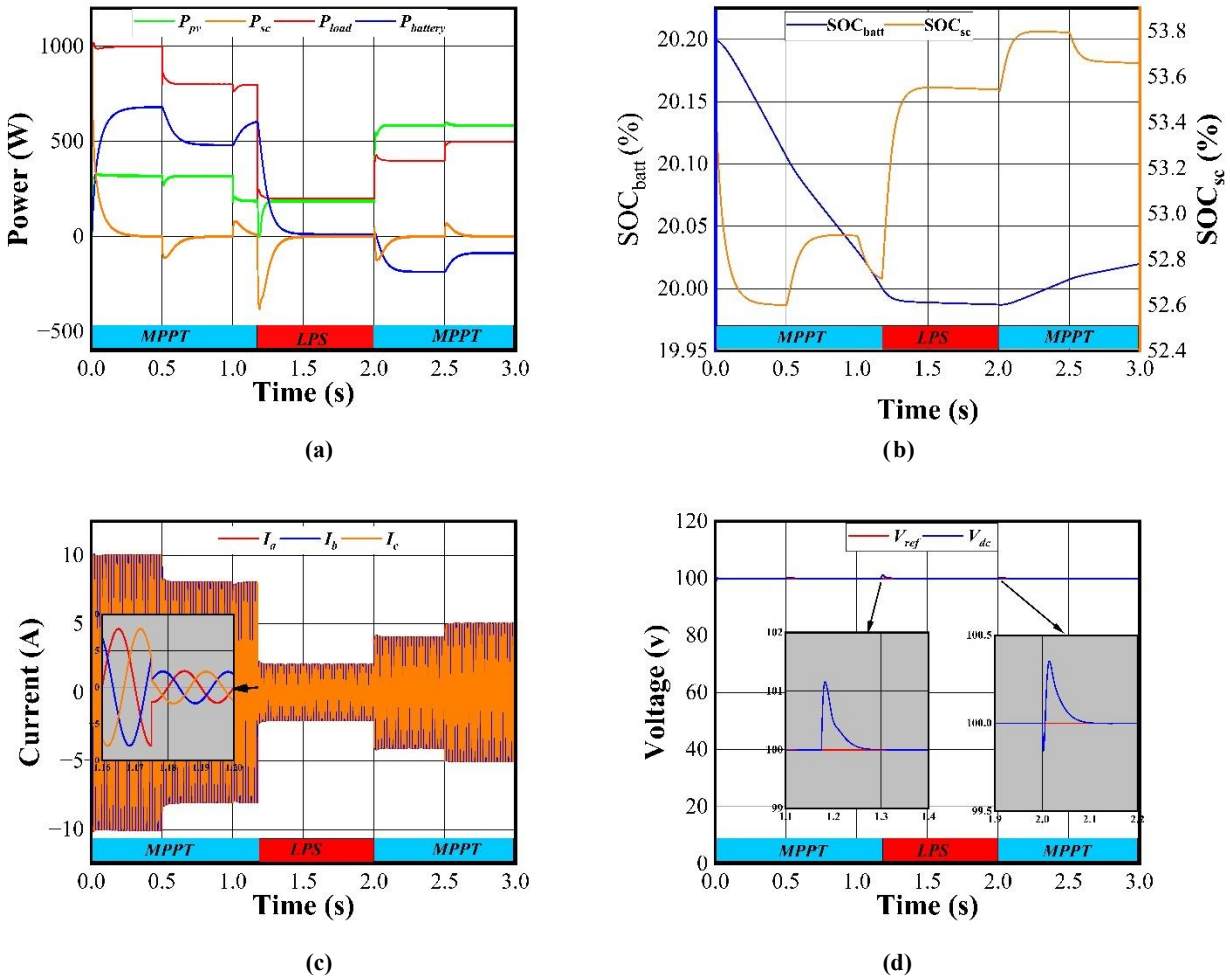


***Fig IV. 38**:(a) power evaluations; (b) SOCHESS; (c) Current load;(d) Dc link voltage*

IV.8 Conclusion

In conclusion, this chapter has provided a detailed examination of energy management systems, highlighting the significance of filter-based control methodologies in the operation of microgrids. The proposed energy management technique has been rigorously tested through simulations, demonstrating its effectiveness in managing the variability of RES outputs and the demands of the load. The one-day continuous test, along with scenarios assessing HESS under different SOC conditions, showcases the adaptability and robustness of the fuzzy logic energy management system. The results affirm that an effective EMS not only enhances the reliability of

microgrid operations but also optimizes energy utilization. As we advance, further exploration of innovative control strategies will be essential for addressing the complexities of microgrid management, ultimately contributing to the development of sustainable and resilient energy systems.

General conclusion

This thesis has provided an in-depth exploration of microgrid systems, underscoring their pivotal role in modern energy management and sustainability. As the global energy landscape shifts towards decentralization and renewable resources, microgrids emerge as a crucial solution to address the pressing challenges of energy security, reliability, and environmental sustainability.

The first chapter established a foundational understanding of microgrids, detailing their definition, components, and classifications. It highlighted essential elements such as distributed generation, demand response, and energy management systems, illustrating how these factors contribute to the resilience of power systems. The alternative classifications of microgrids—AC, DC, and hybrid systems—were analyzed, revealing their respective advantages and limitations. This chapter also shed light on the economic and technical challenges that microgrid operators face, such as operational management, compatibility of components, protection mechanisms, and market dynamics. These insights form a basis for addressing the complexities that arise in the implementation of microgrid systems.

The second chapter focused on the integration of renewable energy sources and energy storage systems within microgrids. By modeling photovoltaic and wind energy sources, alongside energy storage solutions like battery storage, this research evaluated the potential for optimizing energy generation and consumption balance. The modeling frameworks established in this chapter, particularly through the implementation of Maximum Power Point Tracking (MPPT) and the optimization of Hybrid Energy Storage Systems (HESS), demonstrate significant avenues for increasing the efficiency and effectiveness of renewable integration in microgrids. Simulation results validated the strategies discussed, illustrating the feasibility of leveraging diverse renewable sources in conjunction with energy storage to create a stable and reliable supply.

In the third chapter, a detailed techno-economic analysis was conducted using HOMER software to assess the optimal sizing of microgrid components. The analysis included a diverse range of potential microgrid configurations, weighing factors such as the net present cost, levelized cost of energy, capacity shortage fraction, and renewable fraction. This techno-economic insight is essential for policymakers and stakeholders to make informed investment decisions regarding microgrid implementation. The simulation results underscored the importance of careful planning and analysis to minimize costs while maximizing performance and sustainability outcomes.

The fourth chapter explored various energy management techniques to improve the operational efficiency of microgrids. It focused on the classification of different EMS strategies, emphasizing the significance of frequency decoupling and the implications of control algorithms such as Load Power Tracking (LPT) and Load Power Shedding (LPS). Simulated results demonstrated how these energy management strategies could optimize power distribution among renewable sources and storage systems, ensuring load requirements are met while maintaining system stability. Advanced techniques, including fuzzy logic-based control, were proposed to enhance decision-making processes within microgrids, showcasing the path towards more intelligent energy management systems.

Collectively, this research contributes to the understanding and advancement of microgrid technology by providing a comprehensive overview of their structure, operational challenges, and economic viability. The intricacies discussed throughout the thesis not only reflect current technological advancements but also present a foundation for future innovations that are essential in realizing the full potential of microgrids in a sustainable energy future. By facilitating decentralized energy production and consumption, microgrids can significantly reduce reliance on traditional energy systems and contribute to lower carbon emissions, thereby addressing global climate change challenges.

Bibliography

[1] Erdiwansyah, Mahidin, H. Husin, Nasaruddin, M. Zaki, and Muhibbuddin, "A critical review of the integration of renewable energy sources with various technologies," *Protection and Control of Modern Power Systems*, vol. 6, no. 1, pp. 1–18, Jan. 2021, doi: 10.1186/s41601-021-00181-3.

[2] S. R. Sinsel, R. L. Riemke, and V. H. Hoffmann, "Challenges and solution technologies for the integration of variable renewable energy sources—a review," *Renewable Energy*, vol. 145, pp. 2271–2285, Jan. 2020, doi: 10.1016/j.renene.2019.06.147.

[3] A. Q. Al-Shetwi, M. A. Hannan, K. P. Jern, M. Mansur, and T. M. I. Mahlia, "Grid-connected renewable energy sources: Review of the recent integration requirements and control methods," *Journal of Cleaner Production*, vol. 253, p. 119831, Apr. 2020, doi: 10.1016/j.jclepro.2019.119831.

[4] A. Q. Al-Shetwi, "Sustainable development of renewable energy integrated power sector: Trends, environmental impacts, and recent challenges," *Science of The Total Environment*, vol. 822, p. 153645, May 2022, doi: 10.1016/j.scitotenv.2022.153645.

[5] M. Parvin, H. Yousefi, and Y. Noorollahi, "Techno-economic optimization of a renewable micro grid using multi-objective particle swarm optimization algorithm," *Energy Conversion and Management*, vol. 277, p. 116639, Feb. 2023, doi: 10.1016/j.enconman.2022.116639.

[6] B. Dey, S. Dutta, and F. P. Garcia Marquez, "Intelligent Demand Side Management for Exhaustive Techno-Economic Analysis of Microgrid System," *Sustainability*, vol. 15, no. 3, Art. no. 3, Jan. 2023, doi: 10.3390/su15031795.

[7] T. F. Agajie *et al.*, "A Comprehensive Review on Techno-Economic Analysis and Optimal Sizing of Hybrid Renewable Energy Sources with Energy Storage Systems," *Energies*, vol. 16, no. 2, Art. no. 2, Jan. 2023, doi: 10.3390/en16020642.

[8] S. Y. Wong and C. Li, "Techno-economic analysis of optimal hybrid renewable energy systems – A case study for a campus microgrid," *Energy Reports*, vol. 9, pp. 134–138, Nov. 2023, doi: 10.1016/j.egyr.2023.09.153.

[9] B. A. Thango and L. Obokoh, "Techno-Economic Analysis of Hybrid Renewable Energy Systems for Power Interruptions: A Systematic Review," *Eng*, vol. 5, no. 3, Art. no. 3, Sep. 2024, doi: 10.3390/eng5030112.

[10] A. R. Abbasi and D. Baleanu, "Recent developments of energy management strategies in microgrids: An updated and comprehensive review and classification," *Energy Conversion and Management*, vol. 297, p. 117723, Dec. 2023, doi: 10.1016/j.enconman.2023.117723.

[11] A. G. Alharbi, A. G. Olabi, H. Rezk, A. Fathy, and M. A. Abdelkareem, "Optimized energy management and control strategy of photovoltaic/PEM fuel cell/batteries/supercapacitors DC microgrid system," *Energy*, vol. 290, p. 130121, Mar. 2024, doi: 10.1016/j.energy.2023.130121.

[12] X. Wang, J. Huang, Z. Xu, C. Zhang, and X. Guan, "Real-World Scale Deployment of Hydrogen-Integrated Microgrid: Design and Control," *IEEE Transactions on Sustainable Energy*, vol. 15, no. 4, pp. 2380–2392, Oct. 2024, doi: 10.1109/TSTE.2024.3418494.

[13] R. H. Lasseter and P. Paigi, "Microgrid: a conceptual solution," in *2004 IEEE 35th Annual Power Electronics Specialists Conference (IEEE Cat. No.04CH37551)*, Jun. 2004, pp. 4285-4290 Vol.6. doi: 10.1109/PESC.2004.1354758.

[14] E. Unamuno and J. A. Barrena, “Hybrid ac/dc microgrids—Part I: Review and classification of topologies,” *Renewable and Sustainable Energy Reviews*, vol. 52, pp. 1251–1259, Dec. 2015, doi: 10.1016/j.rser.2015.07.194.

[15] D. T. Ton and M. A. Smith, “The U.S. Department of Energy’s Microgrid Initiative,” *The Electricity Journal*, vol. 25, no. 8, pp. 84–94, Oct. 2012, doi: 10.1016/j.tej.2012.09.013.

[16] *Microgrids: Advances in Operation, Control, and Protection*. in Power Systems. Springer, 2021. doi: 10.1007/978-3-030-59750-4.

[17] “A View of Microgrids - Advances in Energy Systems - Wiley Online Library.” Accessed: Sep. 23, 2024. [Online]. Available: https://onlinelibrary.wiley.com/doi/abs/10.1002/9781119508311.ch9

[18] “Microgrid: a conceptual solution | IEEE Conference Publication | IEEE Xplore.” Accessed: Sep. 23, 2024. [Online]. Available: https://ieeexplore.ieee.org/abstract/document/1354758

[19] “Cyber-Physical Microgrids: Toward Future Resilient Communities | IEEE Journals & Magazine | IEEE Xplore.” Accessed: Sep. 23, 2024. [Online]. Available: https://ieeexplore.ieee.org/abstract/document/9205672

[20] Y. Li, L. Fu, K. Meng, Z. Y. Dong, K. Muttaqi, and W. Du, “Autonomous Control Strategy for Microgrid Operating Modes Smooth Transition,” *IEEE Access*, vol. 8, pp. 142159–142172, 2020, doi: 10.1109/ACCESS.2020.3014255.

[21] R. H. Lasseter *et al.*, “CERTS Microgrid Laboratory Test Bed,” *IEEE Transactions on Power Delivery*, vol. 26, no. 1, pp. 325–332, Jan. 2011, doi: 10.1109/TPWRD.2010.2051819.

[22] E. Alegria, T. Brown, E. Minear, and R. H. Lasseter, “CERTS Microgrid Demonstration With Large-Scale Energy Storage and Renewable Generation,” *IEEE Transactions on Smart Grid*, vol. 5, no. 2, pp. 937–943, Mar. 2014, doi: 10.1109/TSG.2013.2286575.

[23] “Microgrids: A review, outstanding issues and future trends - ScienceDirect.” Accessed: Sep. 23, 2024. [Online]. Available: https://www.sciencedirect.com/science/article/pii/S2211467X23000779

[24] F. Martin-Martínez, A. Sánchez-Miralles, and M. Rivier, “A literature review of Microgrids: A functional layer based classification,” *Renewable and Sustainable Energy Reviews*, vol. 62, pp. 1133–1153, Sep. 2016, doi: 10.1016/j.rser.2016.05.025.

[25] “State of the Art in Research on Microgrids: A Review | IEEE Journals & Magazine | IEEE Xplore.” Accessed: Sep. 23, 2024. [Online]. Available: https://ieeexplore.ieee.org/abstract/document/7120901

[26] A. M. Bouzid, J. M. Guerrero, A. Cheriti, M. Bouhamida, P. Sicard, and M. Benghanem, “A survey on control of electric power distributed generation systems for microgrid applications,” *Renewable and Sustainable Energy Reviews*, vol. 44, pp. 751–766, Apr. 2015, doi: 10.1016/j.rser.2015.01.016.

[27] A. Dagar, P. Gupta, and V. Niranjan, “Microgrid protection: A comprehensive review,” *Renewable and Sustainable Energy Reviews*, vol. 149, p. 111401, Oct. 2021, doi: 10.1016/j.rser.2021.111401.

[28] G. v. Brahmendra Kumar and K. Palanisamy, “Review of Energy Storage System for Microgrid,” in *Microgrid Technologies*, John Wiley & Sons, Ltd, 2021, pp. 57–90. doi: 10.1002/9781119710905.ch3.

[29] F. Khavari, A. Badri, and A. Zangeneh, “Energy management in multi-microgrids considering point of common coupling constraint,” *International Journal of Electrical Power & Energy Systems*, vol. 115, p. 105465, Feb. 2020, doi: 10.1016/j.ijepes.2019.105465.

[30] "Direct Power Control Based on Point of Common Coupling Voltage Modulation for Grid-Tied AC Microgrid PV Inverter | IEEE Journals & Magazine | IEEE Xplore." Accessed: Sep. 23, 2024. [Online]. Available: https://ieeexplore.ieee.org/abstract/document/9916258

[31] R. A. Badwawi, M. Abusara, and T. Mallick, "A Review of Hybrid Solar PV and Wind Energy System," *Smart Science*, vol. 3, no. 3, pp. 127–138, Jan. 2015, doi: 10.1080/23080477.2015.11665647.

[32] N. S. M. N. Izam, Z. Itam, W. L. Sing, and A. Syamsir, "Sustainable Development Perspectives of Solar Energy Technologies with Focus on Solar Photovoltaic—A Review," *Energies*, vol. 15, no. 8, Art. no. 8, Jan. 2022, doi: 10.3390/en15082790.

[33] P. H. A. Barra, W. C. de Carvalho, T. S. Menezes, R. A. S. Fernandes, and D. V. Coury, "A review on wind power smoothing using high-power energy storage systems," *Renewable and Sustainable Energy Reviews*, vol. 137, p. 110455, Mar. 2021, doi: 10.1016/j.rser.2020.110455.

[34] M. Khalid, "A review on the selected applications of battery-supercapacitor hybrid energy storage systems for microgrids," *Energies*, vol. 12, no. 23, p. 4559, 2019.

[35] H.-J. Kim *et al.*, "A Comprehensive Review of Li-Ion Battery Materials and Their Recycling Techniques," *Electronics*, vol. 9, no. 7, Art. no. 7, Jul. 2020, doi: 10.3390/electronics9071161.

[36] T. Salameh, M. A. Abdelkareem, A. G. Olabi, E. T. Sayed, M. Al-Chaderchi, and H. Rezk, "Integrated standalone hybrid solar PV, fuel cell and diesel generator power system for battery or supercapacitor storage systems in Khorfakkan, United Arab Emirates," *International Journal of Hydrogen Energy*, vol. 46, no. 8, pp. 6014–6027, Jan. 2021, doi: 10.1016/j.ijhydene.2020.08.153.

[37] M. M. Mohamed, H. M. El Zoghby, S. M. Sharaf, and M. A. Mosa, "Optimal virtual synchronous generator control of battery/supercapacitor hybrid energy storage system for frequency response enhancement of photovoltaic/diesel microgrid," *Journal of Energy Storage*, vol. 51, p. 104317, Jul. 2022, doi: 10.1016/j.est.2022.104317.

[38] C. Thai and J. Brouwer, "Decarbonizing a solar PV and gas turbine microgrid with hydrogen and batteries," *Energy Conversion and Management*, vol. 292, p. 117391, Sep. 2023, doi: 10.1016/j.enconman.2023.117391.

[39] S. Shahzad, M. A. Abbasi, H. Ali, M. Iqbal, R. Munir, and H. Kilic, "Possibilities, Challenges, and Future Opportunities of Microgrids: A Review," *Sustainability*, vol. 15, no. 8, Art. no. 8, Jan. 2023, doi: 10.3390/su15086366.

[40] V. Loboichenko, A. Iranzo, M. Casado-Manzano, S. J. Navas, F. J. Pino, and F. Rosa, "Study of the use of biogas as an energy vector for microgrids," *Renewable and Sustainable Energy Reviews*, vol. 200, p. 114574, Aug. 2024, doi: 10.1016/j.rser.2024.114574.

[41] "A Review of Islanding Detection Methods for Biogas-Based Distributed Generation Systems | SpringerLink." Accessed: Sep. 23, 2024. [Online]. Available: https://link.springer.com/chapter/10.1007/978-3-031-37909-3_4

[42] M. A. Azni, R. Md Khalid, U. A. Hasran, and S. K. Kamarudin, "Review of the Effects of Fossil Fuels and the Need for a Hydrogen Fuel Cell Policy in Malaysia," *Sustainability*, vol. 15, no. 5, Art. no. 5, Jan. 2023, doi: 10.3390/su15054033.

[43] M. A. Aminudin, S. K. Kamarudin, B. H. Lim, E. H. Majilan, M. S. Masdar, and N. Shaari, "An overview: Current progress on hydrogen fuel cell vehicles," *International Journal of Hydrogen Energy*, vol. 48, no. 11, pp. 4371–4388, Feb. 2023, doi: 10.1016/j.ijhydene.2022.10.156.

[44] A. Pramuanjaroenkij and S. Kakaç, "The fuel cell electric vehicles: The highlight review," *International Journal of Hydrogen Energy*, vol. 48, no. 25, pp. 9401–9425, Mar. 2023, doi: 10.1016/j.ijhydene.2022.11.103.

[45] K. Gandhi and S. K. Gupta, "Operational strategies and electricity market structure of microgrid: A critical review," *Renewable Energy Focus*, vol. 39, pp. 163–171, Dec. 2021, doi: 10.1016/j.ref.2021.09.001.

[46] J. Hu *et al.*, "Economic Model Predictive Control for Microgrid Optimization: A Review," *IEEE Transactions on Smart Grid*, vol. 15, no. 1, pp. 472–484, Jan. 2024, doi: 10.1109/TSG.2023.3266253.

[47] H. Mo, G. Sansavini, and M. Xie, *Cyber-Physical Distributed Systems: Modeling, Reliability Analysis and Applications*. John Wiley & Sons, 2021.

[48] "Bayesian adversarial multi-node bandit for optimal smart grid protection against cyber attacks - ScienceDirect." Accessed: Sep. 23, 2024. [Online]. Available: https://www.sciencedirect.com/science/article/abs/pii/S0005109821000716

[49] "Executive summary – Renewables 2022 – Analysis - IEA." Accessed: Sep. 23, 2024. [Online]. Available: https://www.iea.org/reports/renewables-2022/executive-summary

[50] "Resilience-oriented operation of microgrids in the presence of power-to-hydrogen systems - ScienceDirect." Accessed: Sep. 23, 2024. [Online]. Available: https://www.sciencedirect.com/science/article/pii/S0306261923007936

[51] S. Sepasi, C. Talichet, and A. S. Pramanik, "Power Quality in Microgrids: A Critical Review of Fundamentals, Standards, and Case Studies," *IEEE Access*, vol. 11, pp. 108493–108531, 2023, doi: 10.1109/ACCESS.2023.3321301.

[52] N. T. Mbungu, A. A. Ismail, M. AlShabi, R. C. Bansal, A. Elnady, and A. K. Hamid, "Control and estimation techniques applied to smart microgrids: A review," *Renewable and Sustainable Energy Reviews*, vol. 179, p. 113251, Jun. 2023, doi: 10.1016/j.rser.2023.113251.

[53] "Impedance Modeling With Stability Boundaries for Constant Power Load During Line Failure | IEEE Journals & Magazine | IEEE Xplore." Accessed: Sep. 23, 2024. [Online]. Available: https://ieeexplore.ieee.org/abstract/document/10267999

[54] "Robust Centralized Control for DC Islanded Microgrid Considering Communication Network Delay | IEEE Journals & Magazine | IEEE Xplore." Accessed: Sep. 23, 2024. [Online]. Available: https://ieeexplore.ieee.org/document/9076643

[55] M. Saleh, Y. Esa, and A. A. Mohamed, "Communication-Based Control for DC Microgrids," *IEEE Transactions on Smart Grid*, vol. 10, no. 2, pp. 2180–2195, Mar. 2019, doi: 10.1109/TSG.2018.2791361.

[56] J. M. Guerrero, J. C. Vasquez, J. Matas, L. G. de Vicuna, and M. Castilla, "Hierarchical Control of Droop-Controlled AC and DC Microgrids—A General Approach Toward Standardization," *IEEE Transactions on Industrial Electronics*, vol. 58, no. 1, pp. 158–172, Jan. 2011, doi: 10.1109/TIE.2010.2066534.

[57] L. Meng, T. Dragicevic, J. Roldán-Pérez, J. C. Vasquez, and J. M. Guerrero, "Modeling and Sensitivity Study of Consensus Algorithm-Based Distributed Hierarchical Control for DC Microgrids," *IEEE Transactions on Smart Grid*, vol. 7, no. 3, pp. 1504–1515, May 2016, doi: 10.1109/TSG.2015.2422714.

[58] S. Ali, Z. Zheng, M. Aillerie, J.-P. Sawicki, M.-C. Péra, and D. Hissel, "A Review of DC Microgrid Energy Management Systems Dedicated to Residential Applications," *Energies*, vol. 14, no. 14, Art. no. 14, Jan. 2021, doi: 10.3390/en14144308.

[59] D. E. Olivares *et al.*, "Trends in Microgrid Control," *IEEE Transactions on Smart Grid*, vol. 5, no. 4, pp. 1905–1919, Jul. 2014, doi: 10.1109/TSG.2013.2295514.

[60] Z. Shuai, J. Fang, F. Ning, and Z. J. Shen, "Hierarchical structure and bus voltage control of DC microgrid," *Renewable and Sustainable Energy Reviews*, vol. 82, pp. 3670–3682, Feb. 2018, doi: 10.1016/j.rser.2017.10.096.

[61] P. C. Loh, F. Blaabjerg, S. Peyghami-Akhuleh, and H. Mokhtari, "Distributed secondary control in DC microgrids with low-bandwidth communication link," in *2016 7th Power Electronics and Drive Systems Technologies Conference (PEDSTC)*, Feb. 2016, pp. 641–645. doi: 10.1109/PEDSTC.2016.7556935.

[62] S. V. Kulkarni and D. N. Gaonkar, "Improved droop control strategy for parallel connected power electronic converter based distributed generation sources in an Islanded Microgrid," *Electric Power Systems Research*, vol. 201, p. 107531, Dec. 2021, doi: 10.1016/j.epsr.2021.107531.

[63] Y. Mi *et al.*, "A Power Sharing Strategy for Islanded DC Microgrid with Unmatched Line Impedance and Local Load," *Electric Power Systems Research*, vol. 192, p. 106983, Mar. 2021, doi: 10.1016/j.epsr.2020.106983.

[64] F. Bandeiras, E. Pinheiro, M. Gomes, P. Coelho, and J. Fernandes, "Review of the cooperation and operation of microgrid clusters," *Renewable and Sustainable Energy Reviews*, vol. 133, p. 110311, Nov. 2020, doi: 10.1016/j.rser.2020.110311.

[65] M. S. Golsorkhi and M. Savaghebi, "A Decentralized Control Strategy Based on V-I Droop for Enhancing Dynamics of Autonomous Hybrid AC/DC Microgrids," *IEEE Transactions on Power Electronics*, vol. 36, no. 8, pp. 9430–9440, Aug. 2021, doi: 10.1109/TPEL.2021.3049813.

[66] D. Li and C. N. M. Ho, "A Module-Based Plug-n-Play DC Microgrid With Fully Decentralized Control for IEEE Empower a Billion Lives Competition," *IEEE Transactions on Power Electronics*, vol. 36, no. 2, pp. 1764–1776, Feb. 2021, doi: 10.1109/TPEL.2020.3009631.

[67] X. Lu, K. Sun, J. M. Guerrero, J. C. Vasquez, and L. Huang, "State-of-Charge Balance Using Adaptive Droop Control for Distributed Energy Storage Systems in DC Microgrid Applications," *IEEE Transactions on Industrial Electronics*, vol. 61, no. 6, pp. 2804–2815, Jun. 2014, doi: 10.1109/TIE.2013.2279374.

[68] A. F. Habibullah, F. A. Padhilah, and K.-H. Kim, "Decentralized Control of DC Microgrid Based on Droop and Voltage Controls with Electricity Price Consideration," *Sustainability*, vol. 13, no. 20, Art. no. 20, Jan. 2021, doi: 10.3390/su132011398.

[69] "Distributed Control and Optimization of DC Microgrids: A Port-Hamiltonian Approach | IEEE Journals & Magazine | IEEE Xplore." Accessed: Sep. 23, 2024. [Online]. Available: https://ieeexplore.ieee.org/abstract/document/9796512

[70] "Distributed Control Strategies for Microgrids: An Overview | IEEE Journals & Magazine | IEEE Xplore." Accessed: Sep. 23, 2024. [Online]. Available: https://ieeexplore.ieee.org/abstract/document/9233319

[71] Z. Fan, B. Fan, and W. Liu, "Distributed Control of DC Microgrids for Optimal Coordination of Conventional and Renewable Generators," *IEEE Transactions on Smart Grid*, vol. 12, no. 6, pp. 4607–4615, Nov. 2021, doi: 10.1109/TSG.2021.3094878.

[72] Z. Liu, J. Li, M. Su, X. Liu, and L. Yuan, "Stability Analysis of Equilibrium of DC Microgrid Under Distributed Control," *IEEE Transactions on Power Systems*, vol. 39, no. 1, pp. 1058–1067, Jan. 2024, doi: 10.1109/TPWRS.2023.3266244.

[73] M. Moradi, M. Heydari, and S. F. Zarei, “An overview on consensus-based distributed secondary control schemes in DC microgrids,” *Electric Power Systems Research*, vol. 225, p. 109870, Dec. 2023, doi: 10.1016/j.epsr.2023.109870.

[74] Q. Liu, L. Zhang, H. Zhang, S. Wang, and X. Ji, “Distributed Secondary Optimal Control with Fast Voltage Recovery and Minimum Generation Cost for Islanded DC Microgrids,” *IEEE Transactions on Smart Grid*, pp. 1–1, 2024, doi: 10.1109/TSG.2024.3443242.

[75] S. Ferahtia, A. Houari, T. Cioara, M. Bouznit, H. Rezk, and A. Djerioui, “Recent advances on energy management and control of direct current microgrid for smart cities and industry: A Survey,” *Applied Energy*, vol. 368, p. 123501, Aug. 2024, doi: 10.1016/j.apenergy.2024.123501.

[76] H. Lotfi and A. Khodaei, “Hybrid AC/DC microgrid planning,” *Energy*, vol. 118, pp. 37–46, Jan. 2017, doi: 10.1016/j.energy.2016.12.015.

[77] R. Chauhan, *Challenges and Opportunities for DC Micro Grid*. 2016. doi: 10.13140/RG.2.1.1923.6240.

[78] M. M. Khaleel, A. A. Ahmed, and A. Alsharif, “Energy Management System Strategies in Microgrids: A Review,” *NAJSP*, pp. 1–8, Jan. 2023.

[79] K. Wang *et al.*, “A method for large-scale WEC connecting to island isolated microgrid based on multiple small power HPGSs,” *Renewable Energy*, vol. 218, p. 119330, Dec. 2023, doi: 10.1016/j.renene.2023.119330.

[80] M. Shirkhani *et al.*, “A review on microgrid decentralized energy/voltage control structures and methods,” *Energy Reports*, vol. 10, pp. 368–380, Nov. 2023, doi: 10.1016/j.egyr.2023.06.022.

[81] W. M. Hamanah, M. I. Hossain, M. Shafiullah, and M. A. Abido, “AC Microgrid Protection Schemes: A Comprehensive Review,” *IEEE Access*, vol. 11, pp. 76842–76868, 2023, doi: 10.1109/ACCESS.2023.3298306.

[82] M. Y. A. Khan, H. Liu, J. Shang, and J. Wang, “Distributed hierarchal control strategy for multi-bus AC microgrid to achieve seamless synchronization,” *Electric Power Systems Research*, vol. 214, p. 108910, Jan. 2023, doi: 10.1016/j.epsr.2022.108910.

[83] “Comparative framework for AC-microgrid protection schemes: challenges, solutions, real applications, and future trends | PSPC Journals & Magazine | IEEE Xplore.” Accessed: Sep. 23, 2024. [Online]. Available: https://ieeexplore.ieee.org/abstract/document/10374447

[84] M. Uzair, L. Li, M. Eskandari, J. Hossain, and J. G. Zhu, “Challenges, advances and future trends in AC microgrid protection: With a focus on intelligent learning methods,” *Renewable and Sustainable Energy Reviews*, vol. 178, p. 113228, May 2023, doi: 10.1016/j.rser.2023.113228.

[85] V. F. Pires, A. Pires, and A. Cordeiro, “DC Microgrids: Benefits, Architectures, Perspectives and Challenges,” *Energies*, vol. 16, no. 3, Art. no. 3, Jan. 2023, doi: 10.3390/en16031217.

[86] B. Modu, M. P. Abdullah, M. A. Sanusi, and M. F. Hamza, “DC-based microgrid: Topologies, control schemes, and implementations,” *Alexandria Engineering Journal*, vol. 70, pp. 61–92, May 2023, doi: 10.1016/j.aej.2023.02.021.

[87] D. Jain and D. Saxena, “Comprehensive review on control schemes and stability investigation of hybrid AC-DC microgrid,” *Electric Power Systems Research*, vol. 218, p. 109182, May 2023, doi: 10.1016/j.epsr.2023.109182.

[88] A. H. Tariq, S. A. A. Kazmi, M. Hassan, S. A. Muhammed Ali, and M. Anwar, "Analysis of fuel cell integration with hybrid microgrid systems for clean energy: A comparative review," *International Journal of Hydrogen Energy*, vol. 52, pp. 1005–1034, Jan. 2024, doi: 10.1016/j.ijhydene.2023.07.238.

[89] "A Comprehensive Review: Study of Artificial Intelligence Optimization Technique Applications in a Hybrid Microgrid at Times of Fault Outbreaks." Accessed: Sep. 23, 2024. [Online]. Available: https://www.mdpi.com/1996-1073/16/4/1786

[90] S. Patel, A. Ghosh, P. K. Ray, and V. Gurugubelli, "Effective Power Management Strategy and Control of a Hybrid Microgrid With Hybrid Energy Storage Systems," *IEEE Transactions on Industry Applications*, vol. 59, no. 6, pp. 7341–7355, Nov. 2023, doi: 10.1109/TIA.2023.3303862.

[91] "Hybrid optimized-ANFIS based MPPT for hybrid microgrid using zebra optimization algorithm and artificial gorilla troops optimizer - ScienceDirect." Accessed: Sep. 23, 2024. [Online]. Available: https://www.sciencedirect.com/science/article/pii/S019689042301155X

[92] M. Ashraful Islam *et al.*, "Assessing the feasibility and quality performance of a renewable Energy-Based hybrid microgrid for electrification of remote communities," *Energy Conversion and Management: X*, vol. 23, p. 100674, Jul. 2024, doi: 10.1016/j.ecmx.2024.100674.

[93] A. S. Dahane and R. B. Sharma, "Hybrid AC-DC microgrid coordinated control strategies: A systematic review and future prospect," *Renewable Energy Focus*, vol. 49, p. 100553, Jun. 2024, doi: 10.1016/j.ref.2024.100553.

[94] M. R. Zaman, S. Sarker, M. A. Halim, S. Ibrahim, and A. Haque, "A Comprehensive Review of Techno-Economic Perspective of AC/DC Hybrid Microgrid," *Control Systems and Optimization Letters*, vol. 2, no. 1, Art. no. 1, Feb. 2024, doi: 10.59247/csol.v2i1.72.

[95] S. R. and M. Kowsalya, "HESS-based microgrid control techniques empowered by artificial intelligence: A systematic review of grid-connected and standalone systems," *Journal of Energy Storage*, vol. 84, p. 111012, Apr. 2024, doi: 10.1016/j.est.2024.111012.

[96] M. S. Alam *et al.*, "Renewable energy integration with DC microgrids: Challenges and opportunities," *Electric Power Systems Research*, vol. 234, p. 110548, Sep. 2024, doi: 10.1016/j.epsr.2024.110548.

[97] Y. Li, Y. Zhang, Y. Su, W. Wu, and L. Xia, "Optimal economic configuration by sharing hydrogen storage while considering distributed demand response in hydrogen-based renewable microgrid," *Renewable Energy*, vol. 235, p. 121360, Nov. 2024, doi: 10.1016/j.renene.2024.121360.

[98] L. Chen, L. Gao, S. Xing, Z. Chen, and W. Wang, "Zero-carbon microgrid: Real-world cases, trends, challenges, and future research prospects," *Renewable and Sustainable Energy Reviews*, vol. 203, p. 114720, Oct. 2024, doi: 10.1016/j.rser.2024.114720.

[99] Z. Yi, W. Dong, and A. H. Etemadi, "A Unified Control and Power Management Scheme for PV-Battery-Based Hybrid Microgrids for Both Grid-Connected and Islanded Modes," *IEEE Transactions on Smart Grid*, vol. 9, no. 6, pp. 5975–5985, Nov. 2018, doi: 10.1109/TSG.2017.2700332.

[100] N. H. Khan *et al.*, "A novel modified artificial rabbit optimization for stochastic energy management of a grid-connected microgrid: A case study in China," *Energy Reports*, vol. 11, pp. 5436–5455, Jun. 2024, doi: 10.1016/j.egyr.2024.05.018.

[101] A. Yaniv and Y. Beck, "Optimal battery scheduling in solar-plus-storage grid-connected microgrid for profit and cost efficiency: A use case on an Israeli microgrid," *Journal of Energy Storage*, vol. 77, p. 109697, Jan. 2024, doi: 10.1016/j.est.2023.109697.

[102] X. Wu, W. Zhao, X. Wang, and H. Li, "An MILP-Based Planning Model of a Photovoltaic/Diesel/Battery Stand-Alone Microgrid Considering the Reliability," *IEEE Transactions on Smart Grid*, vol. 12, no. 5, pp. 3809–3818, Sep. 2021, doi: 10.1109/TSG.2021.3084935.

[103] R. Zahira, D. Lakshmi, G. Ezhilarasi, P. Sivaraman, C. N. Ravi, and C. Sharmeela, "6 - Stand-alone microgrid concept for rural electrification: a review," in *Residential Microgrids and Rural Electrifications*, S. Padmanaban, C. Sharmeela, P. Sivaraman, and J. B. Holm-Nielsen, Eds., Academic Press, 2022, pp. 109–130. doi: 10.1016/B978-0-323-90177-2.00013-X.

[104] C. Zhao, P. B. Andersen, C. Træholt, and S. Hashemi, "Grid-connected battery energy storage system: a review on application and integration," *Renewable and Sustainable Energy Reviews*, vol. 182, p. 113400, Aug. 2023, doi: 10.1016/j.rser.2023.113400.

[105] M. Ibrar *et al.*, "A Machine Learning-Based Model for Stability Prediction of Decentralized Power Grid Linked with Renewable Energy Resources," *Wireless Communications and Mobile Computing*, vol. 2022, no. 1, p. 2697303, 2022, doi: 10.1155/2022/2697303.

[106] S. Roth and P. Tricoli, "Linkage of a Decentralised Green Energy Generation System to the Requirements of Railway Operations," in *2024 IEEE 18th International Conference on Compatibility, Power Electronics and Power Engineering (CPE-POWERENG)*, Jun. 2024, pp. 1–6. doi: 10.1109/CPE-POWERENG60842.2024.10604398.

[107] A. Aoun, M. Adda, A. Ilinca, M. Ghandour, and H. Ibrahim, "Centralized vs. Decentralized Electric Grid Resilience Analysis Using Leontief's Input–Output Model," *Energies*, vol. 17, no. 6, Art. no. 6, Jan. 2024, doi: 10.3390/en17061321.

[108] H. Fathabadi, "Novel stand-alone, completely autonomous and renewable energy based charging station for charging plug-in hybrid electric vehicles (PHEVs)," *Applied Energy*, vol. 260, p. 114194, Feb. 2020, doi: 10.1016/j.apenergy.2019.114194.

[109] M. S. Sami *et al.*, "Energy Management of Microgrids for Smart Cities: A Review," *Energies*, vol. 14, no. 18, Art. no. 18, Jan. 2021, doi: 10.3390/en14185976.

[110] F. Bandeiras, Á. Gomes, M. Gomes, and P. Coelho, "Exploring Energy Trading Markets in Smart Grid and Microgrid Systems and Their Implications for Sustainability in Smart Cities," *Energies*, vol. 16, no. 2, Art. no. 2, Jan. 2023, doi: 10.3390/en16020801.

[111] M. KAZERANI and K. TEHRANI, "Grid of Hybrid AC/DC Microgrids: A New Paradigm for Smart City of Tomorrow," in *2020 IEEE 15th International Conference of System of Systems Engineering (SoSE)*, Jun. 2020, pp. 175–180. doi: 10.1109/SoSE50414.2020.9130482.

[112] Q. T. Tran, K. Davies, and S. Sepasi, "Isolation Microgrid Design for Remote Areas with the Integration of Renewable Energy: A Case Study of Con Dao Island in Vietnam," *Clean Technologies*, vol. 3, no. 4, Art. no. 4, Dec. 2021, doi: 10.3390/cleantechnol3040047.

[113] A. D. Bintoudi and C. Demoulias, "Optimal isolated microgrid topology design for resilient applications," *Applied Energy*, vol. 338, p. 120909, May 2023, doi: 10.1016/j.apenergy.2023.120909.

[114] T. Ardriani *et al.*, "A DC Microgrid System for Powering Remote Areas," *Energies*, vol. 14, no. 2, Art. no. 2, Jan. 2021, doi: 10.3390/en14020493.

[115] M. Kermani, B. Adelmanesh, E. Shirdare, C. A. Sima, D. L. Carnì, and L. Martirano, "Intelligent energy management based on SCADA system in a real Microgrid for smart building applications," *Renewable Energy*, vol. 171, pp. 1115–1127, Jun. 2021, doi: 10.1016/j.renene.2021.03.008.

[116] L. Tightiz, H. Yang, and M. J. Piran, "A Survey on Enhanced Smart Micro-Grid Management System with Modern Wireless Technology Contribution," *Energies*, vol. 13, no. 9, Art. no. 9, Jan. 2020, doi: 10.3390/en13092258.

[117] "A brief review on microgrids: Operation, applications, modeling, and control - Shahgholian - 2021 - International Transactions on Electrical Energy Systems - Wiley Online Library." Accessed: Sep. 24, 2024. [Online]. Available: https://onlinelibrary.wiley.com/doi/full/10.1002/2050-7038.12885

[118] K. Kumar, M. Alam, S. Verma, and V. Dutta, "Analysis of metal hydride storage on the basis of thermophysical properties and its application in microgrid," *Energy Conversion and Management*, vol. 222, p. 113217, Oct. 2020, doi: 10.1016/j.enconman.2020.113217.

[119] T. Picard, T. Hong, N. Luo, S. H. Lee, and K. Sun, "Robustness of energy performance of Zero-Net-Energy (ZNE) homes," *Energy and Buildings*, vol. 224, p. 110251, Oct. 2020, doi: 10.1016/j.enbuild.2020.110251.

[120] A. M. Othman and H. A. Gabbar, "Enhanced interconnected microgrids for water-pumps networks towards zero net energy farms," *International Journal of Reasoning-based Intelligent Systems*, vol. 13, no. 3, pp. 182–190, Jan. 2021, doi: 10.1504/IJRIS.2021.117082.

[121] I. Bianchini, J. Knapp, S. Riethmüller, T. Kwiatkowski, X. Yang, and A. Sauer, "Source Management In DC Microgrids: An Industrial Application," pp. 44–53, 2023, doi: 10.15488/13423.

[122] O. Larsson, *On the implementation of green airport facilities by integrating electric airplanes: A case study : A potential solution for future green airports*. 2023. Accessed: Sep. 24, 2024. [Online]. Available: https://urn.kb.se/resolve?urn=urn:nbn:se:kau:diva-93016

[123] G. Er, G. Soykan, and E. Canakoglu, "Stochastic optimal design of a rural microgrid with hybrid storage system including hydrogen and electric cars using vehicle-to-grid technology," *Journal of Energy Storage*, vol. 75, p. 109747, Jan. 2024, doi: 10.1016/j.est.2023.109747.

[124] Z. Qiao, R. Yang, W. Liao, W. Yu, and Y. Fang, "Impedance modeling, Parameters sensitivity and Stability analysis of hybrid DC ship microgrid," *Electric Power Systems Research*, vol. 226, p. 109901, Jan. 2024, doi: 10.1016/j.epsr.2023.109901.

[125] B. Das, P. K. Panigrahi, and C. K. Samant, "Impact Analysis of Plug-in Hybrid Electric Vehicle on Integration with Micro grid -A Review," in *2020 IEEE International Symposium on Sustainable Energy, Signal Processing and Cyber Security (iSSSC)*, Dec. 2020, pp. 1–5. doi: 10.1109/iSSSC50941.2020.9358824.

[126] H. Arya and M. Das, "Fast Charging Station for Electric Vehicles Based on DC Microgrid," *IEEE Journal of Emerging and Selected Topics in Industrial Electronics*, vol. 4, no. 4, pp. 1204–1212, Oct. 2023, doi: 10.1109/JESTIE.2023.3285535.

[127] D. Savio Abraham *et al.*, "Electric Vehicles Charging Stations' Architectures, Criteria, Power Converters, and Control Strategies in Microgrids," *Electronics*, vol. 10, no. 16, Art. no. 16, Jan. 2021, doi: 10.3390/electronics10161895.

[128] Md. R. H. Mojumder, M. Hasanuzzaman, and E. Cuce, "Prospects and challenges of renewable energy-based microgrid system in Bangladesh: a comprehensive review," *Clean Techn Environ Policy*, vol. 24, no. 7, pp. 1987–2009, Sep. 2022, doi: 10.1007/s10098-022-02301-5.

[129] K. Jithin, P. P. Haridev, N. Mayadevi, R. P. Harikumar, and V. P. Mini, "A Review on Challenges in DC Microgrid Planning and Implementation," *Journal of Modern Power Systems and Clean Energy*, vol. 11, no. 5, pp. 1375–1395, Sep. 2023, doi: 10.35833/MPCE.2022.000053.

[130] M. Faisal, M. A. Hannan, P. J. Ker, A. Hussain, M. B. Mansor, and F. Blaabjerg, "Review of Energy Storage System Technologies in Microgrid Applications: Issues and Challenges," *IEEE Access*, vol. 6, pp. 35143–35164, 2018, doi: 10.1109/ACCESS.2018.2841407.

[131] S. Monesha, S. G. Kumar, and M. Rivera, "Microgrid energy management and control: Technical review," in *2016 IEEE International Conference on Automatica (ICA-ACCA)*, Oct. 2016, pp. 1–7. doi: 10.1109/ICA-ACCA.2016.7778452.

[132] A. Kumar, P. Mohanty, D. Palit, and A. Chaurey, "Approach for standardization of off-grid electrification projects," *Renewable and Sustainable Energy Reviews*, vol. 13, no. 8, pp. 1946–1956, Oct. 2009, doi: 10.1016/j.rser.2009.03.008.

[133] H. Zerriffi, "Distributed Rural Electrification in China," in *Rural Electrification: Strategies for Distributed Generation*, H. Zerriffi, Ed., Dordrecht: Springer Netherlands, 2011, pp. 111–135. doi: 10.1007/978-90-481-9594-7_5.

[134] D. Akinyele, J. Belikov, and Y. Levron, "Challenges of Microgrids in Remote Communities: A STEEP Model Application," *Energies*, vol. 11, no. 2, Art. no. 2, Feb. 2018, doi: 10.3390/en11020432.

[135] S. Chen *et al.*, "Butler, Not Servant: A Human-Centric Smart Home Energy Management System," *IEEE Communications Magazine*, vol. 55, no. 2, pp. 27–33, Feb. 2017, doi: 10.1109/MCOM.2017.1600699CM.

[136] H. Wang, Z. Yan, M. Shahidehpour, X. Xu, and Q. Zhou, "Quantitative Evaluations of Uncertainties in Multivariate Operations of Microgrids," *IEEE Transactions on Smart Grid*, vol. 11, no. 4, pp. 2892–2903, Jul. 2020, doi: 10.1109/TSG.2020.2971689.

[137] Y. Yoldaş, A. Önen, S. M. Muyeen, A. V. Vasilakos, and İ. Alan, "Enhancing smart grid with microgrids: Challenges and opportunities," *Renewable and Sustainable Energy Reviews*, vol. 72, pp. 205–214, May 2017, doi: 10.1016/j.rser.2017.01.064.

[138] G. Artale *et al.*, "A Virtual Tool for Load Flow Analysis in a Micro-Grid," *Energies*, vol. 13, no. 12, Art. no. 12, Jan. 2020, doi: 10.3390/en13123173.

[139] U. H. Ramadhani, M. Shepero, J. Munkhammar, J. Widén, and N. Etherden, "Review of probabilistic load flow approaches for power distribution systems with photovoltaic generation and electric vehicle charging," *International Journal of Electrical Power & Energy Systems*, vol. 120, p. 106003, Sep. 2020, doi: 10.1016/j.ijepes.2020.106003.

[140] Y. Wu *et al.*, "Two thermally stable and AIE active 1,8-naphthalimide derivatives with red efficient thermally activated delayed fluorescence," *Dyes and Pigments*, vol. 169, pp. 81–88, Oct. 2019, doi: 10.1016/j.dyepig.2019.04.071.

[141] M. Farrokhabadi *et al.*, "Microgrid Stability Definitions, Analysis, and Examples," *IEEE Transactions on Power Systems*, vol. 35, no. 1, pp. 13–29, Jan. 2020, doi: 10.1109/TPWRS.2019.2925703.

[142] J. Jung and M. Villaran, "Optimal planning and design of hybrid renewable energy systems for microgrids," *Renewable and Sustainable Energy Reviews*, vol. 75, pp. 180–191, Aug. 2017, doi: 10.1016/j.rser.2016.10.061.

[143] A. J. Aristizábal, J. Herrera, M. Castaneda, S. Zapata, D. Ospina, and E. Banguero, "A new methodology to model and simulate microgrids operating in low latitude countries," *Energy Procedia*, vol. 157, pp. 825–836, Jan. 2019, doi: 10.1016/j.egypro.2018.11.248.

[144] J. Zhou, J. Zhang, X. Cai, G. Shi, J. Wang, and J. Zang, "Design and Analysis of Flexible Multi-Microgrid Interconnection Scheme for Mitigating Power Fluctuation and Optimizing Storage Capacity," *Energies*, vol. 12, no. 11, Art. no. 11, Jan. 2019, doi: 10.3390/en12112132.

[145] J. Xu, Q. Sun, H. Mo, and D. Dong, "Online routing for smart electricity network under hybrid uncertainty," *Automatica*, vol. 145, p. 110538, Nov. 2022, doi: 10.1016/j.automatica.2022.110538.

[146] A. Sharma, M. Kolhe, U.-M. Nils, A. Mudgal, K. Muddineni, and S. Garud, "Comparative Analysis of Different Types of Micro-grid Architectures and Controls," in *2018 International Conference on Advances in Computing, Communication Control and Networking (ICACCCN)*, Oct. 2018, pp. 1200–1208. doi: 10.1109/ICACCCN.2018.8748491.

[147] L. Wang, X. Ma, and J. Zhang, "Feature screening for ultrahigh-dimensional additive logistic models," *Journal of Statistical Planning and Inference*, vol. 205, pp. 306–317, Mar. 2020, doi: 10.1016/j.jspi.2019.08.005.

[148] C. Chandraratne, T. Naayagi Ramasamy, T. Logenthiran, and G. Panda, "Adaptive Protection for Microgrid with Distributed Energy Resources," *Electronics*, vol. 9, no. 11, Art. no. 11, Nov. 2020, doi: 10.3390/electronics9111959.

[149] M. S. Alam, F. S. Al-Ismail, S. M. Rahman, M. Shafiullah, and M. A. Hossain, "Planning and protection of DC microgrid: A critical review on recent developments," *Engineering Science and Technology, an International Journal*, vol. 41, p. 101404, May 2023, doi: 10.1016/j.jestch.2023.101404.

[150] A. Chakraborty and S. Ray, "Economic and environmental factors based multi-objective approach for optimizing energy management in a microgrid," *Renewable Energy*, vol. 222, p. 119920, Feb. 2024, doi: 10.1016/j.renene.2023.119920.

[151] V. Khare and P. Chaturvedi, "Design, control, reliability, economic and energy management of microgrid: A review," *e-Prime - Advances in Electrical Engineering, Electronics and Energy*, vol. 5, p. 100239, Sep. 2023, doi: 10.1016/j.prime.2023.100239.

[152] J. Behrendt, "Microgrids and EU law: Three Microgrid models to solve one regulatory puzzle," *Energy Policy*, vol. 177, p. 113483, Jun. 2023, doi: 10.1016/j.enpol.2023.113483.

[153] "Renewables 2023 – Analysis," IEA. Accessed: Sep. 16, 2024. [Online]. Available: https://www.iea.org/reports/renewables-2023

[154] M. A. H. Mujammal, A. Moualdia, S. Boulkhrachef, P. Wira, D. Boudana, and M. A. Albasheri, "Advancing wind energy conversion: smart maximum power point based on M5-Pruned algorithm for enhanced wind energy production," *Prod. Eng. Res. Devel.*, Oct. 2024, doi: 10.1007/s11740-024-01315-w.

[155] M. A. H. Mujammal, A. Moualdia, P. Wira, M. A. Albasheri, and A. Cherifi, "Novel Direct Power Control Based on Grid Voltage Modulated Strategy Using Artificial Intelligence," *Smart Grids and Energy*, vol. 9, no. 2, p. 37, Oct. 2024, doi: 10.1007/s40866-024-00225-1.

[156] R. Engleitner, A. Nied, M. S. M. Cavalca, and J. P. da Costa, "Dynamic Analysis of Small Wind Turbines Frequency Support Capability in a Low-Power Wind-Diesel Microgrid," *IEEE Transactions on Industry Applications*, vol. 54, no. 1, pp. 102–111, Jan. 2018, doi: 10.1109/TIA.2017.2761833.

[157] M. A. Albasheri, O. Bouchhida, Y. Soufi, A. Moualdia, and M. Mujammal, "Control And Power Management of DC Microgrid Based Wind/Battery/Supercapacitor," in *2022 IEEE 2nd International Maghreb Meeting of the Conference on Sciences and Techniques of Automatic Control and Computer Engineering (MI-STA)*, May 2022, pp. 680–685. doi: 10.1109/MI-STA54861.2022.9837665.

[158] C. Messasma, S. E. Chouaba, A. Barakat, and B. Sari, "Innovative real-time deloading approach to wind systems with applications in primary frequency control," *Electric Power Systems Research*, vol. 237, p. 110983, Dec. 2024, doi: 10.1016/j.epsr.2024.110983.

[159] A. M. Abdulelah, B. Ouahid, and S. Youcef, "Control of a Stand-Alone Variable Speed Wind Turbine with a Permanent Magnet Synchronous Generator," in *2021 18th International Multi-Conference on Systems, Signals & Devices (SSD)*, Mar. 2021, pp. 546–550. doi: 10.1109/SSD52085.2021.9429307.

[160] M. A. H. Mujammal, A. Moualdia, S. Boulkhrachef, D. Boudana, P. Wira, and M. A. Albasheri, "Next-Generation MPPT: neural network-driven optimization for superior solar performance," *STUDIES IN ENGINEERING AND EXACT SCIENCES*, vol. 5, no. 2, pp. e7338–e7338, Sep. 2024, doi: 10.54021/seesv5n2-150.

[161] S. Kouro, B. Wu, H. Abu-Rub, and F. Blaabjerg, "Photovoltaic Energy Conversion Systems," in *Power Electronics for Renewable Energy Systems, Transportation and Industrial Applications*, John Wiley & Sons, Ltd, 2014, pp. 160–198. doi: 10.1002/9781118755525.ch7.

[162] M. A. H. Mujammal, A. Moualdia, O. Bouchhida, and M. A. Albasheri, "Upgrade Perturbation and Observation of MPPT Strategy via Fuzzy Logic Controller," in *2023 2nd International Conference on Electronics, Energy and Measurement (IC2EM)*, Nov. 2023, pp. 1–7. doi: 10.1109/IC2EM59347.2023.10419670.

[163] "Review of energy storage services, applications, limitations, and benefits - ScienceDirect." Accessed: Sep. 27, 2024. [Online]. Available: https://www.sciencedirect.com/science/article/pii/S2352484720312464

[164] M. A. Al Basheri, Y. Soufi, O. Bouchhida, and A. Cherifi, "Control and Energy Management Based on Decoupling Frequency of DC Microgrid," in *2024 21st International Multi-Conference on Systems, Signals & Devices (SSD)*, Apr. 2024, pp. 224–229. doi: 10.1109/SSD61670.2024.10549218.

[165] M. A. Albasheri, O. Bouchhida, Y. Soufi, and A. Cherifi, "Energy Management of Wind Energy Hybrid Storage for Remote Area Power System," in *2024 12th International Conference on Smart Grid (icSmartGrid)*, May 2024, pp. 418–422. doi: 10.1109/icSmartGrid61824.2024.10578267.

[166] M. Bahloul and S. K. Khadem, "An analytical approach for techno-economic evaluation of hybrid energy storage system for grid services," *Journal of Energy Storage*, vol. 31, p. 101662, Oct. 2020, doi: 10.1016/j.est.2020.101662.

[167] T. Ma, M. H. Cintuglu, and O. A. Mohammed, "Control of a Hybrid AC/DC Microgrid Involving Energy Storage and Pulsed Loads," *IEEE Transactions on Industry Applications*, vol. 53, no. 1, pp. 567–575, Jan. 2017, doi: 10.1109/TIA.2016.2613981.

[168] F. Naseri, S. Karimi, E. Farjah, and E. Schaltz, "Supercapacitor management system: A comprehensive review of modeling, estimation, balancing, and protection techniques," *Renewable and Sustainable Energy Reviews*, vol. 155, p. 111913, Mar. 2022, doi: 10.1016/j.rser.2021.111913.

[169] K. Raut, A. Shendge, J. Chaudhari, R. Lamba, and N. F. Alshammari, "Modeling and simulation of photovoltaic powered battery-supercapacitor hybrid energy storage system for electric vehicles," *Journal of Energy Storage*, vol. 82, p. 110324, Mar. 2024, doi: 10.1016/j.est.2023.110324.

[170] C. Yin, H. Wu, F. Locment, and M. Sechilariu, “Energy management of DC microgrid based on photovoltaic combined with diesel generator and supercapacitor,” *Energy Conversion and Management*, vol. 132, pp. 14–27, Jan. 2017, doi: 10.1016/j.enconman.2016.11.018.

[171] L. Mamouri, T. Mesbahi, P. Bartholomeus, and T. PAUL, “Design of a DC/DC Power Converter for Li-ion Battery/Supercapacitor Hybrid Energy Storage System in Electric Vehicles,” in *2020 IEEE Vehicle Power and Propulsion Conference (VPPC)*, Nov. 2020, pp. 1–5. doi: 10.1109/VPPC49601.2020.9330905.

[172] T. S. Babu, K. R. Vasudevan, V. K. Ramachandaramurthy, S. B. Sani, S. Chemud, and R. M. Lajim, “A Comprehensive Review of Hybrid Energy Storage Systems: Converter Topologies, Control Strategies and Future Prospects,” *IEEE Access*, vol. 8, pp. 148702–148721, 2020, doi: 10.1109/ACCESS.2020.3015919.

[173] D. Peña, P. Arevalo, Y. Ortiz, and F. Jurado, “Survey of Optimization Techniques for Microgrids Using High-Efficiency Converters,” *Energies*, vol. 17, no. 15, Art. no. 15, Jan. 2024, doi: 10.3390/en17153657.

[174] H. Fu, S. Nižetić, J.-W. Park, K. Y. Lee, and L. Sun, “Thermodynamic analysis of a combined heating and power plant hybrid with compressed air energy storage and molten salt heat storage,” *Journal of Energy Storage*, vol. 98, p. 113174, Sep. 2024, doi: 10.1016/j.est.2024.113174.

[175] A. M. Adeyinka, O. C. Esan, A. O. Ijaola, and P. K. Farayibi, “Advancements in hybrid energy storage systems for enhancing renewable energy-to-grid integration,” *Sustainable Energy res.*, vol. 11, no. 1, p. 26, Jul. 2024, doi: 10.1186/s40807-024-00120-4.

[176] L. Kouchachvili, W. Yaïci, and E. Entchev, “Hybrid battery/supercapacitor energy storage system for the electric vehicles,” *Journal of Power Sources*, vol. 374, pp. 237–248, Jan. 2018, doi: 10.1016/j.jpowsour.2017.11.040.

[177] J. Shen and A. Khaligh, “A Supervisory Energy Management Control Strategy in a Battery/Ultracapacitor Hybrid Energy Storage System,” *IEEE Transactions on Transportation Electrification*, vol. 1, no. 3, pp. 223–231, Oct. 2015, doi: 10.1109/TTE.2015.2464690.

[178] L. W. Chong, Y. W. Wong, R. K. Rajkumar, and D. Isa, “An adaptive learning control strategy for standalone PV system with battery-supercapacitor hybrid energy storage system,” *Journal of Power Sources*, vol. 394, pp. 35–49, Aug. 2018, doi: 10.1016/j.jpowsour.2018.05.041.

[179] S. R. and M. Kowsalya, “HESS-based microgrid control techniques empowered by artificial intelligence: A systematic review of grid-connected and standalone systems,” *Journal of Energy Storage*, vol. 84, p. 111012, Apr. 2024, doi: 10.1016/j.est.2024.111012.

[180] T. R. Ayodele, A. S. O. Ogunjuyigbe, and B. E. Olateju, “Improving battery lifetime and reducing life cycle cost of a PV/battery system using supercapacitor for remote agricultural farm power application,” *Journal of Renewable and Sustainable Energy*, vol. 10, no. 1, p. 013503, Jan. 2018, doi: 10.1063/1.4999780.

[181] J. Zhang, M. Gu, and X. Chen, “Supercapacitors for renewable energy applications: A review,” *Micro and Nano Engineering*, vol. 21, p. 100229, Dec. 2023, doi: 10.1016/j.mne.2023.100229.

[182] P. Singh and J. S. Lather, “Power management and control of a grid-independent DC microgrid with hybrid energy storage system,” *Sustainable Energy Technologies and Assessments*, vol. 43, p. 100924, Feb. 2021, doi: 10.1016/j.seta.2020.100924.

[183] A. M. Abdulelah, B. Ouahid, S. Youcef, C. Abderrezzak, M. Abdelhafidh, and M. Ahmed, “Improve Lifespan of Battery Energy Storage in Remote Area Power System,” in *2023 2nd International Conference on Electronics, Energy and Measurement (IC2EM)*, Nov. 2023, pp. 1–6. doi: 10.1109/IC2EM59347.2023.10419419.

[184] W. Dang *et al.*, "An encoder-decoder fusion battery life prediction method based on Gaussian process regression and improvement," *Journal of Energy Storage*, vol. 59, p. 106469, Mar. 2023, doi: 10.1016/j.est.2022.106469.

[185] M. A. H. Mujammal, A. Moualdia, S. Boulkhrachef, M. A. Albasheri, and P. Wira, "Implementation of Smart MPPT Strategy Based on Fuzzy Logic Controller for Stand-Alone PV System," in *Technological and Innovative Progress in Renewable Energy Systems: Proceedings of the 2024 International Renewable Energy Days (IREN Days'2024).*, O. Guerri, A. H. Arab, and K. Imessad, Eds., Cham: Springer Nature Switzerland, 2025, pp. 55–59. doi: 10.1007/978-3-031-71926-4_9.

[186] M. A. H. Mujammal, M. Abdelhafidh, G. Lorenzini, S. Boulkhrachef, P. Wira, and M. Albasheri, "Three-Phase PWM Rectifier Control: Enhanced Direct Power Control with Neural Networks from Theory to Superior Reality Performance," *Journal Européen des Systèmes Automatisés*, vol. 57, pp. 1743–1752, Dec. 2024, doi: 10.18280/jesa.570622.

[187] M. A. Albasheri, O. Bouchhida, Y. Soufi, and A. Cherifi, "Enhanced energy storage system efficiency for remote area-based DC microgrid," *STUDIES IN ENGINEERING AND EXACT SCIENCES*, vol. 5, no. 2, pp. e5367–e5367, Jul. 2024, doi: 10.54021/seesv5n2-002.

[188] "HOMER Energy User Site- Hybrid Renewable and Distributed Generation System Design Software." Accessed: Aug. 13, 2024. [Online]. Available: https://users.homerenergy.com/

[189] S. Yadav, P. Kumar, and A. Kumar, "Techno-economic assessment of hybrid renewable energy system with multi energy storage system using HOMER," *Energy*, vol. 297, p. 131231, Jun. 2024, doi: 10.1016/j.energy.2024.131231.

[190] M. A. Albasheri, M. A. H. Mujammal, O. Bouchhida, Y. Soufi, and A. Cherifi, "Affordable Clean Energy Through Optimized Hybrid Microgrid Design in Yemen," Dec. 26, 2024, *Research Square*. doi: 10.21203/rs.3.rs-5707101/v1.

[191] S. Singh, M. Singh, and S. C. Kaushik, "Feasibility study of an islanded microgrid in rural area consisting of PV, wind, biomass and battery energy storage system," *Energy Conversion and Management*, vol. 128, pp. 178–190, Nov. 2016, doi: 10.1016/j.enconman.2016.09.046.

[192] T. O. Araoye, E. C. Ashigwuike, M. J. Mbunwe, O. I. Bakinson, and T. I. Ozue, "Techno-economic modeling and optimal sizing of autonomous hybrid microgrid renewable energy system for rural electrification sustainability using HOMER and grasshopper optimization algorithm," *Renewable Energy*, vol. 229, p. 120712, Aug. 2024, doi: 10.1016/j.renene.2024.120712.

[193] N. Ghorbani, A. Kasaeian, A. Toopshekan, L. Bahrami, and A. Maghami, "Optimizing a hybrid wind-PV-battery system using GA-PSO and MOPSO for reducing cost and increasing reliability," *Energy*, vol. 154, pp. 581–591, Jul. 2018, doi: 10.1016/j.energy.2017.12.057.

[194] K. M. Kotb, M. R. Elkadeem, M. F. Elmorshedy, and A. Dán, "Coordinated power management and optimized techno-enviro-economic design of an autonomous hybrid renewable microgrid: A case study in Egypt," *Energy Conversion and Management*, vol. 221, p. 113185, Oct. 2020, doi: 10.1016/j.enconman.2020.113185.

[195] S. W. Chisale, S. Eliya, and J. Taulo, "Optimization and design of hybrid power system using HOMER pro and integrated CRITIC-PROMETHEE II approaches," *Green Technologies and Sustainability*, vol. 1, no. 1, p. 100005, Jan. 2023, doi: 10.1016/j.grets.2022.100005.

[196] "Optimization of an off-grid PV/biogas/battery hybrid energy system for electrification: A case study in a commercial platform in Morocco - ScienceDirect." Accessed: Aug. 12, 2024. [Online]. Available: https://www.sciencedirect.com/science/article/pii/S2590174523001642

[197] M. F. Elmorshedy *et al.*, "Feasibility study and performance analysis of microgrid with 100% hybrid renewables for a real agricultural irrigation application," *Sustainable Energy Technologies and Assessments*, vol. 53, p. 102746, Oct. 2022, doi: 10.1016/j.seta.2022.102746.

[198] E. E. E. Ahmed, A. Demirci, and S. M. Tercan, "Optimal sizing and techno-enviro-economic feasibility assessment of solar tracker-based hybrid energy systems for rural electrification in Sudan," *Renewable Energy*, vol. 205, pp. 1057–1070, Mar. 2023, doi: 10.1016/j.renene.2023.02.022.

[199] P. García, J. P. Torreglosa, L. M. Fernández, F. Jurado, R. Langella, and A. Testa, "Energy management system based on techno-economic optimization for microgrids," *Electric Power Systems Research*, vol. 131, pp. 49–59, Feb. 2016, doi: 10.1016/j.epsr.2015.09.017.

[200] "Techno-economic Assessment of a Hydrogen-based Islanded Microgrid in North-east - ScienceDirect." Accessed: Aug. 12, 2024. [Online]. Available: https://www.sciencedirect.com/science/article/pii/S2352484723001609

[201] A. M. Abdulelah, B. Ouahid, S. Youcef, C. Abderrezzak, M. Abdelhafidh, and M. Ahmed, "Improve Lifespan of Battery Energy Storage in Remote Area Power System," in *2023 2nd International Conference on Electronics, Energy and Measurement (IC2EM)*, Nov. 2023, pp. 1–6. doi: 10.1109/IC2EM59347.2023.10419419.

[202] A. Ngila Mulumba and H. Farzaneh, "Techno-economic analysis and dynamic power simulation of a hybrid solar-wind-battery-flywheel system for off-grid power supply in remote areas in Kenya," *Energy Conversion and Management: X*, vol. 18, p. 100381, Apr. 2023, doi: 10.1016/j.ecmx.2023.100381.

[203] M. R. Elkadeem, S. Wang, A. M. Azmy, E. G. Atiya, Z. Ullah, and S. W. Sharshir, "A systematic decision-making approach for planning and assessment of hybrid renewable energy-based microgrid with techno-economic optimization: A case study on an urban community in Egypt," *Sustainable Cities and Society*, vol. 54, p. 102013, Mar. 2020, doi: 10.1016/j.scs.2019.102013.

[204] K. V. Konneh, O. B. Adewuyi, M. M. Gamil, A. M. Fazli, and T. Senjyu, "A scenario-based multi-attribute decision making approach for optimal design of a hybrid off-grid system," *Energy*, vol. 265, p. 125663, Feb. 2023, doi: 10.1016/j.energy.2022.125663.

[205] A. Al-Sharafi, A. Z. Sahin, T. Ayar, and B. S. Yilbas, "Techno-economic analysis and optimization of solar and wind energy systems for power generation and hydrogen production in Saudi Arabia," *Renewable and Sustainable Energy Reviews*, vol. 69, pp. 33–49, Mar. 2017, doi: 10.1016/j.rser.2016.11.157.

[206] F. A. Khan, N. Pal, and Syed. H. Saeed, "Review of solar photovoltaic and wind hybrid energy systems for sizing strategies optimization techniques and cost analysis methodologies," *Renewable and Sustainable Energy Reviews*, vol. 92, pp. 937–947, Sep. 2018, doi: 10.1016/j.rser.2018.04.107.

[207] M. Husein and I.-Y. Chung, "Optimal design and financial feasibility of a university campus microgrid considering renewable energy incentives," *Applied Energy*, vol. 225, pp. 273–289, Sep. 2018, doi: 10.1016/j.apenergy.2018.05.036.

[208] A. Q. Al-Shetwi, I. E. Atawi, A. Abuelrub, and M. A. Hannan, "Techno-economic assessment and optimal design of hybrid power generation-based renewable energy systems," *Technology in Society*, vol. 75, p. 102352, Nov. 2023, doi: 10.1016/j.techsoc.2023.102352.

[209] K. Benyoucef, A. Moualdia, D. Boudana, M. A. H. Mujammal, and M. A. Albasheri, "Optimal control strategies for DFIG-based wind turbines: simulation and analysis," *STUDIES IN ENGINEERING AND EXACT SCIENCES*, vol. 5, no. 3, pp. e12580–e12580, Dec. 2024, doi: 10.54021/seesv5n3-042.

[210] M. A. Albasheri, O. Bouchhida, Y. Soufi, A. Cherifi, and M. A. H. Mujammal, "Supervisory energy management strategy based-fuzzy logic for a DC microgrid," *Int. J. Dynam. Control*, vol. 13, no. 1, p. 31, Jan. 2025, doi: 10.1007/s40435-024-01510-8.

[211] X. Lü, Y. Qu, Y. Wang, C. Qin, and G. Liu, "A comprehensive review on hybrid power system for PEMFC-HEV: Issues and strategies," *Energy Conversion and Management*, vol. 171, pp. 1273–1291, Sep. 2018, doi: 10.1016/j.enconman.2018.06.065.

[212] H. Hemi, J. Ghouili, and A. Cheriti, "Combination of Markov chain and optimal control solved by Pontryagin's Minimum Principle for a fuel cell/supercapacitor vehicle," *Energy Conversion and Management*, vol. 91, pp. 387–393, Feb. 2015, doi: 10.1016/j.enconman.2014.12.035.

[213] X. Lü, P. Wang, L. Meng, and C. Chen, "Energy optimization of logistics transport vehicle driven by fuel cell hybrid power system," *Energy Conversion and Management*, vol. 199, p. 111887, Nov. 2019, doi: 10.1016/j.enconman.2019.111887.

[214] F. Zhang, L. Wang, S. Coskun, H. Pang, Y. Cui, and J. Xi, "Energy Management Strategies for Hybrid Electric Vehicles: Review, Classification, Comparison, and Outlook," *Energies*, vol. 13, no. 13, Art. no. 13, Jan. 2020, doi: 10.3390/en13133352.

[215] D.-D. Tran, M. Vafaeipour, M. El Baghdadi, R. Barrero, J. Van Mierlo, and O. Hegazy, "Thorough state-of-the-art analysis of electric and hybrid vehicle powertrains: Topologies and integrated energy management strategies," *Renewable and Sustainable Energy Reviews*, vol. 119, p. 109596, Mar. 2020, doi: 10.1016/j.rser.2019.109596.

[216] Q. Li, H. Yang, Y. Han, M. Li, and W. Chen, "A state machine strategy based on droop control for an energy management system of PEMFC-battery-supercapacitor hybrid tramway," *International Journal of Hydrogen Energy*, vol. 41, no. 36, pp. 16148–16159, Sep. 2016, doi: 10.1016/j.ijhydene.2016.04.254.

[217] Q. Li *et al.*, "A State Machine Control Based on Equivalent Consumption Minimization for Fuel Cell/ Supercapacitor Hybrid Tramway," *IEEE Transactions on Transportation Electrification*, vol. 5, no. 2, pp. 552–564, Jun. 2019, doi: 10.1109/TTE.2019.2915689.

[218] Z. Fu, L. Zhu, F. Tao, P. Si, and L. Sun, "Optimization based energy management strategy for fuel cell/battery/ultracapacitor hybrid vehicle considering fuel economy and fuel cell lifespan," *International Journal of Hydrogen Energy*, vol. 45, no. 15, pp. 8875–8886, Mar. 2020, doi: 10.1016/j.ijhydene.2020.01.017.

[219] "Optimization-Based Fuzzy Energy Management Strategy for PEM Fuel Cell/Battery/Supercapacitor Hybrid Construction Excavator | SpringerLink." Accessed: Jul. 30, 2022. [Online]. Available: https://link.springer.com/article/10.1007/s40684-020-00262-y

[220] A. A. Khan, A. F. Minai, R. K. Pachauri, and H. Malik, "Optimal Sizing, Control, and Management Strategies for Hybrid Renewable Energy Systems: A Comprehensive Review," *Energies*, vol. 15, no. 17, Art. no. 17, Jan. 2022, doi: 10.3390/en15176249.

[221] D. A. H. Fakra, D. A. S. Andriatoavina, N. A. M. N. Razafindralambo, K. abdallah Amarillis, and J. M. M. Andriamampianina, "A simple and low-cost integrative sensor system for methane and hydrogen measurement," *Sensors International*, vol. 1, p. 100032, Jan. 2020, doi: 10.1016/j.sintl.2020.100032.

[222] X. Lü *et al.*, "Energy management of hybrid electric vehicles: A review of energy optimization of fuel cell hybrid power system based on genetic algorithm," *Energy Conversion and Management*, vol. 205, p. 112474, Feb. 2020, doi: 10.1016/j.enconman.2020.112474.

[223] A. Prasanthi, H. Shareef, M. Asna, A. Asrul Ibrahim, and R. Errouissi, "Optimization of hybrid energy systems and adaptive energy management for hybrid electric vehicles," *Energy Conversion and Management*, vol. 243, p. 114357, Sep. 2021, doi: 10.1016/j.enconman.2021.114357.

[224] Z. Chen, Y. Liu, M. Ye, Y. Zhang, Z. Chen, and G. Li, "A survey on key techniques and development perspectives of equivalent consumption minimisation strategy for hybrid electric vehicles," *Renewable and Sustainable Energy Reviews*, vol. 151, p. 111607, Nov. 2021, doi: 10.1016/j.rser.2021.111607.

[225] I. M. Abdelqawee, A. W. Emam, M. S. ElBages, and M. A. Ebrahim, "An improved energy management strategy for fuel cell/battery/supercapacitor system using a novel hybrid jellyfish/particle swarm/BAT optimizers," *Journal of Energy Storage*, vol. 57, p. 106276, Jan. 2023, doi: 10.1016/j.est.2022.106276.

[226] L. Kwon, D.-S. Cho, and C. Ahn, "Degradation-Conscious Equivalent Consumption Minimization Strategy for a Fuel Cell Hybrid System," *Energies*, vol. 14, no. 13, Art. no. 13, Jan. 2021, doi: 10.3390/en14133810.

[227] M. SivaramKrishnan, N. Kathirvel, C. Kumar, and S. Barua, "Power management for fuel-cell electric vehicle using Hybrid SHO-CSGNN approach," *Energy Reports*, vol. 11, pp. 6069–6082, Jun. 2024, doi: 10.1016/j.egyr.2024.05.003.

[228] C. Park, Y. Jung, K. Lim, B. Kim, Y. Kang, and H. Ju, "Analysis of a phosphoric acid fuel cell-based multi-energy hub system for heat, power, and hydrogen generation," *Applied Thermal Engineering*, vol. 189, p. 116715, May 2021, doi: 10.1016/j.applthermaleng.2021.116715.

[229] Z. Zhang, C. Guan, and Z. Liu, "Real-Time Optimization Energy Management Strategy for Fuel Cell Hybrid Ships Considering Power Sources Degradation," *IEEE Access*, vol. 8, pp. 87046–87059, 2020, doi: 10.1109/ACCESS.2020.2991519.

[230] D. Rezzak and N. Boudjerda, "Robust energy management strategy based on non-linear cascade control of fuel cells-super capacitors hybrid power system," *International Journal of Hydrogen Energy*, vol. 45, no. 43, pp. 23254–23274, Sep. 2020, doi: 10.1016/j.ijhydene.2020.05.250.

[231] X. Guo *et al.*, "Energy management system for hybrid ship: Status and perspectives," *Ocean Engineering*, vol. 310, p. 118638, Oct. 2024, doi: 10.1016/j.oceaneng.2024.118638.

[232] A. Benmouna, M. Becherif, L. Boulon, C. Dépature, and H. S. Ramadan, "Efficient experimental energy management operating for FC/battery/SC vehicles via hybrid Artificial Neural Networks-Passivity Based Control," *Renewable Energy*, vol. 178, pp. 1291–1302, Nov. 2021, doi: 10.1016/j.renene.2021.06.038.

[233] "Energy management strategy for battery/supercapacitor/fuel cell hybrid source vehicles based on finite state machine - ScienceDirect." Accessed: Sep. 30, 2024. [Online]. Available: https://www.sciencedirect.com/science/article/abs/pii/S0306261919313947

[234] T. Wang, Q. Li, W. Chen, and T. Liu, "Application of energy management strategy based on state machine in fuel cell hybrid power system," in *2017 IEEE Transportation Electrification Conference and Expo, Asia-Pacific (ITEC Asia-Pacific)*, Aug. 2017, pp. 1–5. doi: 10.1109/ITEC-AP.2017.8080854.

[235] S. Changizian, P. Ahmadi, M. Raeesi, and N. Javani, "Performance optimization of hybrid hydrogen fuel cell-electric vehicles in real driving cycles," *International Journal of Hydrogen Energy*, vol. 45, no. 60, pp. 35180–35197, Dec. 2020, doi: 10.1016/j.ijhydene.2020.01.015.

[236] P. Dai, W. Sun, H. Xie, Y. Lv, and Z. Han, "Stability Analysis of FCHEV Energy System Using Frequency Decoupling Control Method," *Journal of Power Electronics*, vol. 17, no. 2, pp. 490–500, 2017, doi: 10.6113/JPE.2017.17.2.490.

[237] Y. Shen, P. Cui, X. Wang, X. Han, and Y.-X. Wang, "Variable structure battery-based fuel cell hybrid power system and its incremental fuzzy logic energy management strategy," *International Journal of Hydrogen Energy*, vol. 45, no. 21, pp. 12130–12142, Apr. 2020, doi: 10.1016/j.ijhydene.2020.02.083.

[238] H. Hemi, J. Ghouili, and A. Cheriti, "A real time fuzzy logic power management strategy for a fuel cell vehicle," *Energy Conversion and Management*, vol. 80, pp. 63–70, Apr. 2014, doi: 10.1016/j.enconman.2013.12.040.

[239] S. Tao *et al.*, "Energy management strategy based on dynamic programming with durability extension for fuel cell hybrid tramway," *Rail. Eng. Science*, vol. 29, no. 3, pp. 299–313, Sep. 2021, doi: 10.1007/s40534-021-00247-w.

[240] Z. Hu *et al.*, "Multi-objective energy management optimization and parameter sizing for proton exchange membrane hybrid fuel cell vehicles," *Energy Conversion and Management*, vol. 129, pp. 108–121, Dec. 2016, doi: 10.1016/j.enconman.2016.09.082.

[241] T. Fletcher, R. Thring, and M. Watkinson, "An Energy Management Strategy to concurrently optimise fuel consumption & PEM fuel cell lifetime in a hybrid vehicle," *International Journal of Hydrogen Energy*, vol. 41, no. 46, pp. 21503–21515, Dec. 2016, doi: 10.1016/j.ijhydene.2016.08.157.

[242] J. Bernard, S. Delprat, F. Buechi, and T. M. Guerra, "Global Optimisation in the power management of a Fuel Cell Hybrid Vehicle (FCHV)," in *2006 IEEE Vehicle Power and Propulsion Conference*, Sep. 2006, pp. 1–6. doi: 10.1109/VPPC.2006.364289.

[243] S. Caux, Y. Gaoua, and P. Lopez, "A combinatorial optimisation approach to energy management strategy for a hybrid fuel cell vehicle," *Energy*, vol. 133, pp. 219–230, Aug. 2017, doi: 10.1016/j.energy.2017.05.109.

[244] D. Pivetta, C. Dall'Armi, and R. Taccani, "Multi-objective optimization of hybrid PEMFC/Li-ion battery propulsion systems for small and medium size ferries," *International Journal of Hydrogen Energy*, vol. 46, no. 72, pp. 35949–35960, Oct. 2021, doi: 10.1016/j.ijhydene.2021.02.124.

[245] X. Liu, Y. Wu, and J. Duan, "Optimal Sizing of a Series Hybrid Electric Vehicle Using a Hybrid Genetic Algorithm," in *2007 IEEE International Conference on Automation and Logistics*, Aug. 2007, pp. 1125–1129. doi: 10.1109/ICAL.2007.4338737.

[246] A. Prasanthi, H. Shareef, M. Asna, A. Asrul Ibrahim, and R. Errouissi, "Optimization of hybrid energy systems and adaptive energy management for hybrid electric vehicles," *Energy Conversion and Management*, vol. 243, p. 114357, Sep. 2021, doi: 10.1016/j.enconman.2021.114357.

[247] Z. Hong, Q. Li, Y. Han, W. Shang, Y. Zhu, and W. Chen, "An energy management strategy based on dynamic power factor for fuel cell/battery hybrid locomotive," *International Journal of Hydrogen Energy*, vol. 43, no. 6, pp. 3261–3272, Feb. 2018, doi: 10.1016/j.ijhydene.2017.12.117.

[248] H.-A. Trinh, V.-D. Phan, H.-V.-A. Truong, and K. K. Ahn, "Energy Management Strategy for PEM Fuel Cell Hybrid Power System Considering DC Bus Voltage Regulation," *Electronics*, vol. 11, no. 17, Art. no. 17, Jan. 2022, doi: 10.3390/electronics11172722.

[249] N. Bizon, "Energy optimization of fuel cell system by using global extremum seeking algorithm," *Applied Energy*, vol. 206, pp. 458–474, Nov. 2017, doi: 10.1016/j.apenergy.2017.08.097.

[250] S. Quan, Y.-X. Wang, X. Xiao, H. He, and F. Sun, “Real-time energy management for fuel cell electric vehicle using speed prediction-based model predictive control considering performance degradation,” *Applied Energy*, vol. 304, p. 117845, Dec. 2021, doi: 10.1016/j.apenergy.2021.117845.

[251] M. A. Albasheri, O. Bouchhida, Y. Soufi, A. Moualdia, and M. Mujammal, “Control And Power Management of DC Microgrid Based Wind/Battery/Supercapacitor,” in *2022 IEEE 2nd International Maghreb Meeting of the Conference on Sciences and Techniques of Automatic Control and Computer Engineering (MI-STA)*, May 2022, pp. 680–685. doi: 10.1109/MI-STA54861.2022.9837665.

[252] M. A. Albasheri, O. Bouchhida, Y. Soufi, and A. Cherifi, “Enhanced supervisor energy management technique of DC microgrid-based PV/wind/battery/SC,” *Electr Eng*, Aug. 2024, doi: 10.1007/s00202-024-02622-2.

[253] W. Jing, C. H. Lai, W. S. H. Wong, and M. L. D. Wong, “A comprehensive study of battery-supercapacitor hybrid energy storage system for standalone PV power system in rural electrification,” *Applied Energy*, vol. 224, pp. 340–356, Aug. 2018, doi: 10.1016/j.apenergy.2018.04.106.

[254] Z. Cabrane, J. Kim, K. Yoo, and M. Ouassaid, “HESS-based photovoltaic/batteries/supercapacitors: Energy management strategy and DC bus voltage stabilization,” *Solar Energy*, vol. 216, pp. 551–563, Mar. 2021, doi: 10.1016/j.solener.2021.01.048.

[255] M. A. Albasheri, O. Bouchhida, Y. Soufi, and A. Cherifi, “Enhanced Vector Control of Induction Motor by Fuzzy Logic Controller,” in *2024 2nd International Conference on Electrical Engineering and Automatic Control (ICEEAC)*, May 2024, pp. 1–5. doi: 10.1109/ICEEAC61226.2024.10576217.